Investigating the molecular mechanisms of Hereditary Spastic Paraplegia neuropathies

Thesis submitted in accordance with the requirements of the University of Liverpool for the degree of Doctor in Philosophy by:

Jennifer Maria McNamee

September 2017

Declaration

This thesis is as a product of my own work, unless otherwise stated. The research presented in this thesis was carried out at the University of Liverpool, Institute of Translational Medicine, Cellular and Molecular Physiology department. Neither this thesis, nor any part of this thesis, has been previously submitted as part of another degree or qualification, at this or at any other University or learning institute.

Jennifer Maria McNamee

Investigating the molecular mechanisms of Hereditary Spastic Paraplegia (HSP) neuropathies

Jennifer Maria McNamee

Abstract

Hereditary spastic paraplegia (HSP) was first described in the late 1800s and has since become a term used to describe this relatively large, clinically and genetically diverse group of inherited neurodegenerative or neurodevelopmental disorders. HSPs are characterised by progressive lower limb spasticity and pyramidal weakness, caused by genetic mutations. This defining clinical feature is thought to be due to the progressive, length-dependent neuronal degeneration or axonopathy, which predominantly involves the lateral corticospinal tracts. Although unified by their defining clinical feature, HSPs are some of the most genetically diverse diseases. To date, 78 spastic gait disease-loci (SPG1-78) and 61 corresponding spastic paraplegia genes have been identified, and these are likely to increase further still.

A critical step towards unravelling the complex molecular relationships in living systems is the mapping of protein-protein interactions. Proteins with similar functions and cellular localisations tend to cluster together within these networks, with the majority sharing at least one function. Proteins that interact with known disease-causing HSP proteins may in some cases also acquire mutations that contribute to specific HSP-related phenotypes. Therefore, identification of proteins that interact with known HSP proteins, or exist in common molecular complexes, may provide new insight into the molecular mechanisms fundamental to the pathogenesis of this group of disorders.

The sequence-verified HSP ORFs generated were used to construct a collection of Y2H HSP bait and prey clones. The 'traditional' yeast two-hybrid system was then used to test a number of predicted binary interactions, using high-throughput

targeted assays, whilst novel HSP interaction partners were identified using high-throughput library screens.

Membrane-associated proteins are one of the most biologically important protein classes, with key roles in various cellular processes including cell signalling, molecular transport, metabolism and cell structure maintenance. However, detection of protein-protein interactions (PPIs) of membrane proteins is challenging, due to their hydrophobic nature and non-nuclear localisation, making them difficult to analyse using conventional interaction detection methods. As there is a significant number of membrane-associated HSP proteins, sequence-verified HSP ORFs were used to generate a collection of membrane yeast two-hybrid (MYTH) HSP bait clones. The MYTH system was used to investigate potentially novel interaction profiles for each of the membrane-associated HSP bait constructs, using the optimised high-throughput MYTH library screen approach.

In total, 365 novel binary HSP interactions were identified in this study, increasing the complexity of the HSP interactome. This high-density, comprehensive HSP interactome can be used to inform future hypothesis-driven research, looking at the physiological mechanisms and functional relevance of these interactions, providing a greater understanding of the pathogenic mechanisms of HSP, as well as for the development of new strategies for therapeutic intervention.

Table of Contents

Appendices

Appendix Files provided on CD:

2.1 Primers

2.2 MYTH strategy optimisation – validation

5.1 List of RING E3 ligases

5.2 List of DUBs

6.1 Summary of all interaction data

6.2 Reactome analysis raw data

6.3 PANTHER analysis raw data

6.4 MGI analysis raw data

6.5 MGI analysis raw data – associated human genes

Abbreviations

3-AT	3-Amino-1,2,4-triazol
AA	Amino Acid
AAA	ATPases Associated with diverse cellular Activities
AD	Autosomal Dominance
AD	Alzheimer's Disease
ALS	Amyotrophic Lateral Sclerosis
AP-MS	Affinity-Purification/Mass Spectrometry
APP	Amyloid Precursor Protein
AR	Autosomal Recessive
ASL	Adenylosuccinate Lyase
ATP	Adenosine Triphosphate
BCPCR	Bacterial Colony PCR
BD	Binding Domain
BMP	Bone Morphogenic Protein
CAM	Cell Adhesion Molecule
cDNA	Complementary DNA
CMA	Chaperone-Mediated Autophagy
CNS	Central Nervous System
DNA	Deoxyribonucleic Acid
DSB	Double-Strand Break
DTT	Dithiothreitol
DULIP	Dual Luminescence-Based Co-Immunoprecipitation
ER	Endoplasmic Reticulum
ERAD	ER-associated Degradation
ERGIC	ER-Golgi Intermediate Compartment
ESCRT	Endosomal Sorting Complexes Required for Transport
FRET	Förster Resonance Energy Transfer
HD	Huntington's Disease
HR	Hydrophobic Region
HSP	Hereditary Spastic Paraplegia
LD	Lipid Droplet
MAPPIT	MAmmalian Protein-Protein Interaction Trap
MCS	Multiple Cloning Site
MGI	Mouse Genome Informatics

MIMs	MIT-Interacting Motifs
MIT	Microtubule Interacting and Trafficking domain
mut	Mutant
MVE	Multivesicular Endosome
MYTH	Membrane Yeast Two-Hybrid
NCBI	National Center for Biotechnology Information
OD	Optical Density
ORF	Open Reading Frame
PANTHER	Protein ANalysis THrough Evolutionary Relationships
PCR	Polymerase Chain Reaction
PD	Parkinson's Disease
PEG	Polyethylene Glycol
PPI	Protein-Protein Interaction
RING	Really Interesting New Gene
RNS	Reactive Nitrogen Species
ROS	Reactive Oxygen Species
RT	Room Temperature
SLiCE	Seamless Ligation Cloning Extract
SPG	Spastic Paraplegia Gene
SSB	Single-Strand Break
SSD	Single-Stranded DNA
TF	Transcription Factor
TGN	Trans-Golgi Network
TM	Transmembrane
UAS	Upstream Activating Sequence
UTR	Untranslated Region
w/o	Without
WASH	WASP and Scar homologue
WASP	Wiskott–Aldrich syndrome protein
WT	Wild-type
X-α-gal	5-Bromo-4-chloro-3-indoxyl-α-D-galactopyranoside
X-gal	5-Bromo-4-Chloro-3-Indolyl β-D-Galactopyranoside
Y2H	Yeast Two-Hybrid
YCPCR	Yeast Colony PCR
β-gal	β-galactosidase

Acknowledgements

First and foremost, I would like to thank my supervisor Professor Chris Sanderson for his support and guidance throughout, but also for allowing me to develop into an independent researcher. I would also like to express my gratitude to Dr Igor Stagljar and his colleagues for providing me with the reagents and materials to set up the membrane yeast two-hybrid (MYTH) system in our lab. Finally, I would like to thank the Wellcome Trust for funding my work.

To all members, past and present, of the Sanderson lab: Amy, Bronwyn, Emily, Dave, Hanna, Joanna, Jonathan, James and Vanessa - thank you all for being there. We all know research can be emotionally demanding and stressful but you all helped relieve some of the tension, whether it was getting coffee and having a chat on the way, helping me find space to store the hundreds (quite literally) of yeast plates I'd ordered, or letting me ramble on about some recipe I was interested in trying, it was all support and encouragement in one form or another and I couldn't have done it without you. Special thanks to Amy who introduced me to all things yeasty and the love of YPAD, thanks for letting me rant and rave and always being around, especially towards the end of the PhD. Also, a special thanks to Bronwyn, who not only brought the Great British Bake Off to the lab on a weekly basis but was always there to talk to. Our endless conversations, usually about baking, food or Harvey-related, kept me somewhat sane for the majority of the PhD, either that or knowing that someone else was in the same boat, so thank you.

A huge thank you goes to Andy, my best friend and my soul-mate, without you I probably would never have even considered doing a PhD. You kept me going through all the tough times, and having been through it yourself, you always seemed to know what to do. You have always encouraged and motivated me to keep going, even when I wanted to give up and even, in the midst of it all, when I wanted to get a dog. Thank you.

I would also like to say a huge thank you to my mum and dad, who have always shown me the unconditional love, support and encouragement that has got me to where I am today. Thank you for believing in me, even when I didn't.

Finally, I would like to dedicate this thesis to the greatest influence in my life, my mum. You have taught me to be the strong, independent and ambitious woman that I am today, and I continue to learn from you every day.

Chapter 1: Introduction

1.1 Introduction

In humans, voluntary movements rely on the multi-synaptic pathways of the central nervous system (CNS) that extend from the cerebral motor cortex to the neuromuscular junctions thereby innervating the skeletal muscle. This is known as the pyramidal motor system (Blackstone, 2012), and it has two parts. In the first, axons of the upper motor neurons (neurons of the cerebral motor cortex) pass through the medullary pyramids, where most decussate in the caudal medulla to form the lateral corticospinal tract of the spinal cord (Soderblom and Blackstone, 2006). These corticospinal axons are able to form synapses either directly or indirectly (via spinal interneurons) with the lower motor neurons in the anterior horn of the spinal cord (Blackstone, O'Kane and Reid, 2011; Blackstone, 2012). In the second, axons originating from the lower motor neurons of the spinal cord terminate in specialised synapses at neuromuscular junctions throughout the body, to mediate skeletal muscle contraction (Blackstone, 2012).

The distances covered by the upper and lower motor neurons are extremely long, some of the longest in the CNS, with axons reaching up to 1 m in length (Soderblom and Blackstone, 2006; Blackstone, O'Kane and Reid, 2011). This length permits the rapid relay of action potentials which mediate voluntary movement, with the additional complex intracellular machineries which are required for the proper sorting and distribution of proteins, lipids, organelles and other molecules (Blackstone, O'Kane and Reid, 2011). These machineries exploit the intricate cytoskeletal scaffold, which serves as a molecular *'rail system'* along which motor proteins can mediate the selective transport of components throughout the cell. This active transport of proteins and other molecules is essential for neuronal function and survival, as most of the proteins required in the nerve terminals and axons need to be transported from the cell body (Erlich *et al.*, 2011). Axonal transport machineries are highly dependent upon microtubules, which can function as

polarised tracks with their plus ends orientated towards the axon terminal (Blackstone, 2012).

Not surprisingly, these long axons are particularly vulnerable to length-dependent defects in cellular processes such as trafficking, transport and cytoskeletal organisation. All of which have been shown to affect axonal development and maintenance (Soderblom and Blackstone, 2006; Blackstone, 2012), giving rise to a host of neurological disorders, including the inherited Mendelian disorder, hereditary spastic paraplegias (HSPs).

1.2 Hereditary Spastic Paraplegias (HSPs)

Hereditary spastic paraplegia (HSP) was first described in the late 1800s and has since become a term used to describe this relatively large, clinically and genetically diverse group of inherited neurodegenerative or neurodevelopmental disorders. Hereditary spastic paraplegias (HSPs) are characterised by progressive lower limb spasticity and pyramidal weakness, caused by genetic mutations (Harding, 1983). This defining clinical feature is thought to be due to the progressive, length-dependent neuronal degeneration or axonopathy, which predominantly involves the lateral corticospinal tracts, and is often more severe at the distal ends (DeLuca, Ebers and Esiri, 2004).

Although unified by their defining clinical feature, HSPs are some of the most genetically diverse diseases. To date, 78 spastic gait disease-loci (SPG1-78) and 61 corresponding spastic paraplegia genes have been identified (Klebe, Stevanin and Depienne, 2015; de Souza *et al.*, 2016). As shown in Table 1.1, this number does not include those genes involved in complex forms not referred to as HSP, such as mitochondrial genes MT-ATP6 (Verny *et al.*, 2011) and MT-TI (Corona *et al.*, 2002), or other causative genes that are not yet part of the spastic paraplegia gene (SPG) classification system, such as LYST (Shimazaki *et al.*, 2014) and CCT5 (Bouhouche *et al.*, 2005).

Inheritance and clinical features of each HSP form are described in Table 1.2, with the age of symptom onset varying greatly, from early childhood to late adulthood (Salinas *et al.*, 2008; Schüle *et al.*, 2016). It depends on the underlying genetic defect, but can also vary significantly even between family members with the same mutation (Soderblom and Blackstone, 2006; Klebe, Stevanin and Depienne, 2015).

Table 1.1

SPG	Gene	Gene ID	Locus[a]	References[b]
SPG1	L1CAM	3897	Xq28	Jouet et al., 1994
SPG2	PLP1	5354	Xq22.2	Saugier-Veber et al., 1994
SPG3	ATL1	51062	14q22.1	Zhao et al., 2001
SPG4	SPAST	6683	2p22.3	Hazan et al., 1999
SPG5A	CYP7B1	9420	8q12.3	Tsaousidou et al., 2008
SPG6	NIPA1	123606	15q11.2	Rainier et al., 2003
SPG7	SPG7	6687	16q24.3	Casari et al., 1998
SPG8	WASHC5	9897	8q24.13	Valdmanis et al., 2007
SPG9	SPG9	9193	10q24.1	Seri et al., 1999, Panza et al., 2016
SPG10	KIF5A	3798	12q13.3	Reid et al., 2002
SPG11	SPG11	80208	15q21.1	Stevanin et al., 2007
SPG12	RTN2	6253	19q13.32	Montenegro et al., 2012
SPG13	HSPD1	3329	2q33.1	Hansen et al., 2002
SPG14	SPG14	57309	3q27-q28	Vazza et al., 2000
SPG15	ZFYVE26	23503	14q24.1	Hanein et al., 2008
SPG16	SPG16	57760	Xq11.2	Steinmuller et al., 1997
SPG17	BSCL2	26580	11q12.3	Windpassinger et al., 2004
SPG18	ERLIN2	11160	8p11.23	Alazami et al., 2011
SPG19	SPG19	140907	9q33-q34	Valente et al., 2002
SPG20	SPART	23111	13q12.3	Patel et al., 2002
SPG21	SPG21	51324	15q22.31	Simpson et al., 2003
SPG22	SLC16A2	6567	Xq13.2	Schwartz et al., 2006
SPG23	SPG23	353293	1q24-q32	Blumen et al., 2003
SPG24	SPG24	338090	13q14	Hodgkinson et al., 2002
SPG25	SPG25	387583	6q23-24.1	Zortea et al., 2002

SPG26	B4GALNT1	2583	12q13.3	Boukhris et al., 2013
SPG27	SPG27	414886	10q22.1-q24.1	Meijer et al., 2004, Ribaï et al., 2006
SPG28	DDHD1	80821	14q22.1	Tesson et al., 2012
SPG29	SPG29	619379	1p31.1-21.1	Orlacchio et al., 2005
SPG30	KIF1A	547	2q37.3	Erlich et al., 2011, Klebe et al., 2012
SPG31	REEP1	65055	2p11.2	Zuchner et al., 2006
SPG32	SPG32	724107	14q12-q21	Stevanin et al., 2007
SPG33	ZFYVE27	118813	10q24.2	Mannan et al., 2006
SPG34	SPG34	724110	Xq24-q25	Macedo-Souza et al., 2008
SPG35	FA2H	79152	16q23.1	Dick et al., 2010
SPG36	SPG36	791228	12q23-24	Schüle et al., 2009
SPG37	SPG37	100049159	8p21.1-q13.3	Hanein et al., 2007
SPG38	SPG38	100049707	4p16-p15	Orlacchio et al., 2008
SPG39	PNPLA6	10908	19p13.2	Rainier et al., 2008
SPG40	-	-	-	Subramony et al., 2009
SPG41	SPG41	100359402	11p14.1-11p.2	Zhao et al., 2008
SPG42	SLC33A1	9197	3q25.31	Lin et al., 2008
SPG43	C19orf12	83636	19p13.11-q12	Landoure et al., 2013
SPG44	GJC2	57165	1q42.13	Orthmann-Murphy et al., 2009
SPG45	SPG45	100322879	10q24.3-q25.1	Dorsun et al., 2009,
SPG46	GBA2	57704	9p13.3	Martin et al., 2013
SPG47	AP4B1	10717	1p13.2	Abou Jamra et al., 2011
SPG48	AP5Z1	9907	7p22.1	Slabicki et al., 2010
SPG49	TECPR2	9895	4q25	Oz-Levi et al., 2012
SPG50	AP4M1	9179	7q22.1	Verkerk et al 2009
SPG51	AP4E1	23431	15q21.2	Abou Jamra et al., 2011, Moreno-De-Luca et al., 2011
SPG52	AP4S1	11154	14q12	Abou Jamra et al., 2011
SPG53	VPS37A	137492	8p22	Zivony-Elboum et al., 2012
SPG54	DDHD2	23259	8p11.23	Schuurs-Hoeijmakers et al., 2012
SPG55	C12orf65	91574	12q24.31	Shimazaki et al., 2012
SPG56	CYP2U1	113612	14q32.31	Oz-Levi et al., 2012
SPG57	TFG	10342	3q12.2	Ishiur et al., 2012, Beetz et al., 2013

SPG58	KIF1C	10749	17p13.2	Novarino et al., 2014, Dor et al., 2014
SPG59	USP8	9101	15q21.2	Novarino et al., 2014
SPG60	WDR48	57599	3p22.2	Novarino et al., 2014
SPG61	ARL6IP1	23204	16p12.3	Novarino et al., 2014
SPG62	ERLIN1	10613	10q24.31	Novarino et al., 2014
SPG63	AMPD2	271	1p13.3	Novarino et al., 2014
SPG64	ENTPD1	953	10q24.1	Novarino et al., 2014
SPG65	NT5C2	22978	10q24.32-q24.33	Novarino et al., 2014
SPG66	ARSI	340075	5q32	Novarino et al., 2014
SPG67	PGAP1	80055	2q33.1	Novarino et al., 2014
SPG68	FLRT1	23769	11q13.1	Novarino et al., 2014
SPG69	RAB3GAP2	25782	1q31	Novarino et al., 2014
SPG70	MARS	4141	12q13.3	Novarino et al., 2014
SPG71	ZFR	51663	5p13.3	Novarino et al., 2014
SPG72	REEP2	51308	5q31.2	Esteves et al., 2014
SPG73	CPT1C	126129	19q13.33	Carrasco et al., 2013, Rinaldi et al., 2015
SPG74	IBA57	200205	1q42.13	Lossos et al., 2015
SPG75	MAG	4099	19q13.1	Novarino et al., 2014, Lossos et al., 2015
SPG76	CAPN1	823	11q13.1	Gan-Or et al., 2016
SPG77	FARS2	10667	6p25.1	Yang et al., 2016
SPG78	ATP13A2	23400	1p36.13	Estrada-Cuzcano et al., 2017
-	AFG3L2	10939	18p11.21	Koppen et al., 2007, Di Bella et al., 2010
-	ALS2	57679	2q33.1	Eymard-Pierre et al., 2002, Rowland 2005, Daud et al., 2016
-	BICD2	23299	9q22.32	Oates et al., 2013, Novarino et al., 2014
-	CCT5	22948	5p15.2	Bouhouche et al., 2006
-	ELOVL4	6785	6q14.1	Aldahmesh et al., 2011 Fink, 2013
-	EXOSC3	51010	9p13.2	Zanni et al., 2013, Halevy et al., 2014
-	RETREG1	54463	5p15.1	Aydinlar et al., 2014
-	GAD1	2571	2q31.1	McHale et al., 1999, Lynex et al., 2004
-	GJA1	2697	6q22.31	Paznekas et al., 2003
-	HACE1	57531	6q16.3	Hollstein et al., 2015

-	IFIH1	64135	2q24.2	Crow et al., 2014
-	KANK1	23189	9p24.3	Novarino et al., 2014
-	KCNA2	3737	1p13.3	Helbig et al., 2016
-	KIDINS220	57498	2p25.1	Josifova et al., 2016
-	LYST	1130	1q42.3	Shimazaki et al., 2014
-	ATP6	4508	-	Verny et al., 2011
-	ND4	4538	-	Clarençon et al., 2006, Sgobbi de Souza et al., 2016
-	TRNI	4565	-	Corona et al., 2002
-	COX3	4514	-	Tiranti et al., 2000, Sgobbi de Souza et al., 2016
-	TPP1	1200	11p15.4	Kara et al., 2016
-	VCP	7415	9p13.3	De Bot et al., 2012

Table 1.1. **List of human HSP loci and genes**. HSP genes are listed by spastic gait disease-loci (SPG), numbered sequentially based on the order of locus discovery (Fink, 2013). HSP genes not part of the SPG classification system are listed alphabetically. Entrez Gene IDs were obtained from the NCBI database (Maglott *et al.*, 2007) and are the most updated identifiers for the corresponding genes at the time of submission.

[a] Loci from OMIM (http://www.ncbi.nlm.nih.gov/omim/)

[b] Locus/gene discovery association with HSP

1.2.1 Clinical Classification

The clinical classification of HSPs as “pure” or “complicated” was based on the description by Anita Harding in 1983. According to this, HSPs are classified based on the absence (pure) or presence (complicated) of any neurological and/or non-neurological features, which arise in addition to the spastic paraplegia phenotype, in the absence of any co-existing diseases (Harding, 1983; Fink, 2013; Noreau, Dion and Rouleau, 2014). These additional features are also shown in Table 1.2, and include neurological manifestations such as, cerebellar dysfunction (ataxia, nystagmus, tremor); axonal or demyelinating peripheral neuropathy (dysautonomia and sensory disturbances); cognitive impairment (dementia and mental retardation/intellectual disability); epilepsy; extrapyramidal features (Parkinsonism, chorea, dystonia); brain and spine MRI abnormalities (including mild white matter changes, thin corpus

callosum, spinal cord atrophy, brain iron accumulation, hydrocephalus, and cerebellar atrophy) (Fink, 2013; Novarino *et al.*, 2014; Klebe, Stevanin and Depienne, 2015; de Souza *et al.*, 2016). The extensive heterogeneous non-neurological manifestations include, ophthalmological abnormalities (cataracts, optic neuropathy, optic atrophy, macular degeneration); dysmorphic features (microcephaly, macrocephaly, facial dysmorphism, short stature); and orthopaedic abnormalities (scoliosis, hip dislocation, foot deformities) (Lo Giudice *et al.*, 2014; Klebe, Stevanin and Depienne, 2015; de Souza *et al.*, 2016).

1.2.2 Genetic Classification

All modes of Mendelian inheritance (autosomal dominant, autosomal recessive and X-linked), and the rarer non-Mendelian mitochondrial maternal inheritance have also been described for HSPs, as shown in Table 1.2 (Finsterer *et al.*, 2012; Lo Giudice *et al.*, 2014; Klebe, Stevanin and Depienne, 2015). Autosomal recessive HSP (AR-HSP) is the most common mode of inheritance in HSP, and is even more common in consanguineous families and non-European populations (de Souza *et al.*, 2016), with mutations in the SPG11 (15q21.1) and SPG15 (14q24.1) genes being the most common causes of AR-HSP (Goizet *et al.*, 2009; Siri *et al.*, 2010; Pensato *et al.*, 2014). Moreover, 'complicated' forms of HSP tend to be autosomal recessive (Salinas *et al.*, 2008; Fink, 2013), while 'pure' forms of HSP tend to be autosomal dominant (AD), with mutations in genes encoding spastin, atlastin and REEP1 accounting for an estimated 50 % of all AD-HSP cases (Finsterer *et al.*, 2012).

Autosomal Dominant (AD) HSPs

Thus far, 26 genetic SPG loci have been identified for AD-HSP, with only 19 known corresponding genes. There are 7 AD-HSP loci, namely SPG19 (Valente *et al.*, 2002), SPG29 (Orlacchio *et al.*, 2005), SPG36 (Schule *et al.*, 2009), SPG37 (Hanein *et al.*, 2007), SPG38 (Orlacchio *et al.*, 2008), SPG40 (Subramony *et al.*, 2009) and SPG41 (Zhao *et al.*, 2008), with unidentified genes associated with both pure and complicated forms of HSP (Table 1.1 and 1.2).

Table 1.2

SPG	Gene	Inheritance	Age of onset	Phenotype	Additional features
SPG1	L1CAM	X-linked	EO	C	Mental retardation, aphasia, shuffling gait, adducted thumbs, hydrocephalus, ACC
SPG2	PLP1	X-linked	VO	P or C	Seizures, mental retardation, nystagmus, ataxia, WMLs, PNP
SPG3A	ATL1	AD	EO	P or C	Lower limb muscle atrophy, seizures, ataxia, optic atrophy, spasticity in the upper limbs, sensorimotor axonal neuropathy, cognitive and cranial nerve impairment, intellectual disability, *pes cavus*, TCC
SPG4	SPAST	AD	VO	P or C	Cognitive decline, epilepsy, ataxia, psychosis, upper limb spasticity, *pes cavus*, posterior fossa abnormalities, PNP, hand tremor, WMLs, amyotrophy of small hand muscles
SPG5A	CYP7B1	AR	VO	P or C	Optic atrophy, WMLs, cerebellar ataxia
SPG6	NIPA1	AD	TO	P or C	Idiopathic generalized epilepsy (IGE), dysarthria, PNP, facial dystonia, atrophy of the small hand muscles and upper limbs spasticity, *pes cavus*
SPG7	SPG7	AR	VO	P or C	Cerebellar signs, cerebellar atrophy, PNP, optic atrophy, supranuclear palsy, cognitive impairment of attention and executive functions, TCC, scoliosis, *pes cavus*
SPG8	WASHC5	AD	AO	P	-
SPG9	SPG9	AD	TO	C	Cataracts, motor neuropathy, skeletal abnormalities, gastroesophageal reflux
SPG10	KIF5A	AD	EO	P or C	Distal amyotrophy in the upper extremities, cognitive decline, PNP, dysautonomia, parkinsonism, deafness, retinitis pigmentosa
SPG11	SPG11	AR	VO	C	Cerebellar signs, PNP, WMLs, cerebellar atrophy, TCC, seizures, cognitive decline, abnormal eye signs, amyotrophy, parkinsonism, maculopathy, action tremor, mental retardation, upper limbs weakness
SPG12	RTN2	AD	EO	P	-
SPG13	HSPD1	AD	VO	P or C	Dystonia
SPG14	SPG14	AR	AO	C	Motor PNP, mental retardation

SPG15	ZFYVE26	AR	EO	C	Pigmentary retinopathy, cerebellar signs, PNP, amyotrophy, seizures, mental retardation, TCC
SPG16	SPG16	X-linked	EO	P or C	Aphasia, nystagmus, mental retardation
SPG17	BSCL2	AD	TO	C	Amyotrophy of small hand and feet muscles, lower motor neuron disease
SPG18	ERLIN2	AR	EO	C	Epilepsy, mental retardation, congenital hip dislocation, multiple joint contractures
SPG19	SPG19	AD	AO	P	-
SPG20	SPART	AR	EO	C	Mental retardation, dysarthria, upper limbs spasticity, cerebellar signs, euphoria, crying, WMLs
SPG21	SPG21	AR	EO	C	Dementia, TCC, WMLs, cerebellar signs, extrapyramidal features, callosal disconnection syndrome
SPG22	SLC16A2	X-linked	EO	C	Mental retardation, muscle atrophy, distal wasting, dyskinesia, nystagmus, ataxia
SPG23	SPG23	AR	EO	C	Cognitive impairment, pigmentary abnormalities, facial and skeletal dysmorphism, tremor
SPG24	SPG24	AR	EO	C	Pseudobulbar signs
SPG25	SPG25	AR	AO	C	Cataracts, neuropathy, disc herniation
SPG26	B4GALNT1	AR	EO	C	Intellectual disability, cortical atrophy, peripheral neuropathy, distal atrophy, cerebellar ataxia, WMLs
SPG27	SPG27	AR	VO	C	Dysarthria, mental retardation, polyneuropathy
SPG28	DDHD1	AR	EO	P or C	Saccadic eye pursuit, axonal neuropathy
SPG29	SPG29	AD	TO	C	*Pes cavus*, hearing loss, hiatal hernia, hyperbilirubinaemia
SPG30	KIF1A	AR	TO	P or C	Sensory PNP, cerebellar signs, hypoacusis, distal muscle wasting
SPG31	REEP1	AD	EO	P or C	PNP, cerebellar ataxia, tremor, dementia, amyotrophy of small hand muscles, *pes cavus*
SPG32	SPG32	AR	EO	C	Mental retardation, pontine dysraphism, TCC

SPG33	ZFYVE27	AD	AO	C	Pes equines
SPG34	SPG34	X-linked	VO	P	-
SPG35	FA2H	AR	EO	P or C	Cognitive decline, epilepsy
SPG36	SPG36	AD	VO	C	Sensory polyneuropathy
SPG37	SPG37	AD	VO	P	-
SPG38	SPG38	AD	VO	C	Amyotrophy of small hand muscles, PNP
SPG39	PNPLA6	AR	EO	C	Distal wasting in all four limbs, axonal neuropathy
SPG40	-	AD	AO	P or C	Hyperreflexia of upper limbs, cognitive impairment
SPG41	SPG41	AD	TO	P	-
SPG42	SLC33A1	AD	VO	P	-
SPG43	C19orf12	AR	VO	C	Amyotrophy of small hand muscles, bilateral optic atrophy, axonal sensory and motor neuropathy
SPG44	GJC2	AR	AO	C	Mild cognitive impairment, moderate cerebellar dysfunction, dysarthria, WMLs. *pes cavus*, TCC, scoliosis, upper limb involvement
SPG45	SPG45	AR	EO	C	Mental retardation, pendular nystagmus, optic atrophy
SPG46	GBA2	AR	EO	C	Mental impairment, cataract, cerebellar atrophy, TCC, hypogonadism in males
SPG47	AP4B1	AR	EO	C	Periventricular WMLs, TCC, microcephaly, epilepsy, waddling gait, joint hyperlaxity
SPG48	AP5Z1	AR	AO	P or C	Spinal cord hyperintensities
SPG49	TECPR2	AR	EO	P or C	TCC, cognitive decline, upper limbs involvement, basal-ganglia calcification. dystonic postures, WMLs Optic atrophy, PNP
SPG50	AP4M1	AR	EO	C	Tetraplegic cerebral palsy, mental retardation, reduction of cerebral white matter, atrophy of the cerebellum

SPG51	AP4E1	AR	EO	C	Microcephaly, growth and intellectual retardation
SPG52	AP4S1	AR	EO	C	Delayed speech, stereotypic laughter, growth retardation
SPG53	VPS37A	AR	EO	C	Spasticity in upper extremities, delays in cognition and speech, kyphosis, pectus carinatum (pigeon chest), hypertrichosis
SPG54	DDHD2	AR	EO	C	Mental retardation, strabismus, dysarthria, dysphagia, optic-nerve hypoplasia, short stature, TCC, laterally deviated feet, WMLs
SPG55	C12orf65	AR	EO	C	Optic atrophy, neuropathy, club foot
SPG56	CYP2U1	AR	EO	C	Delayed psychomotor development, mental retardation, TCC, cerebral and cerebellar dysfunction, dysmorphic features
SPG57	TFG	AR	EO	C	Optic atrophy, PNP
SPG58	KIF1C	AR	EO	P or C	Chorea, myoclonus, ataxia, hypodontia, deafness, short stature, pes planus, ptosis, developmental delay, mental retardation, WMLs
SPG59	USP8	AR	EO	C	Nystagmus, borderline intelligence
SPG60	WDR48	AR	EO	C	Neuropathy in lower limbs, nystagmus
SPG61	ARL6IP1	AR	EO	C	Loss of terminal digits, acromutilation, PNP
SPG62	ERLIN1	AR	EO	P	-
SPG63	AMPD2	AR	EO	C	TCC, WMLs, underweight, short stature
SPG64	ENTPD1	AR	EO	C	Club foot, aggressiveness, delayed puberty, microcephaly, borderline intelligence
SPG65	NT5C2	AR	EO	P or C	TCC, defective myelination, small bilateral cystic occipital leukomalacia, learning disability, club foot
SPG66	ARSI	AR	EO	C	Corpus callosum and cerebellar hypoplasia, colpocephaly, borderline intelligence, PNP, club foot
SPG67	PGAP1	AR	EO	C	Distended abdomen, borderline intelligence, ACC, vermis hypoplasia, defective myelination
SPG68	FLRT1	AR	EO	C	Nystagmus, optic atrophy, PNP, amyotrophy, foot drop

SPG69	RAB3GAP2	AR	EO	C	Intellectual disability, deafness, cataract
SPG70	MARS	AR	EO	C	Scoliosis, bilateral Achilles contracture, borderline intelligence, nephrotic syndrome
SPG71	ZFR	AR	EO	C	TCC
SPG72	REEP2	AR	EO	P	-
SPG73	CPT1C	AD	EO	P	-
SPG74	IBA57	AR	EO	C	Optic atrophy and reduced visual acuity
SPG75	MAG	AR	EO	C	Mental retardation, cerebellar ataxia, amyotrophy
SPG76	CAPN1	AR	VO	C	Upper limb involvement, foot deformities and dysarthria
SPG77	FARS2	AR	EO	P	-
SPG78	ATP13A2	AR	AO	C	Mild cognitive impairment, dysarthria, oculomotor disturbances, cerebellar atrophy
-	AFG3L2	AR	EO	C	Significantly impaired ambulation, cerebellar ataxia, oculomotor apraxia, dystonia, and myoclonic epilepsy
-	ALS2	AR	EO	C	Late dysphagia, *pes cavus*, and slow saccadic eye movement.
-	BICD2	AD	EO	P	-
-	CCT5	AR	VO	C	Severe axonal sensory neuropathy with marked distal pan-modal sensory loss, mutilating acropathy, and vagal hyperactivity
-	ELOVL4	AR	EO	C	Mental retardation, ichthyosis
-	EXOSC3	AR	EO	C	Mild cognitive impairment, mild cerebellar ataxia, strabismus, short stature, distal amyotrophy, tongue atrophy, adducted thumbs, and talipes valgus.
-	RETREG1	AR	EO	C	Painless axonal neuropathy, progressive mutilating ulcerations in hands and feet, hyperhidrosis, urinary incontinence
-	GAD1	AR	EO	C	Mental retardation, occasional seizures, microcephaly, multiple contractures, and scoliosis

-	GJA1	AD	VO	C	Craniofacial and limb dysmorphism, deafness and cardiac abnormalities
-	HACE1	AR	EO	C	Seizures, speech delay, ocular abnormalities, foot deformities
-	IFIH1	AD	EO	P	-
-	KANK1	-	EO	C	Mental retardation
-	KCNA2	AD	EO	C	Mild cognitive defects
-	KIDINS220	AD	TO	C	Intellectual disability, nystagmus and obesity
-	LYST	AR	AO	C	PNP, cerebellar ataxia
-	ATP6	Mitochondrial	AO	C	Diabetes mellitus, hypertrophic cardiomyopathy, supraventricular arrhythmia, cerebellar syndrome
-	ND4	Mitochondrial	AO	C	Visual loss (optic atrophy or other retinal changes)
-	TRNI	Mitochondrial	EO	C	Cerebellar ataxia, mental retardation, chronic progressive external ophthalmoplegia, cardiomyopathy, hearing loss, diabetes
-	COX3	Mitochondrial	EO	C	Mental retardation, ophthalmoplegia, severe lactic acidosis, Leigh-like features, COX deficiency
-	TPP1	AR	EO	C	Bulbar palsy, dystonic neck posturing and also severe cognitive problems
-	VCP	AD	AO	C	Frontotemporal dementia

Table 1.2. List of human HSP inheritance and clinical features. HSP genes are listed by spastic gait disease-loci (SPG), genes not part of the SPG classification system are listed alphabetically. Inheritance and clinical features (including age of onset, clinical phenotype) were obtained from literature and online resources, such as OMIM (http://www.ncbi.nlm.nih.gov/omim/).
Abbreviations: ACC = agenesis corpus callosum; AD = autosomal dominant; AO = adult onset; AR = autosomal recessive; C = complicated; EO = early onset (infancy); IGE = idiopathic generalised epilepsy; P = pure; PNP = polyneuropathy; TCC = thin corpus callosum; TO = teenage onset; VO = variable onset; WMLs = white matter lesions. Adapted from Lo Giudice *et al.*, 2014; de Souza *et al.*, 2016.

Autosomal Recessive (AR) HSPs

So far, 63 genetic SPG loci and 56 genes have been identified for AR-HSP, with 7 AR-HSP loci, namely SPG14 (Vazza *et al.*, 2000), SPG23 (Blumen *et al.*, 2003), SPG24 (Hodgkinson *et al.*, 2002), SPG25 (Zortea *et al.*, 2002), SPG27 (Meijer *et al.*, 2004; Ribai *et al.*, 2006), SPG32 (Stevanin *et al.*, 2007) and SPG45 (Dursun *et al.*, 2009), with gene identity still unknown (Table 1.1 and 1.2).

X-linked (XL) HSPs

Only 5 X-linked SPG loci (SPG1, SPG2, SPG16, SPG22 and SPG34), and 3 corresponding genes (L1CAM, PLP1 and SLC16A2) have been identified to date. For SPG16 (Steinmüller *et al.*, 1997) and SPG34 (Macedo-Souza *et al.*, 2008), gene identity is still unknown (Table 1.1 and 1.2).

1.3 Epidemiology

There are several earlier epidemiological studies, with the reported prevalence of HSP varying considerably between studies (Polo *et al.*, 1991; McMonagle, Webb and Hutchinson, 2002). This discrepancy in part reflects the diverse genetic make-up of the populations, in combination with the diagnostic criteria and epidemiological methodologies employed. Also, for many areas of the world, prevalence rates are as yet unknown (McDermott *et al.*, 2000; Ruano *et al.*, 2014). However, after employing similar criteria and methodologies, the prevalence of HSP was estimated at 3-10 cases per 100,000 population in Europe (Filla *et al.*, 1992; Leone *et al.*, 1995; McDermott *et al.*, 2000). More recently, to gain a better understanding of the global distribution and prevalence of HSP, a systematic review was carried out by Ruano et al. (2014) of all the epidemiological studies published after 1983, following the wide use of Harding's diagnostic and classification criteria for HSP (Harding, 1983). Using predefined methodological parameters, the prevalence estimated was 1.8/100,000 for both autosomal dominant and autosomal recessive HSP (Ruano *et al.*, 2014).

1.4 Diagnosis

The diagnosis of HSP is based on several factors, which include: (i) a clinical history identifying characteristic progressive spastic paraparesis in a pure or complicated form (associated with additional neurological or non-neurological manifestations); (ii) neurological examination demonstrating corticospinal tract deficits; (iii) family history to determine type of transmission (autosomal dominant, recessive or X-linked recessive, or maternal inheritance); (iv) identification of genetic mutation in a *locus* associated with a previously described HSP phenotype; and (v) exclusion of any other differential diagnoses (de Souza *et al.*, 2016).

The diagnosis of 'complicated' forms of HSP is often more difficult due to the additional neurological and non-neurological features typically associated with such forms, which may precede the onset of spastic paraparesis (Lo Giudice *et al.*, 2014; Klebe, Stevanin and Depienne, 2015).

1.5 Functional Modules

The identification of disease-loci/genes implicated in HSPs has been critical to our understanding of the clinical and pathological features of this group of disorders, and has also improved our understanding of the cellular processes required for axonal maintenance or degeneration (Blackstone, O'Kane and Reid, 2011). HSP forms and putative protein function for each HSP gene product are summarised in Table 1.3. Although large numbers of HSP-associated genes have been identified, and continue to be identified, the genetic heterogeneity of HSPs has in fact been advantageous in identifying common disease-related functional modules and cellular pathways (see Figure 1.1), through the recognition that encoded proteins function in similar biological pathways, or perform similar functions (Soderblom and Blackstone, 2006; Blackstone, 2012; Klebe, Stevanin and Depienne, 2015). The same protein is often implicated in several of the functional modules highlighted (Lo Giudice *et al.*, 2014). Identification of these functional modules likely indicates their importance in corticospinal tract axon development and maintenance (Blackstone, 2012).

Table 1.3

Disease/*Gene*	Protein name (UniProt)	Cellular function	Reference
SPG1/*L1CAM*	Neural cell adhesion molecule L1	Neuronal cell adhesion and signalling, Neurite outgrowth	Jouet et al., 1994; Finsterer et al., 2012
SPG2/*PLP1*	Myelin proteolipid protein	Myelination and axonal survival	Saugier-Veber et al., 1994
SPG3A/*ATL1*	Atlastin-1	Membrane trafficking, ER and Golgi morphogenesis and BMP signalling	Park et al., 2010; Guelly et al., 2011
SPG4/*SPAST*	Spastin (M1 and M87 isoforms)	Microtubule dynamics, ER morphogenesis, endosomal trafficking, BMP signalling	Hazan et al., 1999; Solowska et al., 2010
SPG5A/*CYP7B1*	25-hydroxycholesterol 7-alpha-hydroxylase	Cholesterol metabolism in brain	Tsaousidou et al., 2008; Finsterer et al., 2012
SPG6/*NIPA1*	Magnesium transporter NIPA1	Endosomal/ER morphogenesis, protein folding, Mg^{2+} transport and BMP signalling	Rainier et al., 2003; Tsang et al., 2009
SPG7/*PGN*	Paraplegin	Mitochondrial protease, ribosome maturation	Casari et al., 1998; Tzoulis et al., 2008
SPG8/*WASHC5*	WASH complex subunit strumpellin	Endosomal trafficking, cytoskeletal (actin) regulation, protein aggregation	Valdmanis et al., 2007; Derivery et al., 2009
SPG9/*ALDH18A1*	Delta-1-pyrroline-5-carboxylate synthase	Ornithine metabolism	Coutelier et al., 2015; Sgobbi de Souza et al., 2017
SPG10/*KIF5A*	Kinesin heavy chain isoform 5A	Microtubule-based motor protein	Ebbing et al., 2008; Crimella et al., 2011
SPG11	Spatacsin	Autophagy, Endosomal trafficking	Stevanin et al., 2007; Murmu et al., 2011; Ebrahimi-Fakhari et al., 2016
SPG12/*RTN2*	Reticulon-2	ER morphogenesis	Montenegro et al., 2012
SPG13/*HSPD1*	60 kDa heat shock protein, mitochondrial	Mitochondrial chaperone – protein folding and assembly	Hansen et al., 2002; Anderson et al., 2011
SPG14	-	-	-

SPG15/*ZFYVE26*	Zinc finger FYVE domain-containing protein 26	Endosomal trafficking, cytokinesis, autophagy	Hanein et al., 2008; Sagona et al., 2010; Murmu et al., 2011
SPG16	-	-	-
SPG17/*BSCL2*	Seipin	Lipid droplet biogenesis, ER stress response	Windpassinger et al., 2004; Lundin et al., 2006
SPG18/*ERLIN2*	Erlin-2	ERAD regulation	Pearce et al., 2007; Huber et al., 2013
SPG19	-	-	-
SPG20	Spartin	Endosomal trafficking, Lipid droplet turnover, Mitochondrial regulation, BMP signalling, cytokinesis	Patel et al., 2002; Edwards et al., 2009; Finsterer et al., 2012
SPG21	Maspardin	Endosomal trafficking and sorting	Simpson et al., 2003
SPG22/*SLC16A2*	Monocarboxylate transporter 8	Thyroid hormone transporter (axon development)	Friesema et al., 2003; Vaurs-Barriere et al., 2009; Boccone et al., 2010
SPG23	-	-	-
SPG24	-	-	-
SPG25	-	-	-
SPG26/*B4GALNT1*	Beta-1,4 N-acetylgalactosaminyltransferase 1	Ganglioside metabolism	Boukhris et al., 2013
SPG27	-	-	-
SPG28/*DDHD1*	Phospholipase DDHD1	Fatty acid and/or phospholipid metabolism	Tesson et al., 2012
SPG29	-	-	-
SPG30/*KIF1A*	Kinesin-like protein KIF1A	Microtubule-based motor protein (anterograde transport)	Erlich et al., 2011; Finsterer et al., 2012

SPG31/*REEP1*	Receptor expression-enhancing protein 1	ER morphogenesis and ER-microtubule interaction	Züchner et al., 2006; Park et al., 2010
SPG32	-	-	-
SPG33/*ZFYVE27*	Protrudin	ER morphogenesis	Chang et al., 2013
SPG34	-	-	-
SPG35/*FA2H*	Fatty acid 2-hydroxylase	Sphingolipid synthesis	Alderson et al., 2004; Zöller et al., 2008 Cao et al., 2013
SPG36	-	-	-
SPG37	-	-	-
SPG38	-	-	-
SPG39/*PNPLA6*	Neuropathy target esterase	Axonal maintenance, phospholipid homeostasis	Rainier et al., 2008; Hein et al., 2010
SPG40	-	-	-
SPG41	-	-	-
SPG42/SLC33A1	Acetyl-coenzyme A transporter 1	Acetyl-CoA transporter	Hirabayashi et al., 2004
SPG43/*C19orf12*	Protein C19orf12	Function unknown - mitochondrial and ER membrane localisation	Fink et al., 2013
SPG44/*GJC2*	Gap junction gamma-2 protein	Intracellular gap junction channel	Orthmann-Murphy et al., 2007; Orthmann-Murphy et al., 2009
SPG45	-	-	-
SPG46/*GBA2*	Non-lysosomal glucosylceramidase	Ganglioside metabolism	Hammer et al., 2013
SPG47/*AP4B1*	AP-4 complex subunit beta-1	Endosomal trafficking	Abou Jamra et al., 2011

SPG48/*AP5Z1*	AP-5 complex subunit zeta-1	Helicase that repairs DNA double-strand break, endosomal trafficking	Slabicki et al., 2010; Hirst et al., 2011
SPG49/*TECPR2*	Tectonin beta-propeller repeat-containing protein 2	Autophagy	Oz-Levi et al., 2012
SPG50/*AP4M1*	AP-4 complex subunit mu-1	Endosomal trafficking	Abou Jamra et al., 2011
SPG51/*AP4E1*	AP-4 complex subunit epsilon-1	Endosomal trafficking	Abou Jamra et al., 2011
SPG52/*AP4S1*	AP-4 complex subunit sigma-1	Endosomal trafficking	Abou Jamra et al., 2011
SPG53/*VPS37A*	Vacuolar protein sorting-associated protein 37A	Endosomal trafficking	Zivony-Elboum et al., 2012
SPG54/*DDHD2*	Phospholipase DDHD2	Phospholipid metabolism (phospholipase)	Sato et al., 2010; Schuurs-Hoeijmakers et al., 2012
SPG55/*C12orf65*	Probable peptide chain release factor C12orf65, mitochondrial	Peptide chain termination in mitochondrial translation machinery	Antonicka et al., 2010; Shimazaki et al., 2012
SPG56/*CYP2U1*	Cytochrome P450 2U1	Lipid metabolism (fatty acid hydroxylation)	Chuang et al., 2004
SPG57/*TFG*	Protein TFG	Endosomal trafficking, ER shaping	Witte et al., 2011; Beetz et al., 2013
SPG58/*KIF1C*	Kinesin-like protein KIF1C	Microtubule-based motor protein (retrograde Golgi to ER transport)	Dorner et al., 1998
SPG59/*USP8*	Ubiquitin carboxyl-terminal hydrolase 8	Deubiquitinating enzyme, endosomal trafficking.	Row et al., 2006; Coyne and Wing, 2016
SPG60/*WDR48*	WD repeat-containing protein 48	Regulator of deubiquitination	Cohn et al., 2007; Novarino et al., 2014
SPG61/*ARL6IP1*	ADP-ribosylation factor-like protein 6-interacting protein 1	ER morphogenesis, protein transport	Yamamoto et al., 2014; Novarino et al., 2014
SPG62/*ERLIN1*	Erlin-1	ERAD	Pearce et al., 2009; Novarino et al., 2014
SPG63/*AMPD2*	AMP deaminase 2	Purine nucleotide metabolism	Akizu et al., 2013

SPG64/*ENTPD1*	Ectonucleoside triphosphate diphosphohydrolase 1	Nucleotide metabolism to regulate purinergic transmission	Munkonda et al., 2007
SPG65/*NT5C2*	Cytosolic purine 5'-nucleotidase	Purine/pyrimidine nucleotide metabolism	Oka et al., 1994; Dursun et al., 2009
SPG66/*ARSI*	Arylsulfatase I	Hormone biosynthesis	Sardiello et al., 2005
SPG67/*PGAP1*	GPI inositol-deacylase	GPI biosynthesis	Tanaka et al., 2004
SPG68/*FLRT1*	Leucine-rich repeat transmembrane protein FLRT1	Neurite outgrowth, Cell-cell adhesion, Receptor signalling	Lacy et al., 1999; Novarino et al., 2014
SPG69/*RAB3GAP2*	Rab3 GTPase-activating protein non-catalytic subunit	Exocytosis of neurotransmitters and hormones	Nagano et al., 1998; Aligianis et al., 2006
SPG70/*MARS*	Methionine--tRNA ligase, cytoplasmic	Nucleotide metabolism	Deniziaki and Barciszewski, 2001
SPG71/*ZFR*	Zinc finger RNA-binding protein	Neuron development/synapse related	Elvira et al., 2006
SPG72/*REEP2*	Receptor expression-enhancing protein 2	ER morphogenesis	Esteves et al., 2014
SPG73/*CPT1C*	Carnitine O-palmitoyltransferase 1, brain isoform	Lipid (ceramide) metabolism	Carrasco et al., 2013
SPG74/*IBA57*	Putative transferase CAF17, mitochondrial	Maturation of mitochondrial proteins involved in the iron-sulphur cluster assembly pathway	Sheftel et al., 2012
SPG75/*MAG*	Myelin-associated glycoprotein	Cell adhesion molecule involved in myelin maintenance	Lossos et al., 2015
SPG76/*CAPN1*	Calpain-1 catalytic subunit	Calcium-regulated non-lysosomal protease involved in cytoskeletal remodelling	Ohno et al., 1990
SPG77/*FARS2*	Phenylalanine--tRNA ligase, mitochondrial	Mitochondrial phenylalanyl transfer RNA (tRNA) synthetase	Bullard et al., 1999
SPG78/*ATP13A2*	Probable cation-transporting ATPase 13A2	Cation homeostasis and maintenance of neuronal integrity, lysosomal and mitochondrial maintenance	Ramonet et al., 2012; Estrada-Cuzcano et al., 2017
AFG3L2	AFG3-like protein 2	Protease essential for axonal and neuronal development	Koppen et al., 2007
ALS2	Alsin	Endosomal trafficking	Eymard-Pierre et al., 2002;

			Hadano et al., 2006;
BICD2	Protein bicaudal D homolog 2	Motor adaptor protein	Oates et al., 2013 Neveling et al., 2013
CCT5	T-complex protein 1 subunit epsilon	Molecular chaperone - protein folding and assembly	Liou and Willison, 1997
ELOVL4	Elongation of very long chain fatty acids protein 4	Lipid metabolism	Agbaga et al., 2008
EXOSC3	Exosome complex component RRP40	Non-catalytic component of RNA exosome complex	Brouwer et al., 2001
FAM134B	Reticulophagy receptor FAM134B	Autophagy (ER-phagy), ER morphogenesis	Khaminets et al., 2015
GAD1	Glutamate decarboxylase 1	Catalyses production of GABA	Fenalti et al., 2007
GJA1	Gap junction alpha-1 protein	Intracellular gap junction channel protein	De Block et al., 2013
HACE1	E3 ubiquitin-protein ligase HACE1	Regulates GTPase activity and Golgi membrane dynamics	Anglesio et al., 2004; Hollstein et al., 2015
IFIH1	Interferon-induced helicase C domain-containing protein 1	Innate immune receptor	Rice et al., 2014
KANK1	KN motif and ankyrin repeat domain-containing protein 1	Regulates cytoskeleton formation	Roy et al., 2009
KCNA2	Potassium voltage-gated channel subfamily A member 2	Neuron development/synapse related	Sybre et al., 2015; Helbig et al., 2016
KIDINS220	Kinase D-interacting substrate of 220 kDa	Neuron development/synapse related	Iglesias et al., 2000; Arevalo et al., 2004; Josifova et al., 2016
LYST	Lysosomal-trafficking regulator	Endosomal trafficking	Shimazaki et al., 2014
MT-ATP6	ATP synthase subunit a	Mitochondrial function	Carrozzo et al., 2006; Vazquez-Memije et al., 2009; Sgobbi de Souza et al., 2017
MT-ND4	NADH-ubiquinone oxidoreductase chain 4	Mitochondrial function	Clarencon et al., 2006, Sgobbi de Souza et al., 2016

MT-TI	Mitochondrially encoded tRNA isoleucine	Mitochondrial function	Corona et al., 2002; Sgobbi de Souza et al., 2017
MT-CO3	Cytochrome c oxidase subunit 3	Mitochondrial function	Tiranti et al., 2000, Sgobbi de Souza et al., 2016
TPP1	Tripeptidyl-peptidase 1	Lysosomal serine peptidase	Golabeck et al., 2003
VCP	Transitional endoplasmic reticulum ATPase	Autophagy, endosomal trafficking, ERAD	Wojcik et al., 2006; DeLaBarre et al., 2006; Tresse et al., 2010; Kirchner et al., 2013

Table 1.3. Putative function of each HSP. HSP genes are listed by spastic gait disease-loci (SPG), genes not part of the SPG classification system are listed alphabetically. HSP forms and putative protein function of each HSP gene product were obtained from literature.
Abbreviations: BMP = bone morphogenetic protein; ERAD = ER-associated degradation. Adapted from Blackstone, 2012; Lo Giudice *et al.*, 2014; Noreau, Dion and Rouleau, 2014.

Figure 1.1

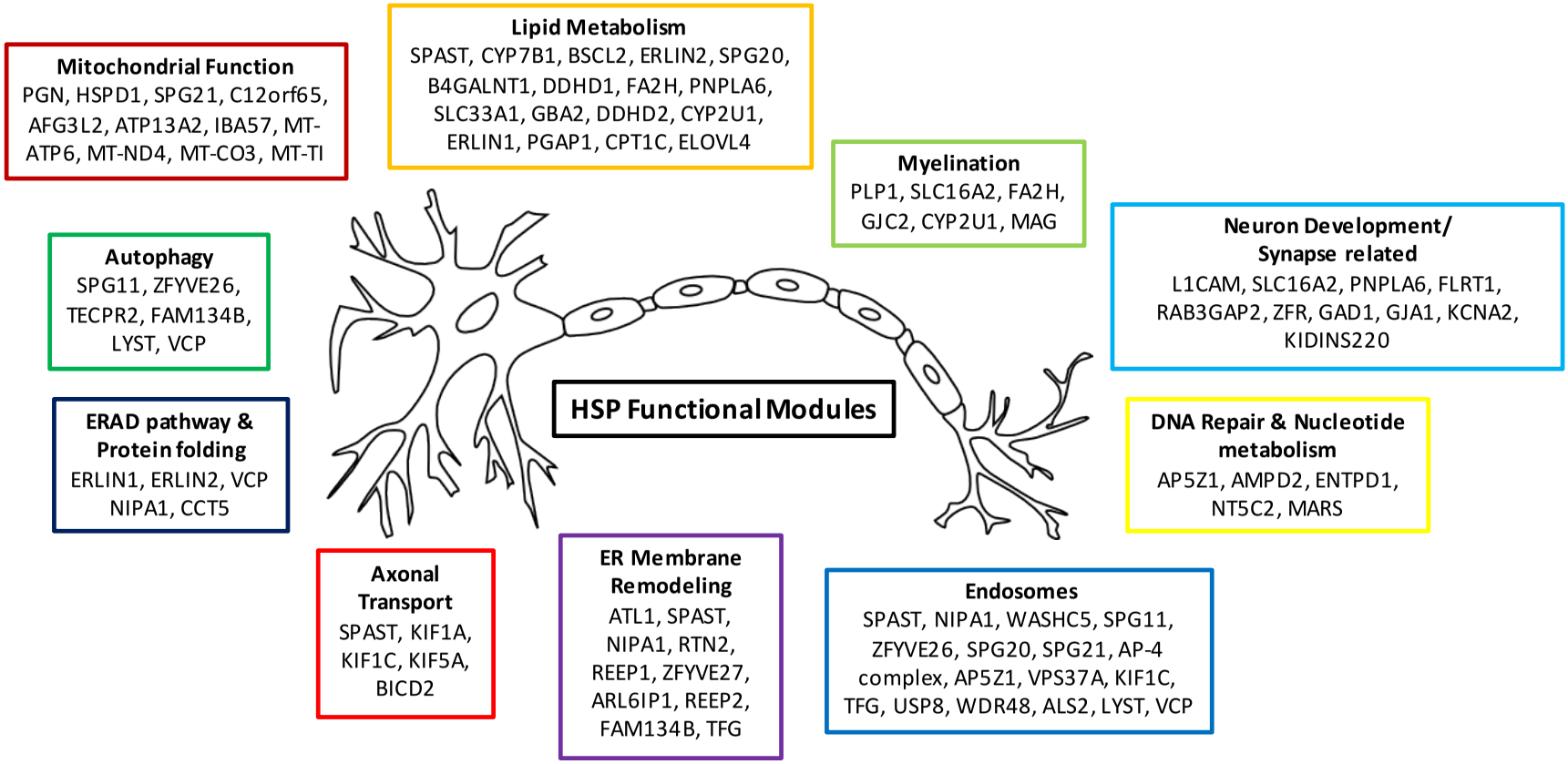

Figure 1.1. Common functional modules identified in HSP seed proteins. Analysis of HSP seed proteins has led to the identification of some common pathogenic themes which link sets of HSP proteins to different function modules. The schematic representation of a corticospinal motor neuron, is annotated to show the major HSP functional modules identified to date. Adapted from Blackstone, 2012; Lo Giudice *et al.*, 2014.

1.5.1 Axon development/pathfinding

In order to form a functional nervous system, neurons extend axons from the cell body (soma) toward specific target cells (axon outgrowth) to form synaptic connections. This neural network is crucial to the complex functioning of the nervous system, and hence both intrinsic and extrinsic factors, or molecular cues, are used to guide and control axonal outgrowth and direction (Chilton, 2006).

Mutations in the *L1 cell adhesion molecule* (*L1CAM*) gene causes the rare X-linked recessive spastic paraplegia type 1 (SPG1) (Jouet *et al.*, 1994). This gene encodes the neuronal cell adhesion molecule L1, an axonal glycoprotein of the immunoglobulin (Ig) superfamily involved in cell-to-cell adhesion processes in the CNS. L1CAM is an axonal guidance molecule, and plays an important role in the development of the nervous system, promoting neuronal migration, axon outgrowth and synapse formation (Kenwrick, Watkins and Angelis, 2000; Maness and Schachner, 2007). These important cellular events are facilitated by interactions with other L1CAM molecules and extracellular ligands, including other cell adhesion molecules (CAMs), integrins and proteoglycans, as well as intracellular proteins (Blackstone, 2012; Lo Giudice *et al.*, 2014).

Mutations in the *fibronectin leucine-rich transmembrane protein 1* (*FLRT1*) gene cause autosomal recessive spastic paraplegia type 68 (SPG68) (Novarino *et al.*, 2014). This gene encodes a member of the fibronectin leucine rich transmembrane (FLRT) proteins, which are involved in cell adhesion and receptor signalling (Lacy *et al.*, 1999; Wheldon *et al.*, 2010).

Mutations in the *RAB3 GTPase activating protein subunit 2* (*RAB3GAP2*) gene cause autosomal recessive spastic paraplegia type 69 (SPG69) (Novarino *et al.*, 2014). This gene encodes the 150-kD non-catalytic subunit of the RAB3GAP protein, one of three proteins that regulate the activity of the RAB3 protein family, which are involved in the regulated exocytosis of neurotransmitters and hormones (Aligianis *et al.*, 2006).

Mutations in the *SLC16A2* gene cause X-linked hereditary spastic paraplegia (HSP) type 22 (SPG22), and this gene encodes the monocarboxylate transporter 8 (MCT8) protein (Schwartz *et al.*, 2005), which is necessary for tri-iodo-thyronine transport into neurons, and axonal pathfinding (Blackstone, O'Kane and Reid, 2011).

1.5.2 Myelination

The myelin sheath is a highly extended, specialised plasma membrane that wraps around the nerve axon, in a process known as myelination (Raine, 1984). The membranes of the myelin sheath originate from Schwann cells in the peripheral nervous system (PNS), and oligodendroglial cells in the central nervous system (CNS) (Bunge, 1968). The myelin sheath acts as an electrical insulator, increasing axonal conduction speed which allows fast transmission of electrical signals over large distances (Fields, 2008).

Demyelination is the loss or destruction of the myelin sheath, whilst the axon remains relatively unaffected. This is caused by diseases that damage myelin sheaths directly or the cells that form them, and is typically seen in neurodegenerative disorders such as multiple sclerosis (MS), one of the most well-known demyelinating diseases (Love, 2006; Streitberger *et al.*, 2012). Myelin defects can be caused by several mechanisms including inflammatory, metabolic or genetic abnormalities, leading to nerve dysfunction from the slowed or blocked signal conduction, resulting in impaired information relay between the brain and body or within the brain (Love, 2006). Dysmyelination on the other hand, is used to describe the defective structure and function of myelin sheaths (Cheon *et al.*, 2002). Dysmyelinating diseases are characterised by abnormal myelination, which often occur as a result of hereditary mutations that affect myelin biosynthesis and formation, and include the missense mutations in the human *proteolipid protein* (*PLP1*) gene (Krämer-Albers *et al.*, 2006).

One of the main myelination defects associated with HSP is known to occur as a result of *proteolipid protein* (*PLP1*) gene mutation. This gene encodes the primary constituent of myelin in the CNS, proteolipid protein 1 (PLP1) and the spliced variant

DM20 (Weimbs and Stoffel, 1992), which are both integral membrane proteins involved in the compaction, stabilisation and maintenance of the myelin sheath (Jahn, Tenzer and Werner, 2009). The variability of genetic mutations results in a wide clinical spectrum of *PLP1*-related disorders, which include both pure and complicated forms of spastic paraplegia type 2 (SPG2), as well as the more severe Pelizaeus–Merzbacher disease (PMD), which typically involves DM20 abnormalities (Inoue, 2005). SPG2 is an X-linked recessive PLP1-related disorder characterised by dysmyelination of the central nervous system, caused by a variety of mutations in the PLP1 gene (Noetzli *et al.*, 2014).

Mutations in the *myelin-associated glycoprotein* (*MAG*) gene cause severe autosomal recessive spastic paraplegia type 75 (SPG75) (Novarino *et al.*, 2014). This gene encodes a component of myelin that belongs to the immunoglobulin (Ig) superfamily of proteins and is involved in myelin maintenance and glial-axon interactions, where it is enriched in myelinating glial cells (Lopez, 2014; Lossos et al., 2015).

Mutations in the *fatty acid 2-hydroxylase (FA2H*) gene cause severe autosomal recessive spastic paraplegia type 35 (SPG35) (Dick et al., 2008). This gene encodes a fatty acid 2-hydroxylase hydroxylase (FA2H), an integral ER membrane protein which catalyses the 2-hydroxylation of the major myelin lipids galactosylceramides (GalCer) and sulfatides (Uchida *et al.*, 2007; Lamari *et al.*, 2013). FA2H is required for the initial step in the incorporation of α-hydroxylated GalCer into myelin, which use free fatty acids as substrates (Alderson *et al.*, 2004; Edvardson *et al.*, 2008). It has been shown to be required for the long-term maintenance of myelin (Zoller *et al.*, 2008).

Mutations in the *gap junction gamma-2* (*GJC2/GJA12*) gene which encodes the gap junction protein connexin47 (Cx47) was originally associated with an early-onset dysmyelinating disorder, Pelizaeus-Merzbacher-like disease (PMLD) of the CNS (Uhlenberg *et al.*, 2004; Salviati *et al.*, 2007; Henneke *et al.*, 2008). However, a novel mutation in *GJC2* (Cx47) was associated with causing complicated spastic paraplegia type 44 (SPG44) in which it was suggested that Cx47/Cx43 channels between astrocytes and oligodendrocytes were disrupted resulting in cell-cell communication

impairment, affecting maintenance of CNS myelin (Orthmann-Murphy *et al.*, 2009). Additional PMLD disorders also associated with HSP, include mutations in the *solute carrier family 16 member 2* (*SLC16A2*) gene which causes X-linked hereditary spastic paraplegia (HSP) type 22 (SPG22) (Vaurs-Barrière *et al.*, 2009), and more recently mutations in the *CYP2U1* gene which causes the autosomal recessive hereditary spastic paraplegia (HSP) type 56 (SPG56) (Minase *et al.*, 2017).

1.5.3 ER membrane modelling

The endoplasmic reticulum (ER) is a multifunctional organelle present in all eukaryotic cells, primarily involved in the synthesis, modification, quality control and transport of integral membrane and secreted proteins. It is also critical for sterol synthesis, lipid synthesis and distribution, carbohydrate metabolism and calcium storage, release and signalling (Clapham, 2007; Fagone and Jackowski, 2009; Braakman and Hebert, 2013). The ER is the largest and one of the most distinctive organelles in the cell. It is a continuous, membranous system that includes the well-defined morphologies of the nuclear envelope, peripheral flat sheet-like structures studded with ribosomes, and a network of interconnected, branched tubules, all of which enable the diverse functions of the ER (Blackstone, 2012; Schwarz and Blower, 2016). The distinctive shape and distribution of the ER architecture is regulated by several integral membrane proteins, as well as dynamic interactions with the cytoskeleton and other organelles (Schwarz and Blower, 2016). These include, (i) ER-shaping proteins of the DP1/Yop1p and reticulon families, which have a characteristic hydrophobic domain, which is thought to sit in the ER membrane as a hairpin loop, occupying more space in the outer leaflet of the phospholipid bilayer, thereby generating membrane curvature through 'hydrophobic wedging' - critical to the formation and stabilisation of high membrane curvature found at ER tubules and sheet edges (Collins, 2006; Voeltz *et al.*, 2006; Hu *et al.*, 2008); (ii) the atlastin family of GTPases, which also contain a hairpin domain, are required for correct formation of the tubular ER network, promoting the formation of three-way junctions through homotypic fusion of ER tubules (Hu *et al.*, 2009); (iii) microtubule cytoskeletal regulators required for distribution of ER network (Park *et al.*, 2010), including the

microtubule-severing ATPase spastin, which also localises to the ER and has a hairpin domain allowing direct interaction with atlastins (Connell *et al.*, 2009; Park *et al.*, 2010), particularly important for neurons (Renvoisé and Blackstone, 2010) and finally, (iv) components of the early secretory pathway which control vesicle biogenesis (Renvoisé and Blackstone, 2010; Zanetti *et al.*, 2011).

In neurons, the ER is particularly important during the expansion of polarised membrane which occurs during axon and dendrite formation (Pfenninger, 2009; Renvoisé and Blackstone, 2010). It also has an important role as an intracellular calcium store, tightly integrated with pre- and post-synaptic signalling mechanisms (Collin, Marty and Llano, 2005; Verkhratsky, 2005). ER morphology changes have been linked to synaptic organisation (Spacek and Harris, 1997).

Mutations that affect the endoplasmic reticulum (ER) architecture are common in HSP patients, with over 50 % of patients harbouring pathogenic mutations in 1 of 3 genes ATL1 (SPG3A), SPAST (SPG4) and REEP1 (SPG31) encoding proteins (spastin, atlastin-1 and REEP1) involved in ER membrane shaping and re-modelling events (Salinas *et al.*, 2008; Blackstone, O'Kane and Reid, 2011). Mutations also occur in other, less common ER-shaping proteins RTN2 (SPG12) and REEP2 (SPG72) which further support a role for abnormal ER morphogenesis in the pathogenesis of HSP.

Mutations in the *ATL1* gene cause autosomal dominant spastic paraplegia type 3A (SPG3A) (Zhao *et al.*, 2001). This gene encodes atlastin-1, a member of the dynamin superfamily of GTPases (Zhao *et al.*, 2001; Rismanchi *et al.*, 2008). Atlastin-1 GTPase is predominantly localised to the tubular ER, where it mediates homotypic fusion of ER membranes, promoting the formation of three-way junctions (Hu *et al.*, 2009; Orso *et al.*, 2009). Atlastin-1 GTPase can also interact directly with the ATP-dependent microtubule-severing protein, spastin (Evans *et al.*, 2006; Sanderson *et al.*, 2006), and the ER tubule-shaping reticulons and DP1/Yop1p/REEP protein family, through hydrophobic hairpin domains within the tubular ER (Hu *et al.*, 2008, 2009), linking membrane and cytoskeletal remodelling proteins (Voeltz *et al.*, 2006; Hu *et*

al., 2008). This provides evidence to suggest a role for atlastins in the formation and morphology of an interconnected tubular ER network.

Mutations in the *SPAST* gene cause autosomal dominant spastic paraplegia type 4 (SPG4), the most common cause of autosomal dominant HSP. SPAST encodes an ATP-dependent microtubule-severing protein, spastin (Hazan *et al.*, 1999). Spastin is a member of the AAA (ATPase Associated with diverse cellular Activities) protein family with various functions including roles in microtubule dynamics (Errico, Ballabio and Rugarli, 2002) and membrane trafficking (Reid *et al.*, 2005). The two translation initiation codons in SPAST allows the synthesis of two isoforms: full-length M1, and the shorter isoform, M87 which lacks the first 86 amino acids (Claudiani *et al.*, 2005). Spastin consists of an N-terminal microtubule-interacting and endosomal-trafficking (MIT) domain, a microtubule-binding domain (MTBD) and the C-terminal AAA catalytic domain. MIT and MTBD are required for association with the microtubule cytoskeleton and subsequent severing, thereby regulating microtubule dynamics (White *et al.*, 2007). The full-length M1 spastin isoform has a longer N-terminal domain as it contains a hydrophobic region (HR), not present in the shorter M87 spastin isoform (Blackstone, O'Kane and Reid, 2011). The hydrophobic region (HR) is predicted to insert into the ER and form a partially membrane-spanning hairpin loop (Park *et al.*, 2010), localising M1 to the ER where it mediates interactions between M1 spastin and three ER-shaping proteins: atlastin-1 (Evans *et al.*, 2006; Sanderson *et al.*, 2006), REEP1 (Park *et al.*, 2010) and RTN2 (Montenegro *et al.*, 2012). M1 spastin is predominantly located at structures of the early secretory pathway, endosomes (Evans *et al.*, 2006; Sanderson *et al.*, 2006) and lipid droplets (Papadopoulos *et al.*, 2015). The shorter M87 spastin isoform is a cytoplasmic protein that can be recruited to endosomes, but not to the early secretory pathway (Connell et al., 2009; Blackstone et al., 2011).

Atlastin-1 and M1 spastin also regulate lipid droplet (LD) formation (Klemm *et al.*, 2013; Papadopoulos *et al.*, 2015) and BMP signalling (Tsang *et al.*, 2009; Zhao and Hedera, 2013), common functional modules also important to HSP.

Mutations in the *REEP1* gene cause autosomal dominant spastic paraplegia type 31 (SPG31) (Züchner *et al.*, 2006). This gene encodes the receptor expression-enhancing protein 1 (REEP1), a member of the DP1/Yop1p protein family involved in ER tubule-shaping (Voeltz *et al.*, 2006). REEP1 localises to the tubular ER where it interacts with both atlastin-1 and spastin through hydrophobic hairpin domains, to co-ordinate the shaping and remodelling of ER tubules (Park *et al.*, 2010). Interestingly, like spastin, REEP1 is also able to mediate microtubule interactions with the tubular ER network (Park *et al.*, 2010). Defects in tubular ER shaping and ER network interactions with the microtubule cytoskeleton seem to be important in the pathogenesis of HSP. *REEP2* encodes the receptor expression-enhancing protein 2, a paralog of REEP1, which also localises to the ER and microtubules where it is thought to participate in ER-shaping (Esteves *et al.*, 2014), possibly through insertion of its hydrophobic domain in the phospholipid bilayer as shown for family member, REEP1 (Beetz, Koch, *et al.*, 2013).

Mutations in the *RTN2* gene cause autosomal dominant spastic paraplegia type 12 (SPG12) (Montenegro *et al.*, 2012). This gene encodes a member of the large, diverse reticulon (RTN) superfamily of ER membrane-shaping proteins (Yang and Strittmatter, 2007). RTNs have a key role in shaping intracellular membrane-bound organelles, especially the ER, where they are involved in generating regions of high membrane curvature found at tubules and ER sheet edges, through hydrophobic insertion (wedging) (Collins, 2006; Voeltz *et al.*, 2006; Hu *et al.*, 2008; Chiurchiù, Maccarrone and Orlacchio, 2014). RTNs are characterised by the conserved reticulon homology domain (RHD), located at the C-terminal, which contains two short hydrophobic domains which are thought to "double back" forming hairpin loops and generating membrane curvature by increasing the area of the cytoplasmic leaflet of the lipid bilayer (Oertle and Schwab, no date; Zurek, Sparks and Voeltz, 2011). RTN2 localises to the ER, where it appears to interact with spastin M1 through the hydrophobic hairpin loop domain, which is only observed in the longer M1 isoform (Montenegro *et al.*, 2012). Given that the conserved RHD is known to mediate interactions between reticulons and other ER morphogens, RTN2 is thought to participate in the hairpin loop-containing network of ER morphogens, which includes

atlastin-1, M1 spastin and REEP1, interacting through hydrophobic hairpin domains within the tubular ER to co-ordinate ER shaping and microtubule dynamics (Park *et al.*, 2010; Montenegro *et al.*, 2012).

Mutations in the *ZFYVE27* gene cause autosomal dominant spastic paraplegia type 33 (SPG33), and encodes a member of the FYVE-finger family of proteins, protrudin (Mannan *et al.*, 2006). Protrudin localises predominantly to the tubular ER where it interacts with ER-shaping proteins spastin, atlastin-1 and REEP1 through hydrophobic hairpin domains to co-ordinate ER membrane curvature, contributing to the formation of the tubular ER network (Mannan *et al.*, 2006; Hashimoto *et al.*, 2014).

Mutations in the *tropomyosin-receptor kinase* (*Trk)-fused gene* (*TFG*) cause autosomal recessive spastic paraplegia type 57 (SPG57) (Beetz, Koch, *et al.*, 2013). This gene encodes a protein which functions at ER exit sites in the regulation of COPII vesicle secretion (Witte *et al.*, 2011; Johnson *et al.*, 2015). TFG is thought to be a key component of the early secretory pathway, regulating anterograde trafficking from ER (Johnson *et al.*, 2015). Mutant TFG is unable to form a matrix at the interface between the ER and ER-Golgi intermediate compartments (ERGIC), critical to its function, altering ER protein secretion and subsequent ER morphology, disrupting ER tubule organisation and causing the ER network to collapse onto the underlying microtubule cytoskeleton (Beetz, Koch, *et al.*, 2013).

Mutations in the *ADP-ribosylation-like factor 6-interacting protein 1* (*ARL6IP1*) gene cause autosomal recessive spastic paraplegia type 61 (SPG61) (Novarino *et al.*, 2014). This gene encodes the ADP-ribosylation factor-like protein 6-interacting protein 1 (ARL6IP1 or ARMER), an anti-apoptotic protein which localises to ER (Lui *et al.*, 2003). ARL6IP1 localises to the ER where the short hairpin structures of the transmembrane domains are required for shaping the ER membrane, in a reticulon-like manner (Yamamoto *et al.*, 2014).

1.5.4 ERAD pathway & Protein folding

Newly synthesized proteins are translocated into the ER lumen, where if destined for secretion, they must undergo correct folding and modifications, such as glycosylation, with the assistance of numerous chaperones and modifying enzymes (Rapoport, 2007). However, even with numerous chaperones and other cellular factors, protein folding is still inefficient, and a significant proportion fail to acquire their native three-dimensional structure and end up misfolded (Hartl and Hayer-Hartl, 2009). Cells have evolved protein quality control systems in the ER to detect and eliminate terminally misfolded proteins, the most well-characterised of these pathways is ER-associated degradation (ERAD). ERAD is a conserved multi-step pathway dedicated to the removal of misfolded proteins from the lumen or membrane of the ER, targeting them for ubiquitin-proteasome-mediated degradation (Hiller *et al.*, 1996; Werner, Brodsky and McCracken, 1996). Recognition of misfolded proteins and subsequent clearance through the ERAD pathway needs to be tightly regulated so that normal cellular function is not affected (Ruggiano, Foresti and Carvalho, 2014).

Mutations in the *CCT5* gene cause autosomal recessive mutilating sensory neuropathy with spastic paraplegia (Bouhouche *et al.*, 2005). This gene encodes subunit 5 of the chaperonin-containing TCP1 (T-complex polypeptide 1) complex, a complex comprised of two stacked rings, each containing 8 different subunits (Liou, Willison and Research, 1997). Molecular chaperones assist misfolded and nascent proteins into their native conformation or protect misfolded proteins from aggregation (Sergeeva *et al.*, 2013). The chaperonin CCT complex is required for the proper folding of cytoskeletal proteins (actin and tubulin) whereby unfolded polypeptides enter the central cavity and are folded in an ATP-dependent manner (Lewis *et al.*, 1996).

ERLIN2 (SPG18) and its paralog ERLIN1 (SPG62) are members of the Stomatin/Prohibitin/Flotillin/HflK/C (SPFH) domain-containing family, and encode lipid raft-associated proteins localised to the endoplasmic reticulum and nuclear

envelope (Browman *et al.*, 2006; Tian *et al.*, 2016). Together, they form an ER membrane complex and mediate the ER-associated degradation (ERAD) of inositol 1,4,5-triphophate (IP3) receptors (Pearce *et al.*, 2009).

Mutations in the *VCP* gene cause a progressive lower limb spasticity which has been associated with hereditary spastic paraplegia (de Bot *et al.*, 2012). This gene encodes a member of the AAA (ATPases Associated with a variety of cellular Activities) family of proteins (DeLaBarre and Brunger, 2005; Pye *et al.*, 2006), which is known to function in a range of cellular processes, including ERAD (Meyer, Bug and Bremer, 2012). VCP/p97 acts as a ubiquitin-selective chaperone, using energy from ATP hydrolysis to re-translocate proteins from the ER to the cytosol during ERAD (Jarosch *et al.*, 2002; Rabinovich *et al.*, 2002; Christianson and Ye, 2014).

1.5.5 Lipid metabolism

The ER is not only where membrane-bound and secretory proteins are synthesised, but together with the Golgi apparatus it forms the endomembrane compartment, the major site of lipid synthesis (Fagone and Jackowski, 2009). The ER region close to the Golgi apparatus is known as the ER-Golgi intermediate compartment (ERGIC). This region is rich in vesicles and tubules and is where phospholipids, the major lipid components of all mammalian membranes, including glycerophospholipids and sphingolipids, are transferred and biochemically modified, together with proteins destined for the cell surface or transport to other organelles (Fagone and Jackowski, 2009; Glick and Nakano, 2009). The structure closest to the ERGIC is the *cis*-Golgi structure leading to the *trans*-Golgi network (TGN), the site where budding vesicles are formed carrying newly synthesised secretory proteins (Fagone and Jackowski, 2009; Schwarz and Blower, 2016). The TGN has traditionally been seen as the main cargo sorting hub, where proteins and lipids are sorted into transport carriers, which requires elaborate cargo sorting machineries allowing them to be transported to downstream destinations which include the plasma membrane and endosomal compartments (Guo, Sirkis and Schekman, 2014).

Brain lipids consist of glycerophospholipids, sphingolipids and cholesterol, which are important structural components of cellular membranes (Korade and Kenworthy, 2008). The brain is the most cholesterol-rich organ in the body (Björkhem and Meaney, 2004), where it is tightly regulated and has been shown to be essential for normal brain development (Orth and Bellosta, 2012). Cholesterol is required for synapse and dendrite formation (Goritz, Mauch and Pfrieger, 2005; Fester *et al.*, 2009) and axonal guidance (de Chaves *et al.*, 1997), and as it is a major constituent of cell membranes, any defects associated with cholesterol metabolism can lead to a number of CNS diseases, including Huntington's disease (Block *et al.*, 2010) and Alzheimer's disease (Di Paolo and Kim, 2011) to name a few. A number of proteins involved in HSP, play various roles in lipid metabolism, and so it is not surprising that a subset of HSPs are caused by disturbances in phospholipid, sphingolipid and fatty acid metabolism. For example, DDHD1 (SPG28) and DDHD2 (SPG54) are members of the mammalian intracellular phospholipase A_1 family of proteins (Inoue *et al.*, 2012), and neuropathy target esterase (PNPLA6/NTE, SPG39) has combined phospholipase A_1 and A_2 activity (Zaccheo *et al.*, 2004).

Mutations in the *DDHD domain-containing protein 1* (*DDHD1*) gene cause autosomal recessive hereditary spastic paraplegia (HSP) type 28 (SPG28) (Tesson *et al.*, 2012). This gene encodes a cytosolic phosphatidic acid (PA)-preferring phospholipase A1 (PA-PLA1), also known as DDHD1 (Higgs *et al.*, 1998; Inoue *et al.*, 2012). DDHD1 is predominantly localised in the cytosol, with partial localisation in microsomes and mitochondria (Yamashita *et al.*, 2010). DDHD1 is also thought to be involved in regulating mitochondrial dynamics, since mutant *DDHD1* causes mitochondrial dysfunction, which is thought to occur as a result of the PA accumulation in mitochondria. Alterations in lipid metabolism may therefore affect mitochondrial bioenergetic function in HSP (Tesson *et al.*, 2012). *DDHD2* encodes a member of the phospholipase A_1 family of proteins, a hydrolysing phospholipid that localise to the cis-Golgi and to the ER-Golgi intermediate compartment (ERGIC) (Morikawa *et al.*, 2009; Sato *et al.*, 2010).

PNPLA6 encodes a neuropathy target esterase (NTE), which is involved in the de-esterification of phosphatidylcholine, a major membrane phospholipid, into glycerophosphocholine and fatty acids, maintaining intracellular phospholipid homeostasis (Synofzik *et al.*, 2014; Topaloglu *et al.*, 2014).

ELOVL4, FA2H (SPG35) and CYP2U1 (SPG53) are all involved in various aspects of fatty acid metabolism. Mutations in the *ELOVL Fatty Acid Elongase 4* (*ELOVL4*) gene cause autosomal recessive conditions such as Sjögren-Larsson syndrome, in which spastic quadriplegia is associated with mental retardation and ichthyosis (Laurenzi *et al.*, 1996; Aldahmesh *et al.*, 2011), and recently associated with HSP (Fink, 2013). This gene encodes a member of the ELO family, a membrane-bound fatty acid elongase essential for biosynthesis of fatty acids (Agbaga *et al.*, 2008). FA2H (SPG35) catalyses the 2-hydroxylation of the major myelin lipids which can then be incorporated into myelin, using the free fatty acids as substrates (Alderson et al., 2004; Edvardson et al., 2008). CYP2U1 (SPG56) is a member of the cytochrome P450 superfamily of enzymes involved in fatty acid hydroxylation, catalysing the hydroxylation of arachidonic acid and related long-chain fatty acids (Chuang et al., 2004; Tesson et al., 2012).

The *SPG20* gene encodes spartin, a multifunctional protein that associates with the surface of lipid droplets (LDs), interacting with TIP47 (tail-interacting protein of 47 kDa), a peripheral membrane protein (Eastman, Yassaee and Bieniasz, 2009). LDs store neutral lipids and have important roles in lipid metabolism (Welte, 2007). These dynamic organelles are thought to be formed within ER membranes, before budding off and being transported along microtubules and mobilised for lipolysis, in response to metabolic changes (Brasaemle, 2007). The membrane layer on the surface of LDs has two main groups of proteins; enzymes important in lipid metabolism and membrane proteins of the perilipin (PAT) family which includes TIP47. TIP47 is involved in stabilising LDs (Thiele and Spandl, 2008). Spartin is involved in the regulation of lipid droplet turnover (Eastman, Yassaee and Bieniasz, 2009), acting as an adaptor protein, it activates and recruits atrophin-1 interacting protein 4 (AIP4)-E3 ubiquitin ligase to lipid droplets, regulating the level of AIP4-mediated

ubiquitination of lipid droplet-associated proteins (Eastman, Yassaee and Bieniasz, 2009; Milewska, McRedmond and Byrne, 2009; Hooper *et al.*, 2010).

Mutations in the *BSCL2* gene cause autosomal dominant hereditary spastic paraplegia (HSP) type 17 (SPG17) (Windpassinger *et al.*, 2004). This gene encodes the ER membrane protein seipin (BSCL2), which is involved in lipid droplet morphology and metabolism (Fei, Du and Yang, 2011). HSP-associated *BSCL2* mutations (N88S and S90L), cause misfolded seipin to accumulate in the ER, leading to ER stress and enhance ubiquitination and degradation (Ito *et al.*, 2008).

In addition, the full-length spastin isoform M1 was recently found to be involved in lipid metabolism, regulating lipid droplet (LD) size and distribution (Papadopoulos *et al.*, 2015).

ERLIN1 (SPG62) and ERLIN2 (SPG18) have also been identified as novel ER regulators of Sterol Regulatory Element Binding Proteins (SREBPs), restricting SREBP activation in the ER and regulating cellular cholesterol homeostasis (Huber *et al.*, 2013).

1.5.6 Endosome dynamics & Vesicle formation

Membrane trafficking involves a wide range of complex, highly regulated processes that are required for the movement of cargo (proteins etc.) using membrane-bound transport vesicles (Herrmann and Spang, 2015). Membrane trafficking can be divided into two pathways, exocytosis and endocytosis, based on the direction of travel. Exocytosis involves the movement of newly synthesised lipids, proteins or carbohydrates from the endoplasmic reticulum (ER) via the Golgi complex to plasma membrane or extracellular space. In contrast, the endocytic pathway involves the internalisation of cargo, such as receptors and transmembrane domains from the plasma membrane and extracellular environment to early endosomes, where they can be recycled back to plasma membrane, targeted to Golgi or transported to late endosomes and lysosomes for degradation (Mellman, 1996; Mellman and Warren, 2000; Maxfield and McGraw, 2004).

The endosomal sorting complexes required for transport (ESCRT) machinery are composed of several cytosolic protein complexes, ESCRT-I to III, which are evolutionary conserved key components of the endocytic pathway that function in a number of cellular contexts to mediate receptor sorting, membrane remodelling and membrane scission (Hurley, 2010). The ESCRT proteins were originally identified as being involved in the biogenesis of multivesicular bodies (MVBs), late endosomal structures that fuse with lysosomes, leading to degradation of endocytosed proteins such as receptors and transmembrane proteins (Katzmann, Odorizzi and Emr, 2002; Metcalf and Isaacs, 2010). The ESCRT pathway is also involved in a number of membrane-scission events, including viral budding (Garrus *et al.*, 2001) and cytokinesis (Carlton and Martin-Serrano, 2007). The endocytic pathway ensures cellular homeostasis and regulates cell-to-cell communication, controlling nutrient uptake, signalling and degradation of transmembrane and misfolded proteins (Huotari and Helenius, 2011).

The endosomal system can provide mechanisms to overcome the spatial challenges presented as a result of the distinctive morphology of neurons, which enable signalling molecules to be trafficked throughout the neuron, and allow intracellular signals to be sustained over long distances (Cosker and Segal, 2014). The endosomal processes remain largely the same in neurons as in other cell types (Yap and Winckler, 2012), with many developmental processes dependent on endocytosis, endosomal recycling and degradation (Shilo and Schejter, 2011). The endocytic machinery is important in a number of neurodevelopmental processes (Yap and Winckler, 2012), particularly endosomes, which are crucial to neuronal signalling, regulating cell survival, axon outgrowth and guidance, dendritic branching and cell migration (Cosker and Segal, 2014).

Adaptor protein complexes (AP1-5) are conserved heterotetrameric complexes that function in vesicle trafficking (Hirst, Irving and Borner, 2013). All APs function as coat proteins which are recruited onto membranes to mediate the formation of different types of vesicles and select cargo for inclusion into these vesicles (Abou Jamra *et al.*, 2011; Hirst, Irving and Borner, 2013). AP-4 and AP-5 both function independently of

clathrin and both are associated with spastic paraplegia (Hirst *et al.*, 2011). AP-4 is thought to be important in brain function and development, it mediates anterograde vesicular trafficking between the trans-Golgi network (TGN) and an endosomal compartment of specific cargos, such as the amyloid precursor protein (APP) (Burgos *et al.*, 2010). AP-4 deficiency has been linked with severe intellectual disability and progressive spastic paraplegia, with mutations identified in several of the AP-4 subunits (Abou Jamra *et al.*, 2011; Moreno-De-Luca *et al.*, 2011). Interestingly, the AP-5 complex, which seems to be involved in endosomal trafficking, is also associated with progressive spastic paraplegia and is therefore likely to be crucial for neuronal development and homeostasis (Hirst *et al.*, 2011; Hirst, Irving and Borner, 2013).

Mutations in the *AP5Z1* gene cause autosomal recessive spastic paraplegia type 48 (SPG48) (Słabicki *et al.*, 2010). This gene encodes the zeta-1 subunit of adaptor-related protein complex 5 (AP5Z1) or KIAA0415, which was originally thought to function in DNA repair (Słabicki *et al.*, 2010), but has since been identified as a subunit of the new adaptor protein complex, AP-5, where it localises to late endosomes and is involved in endosomal dynamics (Hirst *et al.*, 2011). Like AP-4, AP-5 is not associated with clathrin but instead interacts with spatacsin (SPG11) and spastizin (SPG15) in an emerging HSP-related complex related to endocytic trafficking (Słabicki *et al.*, 2010; Hirst *et al.*, 2011; Hirst, Irving and Borner, 2013). It is thought that due to structural features, spatacsin (SPG11) and spastizin (SPG15) may in fact act as accessory proteins in the formation of an AP-5-containing coat-like complex (Słabicki *et al.*, 2010; Hirst *et al.*, 2011). Spatacsin (SPG11) has predicted structures which are similar to clathrin heavy chains, suggesting a role for SPG11 as a membrane scaffold (Hirst *et al.*, 2011), whereas spastizin (SPG15) may facilitate membrane docking through interaction with the endosomal lipid, phosphatidylinositol 3-phosphate (PI3P), via its FYVE domain (Sagona *et al.*, 2010; Park and Guo, 2014).

As discussed previously, the ATP-dependent microtubule-severing protein spastin (SPG4) harbours an N-terminal microtubule-interacting and trafficking (MIT) domain. Through this domain spastin binds strongly with two endosomal sorting complex required for transport III (ESCRT-III) proteins, CHMP1B (charged multivesicular body

protein 1B) and IST1 (increased sodium tolerance 1), coupling microtubule severing with membrane scission (Reid *et al.*, 2005; Agromayor *et al.*, 2009). Specifically, interaction with IST1 is important for spastin recruitment to the midbody and subsequent participation in cytokinesis (Renvoisé and Blackstone, 2010). The MIT domain has been described in several other proteins that are known to have defined roles in endosomal trafficking (Ciccarelli *et al.*, 2003), interacting with components of the endosomal sorting complexes required for transport (ESCRT) machinery, specifically MIT-interacting motifs (MIMs) of ESCRT-III proteins (Hurley and Yang, 2008). The major membrane-remodelling component, ESCRT-III mediates a range of cellular membrane scission processes other than ESCRT-mediated endosomal sorting and multivesicular endosome (MVE) formation (Katzmann, Odorizzi and Emr, 2002), which include virus budding (Morita and Sundquist, 2004) and cytokinesis (Carlton and Martin-Serrano, 2007), a process in which both spastin (Connell *et al.*, 2009) and spartin (Lind *et al.*, 2011) are known to participate. Another cellular membrane scission process mediated by ESCRT-III includes the recruitment of spastin to regulate endosomal tubulation, following interaction with IST1, which promotes fission of recycling tubules from the endosome (Allison *et al.*, 2013). Endosomal tubulation at early sorting endosomes is important for both recycling and endosome-to-Golgi pathways. In the recycling pathway, tubules traffic cargo directly or indirectly from the peripheral early endosome to the plasma membrane (Allison *et al.*, 2013). In the endosome-to-Golgi pathway, the retromer complex is required for cargo-selective endosomal sorting (Seaman, 2004; Bonifacino and Hurley, 2008).

Another HSP protein, strumpellin, is involved in the fission of endosomal tubules. Strumpellin, also known as WASH complex subunit 5 (WASHC5), is a component of the Wiskott Aldrich Syndrome Protein (WASP) and SCAR Homologue (WASH) complex (Derivery *et al.*, 2009). The WASH complex is recruited to endosomes by the retromer complex, via interactions with the vacuolar protein sorting-associated protein 35 (VPS35), a component of the retromer complex (Harbour *et al.*, 2010). The retromer complex is a crucial element of the endosomal protein recycling machinery which sorts cargo into the endosome-to-Golgi pathway (Gomez and Billadeau, 2009; Gomez *et al.*, 2012; Seaman, 2012).

Mutations in the Vacuolar Protein Sorting 37A (VPS37A) gene, have also been associated with impaired endosomal trafficking in HSP, causing autosomal recessive spastic paraplegia type 53(SPG53) (Zivony-Elboum *et al.*, 2012). This gene encodes subunit alpha of the ESCRT-I complex which is involved in vesicular trafficking and ubiquitination (Zivony-Elboum *et al.*, 2012).

Mutations in the neuronal *KIF1C* gene cause autosomal recessive spastic paraplegia type 58 (SPG58) (Dor *et al.*, 2014; Novarino *et al.*, 2014). This gene encodes a microtubule-dependent motor protein which is required for the retrograde transport of Golgi vesicles to the ER (Dorner *et al.*, 1998).

Mutations in the *Ubiquitin Specific Peptidase 8* (*USP8*) gene cause autosomal recessive spastic paraplegia type 59 (SPG59) (Novarino *et al.*, 2014). This gene encodes a deubiquitinating enzyme (DUB) known to associate directly with the early ESCRT-0 complex (Berlin *et al.*, 2010), as well as with chromatin-modifying protein (CHMP) components of the late ESCRT-III machinery (Tsang *et al.*, 2006; Row *et al.*, 2007).

Mutations in the *WD Repeat-Containing Protein 48* (*WDR48*) gene cause autosomal recessive spastic paraplegia type 60 (SPG60) (Novarino *et al.*, 2014).This gene encodes an endosomal protein known to regulate deubiquitination, by forming stable complexes with multiple deubiquitinating enzymes (DUBs) including USP1, USP12 and USP46 (Cohn *et al.*, 2009). Together with KIF1C and USP8, WDR48 has been implicated in the endosomal sorting complexes required for transport (ESCRT) pathway (Novarino *et al.*, 2014).

Mutations in the *33-kD acidic cluster protein (ACP33)* gene have been associated with causing autosomal recessive hereditary spastic paraplegia (HSP) type 21 (SPG21), also known as Mast syndrome (Simpson *et al.*, 2003). This gene encodes 'maspardin' (Mast syndrome, spastic paraplegia, autosomal recessive with dementia), which localises to intracellular endosomal/*trans*-Golgi vesicles, where it likely has a

functional role in the *trans*-Golgi network/endosomal pathway (Simpson *et al.*, 2003; Hanna and Blackstone, 2009).

As discussed previously, VCP is essential for autophagy, a process linked with endosomal trafficking (Ju and Weihl, 2010; Tresse *et al.*, 2010). The *VCP* gene encodes a member of the AAA (ATPases Associated with a variety of cellular Activities) family of proteins (DeLaBarre and Brunger, 2005; Pye *et al.*, 2006), and is known to function in a range of cellular processes. VCP is involved in the early steps of endosomal trafficking as it associates with the endocytic coat protein clathrin and the endosomal sorting factor, EEA1 (early endosome antigen 1) (Pleasure, Black and Keen, 1993; Ramanathan and Ye, 2012). VCP can affect the oligomeric state of EEA1, to regulate the size of early endosomes (Ramanathan and Ye, 2012).

1.5.7 Autophagy

Autophagy is the general term used to describe the regulated catabolic process in which cytosolic components, organelles and misfolded proteins are degraded in lysosomes and recycled (Levine and Kroemer, 2008; Klionsky, 2010). Based on the mechanism of cargo delivery to the lysosomes, there are 3 distinct types of autophagy: chaperone-mediated autophagy (CMA), micro-autophagy and macro-autophagy (Cuervo, 2004). In micro-autophagy, lysosomal membrane invaginations directly engulf portions of the cytoplasm, whereas CMA involves the chaperone HSC70 and its co-chaperones which are able to recognise and unfold substrate proteins with the specific 'KFERQ' amino-acid motif. These substrates bind to the lysosomal protein LAMP-2A and are translocated across the lysosomal membrane for degradation (Nikoletopoulou, Papandreou and Tavernarakis, 2015). The main pathway is thought to be macro-autophagy, which differs from the other two pathways in that the cytoplasmic cargo is sequestered inside a double membranous structure known as the autophagosome. The autophagosome is then transported along microtubules to lysosomes, which they fuse with to form autolysosomes. Together, the cellular components and the inner membrane are degraded by lysosomal enzymes and recycled (Levine and Kroemer, 2008).

Neuronal autophagy is essential for the maintenance of neuronal homeostasis and neuronal survival (Liang and Jia, 2014). There is increasing evidence that autophagy dysfunction, which can lead to the accumulation and aggregation of proteins resulting in cellular toxicity, is involved in the pathogenesis of several neurodegenerative diseases, including Parkinson's disease, Alzheimer's disease, Huntington's disease and other protein-misfolding disorders (Pan *et al.*, 2008; Liang and Jia, 2014; Ciechanover and Kwon, 2015a).

As already mentioned, mutations in the *VCP* gene cause progressive lower limb spasticity, which has been associated with hereditary spastic paraplegia (de Bot *et al.*, 2012), but is not yet classified as such. VCP/p97 monomers form a homohexamer allowing the ATPase domains to orientate as two stacked rings to form a central pore (Zhang *et al.*, 2000; DeLaBarre and Brunger, 2003). As one of the most abundant proteins, it functions in a range of independent cellular processes, and although it has a well-established role in proteasomal degradation, it is now also linked to the other cellular degradative system, the lysosome (Meyer, Bug and Bremer, 2012). VCP has been shown to function in both ubiquitin-controlled autophagy pathway (Tresse *et al.*, 2010) and endolysosomal sorting (Ritz *et al.*, 2011). Pathogenic VCP mutants have been identified in a number of different neurodegenerative disorders, including Parkinson's disease, Huntington's disease, and ALS (Kakizuka, 2008) increasing our confidence in its involvement in HSP.

Mutations in the *tectonin beta-propeller repeat containing 2 (TECPR2)* gene cause autosomal recessive spastic paraplegia type 49 (SPG49) (Oz-Levi *et al.*, 2012). This gene encodes the tectonin beta-propeller repeat-containing protein 2 (TECPR2), a positive regulator in intracellular autophagy pathways, regulating autophagosome formation and accumulation (Behrends *et al.*, 2010).

Additionally, autophagy/lysosomal dysfunction has also been associated with SPG11 and SPG15, caused by *SPG11* (spatacsin) and *ZFYVE26* (spastizin) gene mutations (Stevanin *et al.*, 2007; Hanein *et al.*, 2008). Both spatacsin (SPG11) and spastizin (SPG15), are known to co-localise with vesicle, endosomal and ER markers (Murmu

et al., 2011) and are also thought to be involved with autophagic lysosome reformation and initiation of lysosome tabulation (Chang, Lee and Blackstone, 2014; Varga *et al.*, 2015).

The *lysosomal trafficking regulator (LYST)* gene was originally described as the causative gene for the rare autosomal recessive, Chédiak-Higashi syndrome (CHS) (Nagle *et al.*, 1996). However, *LYST* mutations have now been associated with impaired autophagy (Rahman *et al.*, 2012) in autosomal recessive hereditary spastic paraplegia (Shimazaki *et al.*, 2014). This gene encodes the large, cytoplasmic lysosomal trafficking regulator protein, LYST (Barbosa *et al.*, 1996; Nagle *et al.*, 1996). Given that autophagic impairment is observed with the loss-of-function of other HSP-related proteins, this highlights the importance of this function module in the pathogenesis of disease.

1.5.8 Axonal transport

Neurons have a unique morphology, as highly polarised cells with extended axons and dendrites, making them dependent on the active intracellular transport of proteins, RNA and organelles (cargo) along axons (Perlson *et al.*, 2010). Axonal transport allows newly synthesised lipids and proteins to reach the distal synapse, whilst misfolded and aggregated proteins are removed from the axon and transported to the cell body (soma) for efficient degradation (Chevalier-Larsen and Holzbaur, 2006). Axonal transport is also important for intracellular neural transmission between the distal axon and the soma, allowing the neuron to respond efficiently to environmental changes (Perlson *et al.*, 2010). Molecular motors, such as kinesin and dynein superfamily proteins, are required to drive long-distance axonal transport of cargo (membrane-bound organelles and vesicles) along the microtubule 'rails' of the cytoskeleton, using the energy released following ATP hydrolysis (Hirokawa, 1998; Perlson *et al.*, 2010). Kinesins are thought to be the main molecular motors required for the intracellular transport of cargos along the microtubules 'tracts' in the anterograde direction (away from cell body) (Hirokawa *et al.*, 1991), whereas cytoplasmic dynein complexes move in the opposite direction

(towards cell body), to drive retrograde microtubule-based transport (Hirokawa, 1998; Goldstein and Yang, 2000).

Axonal transport defects have emerged as a common factor in the pathogenesis of several neurodegenerative disorders including Alzheimer's disease (Stokin *et al.*, 2005), Parkinson's disease (Saha *et al.*, 2004), Huntington's disease (Gunawardena *et al.*, 2003; Her and Goldstein, 2008) and amyotrophic lateral sclerosis (ALS) (Ligon *et al.*, 2005; Perlson *et al.*, 2010). Given the vulnerability of long motor neuron axons to changes in transport processes, it is not surprising that several HSP-associated genes, encoding proteins involved in axonal transport and intracellular trafficking, have been identified (Blackstone, 2012).

Most pathogenic *SPAST* mutations affect the enzymatic activity of spastin, and as it is a microtubule-severing protein, mutations can cause a redistribution of the microtubule cytoskeleton, disrupting microtubule dynamics (Errico, Ballabio and Rugarli, 2002; McDermott *et al.*, 2003). However, it has also been shown to be involved in axonal transport, as expression in cultured neurons of a short dysfunctional M1 polypeptide (but not a short dysfunctional M87) was found to dramatically inhibit fast axonal transport (FAT), possibly through the activation of specific kinases and phosphatases involved in the regulation of molecular motor proteins, thereby causing a defect in axonal transport (Solowska *et al.*, 2008). As spastin regulates microtubule dynamics, and microtubules are essential in axonal transport, defects in axonal transport are likely to play some part in the pathogenesis of disease.

Axonal transport impairments have also been associated with SPG10 caused by *KIF5A* gene mutation (Reid *et al.*, 2002) and SPG30 caused by *KIF1A* gene mutation (Erlich *et al.*, 2011), both of which encode microtubule-dependent motor proteins involved in vesicular anterograde axonal transport. More recently, SPG58 caused by *KIF1C* gene mutations has been identified (Dor *et al.*, 2014; Novarino *et al.*, 2014). *KIF1C* encodes a microtubule-dependent motor protein required for the retrograde transport of Golgi vesicles to the ER (Dorner *et al.*, 1998).

Mutations in the BICD2 gene, have been associated with axonal transport impairments in autosomal recessive HSP patients (Oates *et al.*, 2013). This gene encodes an evolutionary conserved Golgi-associated motor-adaptor protein involved in anterograde and retrograde transport (Splinter *et al.*, 2010).

The identification of genes that encode motor and motor-adaptor proteins involved in the pathogenesis of HSPs further supports the role of intracellular transport processes in the pathogenesis of hereditary axonopathies such as HSP.

1.5.9 Mitochondrial function

Mitochondria are unique, double membrane-bound organelles central to a number of cellular processes, including adenosine-5'-triphosphate (ATP) production through coupled electron transport chain and oxidative phosphorylation, intracellular Ca^{2+} homeostasis, steroid synthesis and the generation of reactive oxygen species (ROS) (Kann and Kovács, 2007). Consequently, mitochondrial dysfunction has serious implications for cells, with links to cancer, as well as to ageing, metabolic and neurodegenerative diseases (Wallace, 2005).

The central nervous system (CNS) has an extremely high metabolic rate, with a single cortical neuron requiring up to 4.7 billion ATP molecules/second (Zhu *et al.*, 2012). Constant ATP production is required for neuronal function and survival (Nicholls and Budd, 2000), as it supports synapse assembly (Lee and Peng, 2008), generating action potentials (Attwell and Laughlin, 2001), and for synaptic transmission (Verstreken *et al.*, 2005). Since the majority of neuronal ATP is generated by oxidative metabolism, neurons are dependent upon mitochondrial function and oxygen supply (Erecinska, Cherian and Silver, 2004; Kann and Kovács, 2007) and are therefore sensitive to mitochondrial dysfunction (Fiskum, Murphy and Beal, 1999; Nicholls and Budd, 2000). Mitochondrial dysfunction occurs when there is an inadequate number of mitochondria, an inability to supply substrates to mitochondria, or a dysfunction in their electron transport and ATP-synthesis machinery (Nicolson, 2014). As a result, these changes cause a reduced efficiency of oxidative phosphorylation and a

reduction in the synthesis of high-energy molecules such as ATP, a feature observed in most chronic diseases (Reddy, 2008; Swerdlow, 2011; Nicolson, 2014). Mitochondrial dysfunction is a characteristic that is also observed in ageing and in age-related neurodegenerative diseases such as Alzheimer's disease, Parkinson's disease, amyotrophic lateral sclerosis (ALS) and Huntington's disease (Trushina and McMurray, 2007), as well as in cancer (Wallace, 2012) and diabetes (Reddy, 2008). Impaired mitochondrial function has also been implicated in the pathogenesis of several neurodegenerative diseases, including several HSPs.

Frameshift mutations in the *SPG20* gene have been associated with causing autosomal recessive hereditary spastic paraplegia (HSP) type 20 (SPG20), also known as Troyer syndrome (Patel *et al.*, 2002). This gene encodes spartin, a multifunctional protein which is known to interact with multiple binding partners (Milewska, McRedmond and Byrne, 2009) and is associated with several intracellular organelles (Robay *et al.*, 2006), including mitochondria (Lu, Rashid and Byrne, 2006). Spartin has been found to have a functional role in maintaining mitochondrial Ca^{2+} homeostasis via an interaction with cardiolipin, a major mitochondrial phospholipid (Joshi and Bakowska, 2011).

Mutations in the *C12orf65* gene have also been associated with mitochondrial dysfunction in HSP, causing autosomal recessive spastic paraplegia type 55 (SPG55) (Shimazaki *et al.*, 2012). This gene encodes a soluble mitochondrial matrix protein which belongs to a family of four mitochondrial class I peptide release factors, all characterised by a 'GGQ' motif at the active site (Richter *et al.*, 2010). *C12orf65* encodes a protein thought to be critical for the release of newly synthesised proteins from mitochondrial ribosomes (Antonicka *et al.*, 2010). The *C12orf65* nonsense mutation causes autosomal recessive SPG55, resulting in a premature stop codon. The truncated protein leads to a defect in mitochondrial protein synthesis and subsequent defects in respiratory complexes I and IV, leading to a reduction in the activity of the respiratory enzyme complex (Shimazaki *et al.*, 2012).

Abnormal mitochondrial function has also been associated with SPG7 caused by *PGN* gene mutation (Casari *et al.*, 1998) and SPG13 caused by *heat-shock protein 60* (*HSPD1*) gene mutation (Hansen *et al.*, 2002). Paraplegin assembles with AFG3L2 to form the metalo-protease AAA (ATPase Associated with diverse cellular Activities) complex at the mitochondrial inner membrane, where it is essential for mitochondrial protein quality control (Atorino *et al.*, 2003; Nolden *et al.*, 2005), degrading misfolded proteins (Karlberg *et al.*, 2009) and regulating ribosome assembly (Nolden *et al.*, 2005; Koppen *et al.*, 2007). Interestingly, homozygous mutations in the *AFG3L2* gene cause autosomal dominant hereditary ataxia spinocerebellar ataxia type 28 (SCA28), identifying this gene as a novel cause of dominant neurodegenerative disease (Di Bella *et al.*, 2010). HSPD1 is also involved in mitochondrial protein quality control, forming a double barrel chaperonin complex with its co-chaperone, 10 kDa heat shock protein (HSP10), to facilitate the correct folding of imported mitochondrial proteins (Nielsen and Cowan, 1998; Levy-Rimler *et al.*, 2001; Bross and Fernandez-Guerra, 2016).

Mutations in the *IBA57* gene, have also been associated with mitochondrial dysfunction in HSP, causing autosomal recessive spastic paraplegia type 74 (SPG74) (Lossos *et al.*, 2015). This gene encodes a mitochondrial iron-sulphur (Fe/S) protein assembly factor which is involved in the maturation of mitochondrial proteins (Sheftel *et al.*, 2012).

Finally, mutations in MT-ATP6 (Verny *et al.*, 2011), MT-ND4 (Clarençon *et al.*, 2006), MT-CO3 (Tiranti *et al.*, 2000) or MT-TI (Corona *et al.*, 2002) mitochondrial genes, are rare and easily overlooked, but they can contribute to both pure and complex forms of HSP.

1.5.10 DNA repair & Nucleotide metabolism

DNA damage is defined as any DNA modification that alters the chemical structure of DNA and changes its normal function in transcription or replication, or DNA coding properties (Lindahl, 1993; Rao, 1993). DNA damage can occur naturally following

metabolic processes where DNA damaging compounds such as reactive oxygen species (ROS) and reactive nitrogen species (RNS) are released (Rao, 1993), or following hydrolytic processes involving X-rays, ultraviolet (UV) light or various chemicals (Friedberg, 2008; Tubbs and Nussenzweig, 2017). Given that the majority of daily DNA damage is caused by single-stranded DNA (SSD) breaks following oxidative damage during metabolism or base hydrolysis, it is not surprising that cells acquired enzymes during evolution that can repair DNA following damage, restoring genome integrity (Lindahl and Barnes, 2000; Friedberg, 2008). However, mutations in DNA repair genes have been associated with several different diseases including cancer (Hoeijmakers, 2001), aging (Lombard *et al.*, 2005), and several neurodegenerative diseases (Rass, Ahel and West, 2007).

Given the extreme sensitivity of the neuron genome, specifically the motor neuron genome, to ROS and RNS, which cause both single- and double-strand DNA breaks (Martin and Liu, 2002) and the particular vulnerability of neurons to mutations in DNA repair genes (Słabicki *et al.*, 2010), it is unsurprising that neuronal DNA damage has been implicated in the pathogenesis of several neurological disorders, including amyotrophic lateral sclerosis (ALS), Alzheimer's disease, Parkinson disease's, and head trauma, to name a few (Martin, 2008).

Mutations in the *AP5Z1* gene, have been associated with abnormal DNA repair in HSP, causing autosomal recessive spastic paraplegia type 48 (SPG48) (Słabicki *et al.*, 2010). This gene encodes the zeta-1 subunit of adaptor-related protein complex 5 (AP5Z1) or KIAA0415, which has both nuclear and cytoplasmic localisation. According to Slabicki et al., (2010), AP5Z1 is a putative helicase required for efficient homologous recombination-mediated DNA double-strand break (DSB) repair. Although DSBs are less frequent than SSBs, they are more dangerous (Tubbs and Nussenzweig, 2017).

Purine nucleotide metabolism has previously been linked to several inherited neurological disorders including the X-linked recessive Lesch-Nyhan syndrome (LNS) and the autosomal recessive adenylosuccinate lyase (ASL) (Jinnah, Sabina and Van

Den Berghe, 2013), but never to HSP. However, AMPD2, ENTPD1 and NT5C2 are proteins involved in purine nucleotide metabolism, which have recently been implicated in HSP (Novarino *et al.*, 2014). *AMPD2* encodes one of three known adenosine monophosphate (AMP) deaminase enzymes involved in the deamination of AMP in the purine nucleotide cycle (Akizu *et al.*, 2013). *AMPD2* mutations have been associated with an early-onset neurodegenerative condition, a new pontocerebellar hypoplasia (PCH)-like syndrome (Akizu *et al.*, 2013). *ENTPD1* encodes a plasma membrane ectonucleotidase which hydrolyses ATP and other nucleotides in the synaptic cleft, regulating purinergic transmission (Munkonda *et al.*, 2007). *NT5C2* encodes cytosolic a purine 5'-nucleotidase which catalyses the hydrolysis of cytoplasmic purine nucleotides such as AMP, releasing adenosine (Dursun *et al.*, 2009).

1.6 Treatment & Management

Currently, there is no specific disease modifying cure or treatment that targets the underlying genetic defect in HSP. Instead, treatment involves targeting the main symptoms to reduce or manage muscle spasticity. Anti-spasticity drugs are often used to reduce muscle tightness, alongside regular physiotherapy which focuses on reducing muscle tone, maintaining muscle flexibility and improving range of motion and mobility (Fink, 2013).

The identification of specific disease genes and their corresponding proteins is already providing major advances in our understanding of the pathogenesis of HSPs, and this will continue, contributing to the identification of common pathways targetable with drugs. There is also the potential for future personalised treatments, depending on the altered pathway(s) of a particular individual (Klebe, Stevanin and Depienne, 2015).

1.7 Protein-Protein Interactions (PPIs)

Since the completion and release of high-quality sequencing of the human genome well over a decade ago (International Genome Sequencing Consortium, 2004), progress has been made in our understanding of the mechanisms that underlie human diseases, and in particular genetically inherited disorders, as our ability to assign genotypes to phenotypes has dramatically increased (Hamosh *et al.*, 2004; Rolland *et al.*, 2014). The actual causal mutations that connect genotype to phenotype are usually unknown, and this is especially true for complex trait loci and cancer-associated mutations. However, even when identified, how the causal mutation alters the function of the corresponding gene or gene product is often unclear (Rolland *et al.*, 2014).

Complex cellular systems are formed by interactions between genes and gene products located in the same cell, across cells, or even across organs, which appear to underlie most cellular functions, including most genotype-to-phenotype relationships (Vidal, Cusick and Barabási, 2011). A critical step towards unravelling the complex molecular relationships in living systems is the mapping of protein-protein interactions, or interactome networks, to understand more about the mechanisms involved following network perturbation as a result of inherited or somatic disease susceptibilities (Rolland *et al.*, 2014).

1.7.1 Protein-Protein Interaction (PPI) networks

Network construction and analysis is a relatively modern approach which has been used to investigate a number of diseases, including Alzheimer's disease (Goñi *et al.*, 2008; Soler-Lopez *et al.*, 2011), multiple sclerosis (Satoh, Tabunoki and Yamamura, 2009), and cancer (Pujana *et al.*, 2007; Su, Yoon and Dougherty, 2010). The disease networks were generated using experimental data, as well as protein interaction datasets from publicly available databases.

Disease networks are of particular interest as they not only increase our understanding of the molecular mechanisms involved in a disease process, but they can also help to identify potential disease drug targets, and in some diseases the identification of multiple targets is necessary if disease mechanisms bypass the inhibition of a single gene and instead target multiple genes (Schrattenholz, Groebe and Soskic, 2010). Moreover, it has been suggested that partial inhibition of multiple targets can be more efficient than complete inhibition of a single target (Csermely, Agoston and Pongor, 2005). Disease networks can also be used to characterise disease-related proteins, with some studies having shown a highly interconnected protein network with disease proteins compared with non-essential proteins, and these disease-related proteins have also been shown to be important to the overall network structure (Gandhi *et al.*, 2006; Jonsson and Bates, 2006; Xu and Li, 2006). However, Goh et al. (2007) found that the majority of disease genes were in fact non-essential and were not more likely to be highly interconnected than non-disease genes (Goh *et al.*, 2007). Other studies have also shown that disease-related proteins have a tendency to interact with proteins involved in the same disease (Barabási, Gulbahce and Loscalzo, 2011), like in the biological concept of "guilt by association". This observation is important for the identification of potentially novel candidate proteins involved in disease progression and development.

Additionally, interolog interactions are valuable datasets which can be used to predict human protein-protein interactions, and to prioritise interactions for further study. Walhout et al., (2000) introduced the concept of 'interologs', orthologous pairs of interacting proteins in different organisms, from which interaction annotation can be transferred from one organism to another (Walhout *et al.*, 2000; Yu *et al.*, 2004).

1.7.2 Detecting binary and co-complex PPIs

Experimental techniques used to detect protein-protein interactions (PPIs) can be divided into two major classes. The first include methods that are used to measure

direct physical interactions between a specific pair of proteins. These are known as "binary" methods, and include techniques such as yeast two-hybrid (Y2H) and membrane yeast two-hybrid (MYTH) (Rual *et al.*, 2005; Suter, Auerbach and Stagljar, 2006). The second class includes methods that are used to measure physical interactions between a tagged protein and a group of proteins without pairwise determination of protein pairs. These are known as "co-complex" or "non-binary" methods, because they are designed to identify proteins in stable complexes within a cellular context, and include techniques such as tandem affinity purification coupled to mass spectrometry (TAP-MS) or co-immunoprecipitation (Co-IP) (Berggård, Linse and James, 2007). Both of these methodologies can be used to detect protein-protein interactions in a high-throughput manner, producing different types of PPI data which can be used to generate large-scale interaction maps (Yu *et al.*, 2008; De Las Rivas and Fontanillo, 2010). These protein-protein interaction network maps have nodes which represent proteins, and edges which represent a physical interaction between each pair of proteins (Vidal, Cusick and Barabási, 2011).

1.7.3 Yeast two-Hybrid

The yeast two-hybrid (Y2H) system, which was originally devised by Stanley Fields and Ok-kyu Song (1989), utilises the powerful genetic system of the model organism *Saccharomyces cerevisiae* (yeast) to detect protein-protein interactions between any two proteins, X and Y (Fields and Song, 1989). As shown in Figure 1.2, Y2H is based on the functional reconstitution of a yeast transcription factor (e.g. *GAL4*) and subsequent activation of a selective reporter gene. To test whether two proteins (X and Y) interact, two expression constructs are made so that: bait protein (X) is fused to the DNA-binding domain (BD), whilst prey protein (Y) is fused to the activation domain (AD) of a transcription factor (Fields and Song, 1989). The DNA-binding domain (BD) binds to an upstream activating sequence (UAS), whereas the activation domain (AD) recruits the RNA polymerase II complex to the transcriptional start site of the reporter gene (Fields and Song, 1989). Therefore, following direct interaction between bait and prey proteins, the reconstituted functional transcription factor (TF), binds onto an upstream activating sequence (UAS), resulting in the activation of

detectable downstream reporter genes that enable growth under selective conditions or a change in colour of yeast colonies (β-galactosidase assay) (Fields and Song, 1989; Brückner *et al.*, 2009).

Figure 1.2

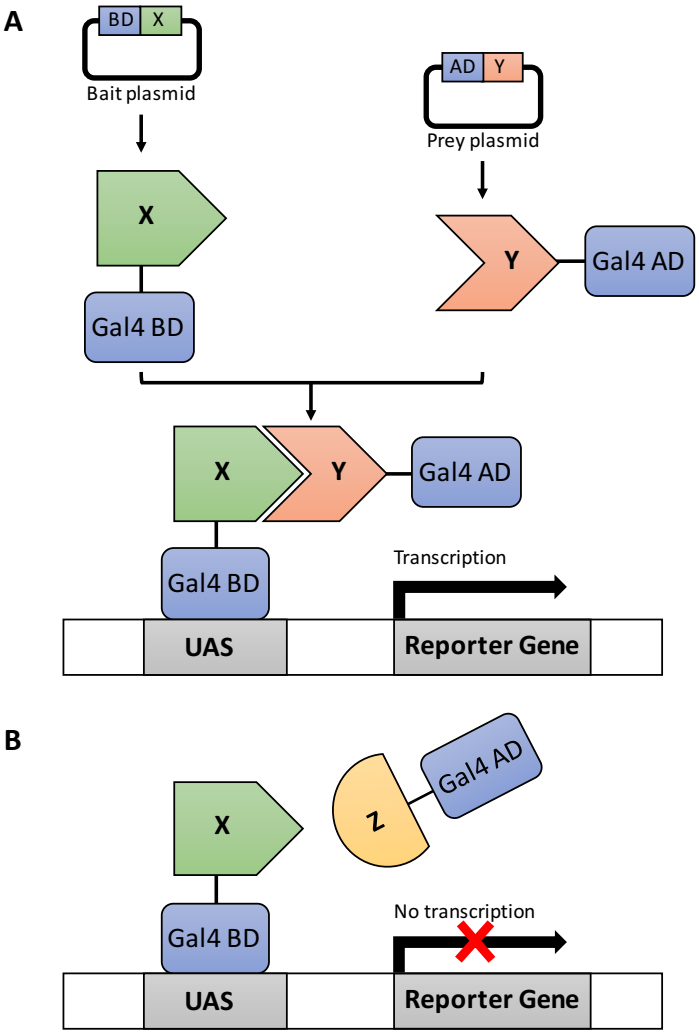

Figure 1.2. Yeast two-hybrid (Y2H) system. The *GAL4* transcription factor can be divided into two fragments: DNA-binding domain (Gal4 BD) and activation domain (Gal4 AD). The BD is responsible for binding to the UAS, whilst the AD is responsible for the activation of transcription. (A) To assess whether two proteins (X and Y) interact, fusion constructs can be co-expressed in yeast cells to produce BD-X and AD-Y. If X and Y interact the fragmented GAL4 transcription factor is functionally reconstituted, thereby driving the expression of reporter genes (e.g. *HIS3, ADE2* or *lacZ*). (B) If X and Y do not interact, the *GAL4* transcription factor BD and AD fragments remain in isolation, and transcription of the reporter gene does not occur.

Reporter genes must encode proteins whose function/phenotype can be easily assessed, and these include the more commonly used auxotrophic growth markers (e.g. *LEU2, HIS3, ADE2, URA3, LYS2*), whose activation enables yeast to grow on defined minimal media lacking specific amino acids, as well as the *lacZ* gene, which encodes the beta-galactosidase enzyme. Therefore, interactions between bait and prey proteins in yeast, can be translated into a transcriptional readout which results in growth of yeast on selective media and colour development when using a colorimetric substrate such as X-Gal in the β-galactosidase assay (Brückner *et al.*, 2009). Current Y2H screens usually assay two or more reporter genes in parallel, increasing stringency of the screen and the reliability of data.

The Y2H system is efficient and easy to use, and as such it has become one of the most common and successfully used high-throughput methods to investigate binary protein interactions (Dreze *et al.*, 2010). For large-scale screenings, there are two distinct, commonly used screening approaches: the matrix mating (or array) approach, in which baits are screened against an array of defined preys (pair-wise interaction analysis), and the library approach, in which baits are screened against high complexity prey cDNA libraries (cDNA library screening). In the matrix approach, various combinations of full-length or truncated open reading frames (ORFs) can be systematically tested through direct mating with a collection of defined bait and prey clones expressed in yeast with different mating types (e.g. mating type *a* for baits against type *α* for preys) (Brückner *et al.*, 2009). This approach is easily automated and has been fundamental for global interactome studies. It was originally used to generate an overview of the yeast proteome, screening various combinations of the 6,000 ORFs which were cloned into bait and prey vectors, identifying over 5,600 interactions, a 70% coverage of the yeast proteome (Fields *et al.*, 2000; Ito *et al.*, 2001). The defined bait position in a matrix allows quick identification of interacting preys without sequencing. In the 'classical' library approach, a defined bait is used to carry out a comprehensive screen of cDNA-libraries, which contain pools of random full-length and fragmented prey ORF clones, identifying large numbers of novel interaction partners for a given bait protein of interest (Brückner *et al.*, 2009).

Several variations on the 'classical' Y2H system have since been devised, involving different DNA-binding domains derived from the *Escherichia coli* LexA protein, transcriptional activation domains derived from the herpes simplex virus VP16 protein, and various reporter gene combinations (Brückner *et al.*, 2009).

1.7.3.1 Advantages and limitations *of Y2H*

The yeast two-hybrid (Y2H) system is able to detect protein interactions in a cellular '*in vivo'* environment, and since it is a relatively simple, cost-effective technique which can be easily adapted for high-throughput studies, it is now considered one of the most widely and successfully used systems of choice for the detection of binary protein-protein interactions (Brückner *et al.*, 2009).

There are limitations associated with yeast two-hybrid (Y2H) methods which are imposed by the occurrence of false negative and false positive interactions. False negative interactions are true interactions that cannot be detected in the 'classical' Y2H screening methodology due to inherent technical limitations. These include interactions involving membrane proteins, proteins which require post-translational modifications, or self-activating proteins. False negative interactions can be caused by a number of factors: (i) failure in nuclear localisation – once bait and prey are expressed they must be able to enter or be stably expressed in the yeast nucleus in order to activate transcription of downstream reporter gene; (ii) incorrect folding of the fusion proteins – the BD or AD fusion moiety may obstruct the site of interaction, or cause steric hindrance which prevents protein interaction; (iii) co-factors or post-translational modifications – may be different or lacking in yeast (host organism). Proper folding or post-translational protein modification may be required for certain protein interactions, particularly interactions between proteins of higher eukaryotes (Brückner *et al.*, 2009; Rodríguez-Negrete, Bejarano and Castillo, 2014).

False positive interactions detected in the context of the 'classical' Y2H methodology are non-specific interactions. These are not reproducible in any independent system and are therefore physiologically meaningless. Some of the possible reasons for the

occurrence of false positive interactions in yeast include: (i) overexpression of bait and prey proteins and their localisation in a 'foreign' environment. Human proteins in particular, are localised in a compartment which is not their natural environment, and this promotes the formation of non-specific interactions; (ii) self-activating bait protein – which can activate reporter gene transcription in the absence of prey; (iii) proteins that directly bind and activate reporter promoters – this can be reduced when two or more reporter genes are assayed increasing the stringency of the assay; (iv) proteins known to be intrinsically "sticky" or incorrectly folded can lead to formation of non-specific interactions (Brückner *et al.*, 2009; Rodríguez-Negrete, Bejarano and Castillo, 2014). Regardless of the limitations highlighted above, the Y2H system remains a powerful tool for large-scale binary protein-protein interaction screening.

The 'classical' Y2H system generated by Fields and Song (1989), has been used to develop several alternative variants to overcome the limitations associated with compartment and cell-type, increasing coverage and reliability associated with Y2H systems (Suter, Auerbach and Stagljar, 2006). Some of these variant Y2H methodologies are designed to detect interactions between membrane proteins (e.g. membrane yeast two-hybrid, MYTH), cytosolic proteins (e.g. split-TEV system), or even protein interactions in mammalian cells (e.g. mammalian protein-protein interaction trap, MAPPIT), some of which have been adapted for large-scale screens (Suter, Kittanakom and Stagljar, 2008).

1.7.4 Membrane Yeast two-Hybrid (MYTH)

Almost one-third of all genes across various organisms encode integral membrane and/or membrane-associated proteins (Stagljar and Fields, 2002). Integral membrane proteins are one of the most biologically important protein classes, with key roles in various cellular processes which includes cell signalling, molecular transport, metabolism and cell structure maintenance (Stagljar and Fields, 2002; Engel and Gaub, 2008; Cordwell and Thingholm, 2010). Many integral membrane proteins have been functionally linked to disease, making them particularly

significant as potential drug targets, with the majority of current therapeutics directed towards altering their function (Overington, Al-Lazikani and Hopkins, 2006). The identification and characterisation of membrane protein-protein interactions and subsequent 'interactome' maps, are key to gaining an insight into the function and mechanism of action associated with this class of proteins (Stagljar and Fields, 2002; Suter, Kittanakom and Stagljar, 2008). Detection of membrane protein-protein interactions (PPIs) is particularly challenging due to their hydrophobic nature and non-nuclear localisation, making them difficult to analyse using conventional interaction detection methods (Stagljar *et al.*, 1998). However, the biological and clinical importance of this class of proteins encouraged the development of the membrane yeast two-hybrid (MYTH) system, which allows the high-throughput identification of PPIs involving full-length integral membrane proteins and membrane-associated proteins in an *in vivo* setting inside cellular membranes, using the model organism *Saccharomyces cerevisiae* as a host (Stagljar *et al.*, 1998; Iyer *et al.*, 2005; Paumi *et al.*, 2007). In contrast to the 'classical' Y2H system, there is no need for the bait and prey proteins, once expressed, to enter the nucleus.

MYTH is a powerful tool which exploits the concept of 'split-ubiquitin', the notion that ubiquitin, a small and evolutionary conserved protein that functions as a tag, marking proteins for degradation by the 26S proteasome (Hershko, 2005), can be separated into two moieties: C-terminal (C_{ub}) and N-terminal (N_{ub}) fragments, that can spontaneously re-associate *in vivo* to form a full-length 'pseudo-ubiquitin' molecule due to their high affinity for one another (Figure 1.3 A). This strong affinity can be blocked though the introduction of an isoleucine 13 to glycine mutation, producing a mutated $N_{ub}G$ fragment which has almost no affinity for C_{ub} when co-expressed in the same cell (Figure 1.3 B). As shown in Figure 1.3 C, the 'split-ubiquitin' principle is easily adapted for use as a protein-protein interaction 'sensor' (Johnsson and Varshavsky, 1994; Stagljar *et al.*, 1998).

Figure 1.3

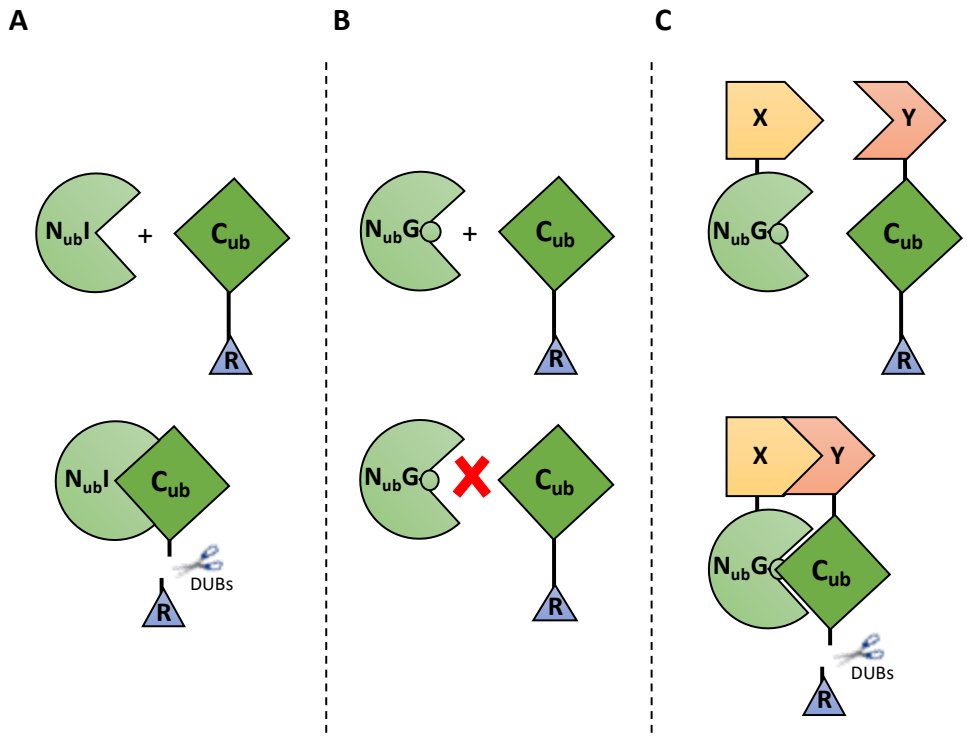

Figure 1.3. Principle of 'split-ubiquitin'. (A) Wild-type ubiquitin can be split into N-terminal ($N_{ub}I$, light green) and C-terminal (C_{ub}, dark green) fragments, which can spontaneously re-associate. The 'pseudo-ubiquitin' molecule formed can be recognized by cytosolic deubiquitinating enzymes (DUBs) which releases the reporter. (B) A point mutation at position 13 from an isoleucine to glycine ($N_{ub}G$) prevents spontaneous re-association. Interacting proteins, X and Y, are fused to the $N_{ub}G$ and C_{ub} domains, respectively. If X and Y interact, $N_{ub}G$ and C_{ub} domains are brought into close proximity which causes partial re-association of ubiquitin, recognition by DUBs and release of reporter. Adapted from Fetchko and Stagljar, 2004.

In the 'split-ubiquitin'-based membrane yeast two-hybrid (MYTH) system (Figure 1.4), the membrane protein of interest (bait) is tagged at its N or C terminus to the C-terminal half of ubiquitin (C_{ub}), along with an artificial transcription factor (TF) composed of the bacterial LexA DNA-binding domain (BD) and the herpes simplex virus VP16 transcriptional activation domain (AD), which is used as a cleavable reporter protein (Brückner *et al.*, 2009). Membrane-bound or cytosolic interacting proteins (preys) are tagged at either their N or C terminus to the mutated N-terminal half of ubiquitin (N_{ub}) fragment, $N_{ub}G$, so as to prevent spontaneous re-association

of the split-ubiquitin fragments. For high-throughput applications, prey $N_{ub}G$-fused cDNA libraries can also be generated and used to identify novel interaction partners for a given membrane protein of interest (bait) (Snider *et al.*, 2010).

Both bait and prey proteins are co-expressed in an *S.cerevisiae* host. Following a direct interaction between bait and prey proteins, the C_{ub} and $N_{ub}G$ fragments are brought into close proximity, allowing the reconstitution of the 'pseudo-ubiquitin' molecule which can be recognised by the cytosolic proteases, DUBs (Johnsson and Varshavsky, 1994; Stagljar *et al.*, 1998; Snider *et al.*, 2010). DUBs (deubiquitinating enzymes) are a class of proteases involved in the de-conjugation of ubiquitin from proteins targeted for degradation, through the hydrolysis of the amide bond between the protein and the C-terminal residue of ubiquitin (Love *et al.*, 2007; Snider *et al.*, 2010). As a result of this reaction, the artificial TF (LexA-VP16) is released from the membrane and translocates to the nucleus, where it activates reporter gene transcription (e.g. *HIS3, ADE2* and *lacZ*) (Snider *et al.*, 2010).

Figure 1.4

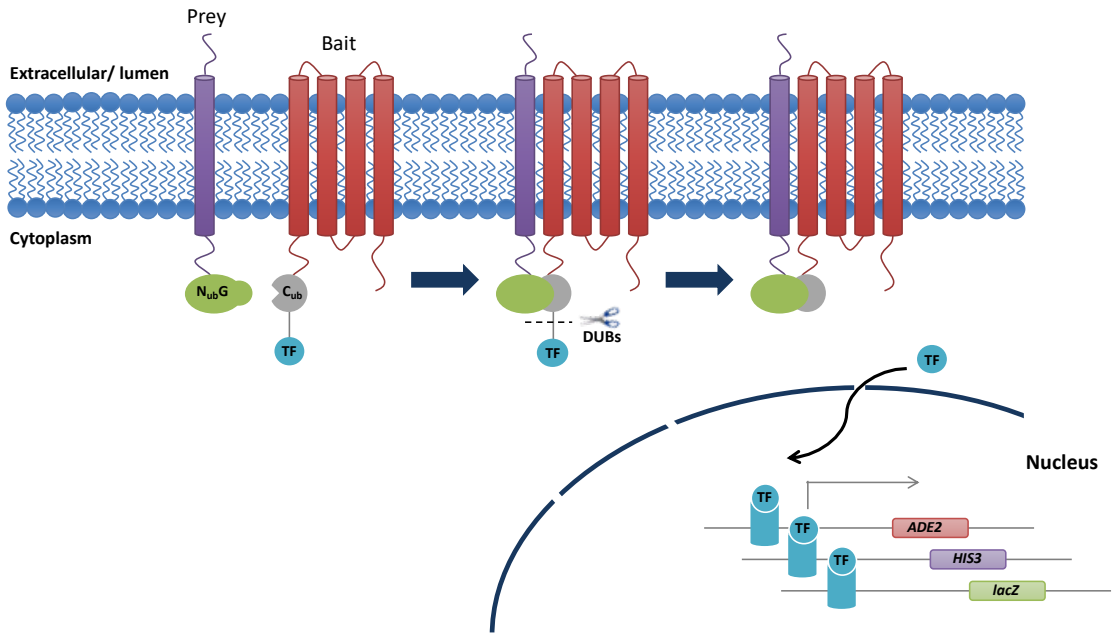

Figure 1.4. 'Split-ubiquitin' based membrane yeast two-hybrid (MYTH) system. Bait (red) and prey (purple) proteins are tagged with C_{ub}-LexA-VP16 and $N_{ub}G$, respectively. Interaction between bait and prey proteins enables the $N_{ub}G$ and C_{ub} fragments to associate and form a 'pseudo-ubiquitin' which can be recognized by

cytosolic DUBs. DUBs cleave after the terminus of the C_{ub} tag, releasing the LexA-VP16 transcription factor (TF). The TF can enter the nucleus and activate the reporter system. Additionally, even though a membrane-bound prey protein is depicted in the figure above, the MYTH system is just as effective using preys with cytosolic localisation. Adapted from Snider *et al.*, 2010.

Reporter genes typically used in the MYTH screen are the same as those used in the 'classical' Y2H system, which include the more commonly used auxotrophic growth markers (e.g. *HIS3,* and *ADE2*) as well as the *lacZ* gene, which encodes the beta-galactosidase enzyme. Interactions between bait and prey proteins in yeast can therefore be translated into a transcriptional readout resulting in growth of yeast on selective media and yeast colour development in a β-galactosidase assay (Stagljar *et al.*, 1998; Iyer *et al.*, 2005; Paumi *et al.*, 2007).

This system has been successfully adapted for use in cDNA library screens (Thaminy *et al.*, 2003; Wang *et al.*, 2004) and large-scale matrix approaches (Pandey and Assmann, 2004; Miller *et al.*, 2005) to identify and characterise binary protein-protein interactions between integral membrane proteins, membrane-associated proteins and cytosolic proteins in their natural environment. MYTH is sensitive enough to be able to detect both transient and stable interactions of exogenously and endogenously expressed proteins (Snider *et al.*, 2010).

1.7.4.1 Advantages and limitations of MYTH

The membrane yeast two-hybrid (MYTH) system is a powerful tool which, unlike the 'classical' Y2H system, allows the investigation of protein-protein interactions involving full-length membrane proteins and/or membrane-associated proteins *in vivo* and *in situ*, as there is no need for nuclear localisation (Stagljar *et al.*, 1998; Iyer *et al.*, 2005; Paumi *et al.*, 2007). There is however a requirement for membrane proteins to have their N and/or C terminus located in the cytosol (Snider *et al.*, 2010). In addition, the MYTH system is relatively simple and can easily be adapted for high-throughput studies, which include large-scale matrix and library screening applications, as well as smaller-scale interaction studies. Although it is not suitable

for use with cytosolic bait proteins, interactions involving both membrane-bound and cytosolic proteins can be detected (Snider *et al.*, 2010).

All yeast two-hybrid (Y2H) methods have limitations associated with the occurrence of false positive and false negative interactions, caused by a number of common factors. For example, false negative interactions can occur as a result of increased steric hindrance caused by either the C_{ub}-LexA-VP16 tag on the bait protein in the MYTH system or the BD or AD fusion moiety in the 'classical' Y2H system, which affects certain protein-protein interactions (Brückner *et al.*, 2009). Alternatively, false positive interactions can occur in both the MYTH system and the 'classical' Y2H system, if the bait protein can activate the reporter system in the absence of an interacting prey, it is known to 'self-activate'. In the MYTH system, the level of 'self-activation' can be assessed using the $N_{ub}G/N_{ub}I$ control test. If a bait shows some level of 'self-activation' the stringency of the selective medium can be increased using the *HIS3* competitive inhibitor 3-amino-1,2,4-triazole (3-AT), which, if used, must be consistent throughout the screening process (Snider *et al.*, 2010).

1.8 Aims

Hereditary spastic paraplegias (HSPs) are a large, genetically diverse group of disorders characterised by progressive lower limb spasticity and pyramidal weakness. This defining clinical feature is thought to be length-dependent axonopathy affecting the distal ends of corticospinal tract axons, for which gene mutation is a major causative factor. However, the genetic basis of many cases of HSP and the factors that control age-of-onset or severity remain unclear. Identification of genetic mutations that contribute to inherited forms of HSP provides valuable insight into the molecular mechanisms and pathogenesis of this group of disorders, as well as improving our understanding of the cellular processes required for axonal maintenance or degeneration.

Although increasing numbers of HSP-related genes are being identified, in many cases the underlying mechanistic changes that lead to an HSP phenotype remain

uncharacterised. We hypothesise that proteins that interact with known disease-causing HSP proteins may in some cases also acquire mutations that contribute to specific HSP-related phenotypes. Therefore, identification of proteins that interact with known HSP proteins, or exist in common molecular complexes, may provide new insight into the molecular mechanisms fundamental to the pathogenesis of this group of disorders.

To improve our understanding of the pathogenic mechanisms that contribute to the onset and progression of HSPs, we aim to perform a systematic investigation of HSP protein interactions. The net result will be an extended high-density map of the human HSP interactome, thereby providing a resource to guide future hypothesis-driven research, as well as for the development of new strategies for therapeutic intervention.

Specific aims of the project:

1. To generate an initial high-density HSP interactome consisting of all known and predicted interaction partners.
2. To selectively test a set of binary HSP:HSP interactions using the 'classical' yeast two-hybrid system.
3. To selectively test a set of predicted binary HSP:RING E3 ligase and HSP:DUB interactions using the 'classical' yeast two-hybrid system to understand more about changes in ubiquitination in HSP.
4. To generate a set of HSP disease-related mutant proteins which can be used to conduct high-throughput interaction profiling, in order to identify novel edgetic effects within the HSP interactome.
5. To identify novel binary HSP interaction partners using the 'classical' yeast two-hybrid library system.
6. To identify novel binary protein-protein interactions involving full-length membrane and membrane-associated HSP proteins using the optimised membrane yeast two-hybrid library system.
7. To integrate all binary HSP interaction data obtained, into an updated HSP interactome, which can then be used for bioinformatics analyses to predict areas

of interest and functional relevance, as well to guide future hypothesis-driven research.

Chapter 2: Materials & Methods

2.1 Molecular Biology

2.1.1 Reagents

Custom DNA Primers, TRIzol® reagent (#15596026), SuperScript™ III Reverse Transcriptase (#18080093), SYBR® Safe DNA Gel Stain (#S33103), Gateway® BP clonase® II (#11789020) and LR clonase® II (#11791020) enzyme kits were all obtained from Invitrogen (paisley, UK). dNTP Set (100 mM, #28-4065-52) was purchased from GE Healthcare Life Sciences (Buckinghamshire, UK). KOD Hot Start DNA Polymerase (#71086-3) was from Novagen (distributed by Merck Chemicals Ltd, Nottingham, UK). BIOTAQ™ DNA Polymerase (#BIO-21060), Hyperladder™ 1kb (#BIO-33026), Agarose, Molecular Grade (#BIO-41025) and α-Select Competent Cells, Silver Efficiency (#BIO-85026) were all purchased from Bioline Reagents Ltd (London, UK). Tris-Borate-EDTA (TBE) buffer 10X (#10031223) was from Fisher Scientific (Loughborough, UK). Antarctic phosphatase (#M0289S) and all restriction endonucleases used, were obtained from New England Biolabs (Hertfordshire, UK). Wizard ® *Plus* SV Minipreps DNA Purification System (#A1460) and RQ1 RNase-Free DNase (#M6101) was from Promega (Southampton, UK) whilst HiSpeed Plasmid Maxi kits (#12662), QIAquick® Gel Extraction kit (#28704) and QIAquick® PCR Purification kit (#28104) were all from QIAGEN (Manchester, UK). Yeast Extract (#YEA03), D(+)-Glucose Anhydrous (#GLU03), Tryptone (#TRP02) were all from Foremedium (Norfolk, UK), whilst the BioAgar (#400-050) was obtained from BioGene (Huntingdon, UK). All other reagents, unless otherwise stated, were obtained from Sigma-Aldrich (Dorset, UK).

2.1.2 Amplification of α-Select Competent Cells

The α-Select Competent Cells were initially purchased from Bioline and then amplified using the following protocol. A 5 μL aliquot of α-Select Competent Cells was grown in 5 mL SOC media (Table 2.1) at room temperature (RT), with gentle

rocking for 20 h or until the OD_{600} reached 0.6-0.8. Once grown, 200 μL of culture was used to inoculate 250 mL SOC media and grown at room temperature (RT) with gentle rocking, until the OD_{600} reached 0.6-0.8 (approx. 40 h). The culture was cooled and stored at 4 °C for 3 h prior to centrifugation at 2600 rpm, 4 °C for 15 min. 80 mL of the CCMB80 buffer, pH 6.4 (Table 2.2) was used to resuspend the bacterial pellet, and left on ice for 30 min prior to centrifugation at 2600 rpm, 4 °C for 15 min. 8 mL of the CCMB80 buffer was used to resuspend the bacterial pellet to achieve an OD_{600} of 1.5-2.0, and left on ice for 15 min. Aliquots (100-200 μL) were flash-frozen in methanol cooled to -80 °C, and stored at -80 °C.

Table 2.1

Reagent	Final concentration
KCl	2.5 mM
NaCl	10 mM
$MgCl_2$	10 mM
$MgSO_4$	10 mM
D-(+)-Glucose	20 mM
Yeast Extract	0.5 % (w/v)
Tryptone	2 % (w/v)

Table 2.1. Constituents required to make SOC medium. Media was made up with double-distilled water and autoclaved.

Table 2.2

Reagent	Final concentration
KOAc (pH 7)	10 mM
$CaCl_2.2H_2O$	80 mM
$MnCl_2.4H_2O$	20 mM
Glycerol	10 % (w/v)

Table 2.2. Constituents required to make the CCMB80 buffer. Buffer was made up in double-distilled water and pH adjusted to 6.4.

2.1.3 Agarose gel electrophoresis

Agarose gels (0.6-1.0 % w/v) were prepared by adding molecular grade agarose to 0.5X TBE buffer. The mixture was heated, allowing the agarose to dissolve completely. SYBR® Safe DNA Gel Stain (1:20,000) was added once cooled, the gel was poured and left at room temperature to set. DNA samples were made up in 1%

Orange G DNA loading buffer (5 % w/v glycerol, 0.05 % Orange G) and resolved in 0.5X TBE buffer in a horizontal mini/midi-electrophoresis tank (Bio-Rad, Hertfordshire, UK) alongside Hyperladder™ 1kb standard (5 μL/well), at 120 V for 15 min to 1 h. DNA bands were visualised using an ultraviolet (UV) light source.

2.1.4 Sequencing

Sequencing of all DNA constructs was performed by automated fluorescent DNA sequencing by GATC Biotech (Konstanz, Germany). Following purification, sequencing of the 5' end of yeast colony PCR products was performed by automated fluorescent DNA sequencing by GATC Biotech (Konstanz, Germany).

2.1.5 Bacterial glycerol stocks

Glycerol stocks of transformed bacterial cells, containing sequence-verified constructs, were made from 10 mL 2X TY medium (Table 2.3) plus appropriate antibiotic culture which was previously inoculated with a single bacterial colony and grown at 37 °C, 220 rpm for 16 h. A 200 μL aliquot of overnight bacterial culture was combined with 80 μL sterile glycerol (80 % v/v) in a labelled 1.5 mL microcentrifuge tube, prior to storage at -80 °C.

Table 2.3

Reagent	**g/L**
NaCl	5
Yeast Extract	10
Tryptone	16
BioAgar*	20

Table 2.3. Constituents required to make 2X TY medium. All media was made up with double-distilled water and autoclaved. (*for solid media only)

2.1.6 RNA extraction and cDNA synthesis

2.1.6.1 RNA extraction

RNA was extracted from HEK293T, A549, HeLa and K-562 cell lines. RNaseZAP™ (Sigma-Aldrich) was used on all work surfaces, removing any RNase. To a 10 cm dish of confluent cells (80-100 %), 1 mL TRIzol® reagent (Invitrogen) was added and incubated at room temperature until all the cells had detached from the dish. Cells were transferred into a 1.5 mL microcentrifuge tube, with the help of a cell scraper. Next, 200 μL chloroform was added, and samples shaken vigorously for 15 sec. Samples were centrifuged at 13,000 rpm, RT for 15 min separating into three layers: a clear, aqueous phase (top), white precipitated DNA (middle) and a pink organic phase (bottom). The clear phase (top layer) was carefully transferred into a clean 1.5 mL microcentrifuge tube and gently mixed with 500 μL isopropanol. Samples were incubated at room temperature for 10 min, followed by centrifugation at 13,000 rpm, RT for 10 min. The RNA pellet was washed with 1 mL 75 % ethanol solution, centrifuged at 7,000 rpm, RT for 5 min and washed again with 1 mL 75 % ethanol solution. Samples were kept on ice or stored at -20 °C.

2.1.6.2 DNase treatment and cDNA synthesis

Ethanol was removed, and RNA pellets left to air-dry for 10-20 min, before 30 μL DEPC-treated water was added and gently mixed. RNA concentration was estimated, using a spectrophotometer to measure the optical density at 260 nm. The DNase reaction mixture (Table 2.4 A) was set up in 0.2 mL PCR tubes and incubated at 37 °C for 30 min. Next, 1 μL RQ1 DNase Stop Solution was added and incubated at 60 °C for 15 min, inactivating the DNase and terminating the reaction. DNase treated RNA samples were placed on ice. The reaction mixture (Table 2.4 B) was set up using DNase-treated RNA from the previous step in clean 0.2 mL PCR tubes and incubated at 65 °C for 5 min. Samples were immediately placed on ice. These samples were used in the reaction mixture shown in Table 2.4 C and cycled in a thermocycler as described (Table 2.4 D). The RNA samples are now thought to be successfully converted into cDNA, which can be used immediately or stored at -20 °C.

Table 2.4

A

Reagent	µL/reaction	Final concentration
RQ1 RNase-free DNase	1	-
RQ1 DNase 10X reaction buffer	1	-
RNA sample	X (1.4 µg)	1X
DEPC-treated H_2O	8-X	-
TOTAL	10	-

B

Reagent	µL/reaction	Final concentration
DNase-treated RNA	**4**	**-**
Random hexamers (100 ng/µL)	2	14.29 ng/µL
dNTPs (10 mM)	1	0.714 mM
DEPC-treated H_2O	7	-
TOTAL	14	-

C

Reagent	µL/reaction	Final concentration
DNase-treated RNA sample	**14**	**-**
SuperScript™ III RT (200 U/µL)	1	10 U
5X First-Strand Buffer	4	1X
DTT (0.1 M)	1	5 mM
TOTAL	20	-

D

Step	Temperature (°C)	Duration
1	25	5 min
2	50	60 min
3	70	15 min
4	4	Forever

Table 2.4. Multi-step reaction mixtures and cycling parameters for cDNA synthesis. Reagents and volumes required for each of the following steps: (A) DNase treatment of RNA, (B) and (C) Reverse transcription of DNase-treated RNA. Thermal cycling parameters for cDNA synthesis (D).

2.1.7 ORF cloning from cDNA and cDNA libraries

Open reading frames (ORFs) were initially amplified from cDNA or cDNA libraries by polymerase chain reaction (PCR) using KOD Hot Start DNA polymerase and specific primers designed to the 5' and 3' end of the coding mRNA sequence (CDS) and

containing the Gateway® *attB* recombination site sequences necessary for the subsequent BP reaction. These recombination sequences were:

Forward primer:

5' GAATTCACAAGTTTGAAAAAAGCAGGCTGGATG [gene-specific sequence] 3'

Reverse primer:

5' GTCGACCACTTTGTACAAAGCTGGGTG [gene-specific sequence] 3'

A typical KOD PCR reaction is shown in Table 2.5. Following PCR amplification, a sample (10 μL) of the reaction was analysed by gel electrophoresis, for correct fragment size, before continuing with subsequent Gateway® cloning.

Table 2.5

A

Reagent	μL/reaction	Final concentration
Forward primer (10 μM)	0.5	0.2 μM
Reverse primer (10 μM)	0.5	0.2 μM
10X KOD buffer	2.5	1X
$MgSO_4$ (25 mM)	1.5	1.5 mM
dNTPs (2 mM)	2.5	0.2 mM
KOD polymerase	0.5	-
cDNA/cDNA library	X (280 ng)	-
Nuclease-free H_2O	17-X	-
TOTAL	25	-

B

Step	Cycles	Temperature (°C)	Duration
1	1	95	2 min
2	30-40*	95	30 s
		55-68**	1 min
		72	30 s/kb
3	1	4	Forever

Table 2.5. Master mix and cycling parameters for a typical KOD Hot Start DNA polymerase chain reaction. (A) Reaction master mix was set up in thin-walled PCR tubes, using reagents and volumes stated. (B) KOD PCR was cycled as indicated.
*30 cycles for amplification from plasmid DNA, 40 cycles from cDNA.
**Annealing temperatures vary depending on the predicted melting temperature (Tm) of the individual primers used.

2.1.8 Gateway® Cloning

Gateway® Technology (Invitrogen) was employed as the main cloning strategy for the generation of the HSP constructs used in this study, which enables quick and easy shuttling of ORFs into a range of expression vectors.

2.1.8.1 Gateway® BP reaction

Following PCR amplification, *in vitro* recombination of ORFs containing *attB* sites and the donor vector pDONR223 (containing *attP* sites) was performed to generate entry clones, via a BP recombination reaction using the Gateway® BP clonase® II enzyme kit.

The reactions were set up on ice as detailed in Table 2.6 and incubated at 25 °C for 16 h. Following incubation, Proteinase K (0.5 μL) was added to each reaction and further incubated at 37 °C for 10 min, allowing the remaining clonase enzymes to be digested, before storing at -20 °C or immediately using in bacterial transformation.

Table 2.6

Reagent	μL/reaction
attB-PCR product	1.5
attP donor vector (pDONR223)	X (100 ng)
BP clonase® II enzyme mix	1
Nuclease-free H_2O	2.5-X
TOTAL	5

Table 2.6. BP recombination reaction mixture. Reaction mixture was set up on ice, using reagents and volumes stated.

2.1.8.2 Gateway ® LR reaction

LR recombination reactions involve the *in vitro* recombination of entry clones (containing *attL* sites) and various destination vectors (containing *attR* sites), to generate expression clones, using the Gateway® LR clonase® II enzyme kit. The reactions were set up on ice, as detailed in Table 2.7, with equal amounts of entry clone and destination vector (100 ng). They were incubated at 25 °C for 16 h,

followed by Proteinase K (0.5 μL) addition and further incubation at 37 °C for 10 min, allowing the remaining clonase enzymes to be digested, before storing at -20 °C or immediately using in bacterial transformation.

Table 2.7

Reagent	μL/reaction
attL entry clone	X (100 ng)
attR destination vector	Y (100 ng)
LR clonase® II enzyme mix	1
Nuclease-free H_2O	4-X-Y
TOTAL	5

Table 2.7. LR recombination reaction mixture. Reaction mixture was set up on ice, using reagents and volumes stated.

2.1.9 Seamless Ligation Cloning Extract (SLiCE)

The Seamless Ligation Cloning Extract (SLiCE) method, recently developed in the Motohashi lab (Kyoto, Japan), exploits the homologous recombination activities of *E. coli* cell lysates to assemble DNA fragments into a vector, and as such is a relatively novel seamless DNA cloning tool (Motohashi, 2015). SLiCE is a relatively simple, low-cost homemade alternative to the many commercially available seamless DNA cloning kits. The primer sequences contain 15-21 bases homologous to the linear ends of the vector, followed by 18-21 bases homologous to the gene of interest. PCR reagents and cycling parameters are outlined in Table 2.5.

2.1.9.1 SLiCE extract preparation

The SLiCE extract can be prepared from any RecA (-) strain of bacteria, using the following protocol. 5 mL 2X LB media was inoculated (Table 2.8) with 5 μL RecA (-) bacterial strain (α-select competent cells) and incubated at 37 °C, 220 rpm for 16 h.

Table 2.8

Reagent	g/L
NaCl	20
Yeast Extract	10
Tryptone	20
BioAgar*	20

Table 2.8. Constituents required to make 2X LB medium. All media was made up with double-distilled water and autoclaved (*for solid media only).

The culture was diluted with a further 45 mL 2X LB media, transferred to a 500 mL flask and incubated at 37 °C, 220 rpm for 3 h or until the OD_{600} reached 0.3 for a 1:10 dilution sample. Bacteria were harvested by centrifugation at 4 °C, 4,300 rpm for 20 min and supernatant discarded. Bacterial pellet was resuspended in 50 mL ice-cold sterile ddH_2O before centrifugation at 4 °C, 4,300 rpm for 10 min. Again, supernatant was discarded, and pellet was resuspended in 1.2 mL 3 % (w/v) Triton X-100 in 50 mM Tris-HCl (pH 8) and transferred to 2 mL microcentrifuge tube. The mixture was incubated at RT for 10 min, followed by centrifugation at 4 °C, 13,000 rpm for 5 min. Supernatant was transferred to a microcentrifuge tube and one volume of ice-cold 80 % glycerol was added. Aliquots (50 μL) were flash-frozen in liquid nitrogen and stored at -80 °C. The SLiCE buffer was prepared as shown in Table 2.9, sterile filtered, and stored at -20 °C in 1 mL aliquots.

Table 2.9

Reagent	Volume (mL)	Final concentration
1 M Tris-HCL, pH 7.5	5	500 mM
1 M $MgCl_2$	1	100 mM
100 mM ATP	1	10 mM
100 mM DTT	1	10 mM
ddH_2O	2	-

Table 2.9. Constituents required to make the SLiCE buffer.

2.1.9.2 SLiCE reaction

The SLiCE reactions were set up on ice, as detailed in Table 2.10, and incubated at 37 °C for 15-30 min, followed by immediate bacterial transformation or storage at -20 °C.

Table 2.10

Reagent	μL/reaction
PCR insert	X (30 ng)
Linearised vector	Y (10 ng)
10X SLiCE buffer	1
SLiCE extract	1
Nuclease-free H_2O	8-X-Y
TOTAL	10

Table 2.10. SLiCE reaction mixture. Reaction mixture was set up on ice, using reagents and volumes stated, and then incubated at 37 °C for 30 min.

2.1.10 Transformation of chemically competent bacterial cells

Gateway® BP and LR reactions were transformed into chemically competent α-select silver efficiency cells. α-select cells were thawed on ice and 25 μL aliquots were added to pre-cooled 2 mL microcentrifuge tubes. 2 μL BP or LR reaction mixture was added to the thawed cells and incubated on ice for 30 min. Cells were heat-shocked (42°C for 45 sec) in a water bath and immediately returned to ice for 2 min. SOC media (250 μL) was added to the cells followed by incubation at 37 °C, 220 rpm for 1 h. 200 μL sample of the culture was plated onto 2X TY agar plates supplemented with the appropriate antibiotic, depending on the plasmid and incubated at 37 °C for 16 h.

2.1.11 Diagnostic bacterial colony PCR (BC-PCR)

Diagnostic BC-PCR was performed to test Gateway® cloning reactions, and whether bacterial transformation of a DNA construct had been successful. All BC-PCR reactions were carried out using BIOTAQ™ DNA Polymerase using vector-specific primers (see Appendix 2.1). A typical BC-PCR reaction and cycle are shown in Table 2.11. Following BC-PCR, samples were analysed by gel electrophoresis, for correct insert size.

Table 2.11

A

Reagent	μL/reaction	Final concentration
Forward primer (10 μM)	0.7	0.7 μM
Reverse primer (10 μM)	0.7	0.7 μM
10X NH_4 buffer	1.0	1X
$MgCl_2$ (50 mM)	0.4	2 mM
dNTPs (25 mM)	0.25	0.625 mM
BIOTAQ™ DNA polymerase	0.05	-
Nuclease-free H_2O	6.9	-
TOTAL	10	-

B

Step	Cycles	Temperature (°C)	Duration
1	1	95	5 min
2	35	95	1 min
		55-68*	1 min
		72	1 min/kb
3	1	72	5 min
4	1	4	Forever

Table 2.11. Master mix and cycling parameters for a typical BC-PCR. (A) Reaction master mix was set up in thin-walled PCR tubes on ice, using reagents and volumes stated. Half of a bacterial colonies were picked with sterile toothpicks and resuspended in the BC-PCR reaction mixture. (B) BC-PCR was cycled as indicated. *Annealing temperatures vary depending on the predicted melting temperature (Tm) of the individual primers used.

2.1.12 DNA plasmid purification

Positive bacterial colonies were selected for subsequent plasmid DNA purification. The remainder of the bacterial colony was picked with a sterile toothpick and used to inoculate 9 mL 2X TY broth supplemented with appropriate antibiotic and grown at 37°C, 220 rpm for 16 h. Bacterial glycerol stocks were made from the overnight culture as described previously in section 2.1.5. The remainder of the bacterial culture was then pelleted by centrifugation (4000 rpm, 4 °C, 10 min), supernatant was removed, and DNA purified using the Wizard ® *Plus* SV Minipreps DNA Purification System (Promega) according to the manufacturer's protocol. Following correct sequencing analysis, the glycerol stocks of the positive bacterial colonies were used to inoculate 2X TY broth supplemented with appropriate antibiotic and

overnight cultures were then used for DNA purification using the HiSpeed Maxiprep kit (QIAGEN). The concentration for both mini/maxi-prep DNA was estimated, by measuring the optical density at 260 nm, using a spectrophotometer.

2.1.13 Site-directed mutagenesis

To investigate the potential interaction profile changes caused by disease-specific mutations, mutants were made using a similar protocol (see Figure 2.1) to that developed for the QuickChange II Site-Directed Mutagenesis approach (Agilent Genomics). Reactions were set up using KOD Hot Start DNA polymerase (Table 2.12) with sequence-verified pDONR223-ORF constructs and two complementary primers carrying base substitutions in the centre of the primers.

Table 2.12

A

Reagent	μL/reaction	Final concentration
Forward primer (10 μM)	0.5	0.2 μM
Reverse primer (10 μM)	0.5	0.2 μM
10X KOD buffer	2.5	1X
$MgSO_4$ (25 mM)	1.5	1.5 mM
dNTPs (2 mM)	2.5	0.2 mM
KOD polymerase	0.5	-
DNA	X (10 ng)	-
Nuclease-free H_2O	17-X	-
TOTAL	25	-

B i

Step	Cycles	Temperature (°C)	Duration
1	1	95	30 s
2	12-18	95	30 s
		55-60*	1 min
		68	30 sec/kb
3	1	4	Forever

B ii

Type of mutation	Number of cycles
Point mutation	12
Single amino acid change	16
Multiple amino acid insertions/deletions	18

Table 2.12. Master mix and cycling parameters for a typical KOD Hot Start DNA polymerase mutagenesis reaction. (A) Reaction master mix was set up in thin-walled PCR tubes, using reagents and volumes stated. (B i) Mutagenesis KOD PCR was cycled as indicated. (B ii) Step 2 of the cycling parameters changes according to mutation type desired.
*Annealing temperatures vary depending on the predicted melting temperature (Tm) of the individual primers used.

A sample of the PCR reaction mixture was analysed by gel electrophoresis to check that the whole plasmid had been amplified. Following successful amplification, reactions were incubated with 1 μL DpnI and incubated at 37 °C for 1 h. DpnI, a restriction endonuclease, was added to digest any of the original DNA template as it recognizes methylated adenine in the short DNA sequence GATC. DNA replicated in bacteria, like the original template, will be methylated unlike products synthesized *in vitro*, therefore the original product will be digested leaving the mutated DNA construct. A sample of the digest mixture was analysed by gel electrophoresis to check the digest had worked. The remainder was purified using a PCR purification kit (QIAGEN), according to the manufacturer's protocol, followed by bacterial transformation (see section 2.1.10). Following diagnostic BC-PCR, positive colonies were selected for plasmid DNA purification (see section 2.1.12) and sequenced to check that the mutagenesis had worked.

2.1.14 Restriction endonuclease assays

Restriction enzymes and buffers from New England Biolabs (NEB), were used for restriction digests according to the manufacturer's protocol. An initial diagnostic digest was performed for 1 h, digesting 1 μg DNA in a total volume of 10 μL. For cloning reactions, 2-5 μg DNA was digested in a total volume of 50 μL for 2-4 h. An excess of enzyme, equating to no more than 10 % of the total volume, was used.

Figure 2.1

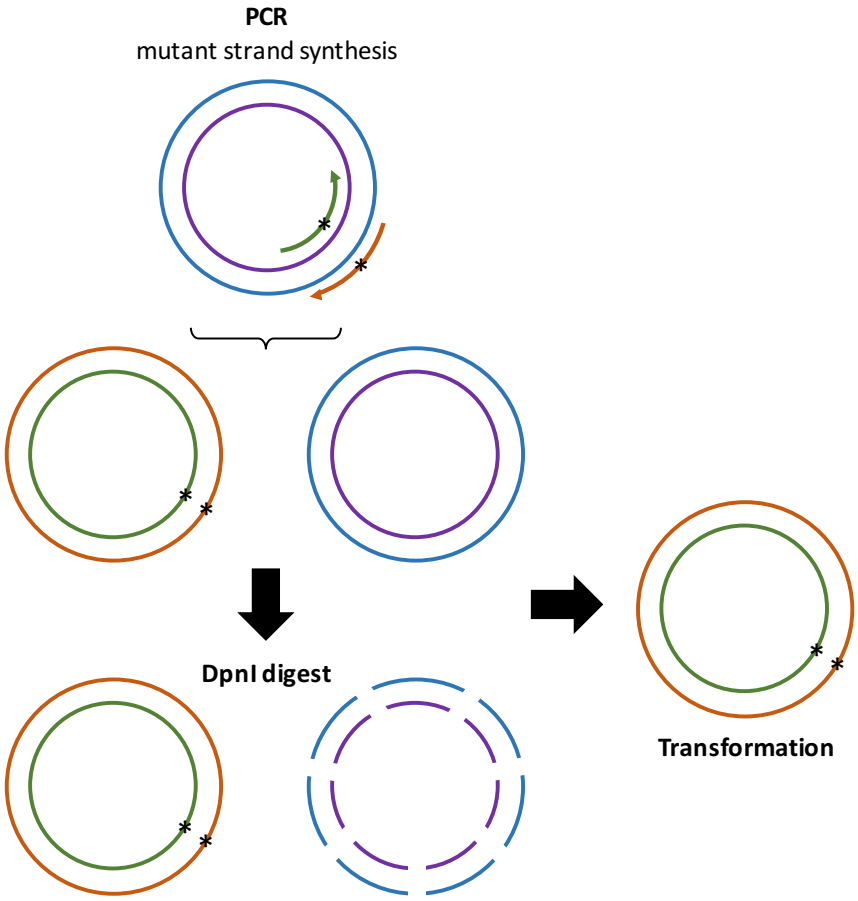

Figure 2.1. Overview of the site-directed mutagenesis method. Complementary primer pairs were designed with the appropriate base substitutions and used to amplify the mutant strand using the original as a template. DpnI digestion of the template DNA was performed prior to bacterial transformation of the mutant. (Adapted from Agilent Genomics)

2.2 Yeast two-Hybrid clone generation and matrix mating

2.2.1 Reagents and media

The yeast two-hybrid strain PJ69-4A (MATa trp1-901 leu2-3, 112 ura3-52, his3-200 gal4Δ gal80Δ LYS2::GAL1-HIS3 GAL2-ADE2 met2::GAL7-lacZ), was used as the bait strain for all Y2H matrix mating assays (provided by Phil James, University of Wisconsin, USA). The PJ69-4A strain carries three independent *GAL4*-responsive reporter genes and was used to create the switched mating-type strain PJ69-4α, a suitable mating partner with an identical genotype.

PJ69-4α (provided by Phil James) was used as the prey strain for all Y2H matrix mating assays. Yeast Extract (#YEA03), D(+)-Glucose Anhydrous (#GLU03), Tryptone (#TRP02), Peptone (#PEP03) and Yeast Nitrogen Base without Amino Acids (#CYN0405) were all from Foremedium (Norfolk, UK), whilst the BioAgar (#400-050) was obtained from BioGene (Huntingdon, UK). Adenine hemisulphate salt (#A9126), DMSO (#D8418), Sodium hydroxide solution (#3574), Lithium acetate dehydrate (LiOAc, #L4158), Poly(ethylene) glycol (PEG 3350, #202444), Deoxyribonucleic acid, single stranded from salmon testes (#D7656), 3-Amino-1,2,4-triazole (3-AT, #A8056) and all amino acids were from Sigma-Aldrich (Dorset, UK). Custom DNA Primers, SYBR® Safe DNA Gel Stain (#S33103) were from Invitrogen (paisley, UK). dNTP Set (100 mM, #28-4065-52) was purchased from GE Healthcare Life Sciences (Buckinghamshire, UK). KOD Hot Start DNA Polymerase (#71086-3) was from Novagen (distributed by Merck Chemicals Ltd, Nottingham, UK). BIOTAQ™ DNA Polymerase (#BIO-21060), Hyperladder™ 1kb (#BIO-33026) and Agarose, molecular grade (#BIO-41025) were all purchased from Bioline Reagents Ltd (London, UK). Tris-Borate-EDTA (TBE) buffer 10X (#10031223) was from Fisher Scientific (Loughborough, UK). 5-bromo-4-chloro-3-indoyl-β-D-galactoside (X-GAL, #7240906) was from Melford Laboratories Ltd (Suffolk, UK). All plastic ware was from STARLAB (Milton Keynes, UK) except for the plastic plates which were from Greiner Bio-One (Gloucester, UK). All other reagents, unless otherwise stated, were obtained from Sigma-Aldrich (Dorset, UK).

Media required for yeast two-hybrid clone generation and matrix matings were prepared in-house (Table 2.13-19). Table 2.13 provides an overview of the various media used in these studies.

Table 2.13

Media	Description	Function
YPAD	Nutrient rich **Y**east Extract **P**eptone **A**denine **D**extrose	Routine yeast growth
SD-W	**S**ynthetic **D**efined Deficient in tryptophan	pGBAE-B (bait) selection and growth
SD-L	Deficient in leucine	pACTBE-B (prey) selection and growth

SD-U	Deficient in uracil	pGBDU (bait) selection and growth
SD-W,LA	Deficient in tryptophan, low adenine	MATa (bait) selection and growth
SD-L,LA	Deficient in leucine, low adenine	MATα (prey) selection and growth
SD-WA	Deficient in tryptophan and adenine	Testing for the auto-activation of pGBAE-B (bait) constructs
SD-WH (3-AT)	Deficient in tryptophan and histidine, supplemented with 3-AT	
SD-UA	Deficient in uracil and adenine	Testing for the auto-activation of pGBDU-GW (bait) constructs
SD-UH (3-AT)	Deficient in uracil and histidine, supplemented with 3-AT	
SD-LA	Deficient in leucine and adenine	Testing for the auto-activation of pACTBE-B (prey) constructs
SD-LH (3-AT)	Deficient in leucine and histidine, supplemented with 3-AT	
SD-WL	Deficient in tryptophan and leucine	Selection and growth of diploid clones pGBAE-B (bait) and pACTBE-B (prey)
SD-UL	Deficient in uracil and leucine	Selection and growth of diploid clones pGBDU-GW (bait) and pACTBE-B (prey)
SD-WLA	Deficient in tryptophan, leucine and adenine	Triple selection, used to select positive protein interactions between pGBAE-B (bait) and pACTBE-B (prey) clones
SD-WLH (3-AT)	Deficient in tryptophan, leucine and histidine, supplemented with 3-AT	
SD-ULA	Deficient in uracil, leucine and adenine	Triple selection, used to select positive protein interactions between pGBDU-GW (bait) and pACTBE-B (prey) clones
SD-ULH (3-AT)	Deficient in uracil, leucine and histidine, supplemented with 3-AT	

Table 2.13. Summary of all yeast media and their uses. All media could be made into solid media by the addition of BioAgar (20 g/L).

Table 2.14

YPAD	
Reagent	**g/L**
Peptone	20
D-(+)-Glucose	20
Yeast extract	10
Adenine hemisulphate	0.3
BioAgar*	20

Table 2.14. Constituents required to make YPAD medium. YPAD is required for basic MATa and MATα yeast growth. All media was made up with double-distilled water and autoclaved. *for solid media only.

Table 2.15

SD-X	
Reagent	**g/L**
Yeast nitrogen base w/o AA	6.7
D-(+)-Glucose	20
Amino acid supplement mix	X
BioAgar*	20

Table 2.15. Constituents required to make Synthetic Defined (SD-X) media. All media was made up with double-distilled water and autoclaved. *for solid media only.

Table 2.16

A/H/L/W/U DO mix	
Amino acid	**g/100 L**
Arginine	2
Isoleucine	3
Lysine	3
Methionine	2
Phenylalanine	5
Threonine	20
Tyrosine	3
Valine	15

Table 2.16. Constituents required to make the amino acid dropout (DO) mix. The DO mix was added to all SD-X media with the addition of amino acids according to the selection required (Table 2.17-19).

Table 2.17

Amino acid	SD-X mix (g/10 L)				
	-L	-W	-U	-L, LA	-W, LA
Adenine hem. (A)	0.6	0.6	0.6	0.06	0.06
Histidine (H)	0.2	0.2	0.2	0.2	0.2
Leucine (L)	-	1.0	1.0	-	1.0
Uracil (U)	0.2	0.2	-	0.2	0.2
A/H/W/U DO mix	5.3	5.3	5.3	5.3	5.3
Total (g/L)	0.63*	0.73	0.71*	0.58*	0.68

Table 2.17. Amino acid supplement mix for SD-X media for bait and prey yeast gap-repair and transformation.

* post-autoclaving, supplement media with filter-sterile tryptophan to a final concentration of 20 mg/L.

Table 2.18

Amino acid	SD-X mix (g/10 L)					
	-LA	-LH	-WA	-WH	-UA	-UH
Adenine hem. (A)	-	0.6	-	0.6	-	0.6
Histidine (H)	0.2	-	0.2	-	0.2	-
Leucine (L)	-	-	1.0	1.0	1.0	1.0
Uracil (U)	0.2	0.2	0.2	0.2	-	-
A/H/W/U DO mix	5.3	5.3	5.3	5.3	5.3	5.3
Total (g/L)	0.57*	0.61***	0.67	0.71**	0.65*	0.69***

Table 2.18. Amino acid supplement for SD-X media for the detection of auto-activating bait and prey constructs.

* post-autoclaving, supplement media with filter-sterile tryptophan to a final concentration of 20 mg/L.

**supplement with 3-amino-1,2,4-triazole (3-AT) to a final concentration of 2.5 mM.

***supplement media with 3-AT and tryptophan.

Table 2.19

Amino acid	SD-X mix (g/10 L)					
	-WL	-WLA	-WLH	-UL	-ULA	-ULH
Adenine hem. (A)	0.6	-	0.6	0.6	-	0.6
Histidine (H)	0.2	0.2	-	0.2	0.2	-
Leucine (L)	-	-	-	-	-	-
Uracil (U)	0.2	0.2	0.2	-	-	-
A/H/W/U DO mix	5.3	5.3	5.3	5.3	5.3	5.3
Total (g/L)	0.63	0.57	0.61**	0.61*	0.55*	0.59***

Table 2.19. Amino acid supplement for SD-X media for the detection of protein-protein interactions.

* post-autoclaving, supplement media with filter-sterile tryptophan to a final concentration of 20 mg/L.
**supplement with 3-AT to a final concentration of 2.5 mM.
***supplement media with 3-AT to a final concentration of 2.5 mM and tryptophan.

2.2.2 Yeast vectors

Conventional Y2H vectors encode either *GAL4* Activation Domain (AD) or DNA-binding domain (BD) at the 5' or 3' end of the recombination site, however pGBAE-B (bait) and pACTBE-B (prey) are frame-shift vectors. These frame-shift vectors have both *GAL4* domain sequences and maintain an open reading frame with the cloning site. Instead of a multiple cloning site (MCS), pGBAE-B and pACTBE-B vectors have a synthetic DNA fragment containing a *Bam*HI restriction site flanked by *attB1* and *attB2* sequences (Figure 2.2). The addition of one base pair insertion between the recombination sequences, allows a frame-shift and stop codon insertion, following homologous recombination of an ORF by gap-repair (Semple *et al.*, 2005).

Figure 2.2

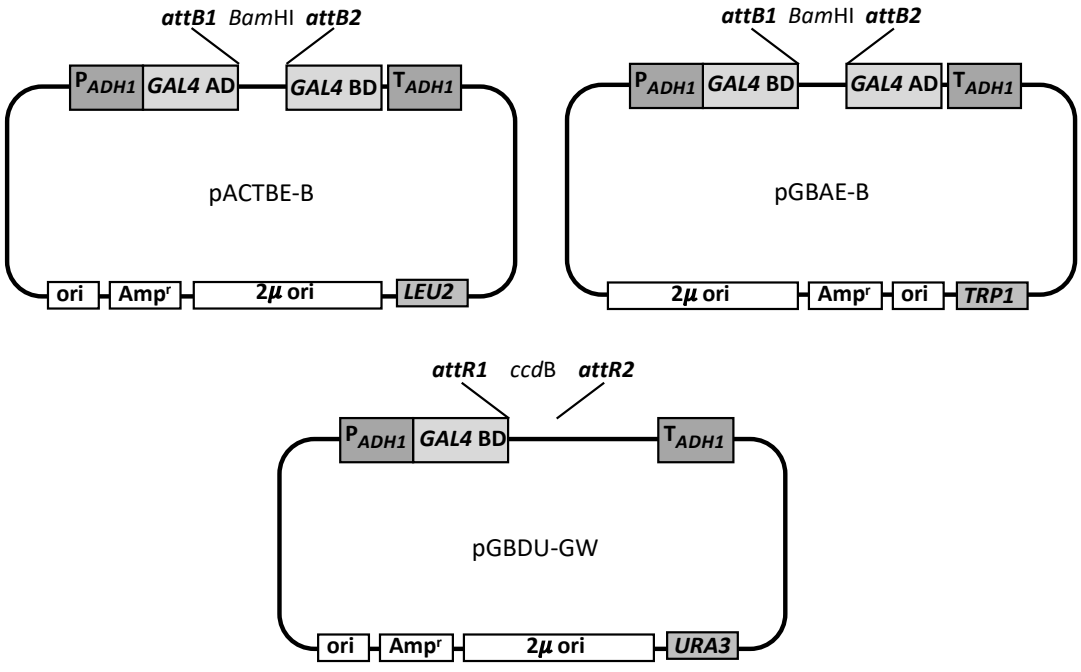

Figure 2.2. Schematic representations of the yeast two-hybrid vectors. pACTBE-B prey vector based on pACT2 encodes the *GAL4* Activation Domain (AD), whereas pGBAE-B bait vector based on pGBD-C1 and pGBDU-GW bait vector based on pGBT9

encode the *GAL4* DNA-binding domain (BD). They all utilize the modified, enhanced ADH1 promoter giving rise to moderate expression levels.

The addition of a stop codon causes a disruption in *GAL4* function which fails to activate the *ADE2* reporter gene. Consequently, this enables the identification of successfully transformed yeast clones as there is a production of red-pigmented colonies for clones that contain an insert, and this can be observed on selective media containing low amounts of adenine. Empty pGBAE-B and pACTBE-B vectors express the *GAL4* BD and AD as one in-frame fusion protein, activating the *ADE2* reporter gene and thereby allowing the growth of healthy, white yeast colonies on low adenine media. In contrast, pGBDU-GW is a Gateway® converted vector based on pGBT9. The *attR1* and *attR2* recombination sites, enable any ORF to be easily and quickly inserted by LR recombination cloning (see section 2.1.8.2).

As a large proportion of WT and all mutant HSP ORFs generated were lacking a stop codon, they were put into pACTBE-B (prey) and/or pGBAE-B (bait) vectors. The prey E3 RING ligases (pACTBE-B) and the bait DUBs (pGBDU-GW), had been previously generated within the laboratory, and were used in subsequent interaction studies discussed in Chapter 5.

2.2.3 Proof-reading KOD PCR from pDONR223

Due to sequence variation between the Gateway® *attB* recombination site sequences flanking ORFs in pDONR223 and those in yeast required for *in vivo* homologous recombination, primers were designed which allowed both the amplification of any ORF from pDONR223 and yeast homologous recombination.

The primers, shown below, contain bases from the yeast sequence (blue), pDONR223 sequence (green) and sequence present in both (black).

pDONR223 gap repair F: 5’ **GAATTCA**CAAGTTTGTACAAAAAA**GCAGGA**ATG 3’
pDONR223 gap repair R: 5’ **GTCGACC**ACTTTGTACAAGAAAGCTGGG 3’

Sequence-verified pDONR223-ORFs were amplified (using primers above) and combined with linearised pGBAE-B (bait) or pACTBE-B (prey) Y2H vector to transform yeast. Following PCR amplification, a sample (10 μL) of the reaction was analysed by gel electrophoresis, for correct fragment size, before continuing with gap-repair cloning.

2.2.4 Gap-repair homologous recombination

pGBAE-B and pACTBE-B vectors were linearized prior to use via restriction digest with *Bam*HI restriction enzyme, as described in section 2.1.14. MATa and MATα yeast glycerol stocks were streaked onto YPAD agar (Table 2.14) plates and grown at 30 °C for 3-5 days. A single MATa or MATα colony was used to inoculate 2 mL YPAD broth and grown at 30 °C, 200 rpm for 16 h. An additional 8 mL YPAD broth was added to the culture and further incubated at 30 °C, 200 rpm for 5 h.

Yeast were harvested by centrifugation at 2,300 rpm, RT for 5 min and supernatant discarded. The yeast pellet was resuspended in 5 mL 100 mM LiOAc. 1.5 mL aliquots of LiOAc-yeast mixture (each enough for 10 reactions) was added to 2 mL microcentrifuge tubes and pelleted as above. Supernatant was discarded, and the pellet was resuspended in 230 μL 50 % (w/v) PEG 3350, 45 μL sterile ddH_2O, 35 μL 1 M LiOAc, 9 μL 10.5 mg/mL heat-denatured salmon testes DNA and 20 ng *Bam*HI-linearized Y2H vector. The yeast suspension was mixed before transferring 32 μL into individual 0.2 mL PCR tubes, followed by 4 μL of a specific gap-repair KOD PCR and gentle mixing. As a negative control 4 μL ddH_2O was added to 32 μL yeast suspension, to assess the level of background growth of red and white colonies. All samples were incubated in a thermocycler at the following conditions: 30 °C for 30 min, 42 °C for 25 min and 30 °C for 1 min. All the reaction mixture was plated out onto appropriate low adenine media lacking vector selection marker (Table 2.17), and incubated at 30 °C for 3-5 days, allowing yeast colonies to grow. Homologous recombination (gap repair) between the linearized plasmid and the amplified bait or prey constructs occurs in the transformed yeast, which results in recombinant vector construction.

The production of red colonies is indicative of positive yeast transformation and ORF insertion, and as such a number of red colonies are selected for diagnostic yeast colony PCR (YC-PCR) and auto-activation testing (see Figure 2.3 A).

2.2.5 Diagnostic yeast colony PCR (YC-PCR)

To establish whether the correct ORF was inserted into the correct bait and/or prey Y2H vector during gap-repair cloning, diagnostic YC-PCR was performed. Several red colonies were picked and lysed in 5 μL 20 mM NaOH in 0.2 mL PCR tubes and incubated at RT for 20 min. Following incubation, 3 μL NaOH-yeast lysate suspension was added to 12 μL of the YC-PCR mix (see Table 2.20 A) and incubated in a thermocycler as described in Table 2.20 B. A 5 μL sample of the PCR product was analysed by gel electrophoresis, for correct fragment size. Positive colonies were taken through to the auto-activation assay.

Table 2.20

A

Reagent	μL/reaction	Final concentration
Forward primer (10 μM)	0.75	0.5 μM
Reverse primer (10 μM)	0.75	0.5 μM
10X NH_4 buffer	1.5	1X
$MgCl_2$ (50 mM)	0.75	2.5 mM
dNTPs (25 mM)	0.45	750 μM
BIOTAQ™ polymerase	0.15	-
DMSO	0.3	
Nuclease-free H_2O	7.35	-
NaOH yeast lysate suspension	3.0	
TOTAL	15	-

B

Step	Cycles	Temperature (°C)	Duration
1	1	95	5 min
2	40	95	1 min
		55-68*	1 min
		72	1 min/kb
3	1	72	5 min
4	1	4	Forever

Table 2.20. Master mix and cycling parameters for a typical YC-PCR. (A) Reaction master mix was set up in thin-walled PCR tubes on ice, using reagents and volumes

stated. Yeast colonies were lysed in 20 mM NaOH before the addition of YC-PCR reaction mixture. (B) YC-PCR was cycled as indicated.
*Annealing temperatures vary depending on the predicted melting temperature (Tm) of the individual primers used.

2.2.6 Auto-activation testing

False positive interactions can occur in Y2H screens if an ORF, when inserted into bait or prey Y2H expression vector, causes constitutive activation of reporter genes *HIS3, ADE2* and/or *lacZ,* in the absence of a positive interacting protein. This is also known as "auto-activation". To test for auto-activation in yeast clones, the remainder of the YC-PCR positive bait and prey yeast colonies were picked from gap-repair transformation plates and resuspended in 20 μL ddH_2O. The yeast suspension was spotted onto double dropout media lacking vector selection marker and one of the biosynthetic reporter nutrients (Table 2.18). *ADE2* and *HIS3* are two of the three *GAL4*-independent reporter genes assayed for auto-activation. Yeast colonies were left to grow at 30 °C for up to 14 days, and any colony growth on the double dropout media (i.e. auto-activated) were discarded and not taken any further. Those that did not auto-activate were used to make glycerol stocks, pooled and used in subsequent studies.

2.2.7 Yeast glycerol stocks

In *S. cerevisiae,* almost all mutations that inhibit *GAL4* function are found in the region of the gene that encodes the DNA-binding domain (Johnston and Dover, 1987), and so false negatives may arise from spontaneous mutations within this region. Therefore, only pooled glycerols stocks of positive colonies will be used for subsequent experimentation, to try and counterbalance any possible spontaneous mutations which may arise.

Glycerol stocks of transformed yeast strains were made in synthetic deficient (SD) medium lacking appropriate nutrients (SD-X). Yeast colonies were grown for 3 days, post-transformation on SD-X agar plates. Following successful YC-PCR, positive

colonies were used to inoculate SD-X liquid medium (200 μL) and grown at 30 °C, 220 rpm for 24 h. Overnight cultures were combined with 80 % (v/v) sterile glycerol (80 μL) in a 1.5 mL microcentrifuge tube and mixed, prior to storage at -80 °C. Pooled glycerol stocks were made from glycerol aliquots of up to 4 positive yeast clones to a total volume of 200 μL in a 1.5 mL microcentrifuge tube and stored at -80 °C.

2.2.8 Yeast two-Hybrid matrix mating

2.2.8.1 Matrix mating protocol

A summary of the yeast two-hybrid matrix mating protocol can be seen in Figure 2.3. Yeast glycerol stocks for each clone to be mated, were spotted onto appropriate selective media (Table 2.17) and grown at 30 °C for 3-5 days. Individual yeast clones were then picked and resuspended in 4 μL ddH_2O x number of individual constructs to be mated against (e.g. to screen a bait construct against a 96-well plate of different prey yeast clones, the bait would be resuspended in a total volume of 384 μL ddH_2O). The bait and prey suspensions used in each screen were of similar opacity (assessed by eye) and this was dependent on the amount of individual bait and prey yeast picked. 3 μL of the bait yeast suspension, was spotted in a 96-array plate format onto YPAD agar in 150 mm, triple vented sterile plates, and allowed to dry. 3 μL of the individual prey yeast suspension was spotted on top of the dried bait spot and allowed to dry before incubating at 30 °C for 24 h to allow the mating of the MATα and MATa yeast. The newly mated yeast was then replicated using sterile velvet cloths, onto 2 double dropout media (SD-WL) plates to select for diploid yeast containing both bait and prey vectors, before incubating at 30 °C for 48 h. One diploid yeast plate was used for the β-Galactosidase (β-Gal*)* assay (see below Section 2.2.8.2). The second diploid plate was used to further replicate onto triple dropout media (Table 2.19) plates, first the more stringent SD-WLA followed by the less stringent SD-WLH(3-AT). The order is important for the reduction of background growth on the less stringent SD-WLH(3-AT) media. The triple dropout plates were incubated at 30 °C for 14 days allowing the selective growth of potential positive interactions between specific bait-prey pairs. Images were taken, and positive yeast

growth was scored every 3-4 days. Interaction scoring criteria were as follows; 0-5 colonies: background growth (0), 5-20 colonies: weak growth (+), 20-100 colonies: medium growth (++), full plaque: strong growth (+++).

Figure 2.3

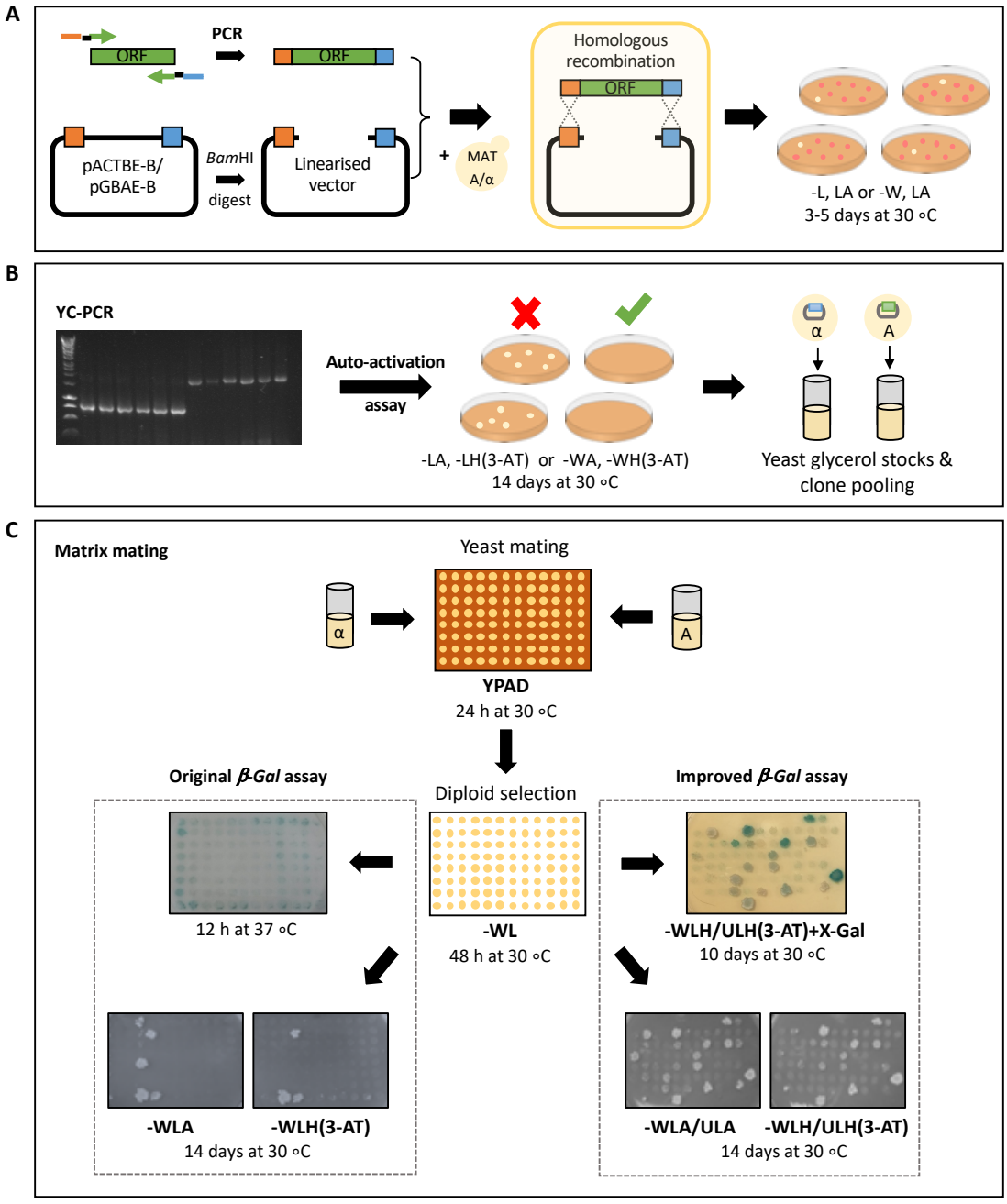

Figure 2.3. Schematic representation of yeast two-hybrid clone generation and matrix mating. (A) PCR product containing flanking sequences homologous to the vector enables *in vivo* recombination between linearised plasmid and PCR product in yeast, resulting in the growth of red colonies. (B) Red colonies were selected for

diagnostic YC-PCR, followed by auto-activation testing and production of yeast glycerol stocks of positive hits. (C) Matrix mating protocol comparing the original and improved *β*-Galactosidase assay.

2.2.8.2 β-Galactosidase assay – colony filter lift assay

The *β*-Galactosidase (*β-Gal)* assay was used to measure the level of the *lacZ* reporter construct expression, using the diploid yeast plate not used for further replication and selection (see above). Equal amounts of yeast from diploid array plates were transferred onto a Whatman® filter paper, diam. 150 mm and freeze-thawed twice by submersion in liquid nitrogen for 10 seconds, to lyse yeast cells. Following this, the filter paper was placed yeast side up onto two Whatman® filter papers which had been placed in a 150 mm petri dish and saturated in *β*-gal reagent (6 mL β-gal Z-buffer (60 mM Na_2HPO_4, 40 mM $Na_2H_2PO_4$, 10 mM KCl, 1 mM $MgSO_4$), 1.6 mg/mL X-Gal reagent (100 mg/mL X-Gal in *N,N*-dimethylforamide) and 11 μL *β*-mercaptoethanol). The plate was sealed and incubated at 37 °C for up to 12 h to allow for the blue colour change to occur in lysed yeast, indicative of the presence of *β*-galactosidase and therefore a positive protein-protein interaction (see Figure 2.3). Images were taken and scored every 30 min based on the intensity of blue colour change appearing on the filter paper. Scoring criteria were as follows; white colonies (0), light blue colonies: weak growth (+), light-dark blue colonies: medium growth (++), dark blue colonies: strong growth (+++).

2.2.9 Yeast two-hybrid matrix mating with improved β-Gal assay

2.2.9.1 Matrix mating protocol

A summary of the yeast two-hybrid matrix with improved *β-Gal* assay can be seen in Figure 2.3. The original matrix mating method was used, as previously described (2.2.8.1).

2.2.9.2 β-Galactosidase assay – agar overlay assay

The improved β-Galactosidase (*β-Gal)* assay was used to assess *lacZ* activity using the second diploid plate which was instead used to replicate onto SD-WLH(3-AT)/-ULH(3-AT) + X-Gal plates. SD-WLH(3-AT)/-ULH(3-AT) media containing agar was prepared, as previously described. After autoclaving, media was allowed to cool before adding 1/10th volume of sterile sodium phosphate solution (493 mM sodium phosphate dibasic, 250 mM sodium phosphate monobasic in ddH_2O) followed by X-Gal reagent (100 mg/mL in *N,N*-dimethylforamide) up to a final concentration of 80 μg/mL. The triple dropout plates containing X-Gal were incubated at 30 °C for 10 days allowing the selective growth of potential positive protein-protein interactions. Images were taken and scored every 3-4 days based on the intensity of blue colour change of the yeast colonies as described in section 2.2.8.2.

2.3 Yeast two-Hybrid library screens

2.3.1 Matchmaker® yeast two-hybrid system

2.3.1.1 Reagents and media

Traditional Matchmaker® Yeast two-hybrid cDNA library was from Clontech Laboratories Inc. (distributed by Takara Bio Europe, France). All other reagents are listed in section 2.2.1.

2.3.1.2 Initial mating

Initially, several pGBAE-B HSP bait proteins were screened against the K-562 pACT2 prey cDNA library. HSP bait yeast glycerol stocks were streaked onto SD-W agar plates and grown at 30 °C for 3-5 days. Two colonies were used to inoculate 2 x 25 mL SD-W broth and grown at 30 °C, 200 rpm for 16-20 h or until the OD_{600} reached 0.8. Following this, yeast cultures were harvested by centrifugation at 2,300 rpm, RT for 5 min and supernatant discarded before re-suspending each pellet in 500 μL YPAD and combining both. The bait suspension was mixed with 300 μL prey Matchmaker Y2H library, plated onto YPAD agar in 150 mm, triple vented sterile plates and

incubated at 30 °C for 6 h to allow the mating of the prey library and bait HSP yeast. Following incubation, newly mated yeast cells were harvested using 5 mL sterile ddH_2O and a cell scraper, transferring the yeast suspension to a 15 mL Falcon tube and repeating the process with another 1 mL sterile ddH_2O. To assess the mating efficiency, a 2 μL sample of the yeast suspension was used to make 10^{-2}, 10^{-3} and 10^{-4} serial dilutions and 100 μL plated onto SD-WL agar plates (90 mm) and incubated at 30 °C for 3-5 days. The remaining yeast suspension was plated equally onto 16 x SD-WLA agar in 150 mm, triple vented sterile plates and incubated at 30 °C for 14 days.

2.3.1.3 Diagnostic YC-PCR

Colonies growing on SD-WLA agar, are diploid colonies containing both bait and prey clones which are also able to activate the *ADE2* reporter gene and as such are representative of a potential protein-protein interaction. As such, up to 2 x 96 colonies were selected for diagnostic YC-PCR and reconfirmation mating. Colonies from SD-WLA library plates were resuspended in 20 μL H_2O, spotted (4 μL) onto fresh SD-WLA agar plates and incubated at 30 °C for 3-5 days. Once grown, yeast colonies were subjected to diagnostic YC-PCR, amplifying the prey clone with the use of the following primers:

Forward primer:
5' **GAATTCACAAGTTTGTACAAAAAAGCAGG**CTGGATGGCTTACCCATACGATGTTCC 3'

Reverse primer:
5' **GTCGACCACTTTGTACAAGAAAGCTGG**TTTTTCAGTATCTACGATTCATAG 3'

These primers contain flanking sequences (shown in green) which allow amplification of the prey clone and *in vivo* yeast homologous recombination (gap repair) into pACTBE-B prey vector for reconfirmation mating of positive clones.
In brief, a small amount of yeast was lysed in 5 μL 20 mM NaOH in 0.2 mL PCR tubes and incubated at RT for 20 min. Following lysis, 25 μL of the YC-PCR mixture (Table 2.21 A) was added to each sample and incubated in a thermocycler as described in

Table 2.21 B. The PCR product was analysed by gel electrophoresis, as described previously, to identify insert size for each clone. Positive colonies were taken through to the gap repair and reconfirmation stage.

Table 2.21

A

Reagent	μL/reaction	Final concentration
Forward primer (10 μM)	1.5	0.5 μM
Reverse primer (10 μM)	1.5	0.5 μM
10X NH_4 buffer	3	1X
$MgCl_2$ (50 mM)	1.5	2.5 mM
dNTPs (25 mM)	0.9	750 μM
BIOTAQ™ polymerase	0.3	-
DMSO	0.6	
Nuclease-free H_2O	15.7	-
NaOH yeast lysate suspension	5	
TOTAL	30	-

B

Step	Cycles	Temperature (°C)	Duration
1	1	95	5 min
2	40	95	1 min
		58	1 min
		72	1 min/kb
3	1	72	5 min
4	1	4	Forever

Table 2.21. Master mix and cycling parameters for a library diagnostic YC-PCR. (A) Reaction master mix was set up in thin-walled PCR tubes on ice, using reagents and volumes stated. (B) YC-PCR was cycled in as indicated.

2.3.1.4 Library Gap Repair

Library colonies were amplified with the intention of performing *in vivo* recombination (gap repair) of prey library hits into the pACTBE-B prey vector to carry out a reconfirmation mating. pACTBE-B, as described previously, is a frame-shift vector allowing the easy identification of successfully transformed yeast colonies through the production of red-pigmented colonies.

MATα yeast strain glycerol stock was streaked onto YPAD agar and grown at 30 °C for 3-5 days. A single MATα colony was used to inoculate 4 mL YPAD broth and grown

at 30 °C, 200 rpm for 16 h. An additional 16 mL YPAD broth was added to the culture and further incubated at 30 °C, 200 rpm for 5 h. Yeast were harvested by centrifugation at 2,300 rpm, RT for 5 min and supernatant discarded. The yeast pellet was resuspended in 5 mL 100 mM LiOAc and pelleted as above. Supernatant was discarded, and the pellet was resuspended in 1100 μL 50 % (w/v) PEG 3350, 170 μL sterile ddH_2O, 167 μL 1M LiOAc, 40 μL 10.5 mg/mL heat denatured salmon testes DNA and 50 ng *Bam*HI linearized pACTBE-B vector. The yeast suspension was mixed and 8 μL was added to each well of a sterile 96-well PCR plate, followed by 2 μL of a specific YC-PCR reaction (from above) and gentle mixing. As a negative control 2 μL H_2O was added to 8 μL yeast suspension, to assess the level of background growth of red and white colonies. All samples were incubated in a thermocycler at the following conditions: 30 °C for 30 min, 42 °C for 25 min and 30 °C for 1 min. Each reaction mixture was spotted 3 μL at a time, onto SD-L, low adenine media, allowing the spots in between. The plates were then incubated at 30 °C for 3-5 days, allowing yeast colonies to grow.

2.3.1.5 Reconfirmation mating

To distinguish between false positives and genuine positive interactions it was important to re-confirm the interactions using the original bait and a negative bait control, thereby eliminating any auto-activating or non-specific prey clones. Unlike the initial mating, the reconfirmation mating will involve utilising all three *GAL4*-independent reporter genes *(HIS3, ADE2* and *lacZ),* and only interactions that activate all three will be considered genuine positive interactions. The negative bait control used in the reconfirmation matings was LSM2, due to its specificity for other LSM proteins.

The successful gap repair of prey clones into the pACTBE-B vector was observed by the growth of red-pigmented colonies. Several red colonies from each spot were picked, resuspended in 20 μL H_2O in a sterile 96-well mating plate and 3 μL spotted onto SD-L agar plate. At the same time 3 μL of the original bait and LSM2 bait clone were spotted onto SD-W agar plates and all yeast colonies were grown at 30 °C for

3-5 days. Prey colonies were resuspended in 20 μL ddH_2O, whilst the bait (original and LSM2) were each resuspended in 384 μL ddH_2O (enough to screen against for 96 prey clones). The bait and prey suspensions used in each screen were of similar opacity (assessed by eye), dependent on the amount of individual bait and prey yeast picked. Next, 3 μL of the bait yeast suspension (original or LSM2), was spotted in a 96-array plate format onto YPAD agar in 150 mm, triple vented sterile plates, and allowed to dry. Following this, 3 μL of the individual prey yeast suspension was spotted on top of the dried bait spot and allowed to dry before incubating at 30 °C for 24 h to allow mating to occur. The newly mated yeast was then replicated using sterile velvet cloths, onto 2 X SD-WL agar plates to select for diploid yeast, before incubating at 30 °C for 48 h. One SD-WL yeast plate was used for the β-Galactosidase (β-Gal*)* assay as described previously in section 2.2.8.2. The second plate of diploid yeast was used to replicate onto triple dropout media SD-WLA followed by SD-WLH(3-AT). These plates were incubated at 30 °C for 14 days allowing the selective growth of potential positive interactions between specific bait-prey pairs. Images were taken, and positive yeast growth was scored every 3-4 days as described in section 2.2.8.2.

2.3.1.6 Yeast prey sequencing

Colonies grown on all three reporter assays with the original bait and not the negative control were selected for DNA sequencing analysis. The remaining 20 μL of the diagnostic YC-PCR product was sent to GATC Biotech (Konstanz, Germany), for purification followed by sequencing by automated fluorescent DNA sequencing. Sequence information was analysed using the NCBI Basic Local Alignment Search Tool (BLAST) tool (McGinnis and Madden, 2004) to identify prey interactors.

2.3.2 Matchmaker® Gold Yeast two-Hybrid System

2.3.2.1 Reagents and media

Matchmaker® Gold Yeast two-hybrid cDNA library system was from Clontech (distributed by Takara Bio Europe, France). The yeast host strain Y2HGold (MATa

trp1-901 leu2-3, 112 ura3-52, his3-200 gal4Δ gal80Δ LYS2::GAL1$_{UAS}$-Gal1$_{TATA}$-His3, GAL2$_{UAS}$-Gal2$_{TATA}$-Ade2 URA3::MEL1$_{UAS}$-Mel1$_{TATA}$ AUR1-C MEL1), was used as the bait strain for all Y2H matrix mating assays. The Y2HGold yeast strain is a derivative of the PJ69-2A strain (James et al., 1996) and carries four independent *GAL4*-responsive reporter genes. The yeast host strain Y187 (MATα ura3-52, his3-200, ade2-101, trp1-901, leu2-3, 112, gal4Δ, gal80Δ, met1, URA3::GAL1$_{UAS}$-Gal1$_{TATA}$-LacZ, MEL1) was used as the prey library strain and carries two independent *GAL4*-responsive reporter genes. All other reagents and media are stated in section 2.2.1.

2.3.2.2 Matchmaker® Gold yeast vectors

Matchmaker® Gold Y2H vectors encode either *GAL4* Activation Domain (AD) or DNA-binding domain (BD) at the 5' or 3' end of the recombination site, like most other conventional Y2H vectors. The bait protein is expressed as a fusion to the *GAL4* DNA-binding domain (BD) using the DNA-BD cloning vector pGBKT7, whilst the library of prey proteins are expressed as fusions to the *GAL4* activation domain (AD) using the AD cloning vector, pGADT7 (Figure 2.4).

Figure 2.4

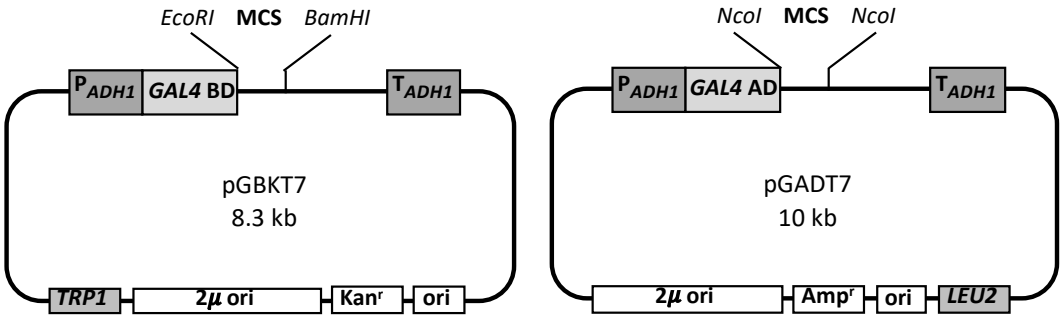

Figure 2.4. Schematic representations of Matchmaker® Gold yeast two-hybrid vectors. pGBKT7 bait vector encode the *GAL4* DNA-binding domain (BD), whereas pGADT7 prey vector encodes the *GAL4* Activator domain (AD). They all utilize the modified, enhanced ADH1 promoter giving rise to moderate expression levels.

2.3.2.3 pGBKT7 bait generation

An overview of the SLiCE cloning method, used to generate pGBKT7 bait constructs used in the Matchmaker® Gold yeast two-hybrid system, is presented in Figure 2.5.

Primers were designed to enable seamless DNA cloning of the desired bait ORF, in-frame with the *GAL4* DNA-binding domain of the pGBKT7 plasmid. The primers included 15-21 bases from the pGBKT7 vector, followed by 18-21 bases homologous to the bait (see Figure 2.5 A). Sequence-verified pDONR223-ORFs were amplified using these specifically designed primers and combined with the pGBKT7 vector, via a SLiCE reaction (see section 2.1.9.2). The pGBKT7 vector is linearized prior to use via restriction digest with *Bam*HI and *Eco*RI restriction enzymes, as described in section 2.1.14. Following PCR amplification, a sample (10 µL) of the reaction was analysed by gel electrophoresis for correct fragment size before continuing with bacterial transformation, BC-PCR and sequencing.

Figure 2.5

A

GBKT7_F:
5’ catggaggccgaattcXXX22233444555666777888 3’

GBKT7_RS:
5’ gcaggtcgacggatccYYY22233444555666777888 3’

B

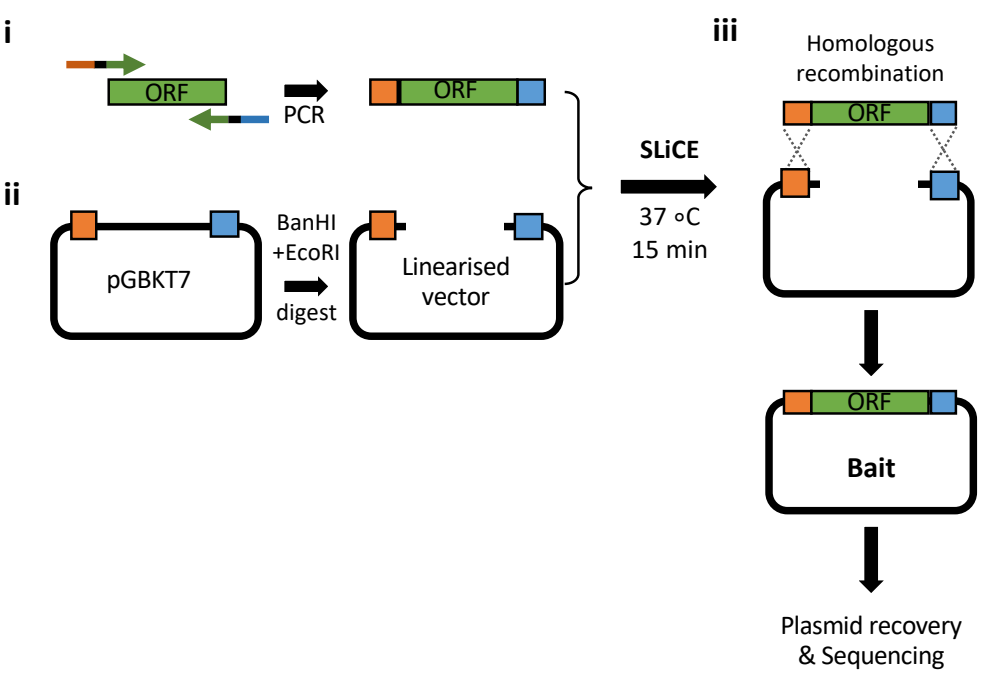

Figure 2.5. Matchmaker® Gold pGBKT7 bait generation. (A) Primer design for use with pGBKT7 bait vector. Primer sequences contain a 16bp sequence that is homologous to the ends of the linearised pGBKT7 vector, together with a 24bp region that is homologous to the required bait protein. XXX = first codon of the bait, YYY = reverse complement of the last codon of the bait protein. (B) Schematic diagram showing the strategy for cloning bait inserts into the linearised pGBKT7 bait vector by homologous recombination, using the Seamless Ligation Cloning Extract (SLiCE) method. (i) The gene of interest (bait) is first amplified using the primers with recombination compatible flanking sequences. (ii) The bait cDNA inserts flanked by vector homologous sequences are mixed with linearised vector and *E.Coli* cell lysates. (iii) The SLiCE method uses the homologous recombination activities in *E.Coli* cell lysates to assemble the bait insert into the pGBKT7 vector. Following *in vitro* assembly, all plasmids were amplified, and sequence verified before use in matchmaker Y2H library screens.

2.3.2.4 Auto-activation and toxicity testing

An overview of the auto-activation testing method, used for Matchmaker® pGBKT7 bait validation, is shown in Figure 2.6. Y2HGold yeast glycerol stocks were streaked onto YPAD agar plates and grown at 30 °C for 3-5 days. A single Y2HGold colony was used to inoculate 10 mL YPAD broth and grown at 30 °C, 200 rpm for 16 h. A 5 mL culture sample was discarded and 45 mL YPAD broth was added to the remaining culture and further incubated at 30 °C, 200 rpm for 90 min or until the OD_{600} reached 0.4-0.5. Yeast were harvested by centrifugation at 2,300 rpm, RT for 5 min and supernatant discarded. The yeast pellet was resuspended in 30 mL ddH_2O and pelleted as above. Supernatant was discarded, and the pellet resuspended in 1.5 mL LiOAc/TE solution (Table 2.22) before transferring the yeast suspension into two 1.5 mL microcentrifuge tubes and centrifugation at high speed for 15 s.

Table 2.22

Reagent	Volume (mL)
10X Tris EDTA buffer (pH 7.5)	1.1
1M Lithium acetate	1.1
ddH_2O	7.8

Table 2.22. Constituents required to make LiOAc/TE solution. Vortex thoroughly and prepare just before use.

Supernatant was discarded, and each pellet was resuspended in 600 μL LiOAc/TE solution. To pre-cooled 1.5 mL microcentrifuge tubes 50 μL cell suspension, 100 ng sequence-verified plasmid DNA (or 100 ng empty pGBKT7 as a negative control) and 500 μL PEG/LiOAc solution (Table 2.23) were added and mixed gently. The transformation mixture was incubated at 30 °C for 30 min, gently vortexing every 10 min, followed by the addition of 20 μL DMSO. The solution was mixed before incubating at 42 °C for 15 min, gently vortexing every 5 min, followed by centrifugation at high speed for 15 s. Supernatant was discarded and pellet was resuspended in 1 mL YPD Plus broth and grown at 30 °C, 200 rpm for 1 h. Yeast was harvested by centrifugation at high speed for 15 s, supernatant discarded and pellet resuspended in 1 mL 0.9 % (w/v) NaCl.

Table 2.23

Reagent	Volume (mL)
50 % (v/v) PEG 3350	12
1M Lithium acetate	1.5
10X Tris EDTA buffer (pH 7.5)	1.5

Table 2.23. Constituents required to make PEG/LiOAc solution. Vortex thoroughly and prepare just before use.

To assess bait auto-activation, 100 μL of a 1/10 and 1/100 dilution of the transformation mixture was plated onto SD-W, SD-W/X-α-Gal and SD-W/X-α-Gal/AbA agar plates (90 mm) and incubated at 30 °C for 3-5 days.

Expected results:

SD-W	White, 2mm colonies
SD-W/X-α-Gal	White/blue, 2mm colonies
SD-W/X-α-Gal/Aba	No colony growth

To assess bait toxicity, 100 μL of a 1/10 and 1/100 dilution of the transformation mixture containing plasmid DNA or empty pGBKT7 vector was plated onto SD-W agar plates (90 mm) and incubated at 30 °C for 3-5 days. If bait is toxic to the yeast, colonies may appear smaller than those containing empty vector. Those pGBKT7 bait constructs that were not toxic to yeast and did not auto-activate, were used to make

yeast glycerol stocks (see section 2.2.7) for use in subsequent Matchmaker® Gold interaction studies.

Figure 2.6

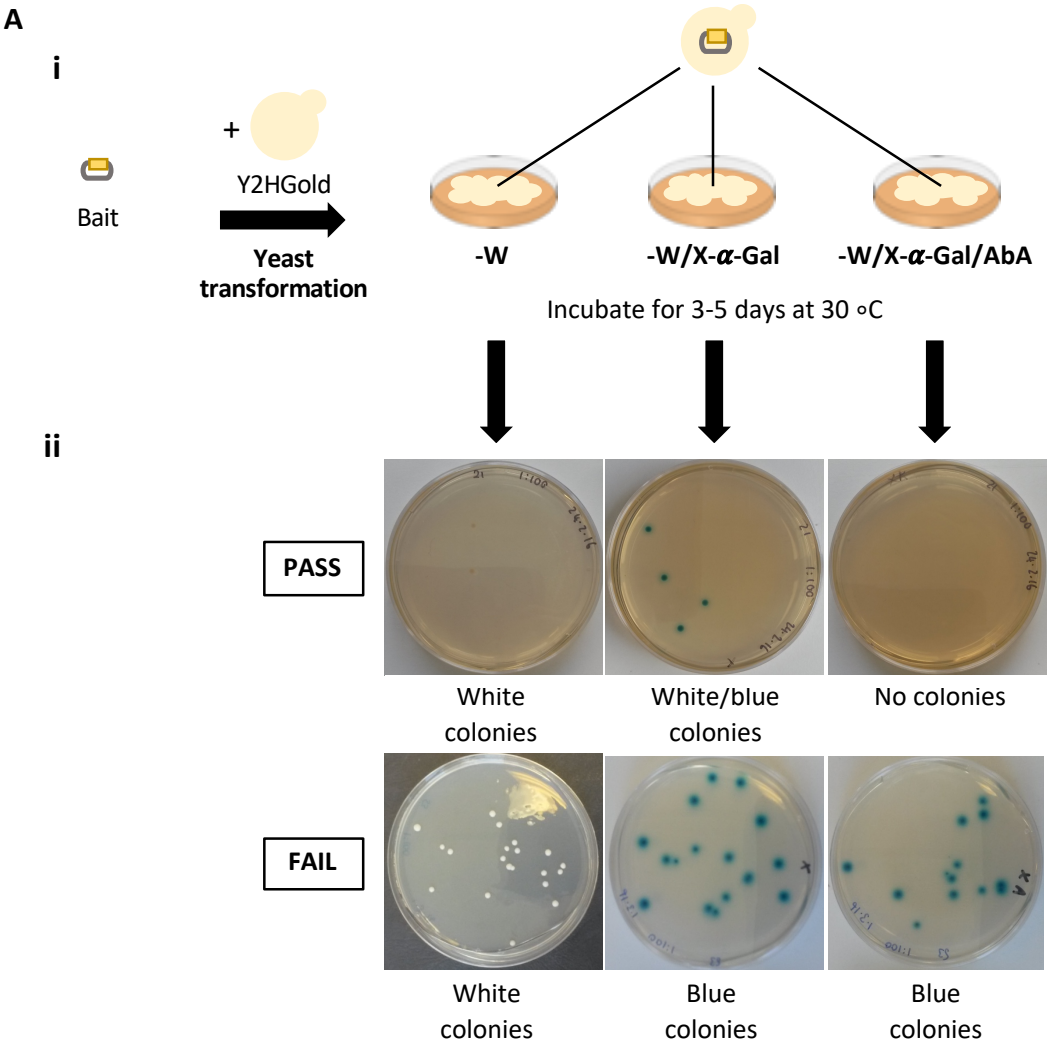

B

Matchmaker baits:	
pGBKT7-WASHC5	pGBKT7-AP4S1
pGBKT7-ERLIN2	pGBKT7-TFG
pGBKT7-SPART	pGBKT7-USP8
pGBKT7-SPG21	pGBKT7-CCT5

Figure 2.6. Matchmaker® Gold pGBKT7 bait validation. (A) For each bait, auto-activation tests are first performed to confirm that the bait does not activate reporter genes in the Y2HGold yeast strain, in the absence of prey proteins. (i) sequence-verified pGBKT7 baits are transformed into Y2HGold yeast cells and plated onto SD-W plates or SD-W plates supplemented with either X-α-Gal alone, or X-α-Gal plus Aureobasidin A (AbA). (ii) Example of results from a successful, non-auto activating

bait (top row), or from an unsuccessful auto-activating bait (bottom row). (B) List of pGBKT7 baits which passed auto-activation and toxicity tests and were subsequently taken through to the library screening.

2.3.2.5 Yeast two-Hybrid library screen: Initial mating

Several pGBKT7-HSP bait proteins were screened against the Matchmaker® human brain pGADT7 prey cDNA library. HSP bait yeast glycerol stocks were streaked onto SD-W agar plates and grown at 30 °C for 3-5 days. A single colony was used to inoculate 5 mL SD-W broth and grown at 30 °C, 220 rpm for 8 h. The culture was diluted with a further 45 mL SD-W broth, transferred to a 500 mL flask and incubated at 37 °C, 220 rpm for 16 h or until the OD_{600} reached 0.8. Following this, yeast cultures were harvested by centrifugation at 2,300 rpm, RT for 5 min, supernatant discarded and pellet resuspended in 1 mL 2X YPAD. The bait suspension was mixed with 1 mL prey Matchmaker Gold Human Brain Y2H library, plated onto YPAD agar in 150 mm, triple vented sterile plates and incubated at 30 °C for 5 h to allow the mating of the prey library and bait HSP yeast. Following incubation, newly mated yeast cells were harvested using 4 mL 0.5X YPAD broth (with 50 μg/mL kanamycin) and a cell scraper, transferring the yeast suspension to a Falcon and repeating the process with another 0.5 mL 0.5X YPAD/Kan liquid medium. To assess the mating efficiency, a 4 μL sample of the yeast suspension was used to make 10^{-2}, 10^{-3} and 10^{-4} serial dilutions and plate 100 μL of each onto SD-W, -L and -WL agar plates (90 mm) and incubated at 30 °C for 3-5 days. The remaining yeast suspension was plated equally onto 16 x SD-WL/AbA agar in 150 mm, triple vented sterile plates and incubated at 30 °C for 3-5 days.

2.3.2.6 Diagnostic YC-PCR

Colonies growing on SD-WL/AbA agar, are diploid colonies containing both bait and prey clones and are therefore representative of a potential protein-protein interaction. As such, up to 2 x 96 colonies were selected for diagnostic yeast YC-PCR and reconfirmation mating. Colonies from SD-WL/AbA library plates were resuspended in 100 μL 0.9 % (w/v) NaCl, spotted (3 μL) onto SD-WLAH and SD-

WLAH/X-α-Gal/AbA agar plates and incubated at 30 °C for 3-5 days. Once grown, yeast colonies which were shown to activate all four reporter genes (i.e. blue colonies on WLAH/X-α-Gal/AbA agar plates) were subjected to diagnostic YC-PCR, amplifying the prey clone with the following primers:

pGADT7.F primer: 5' CGACTCACTATAGGGCGAGC 3'
pGADT7.R primer: 5' GATGGTGCACGATGCACAG 3'

These primers allow amplification of the prey clone and *in vivo* yeast homologous recombination (gap repair) back into the pGADT7 prey vector for reconfirmation mating of positive clones. In brief, a small amount of yeast was lysed in 5 μL 20 mM NaOH in 0.2 mL PCR tubes and incubated at RT for 20 min. Following lysis, 25 μL of the YC-PCR mixture (Table 2.21 A) was added to each sample and incubated in a thermocycler as described in Table 2.21 B. The PCR product was analysed by gel electrophoresis, as described previously, to identify correct insert size for each clone with positive colonies taken through to the gap repair and reconfirmation stage.

2.3.2.7 Gap Repair homologous recombination

Positive YC-PCR library colonies were amplified with the intention of performing *in vivo* recombination (gap repair) of prey library hits back into the pGADT7 prey vector for the reconfirmation mating of positive interactions. Y187 yeast glycerol stock was streaked onto YPAD agar and grown at 30 °C for 3-5 days. Two Y187 colonies were used to inoculate 10 mL YPAD broth and grown at 30 °C, 200 rpm for 16 h. 5 mL culture was discarded and 45 mL YPAD broth was added to the remaining culture and further incubated at 30 °C, 200 rpm for 90 min. Yeast were harvested by centrifugation at 2,300 rpm, RT for 5 min and supernatant discarded. The yeast pellet was resuspended in 30 mL ddH_2O and pelleted as above. Supernatant was discarded, and the pellet resuspended in 1.5 mL LiOAc/TE solution (Table 2.22) before transferring suspension into two 1.5 mL microcentrifuge tubes and centrifugation at high speed for 15 s. Again, discard supernatant and resuspend each pellet in 1100 μL 50 % (v/v) PEG 3350, 170 μL sterile ddH_2O, 167 μL 1M LiOAc, 40 μL 10.5 mg/mL heat

denatured salmon testes DNA and 60 ng *Nco*I linearized pGADT7 vector. The yeast suspension was mixed and 8 μL was added to each well of a sterile 96-well PCR plate, followed by 4 μL of a specific YC-PCR reaction (from above) and gentle mixing. As a negative control 4 μL sterile ddH_2O was added to 8 μL yeast suspension, to assess the level of background growth of red and white colonies. All samples were incubated in a thermocycler at the following conditions: 30 °C for 30 min, 42 °C for 25 min and 30 °C for 1 min. Each reaction mixture was spotted onto SD-L agar in 150 mm, triple vented sterile plates, 4 μL at a time, allowing the spots to dry before spotting out again. The plates were then incubated at 30 °C for 3-5 days, allowing yeast colonies to grow.

2.3.2.8 Yeast two-Hybrid library screen: reconfirmation mating

To distinguish between false positives and genuine positive interactions it was important to re-confirm the interactions using the original pGBKT7 bait and a negative bait control (empty pGBKT7), thereby eliminating any auto-activating or non-specific prey clones. The successful gap repair of prey clones into the pGADT7 vector was observed by the growth of colonies within each spot. Several colonies from each spot were picked, resuspended in 20 μL sterile ddH_2O in a sterile 96-well mating plate and 3 μL spotted onto SD-L agar plate. At the same time 3 μL of the original pGBKT7 bait and empty pGBKT7 were spotted onto SD-W agar plates and all yeast colonies were grown at 30 °C for 3-5 days. Prey colonies were resuspended in 20 μL sterile ddH_2O, whilst the bait (original and empty) were each resuspended in 384 μL sterile ddH_2O (enough to screen against for 96 prey clones). The bait and prey suspensions used in each screen were of similar opacity (assessed by eye), dependent on the amount of individual bait and prey yeast picked. Next, 3 μL of the bait yeast suspension (original or empty), was spotted in a 96-array plate format onto YPAD agar in 150 mm, triple vented sterile plates, and allowed to dry. Following this, 3 μL of the individual prey yeast suspension was spotted on top of the dried bait spot and allowed to dry before incubating at 30 °C for 24 h to allow mating to occur. The newly mated yeast was then replicated using sterile velvet cloths, onto SD-WL agar plate to select for diploid yeast, before incubating at 30 °C for 48 h. The SD-WL diploid yeast

plate was used to replicate onto double dropout media SD-WL/X-α-Gal and quadruple dropout media SD-WLAH/X-α-Gal/Aba. These plates were incubated at 30 °C for 14 days allowing the selective growth of potential positive interactions between specific bait-prey pairs. Images were taken every 3-4 days.

Expected results:

Genuine positive		
pGBKT7 bait + candidate prey	SD-WL/X-α-Gal	Blue, 2mm colonies
	SD-WLAH/X-α-Gal/Aba	Blue, 2mm colonies
Empty pGBKT7 + candidate prey	SD-WL/X-α-Gal	White, 2mm colonies
	SD-WLAH/X-α-Gal/Aba	No colony growth

False positive		
pGBKT7 bait + candidate prey	SD-WL/X-α-Gal	Blue, 2mm colonies
	SD-WLAH/X-α-Gal/Aba	Blue, 2mm colonies
Empty pGBKT7 + candidate prey	SD-WL/X-α-Gal	Blue, 2mm colonies
	SD-WLAH/X-α-Gal/Aba	Blue, 2mm colonies

2.3.2.9 Yeast prey sequencing

Colonies grown on all four reporter assays with the original bait and not the negative control were selected for DNA sequencing analysis. The remaining 20 μL of the diagnostic YC-PCR product was sent to GATC Biotech (Konstanz, Germany), for purification followed by sequencing by automated fluorescent DNA sequencing. Sequence information was analysed using the NCBI Basic Local Alignment Search Tool (BLAST) tool (McGinnis and Madden, 2004) to identify prey interactors.

2.4 Membrane Yeast two-Hybrid (MYTH) library screens

2.4.1 Reagents and media

The NMY51 yeast strain, MYTH empty plasmids, control plasmids and human embryonic, whole brain cDNA library used was obtained from Igor Stagljar (University of Toronto, Canada), whilst all other reagents are stated in section 2.2.1.

2.4.2 MYTH vectors

When using the MYTH Y2H system, the bait must be cloned in-frame with the C_{ub}-LexA-VP16 tag of an appropriate vector. Vector choice is dependent upon membrane topology of the bait (protein of interest). At present, there are several MYTH Y2H vectors available (Figure 2.7), allowing for both N- and C-terminal tagging. C-terminal vectors pCMBV4, pAMBV4 and pTMBV4 (BAIT- C_{ub}-LexA-VP16) are used to generate baits under the control of CYC1 (weak), ADH1 (strong) and TEF1 (very strong) promoters, respectively. N-terminal vectors pTLB1 and pBT3N (LexA-VP16- C_{ub}-BAIT) generate baits under the control of TEF1 and CYC1 promoters, respectively.

Figure 2.7

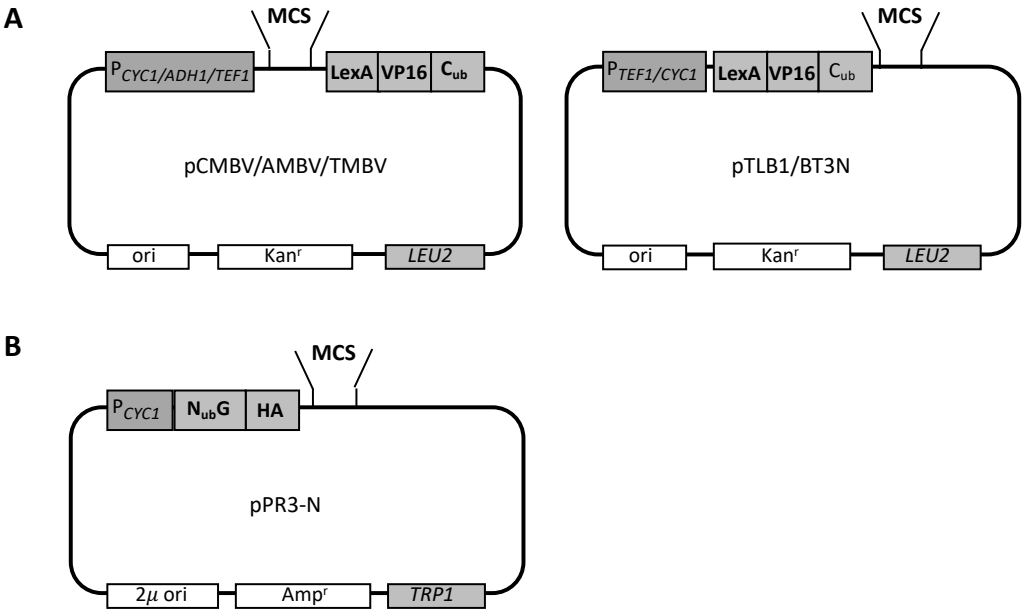

Figure 2.7. Schematic representations of the Membrane yeast two-hybrid (MYTH) vectors. (A) Commonly used C- and N-terminal MYTH bait vectors. (B) N-terminal MYTH prey vector.

2.4.3 Bait Generation

2.4.3.1 Proof-reading KOD PCR from pDONR223

Forward and reverse primers were designed such that they contained 35-40 bases homologous to the linear ends of each bait vector in-frame with 18-21 bases homologous to the cDNA reading frame of the bait (shown below). These primers

allowed the amplification of the desired ORF from pDONR223 and *in vivo* homologous recombination in yeast. Examples shown below:

AMBV_F: 5' AGCATTGCTGCTAAAGAAGAAGGGGTATCTTTGGATAAA**XXX** 3'
AMBV_R: 5' CGACGGTATCGATAAGCTTGATATCGAATTCCTGCAGAT**YYY** 3'

BT3N_F: 5' ACGGTATCGATAAGCTTGATATCGAATTCCTGCAGGGCC**XXX** 3'
BT3N_RS: 5' TGACGTCAGCGCTCCGCGGTTAGCTACTTACCATGGGGC**YYY** 3'

XXX = first codon of the bait,
YYY = reverse complement of last codon of the bait (for N-terminal tagging this is a stop codon).

Sequence-verified pDONR223-ORFs were amplified using KOD Hot Start DNA polymerase and bait-specific MYTH primers (designed as shown above). Typical KOD PCR master mix and cycling parameters in Table 2.5. Following PCR amplification, a sample (10 μL) of the reaction was analysed by gel electrophoresis, for correct fragment size. PCR products were stored at -20 °C.

2.4.3.2 Generation of MYTH baits by Gap Repair

An overview of the homologous recombination method used to generate MYTH bait clones, is shown in Figure 2.8. pAMBV and pBT3N vectors were linearized prior to use via restriction digest with *Sfi*I restriction enzyme, as described in section 2.1.14. NMY51 yeast glycerol stocks were streaked onto YPAD agar plates and grown at 30 °C for 3-5 days. A single NMY51 colony was used to inoculate 5 mL YPAD broth and grown at 30 °C, 200 rpm for 16 h. An additional 45 mL YPAD broth was added to the culture to an OD_{600} of ~0.15 and further incubated at 30 °C, 200 rpm for 3-4 h until an OD_{600} of ~0.6 was reached. Yeast were harvested by centrifugation at 2,300 rpm, RT for 5 min and supernatant discarded. The yeast pellet was resuspended in 25 mL sterile ddH_2O and pelleted as above. Supernatant was discarded, and the pellet was resuspended in 1 mL sterile ddH_2O. To a 1.5 mL microcentrifuge tube: 100 μL yeast

cell suspension, 300 µL PEG/LiOAc solution (Table 2.23), linearised MYTH vector (50 fmol) and KOD PCR product (250-500 fmol) was added and gently mixed.

Figure 2.8

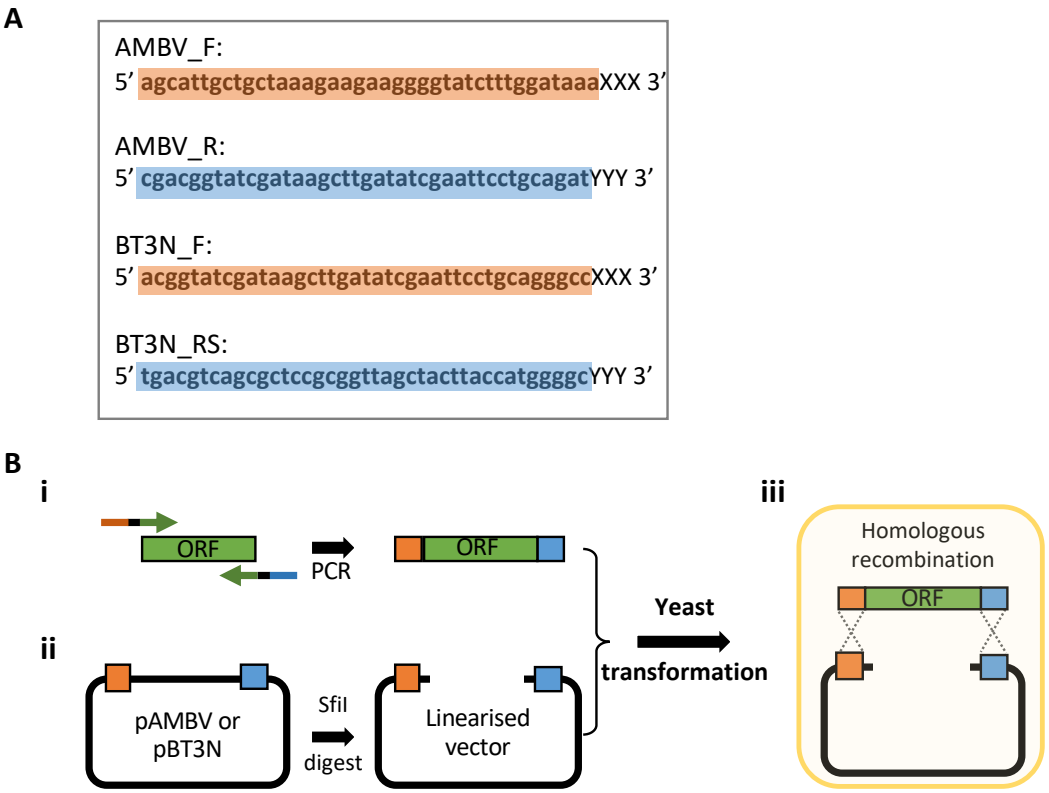

Figure 2.8. Generation of Membrane Yeast Two-Hybrid (MYTH) bait constructs. (A) Forward and reverse Primers designed for *in vivo* recombination cloning into pAMBV (C-terminal tagging) and pBT3N (N-terminal tagging) MYTH bait vectors. Primers are designed to contain a 39 base region of homology to the linear ends of the respective target vectors, together with 18-21 bait specific nucleotides. (XXX = first codon of the bait and YYY = reverse complement of last codon of the selected bait. For N-terminal tagging, this is always a stop codon). (B) Schematic diagram of the homologous recombination method used to generate MYTH bait clones by the *in vivo* gap repair process. (i) Bait cDNA clones were amplified using the primers shown in (A). (ii) The NMY51 MYTH reporter yeast strain was then transfected with a combination of the bait, flanked by vector specific homologous recombination sequences (PCR product) and linearised vector. (iii) *In vivo* homologous recombination facilitates in-frame insertion of the bait into the selected bait vector. Following sequence verification, bait construct is transformed back into MYTH reporter strain, NMY51.

These were incubated at 30 °C for 30 min followed by heat-shock at 42 °C for 60 min, before centrifugation at 2,300 rpm, RT for 5 min. Supernatant was discarded and pellet resuspended in 200 μL sterile ddH_2O and reaction mixture was plated onto SD-L agar plates and grown at 30 °C for 2-4 days. Bait plasmid DNA was isolated from the yeast cell pellet using a commercial miniprep kit (Promega). The manufacturer's bacterial miniprep protocol was modified for yeast plasmid rescue, adding a small volume of 0.5 mm soda lime glass beads to the initial resuspension, followed by 5 min high vortex to ensure sufficient yeast cell lysis. Isolated yeast plasmid DNA was transformed into α-Select competent cells to obtain higher quality, pure plasmid in sufficient quantities for use in subsequent sequencing and analyses. Bait plasmid DNA was isolated from transformed bacterial cells before sequencing construct to confirm proper bait plasmid construction. Sequence-verified bait plasmid DNA was transformed back into NMY51, using the protocol described above, substituting the linearised plasmid and PCR product for the bait plasmid DNA. Yeast glycerol stocks were made as described in section 2.2.7.

2.4.4 Bait Validation – $N_{ub}G$/ $N_{ub}I$ control test

An overview of the $N_{ub}G$/ $N_{ub}I$ control test used for MYTH bait validation, is shown in Figure 2.9. It is necessary to make sure that the bait does not activate the reporter system alone or in the presence of non-interacting preys (i.e. ensure the bait is not auto-activating). The $N_{ub}G/I$ control test is used to assess whether a bait an auto-activator, as it is transformed with interacting (positive) and non-interacting (negative) control preys, and growth assessed on selective media. The following control prey constructs were used: pOST1-$N_{ub}I$, pFUR4-$N_{ub}I$ (positive) and pOST1-$N_{ub}G$, pFUR4-$N_{ub}G$ (negative). OST1 and FUR4 are commonly used control preys. OST1, a component of the N-oligosaccharyl transferase complex, is an integral endoplasmic reticulum (ER) membrane protein (Wilson and High, 2007), whilst FUR4, a uracil permease, is a multi-spanning protein of the plasma membrane in yeast (Silve *et al.*, 1991).

MYTH bait yeast glycerol stocks were streaked onto SD-L agar plates and grown at 30 °C for 3-5 days. A single colony was used to inoculate 5 mL SD-L broth and grown at 30 °C, 200 rpm for 16 h. An additional 45 mL SD-L broth was added to the culture to an OD_{600} of ~0.15 and further incubated at 30 °C, 200 rpm for 3-4 h until an OD_{600} of ~0.6 was reached. Yeast were harvested by centrifugation at 2,300 rpm, RT for 5 min and supernatant discarded.

Figure 2.9

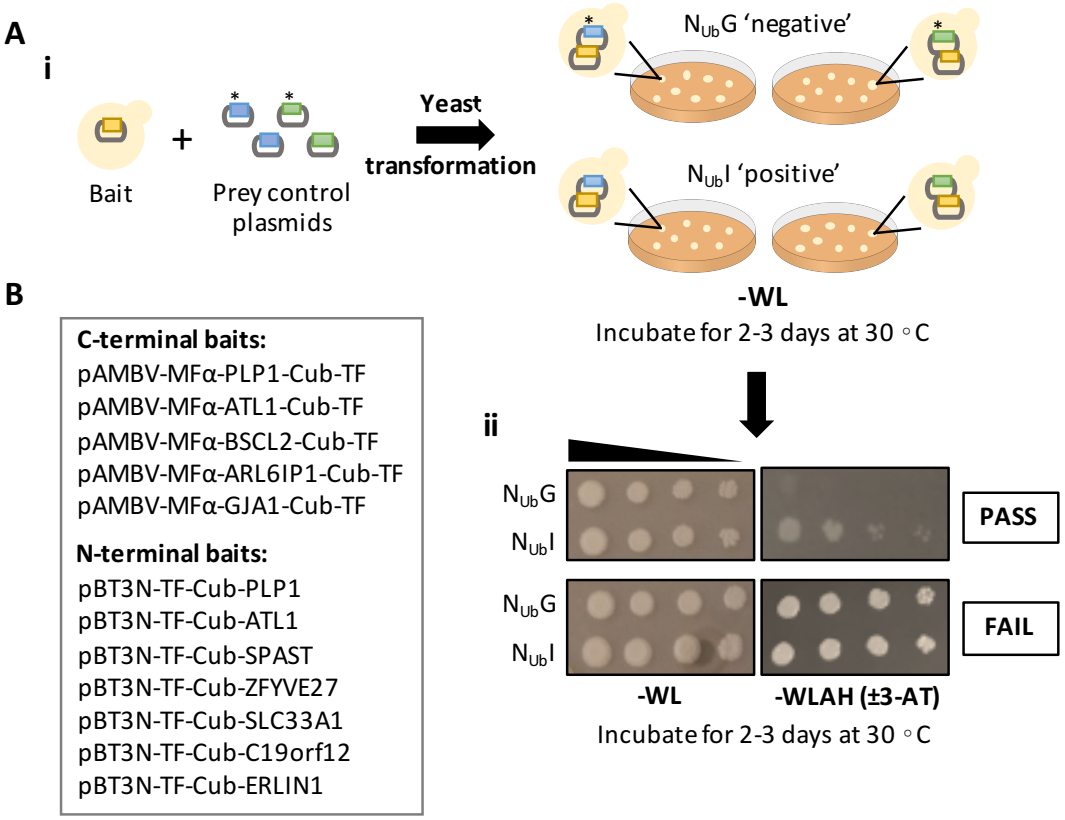

Figure 2.9. Membrane Yeast Two-Hybrid (MYTH) bait validation. (A) Schematic showing the required stages of a MYTH $N_{ub}G/N_{ub}I$ control test. (i) MYTH bait clones, generated as shown in Figure 2.8, were transformed with either $N_{ub}I$ (positive control) or $N_{ub}G$ (negative control) prey plasmids before being plated onto SD-WL plates to select for co-transformed yeast. Positive yeast colonies were then picked and re-spotted onto both SD-WL and a series of SD-WLAH plates supplemented with increasing amounts (0-10 mM) of 3-aminotriazole (3-AT). (ii) Results from a positive (top panel) and negative (bottom panel) $N_{ub}G/N_{ub}I$ control test are shown. Each row of spotted yeast represents a bait transformed with either a negative $N_{ub}G$ (top row) or positive $N_{ub}I$ (bottom row) control prey clone. Spots from left to right represent increasing dilutions (10^0, 10^{-1}, 10^{-2} and 10^{-3}) of yeast. (B) List of MYTH baits which

passed the $N_{ub}G/N_{ub}I$ control tests and were subsequently taken through to MYTH library screening.

The yeast pellet was resuspended in 25 mL sterile ddH_2O and pelleted as above. Supernatant was discarded, and the pellet was resuspended in 1 mL sterile ddH_2O. To a 1.5 mL microcentrifuge tube: 100 μL yeast suspension, 300 μL PEG/LiOAc solution (Table 2.23), 7 μL 10.5 mg/mL heat-denatured salmon testes DNA and 200 ng control prey plasmid was added and gently mixed. These were incubated at 30 °C for 30 min followed by heat-shock at 42 °C for 60 min, before centrifugation at 2,300 rpm, RT for 5 min. Supernatant was discarded and pellet resuspended in 200 μL sterile ddH_2O and reaction mixture was plated onto SD-WL agar plates and grown at 30 °C for 2-4 days. Following diploid colony growth, single colonies from each transformation were resuspended in 100 μL sterile ddH_2O, and used to make 10^{-2}, 10^{-3} and 10^{-4} serial dilutions. Spot 5 μL of undiluted and diluted cells onto SD-WL, SD-WLH±3-AT and SD-WLAH±3-AT (1-10 mM 3-AT) agar plates and grown at 30 °C for 2-4 days.

2.4.5 Large-scale transformation of human embryonic whole brain cDNA prey library with MYTH bait yeast

The initial large-scale transformation step of library screening protocol was performed as described in the DUALmembrane manual (Dualsystems Biotech). Fresh MYTH bait yeast glycerol stocks were streaked onto SD-L agar plates and grown at 30 °C for 3-5 days. Two-three colonies were used to inoculate 10 mL SD-L broth and grown at 30 °C, 200 rpm for 8 h. 100 mL fresh SD-L broth was inoculated with the 10-mL culture and grown at 30 °C, 200 rpm for 16 h. Following incubation, a 1 mL aliquot of culture was pelleted by centrifugation at 2,300 rpm, RT for 5 min and resuspended in 1 mL H_2O. The OD_{600} of the sample was measured and the amount of culture required for 30 OD_{600} units was transferred to a 50-mL Falcon tube and harvested at 2,300 rpm, RT for 5 min. The yeast pellet was resuspended in 10 mL pre-warmed 2X YPAD broth and transferred to a 1 L flask. The Falcon was rinsed with a further 40 mL pre-warmed 2X YPAD broth to recover any remaining cells. An additional 150 mL pre-

warmed 2X YPAD broth (200 mL total volume) was added to the culture resulting in an OD_{600} of ~0.15. The culture was further incubated at 30 °C, 220 rpm for 3-5 h until an OD_{600} of ~0.6 was reached.

The 200 mL yeast culture was divided into four 50 mL Falcon tubes and harvested at 2,300 rpm, RT for 5 min and supernatant discarded. The yeast pellets were each resuspended in 30 mL sterile ddH_2O and pelleted as above. Supernatant was discarded, and each pellet resuspended in 1 mL LiOAc/TE solution (Table 2.22), transferred to a 1.5 mL microcentrifuge tube and pelleted as above. Supernatant was discarded, and the pellet was resuspended in 600 μL LiOAc/TE solution. Four 50 mL Falcon tubes were set up and to each the following was added: 600 μL yeast cell suspension, 2.5 mL PEG/LiOAc solution (Table 2.23), 100 μL 10.5 mg/mL heat denatured salmon testes DNA and 8 μg human adult, whole brain pPR3N (prey) cDNA library. The transformation mixture was incubated at 30 °C for 45 min, gently vortexing every 15 min, followed by addition of 160 μL DMSO. The solution was mixed (by inverting) before incubating at 42 °C for 20 min, followed by centrifugation at 2,300 rpm, 4 °C for 5 min. Each pellet was resuspended in 3 mL 2X YPAD and samples pooled before incubating at 30 °C, 150-200 rpm for 90 min. Yeast were harvested by centrifugation at 2,300 rpm, 4 °C for 5 min and supernatant discarded. The yeast pellet was resuspended in 4.9 mL 0.9 % (w/v) NaCl. To calculate the transformation efficiency, a 100 μL of the yeast suspension was used to make 10^{-2}, 10^{-3} and 10^{-4} serial dilutions and 100 μL was plated onto SD-WL agar plates (90 mm) and incubated at 30 °C for 2-3 days. The remaining yeast suspension was plated equally onto 24 x SD-WLAH (±3-AT depending on control test) agar in 150 mm, triple vented sterile plates and incubated at 30 °C for 3-5 days. Subsequent steps leading to prey identification had to be optimised due to facilities available in the lab (for more details see Appendix 2.2)

2.4.6 Diagnostic YC-PCR

Colonies growing on SD-WL are diploid colonies containing both bait and prey plasmids. Additionally, colony growth on SD-WLAH±3-AT agar plates, indicates

activation of both *HIS3* and *ADE2* reporter genes following successful bait-prey interaction. Up to 2 x 96 colonies from SD-WLAH±3-AT library plates were resuspended in 100 μL 0.9 % (w/v) NaCl, 3 μL spotted onto SD-WLAH and SD-WLAH/X-Gal agar plates and incubated at 30 °C for 3-5 days. Once grown, yeast colonies which could activate all three reporter genes (i.e. blue colonies on WLAH/X-Gal agar plates) were selected for diagnostic YC-PCR using the following primers:

NubGX seq F primer: 5' GTCGAAAATTCAAGACAAGG 3'
pPR3N seq R primer: 5' AAGCGTGACATAACTAATTAC 3'

These primers allow amplification of the prey clone and *in vivo* yeast homologous recombination (gap repair) back into the pPR3N prey vector for reconfirmation mating of positive clones.

In brief, a small amount of yeast was lysed in 5 μL 20 mM NaOH in 0.2 mL PCR tubes and incubated at RT for 20 min. Following lysis, 25 μL of the YC-PCR mixture (Table 2.21 A) was added to each sample and incubated in a thermocycler as described in Table 2.21 B. The PCR product was analysed by gel electrophoresis, as described previously, to identify insert size for each clone. Positive colonies were taken through to the reconfirmation stage.

2.4.7 Reconfirmation gap repair/co-transformation

To distinguish between false positives and genuine positive interactions, prey plasmids are re-transformed with either the original MYTH bait or a negative control. Only those preys which activate all three reporter genes when co-expressed with the original bait only, are considered true positives. The negative bait control used is the empty vector used to construct the MYTH bait. Positive YC-PCR library colonies were amplified with the intention of performing *in vivo* recombination (gap repair) of prey library hits back into the pPR3N prey vector. This was performed simultaneously to the co-transformation of recovered prey and original/control bait, protocol described below.

NMY51 yeast glycerol stocks were streaked onto YPAD agar plates and grown at 30 °C for 3-5 days. A single NMY51 colony was used to inoculate 5 mL YPAD broth and grown at 30 °C, 200 rpm for 16 h. An additional 45 mL YPAD broth was added to the culture to an OD_{600} of ~0.15 and further incubated at 30 °C, 200 rpm for 3-4 h until an OD_{600} of ~0.6 was reached. Yeast were harvested by centrifugation at 2,300 rpm, RT for 5 min and supernatant discarded. The yeast pellet was resuspended in 25 mL sterile ddH_2O and pelleted as above. The pellet was resuspended in 1100 μL 50 % (v/v) PEG 3350, 170 μL sterile ddH_2O, 167 μL 1M LiOAc, 40 μL 10.5 mg/mL heat denatured salmon testes DNA. To a 1.5 mL microcentrifuge tube: 8 μL yeast cell suspension/reaction (i.e. 96x8=768 μL), 5 ng original/control bait/reaction (i.e. 96x5=480 ng) and 5 ng *Sfi*I linearised pPR3N prey vector were added and gently mixed. The yeast suspension was mixed and 8 μL was added to each well of a sterile 96-well PCR plate, followed by 4 μL of a specific YC-PCR reaction (from above) and gentle mixing. As a negative control 4 μL H_2O was added to 8 μL yeast suspension, to assess the level of background growth. All samples were incubated in a thermocycler at the following conditions: 30 °C for 30 min, 42 °C for 25 min and 30 °C for 1 min. Each reaction mixture was spotted onto SD-WL, low adenine media (Table 2.17) 3 μL at a time, allowing the spots to dry before spotting out again. The plates were then incubated at 30 °C for 3-5 days, allowing yeast colonies to grow. Following diploid colony growth, yeast were replicated onto SD-WLAH±3-AT (same as library) and SD-WLAH±3-AT+X-Gal agar plates and grown at 30 °C for 2-4 days, allowing for the selection of positive protein-protein interactions.

2.4.8 Yeast prey sequencing

Only those yeast clones that selectively activate all three reporters (*ADE2, HIS3* and *lacZ*) with the original bait and not the empty bait vector were selected for DNA sequencing analysis. The remaining 20 μL of the diagnostic YC-PCR product was sent to GATC Biotech (Konstanz, Germany), for purification followed by sequencing by automated fluorescent DNA sequencing. Sequence information was analysed using the NCBI Basic Local Alignment Search Tool (BLAST) tool to identify prey interactors.

2.5 Network construction and analysis

It is extremely important to minimise error when dealing with high-throughput data by, accurately collating and storing data. All tested Y2H interactions, both positive and negative, were recorded in Excel spreadsheets (Microsoft, California, USA).

2.5.1 Network construction: database curation

There are many different pathway and molecular databases that have been built to try and collate and store the vast range of interaction network information available in the literature, as well as that being generated in high-throughput, large-scale experiments. There is not one database which provides a fully comprehensive dataset of all published protein-protein interaction data, and soit is necessary to integrate information from several databases to try and increase the coverage of reported interactions.

An 'In-house' interactome network was previously generated by Dr Russell Hyde and Dr Jonathan Woodsmith, combining interaction data collected from several public databases (BioGRID, Human Protein Reference Database (HPRD) and IntAct) as well as interactome data from the Vidal group. This interactome was updated with the most up-to-date version of each database, in combination with experimental interaction data from the Human Integrated Protein-Protein Interaction Reference (HIPPIE) and Biophysical Interactions of ORFeome-based complexes (BioPlex), increasing interaction coverage and providing a final dataset containing both binary (direct) and non-binary (indirect) protein-protein interaction data from which to generate a final network. All identifiers were converted into Entrez Gene IDs to standardise interaction reporting, with the primary gene symbol annotated as a secondary label. This allowed the removal of duplicate interactions, generating an interaction dataset with the highest density and coverage possible at the time of analysis.

2.5.2 Network generation: Cytoscape

Publically available bioinformatics resources such as the Database for Annotation, Visualisation and Integrated Discovery (DAVID) and the Protein ANalysis THrough Evolutionary Relationships (PANTHER) were used on all protein-protein interaction data collated via the final network as well as integrating experimental data generated. Protein-protein interaction data was visualised as complex networks using the open source software platform, Cytoscape (Lopes *et al.*, 2010). Cytoscape allows the integration of networks with any type of attribute data. Figures were generated using Cytoscape version 2.8.2 and will be discussed in more detail in Chapters 3 and 6.

Chapter 3: Constructing a Hereditary Spastic Paraplegia protein-protein interaction (PPI) network

3.1 Introduction

Hereditary spastic paraplegia (HSP or SPG) was first described in the late 1800s (Seeligmüller, 1876; Strümpell, 1880) and has since become a term used to describe this relatively large, clinically and genetically diverse group of inherited neurodegenerative or neurodevelopmental disorders. HSP is characterised by a progressive lower limb spasticity and pyramidal weakness (Harding, 1983; Blackstone, O'Kane and Reid, 2011). Since the identification of the first HSP locus in 1986 (Kenwrick *et al.*, 1986), more recent advances in molecular genetics has led to the identification of over 75 HSP disease-loci with over 60 corresponding genes (Klebe, Stevanin and Depienne, 2015; de Souza *et al.*, 2016). The identification of genes involved in HSP and the functions associated with corresponding proteins, has so far provided a more detailed understanding of the molecular pathways and mechanisms required for axonal maintenance and motor neuron function (Sanderson *et al.*, 2005).

Complex cellular systems are formed by interactions between genes and gene products, located in the same cell, across cells, or even across organs, which appear to underlie most cellular functions, including most genotype-to-phenotype relationships (Vidal, Cusick and Barabási, 2011). A critical step towards unravelling the complex molecular relationships in living systems is the mapping of protein-protein interactions, also known as interactome networks (Rolland *et al.*, 2014). Proteins with similar functions and cellular localisations tend to cluster together within these networks, with the majority sharing at least one function (Vazquez *et al.*, 2003; Chua, Sung and Wong, 2006). Given the inter- and intracellular connectivity within networks, a disease phenotype is rarely the outcome of a specific genetic abnormality in a single gene product, but rather a reflection of the various pathobiological processes that interact within a complex network (Barabási,

Gulbahce and Loscalzo, 2011). Therefore, identifying proteins that either directly or indirectly interact with known HSP proteins, may identify new candidate genes for genetic screening, whilst also providing insights into the molecular mechanisms of HSP pathology. It is therefore important to generate an extended high-confidence human HSP interactome network.

The main aim of the work presented in this section was to prepare a set of tools that would be used to study HSPs systematically. This would be done by: (i) Compiling a comprehensive, up-to-date list of identifiers of all putative human HSPs by literature and database curation; (ii) Using a universal, high-throughput cloning strategy; (iii) Acquiring as many HSP ORFs as possible, and producing expression constructs for use in further studies; (iv) Constructing a predicted HSP PPI network, which can be used to inform interaction predictions, new hypotheses and prioritization of targets for further functional investigation.

3.2 Human HSP ORF library generation

3.2.1 Literature curation

When this study started, there were over 50 spastic gait disease-loci, ("SPastic parapleGia" [SPG] 1-56) identified, with 38 corresponding spastic paraplegia genes (Fink, 2013). This rapidly evolved, and in less than a year, following whole-exome sequencing (WES) and network analysis, there were over 70 different disease-loci (SPG1-71) and a further 16 spastic paraplegia genes identified, as well as other causative genes not yet in the SPG classification (Lo Giudice *et al.*, 2014; Novarino *et al.*, 2014). For this study, information was gathered from a number of literature-based sources including the above-mentioned studies, which were used to acquire Entrez Gene IDs (Maglott *et al.*, 2007) for a total of 58 genes that encode HSP-related proteins (shown in Table 3.1), and are referred to as 'HSP seed 1'.

3.2.2 Obtaining HSP gene identifiers (IDs)

Entrez Gene is an open-access gene-specific database at the National Centre for Biotechnology Information (NCBI, https://www.ncbi.nlm.nih.gov), which generates identifiers (Gene IDs) for individual genes and loci. These unique identifiers correspond to annotated and curated gene-specific information which includes nomenclature, chromosomal localization, protein interactions and phenotypes (Maglott *et al.*, 2011). As such, Entrez Gene IDs were acquired for HSPs identified in section 3.2.1. To maintain consistency throughout this study, HSPs will be annotated and referred to by their gene symbols assigned by Entrez Gene, regardless of any other aliases in use.

Table 3.1

SPG	Gene	Gene ID	Protein	References[a]
SPG1	L1CAM	3897	Neural cell adhesion molecule L1	Jouet et al., 1994
SPG2	PLP1	5354	Myelin proteolipid protein	Saugier-Veber et al., 1994
SPG3	ATL1	51062	Atlastin 1	Zhao et al., 2001
SPG4	SPAST	6683	Spastin	Hazan et al., 1999
SPG5A	CYP7B1	9420	25-hydroxycholesterol 7-alpha-hydroxylase	Tsaousidou et al., 2008
SPG6	NIPA1	123606	Magnesium transporter NIPA1	Rainier et al., 2003
SPG7	SPG7	6687	Paraplegin	Casari et al., 1998
SPG8	WASHC5	9897	WASH complex subunit strumpellin	Valdmanis et al., 2007
SPG10	KIF5A	3798	Kinesin heavy chain isoform 5A	Reid et al., 2002
SPG11	SPG11	80208	Spatacsin	Stevanin et al., 2007
SPG12	RTN2	6253	Reticulon-2	Montenegro et al., 2012
SPG13	HSPD1	3329	60 kDa heat shock protein, mitochondrial	Hansen et al., 2002
SPG15	ZFYVE26	23503	Zinc finger FYVE domain-containing protein 26	Hanein et al., 2008
SPG17	BSCL2	26580	Seipin	Windpassinger et al., 2004
SPG18	ERLIN2	11160	Erlin-2	Alazami et al., 2011
SPG20	SPART	23111	Spartin	Patel et al., 2002
SPG21	SPG21	51324	Maspardin	Simpson et al., 2003

SPG22	SLC16A2	6567	Monocarboxylate transporter 8	Schwartz et al., 2006
SPG28	DDHD1	80821	Phospholipase DDHD1	Tesson et al., 2012
SPG30	KIF1A	547	Kinesin-like protein KIF1A	Erlich et al., 2011, Klebe et al., 2012
SPG31	REEP1	65055	Receptor expression-enhancing protein 1	Zuchner et al., 2006
SPG35	FA2H	79152	Fatty acid 2-hydroxylase	Dick et al., 2010
SPG39	PNPLA6	10908	Neuropathy target esterase	Rainier et al., 2008
SPG42	SLC33A1	9197	Acetyl-coenzyme A transporter 1	Lin et al., 2008
SPG44	GJC2	57165	Gap junction gamma-2 protein	Orthmann-Murphy et al., 2009
SPG47	AP4B1	10717	AP-4 complex subunit beta-1	Abou Jamra et al., 2011
SPG48	AP5Z1	9907	AP-5 complex subunit zeta-1	Slabicki et al., 2010
SPG49	TECPR2	9895	Tectonin beta-propeller repeat-containing protein 2	Oz-Levi et al., 2012
SPG50	AP4M1	9179	AP-4 complex subunit mu-1	Verkerk et al 2009
SPG51	AP4E1	23431	AP-4 complex subunit epsilon-1	Abou Jamra et al., 2011, Moreno-De-Luca et al., 2011
SPG52	AP4S1	11154	AP-4 complex subunit sigma-1	Abou Jamra et al., 2011
SPG53	VPS37A	137492	Vacuolar protein sorting-associated protein 37A	Zivony-Elboum et al., 2012
SPG54	DDHD2	23259	Phospholipase DDHD2	Schuurs-Hoeijmakers et al., 2012
SPG55	C12orf65	91574	Probable peptide chain release factor C12orf65, mitochondrial	Shimazaki et al., 2012
SPG56	CYP2U1	113612	Cytochrome P450 2U1	Oz-Levi et al., 2012
SPG58	KIF1C	10749	Kinesin-like protein KIF1C	Novarino et al., 2014, Dor et al., 2014
SPG59	USP8	9101	Ubiquitin carboxyl-terminal hydrolase 8	Novarino et al., 2014
SPG60	WDR48	57599	WD repeat-containing protein 48	Novarino et al., 2014
SPG61	ARL6IP1	23204	ADP-ribosylation factor-like protein 6-interacting protein 1	Novarino et al., 2014
SPG62	ERLIN1	10613	Erlin-1	Novarino et al., 2014
SPG63	AMPD2	271	AMP deaminase 2	Novarino et al., 2014
SPG64	ENTPD1	953	Ectonucleoside triphosphate diphosphohydrolase 1	Novarino et al., 2014
SPG65	NT5C2	22978	Cytosolic purine 5'-nucleotidase	Novarino et al., 2014

SPG66	ARSI	340075	Arylsulfatase I	Novarino et al., 2014
SPG67	PGAP1	80055	GPI inositol-deacylase	Novarino et al., 2014
SPG68	FLRT1	23769	Leucine-rich repeat transmembrane protein FLRT1	Novarino et al., 2014
SPG69	RAB3GAP2	25782	Rab3 GTPase-activating protein non-catalytic subunit	Novarino et al., 2014
SPG70	MARS	4141	Methionine--tRNA ligase, cytoplasmic	Novarino et al., 2014
SPG71	ZFR	51663	Zinc finger RNA-binding protein	Novarino et al., 2014
-	AFG3L2	10939	AFG3-like protein 2	Koppen et al., 2007, Di Bella et al., 2010
-	ALS2	57679	Alsin	Eymard-Pierre et al., 2002
-	ATP6	4508	Protein bicaudal D homolog 2	Verny et al., 2011
-	CCT5	22948	T-complex protein 1 subunit epsilon	Bouhouche et al., 2006
-	ELOVL4	6785	Elongation of very long chain fatty acids protein 4	Aldahmesh et al., 2011 Fink, 2013
-	GAD1	2571	Glutamate decarboxylase 1	McHale et al., 1999, Lynex et al., 2004
-	GJA1	2697	Gap junction alpha-1 protein	Paznekas et al., 2003
-	KANK1	23189	KN motif and ankyrin repeat domain-containing protein 1	Novarino et al., 2014
-	VCP	7415	Transitional endoplasmic reticulum ATPase	De Bot et al., 2012

Table 3.1. List of 'HSP seed 1' loci and genes. HSP genes are listed by spastic gait disease-loci (SPG), numbered sequentially based on the order of locus discovery (Fink, 2013). HSP genes not part of the SPG classification system are listed alphabetically. Entrez Gene IDs were obtained from the NCBI database (Maglott *et al.*, 2007) and are the most updated identifiers for the corresponding genes at the time of submission.

[a] Locus/gene discovery association with HSP

3.2.3 DNA sequence collection

The NCBI Reference Sequence (RefSeq) database (Pruitt, Tatusova and Maglott, 2005) is an open-access, non-redundant and comprehensive collection of well-annotated sequences, including genomic DNA, transcripts and proteins in which Entrez Gene IDs were used to obtain a Reference Sequence (RefSeq) for each HSP. Some HSP genes have more than one variant annotated in the RefSeq database, only

those variants that encode the longest isoform were selected. RefSeq sequences are continually updated and annotated with newer versions often including longer 5' and 3' untranslated regions (UTR), however the protein coding sequence generally remains the same, and as such the complementary DNA (cDNA) sequence information of the selected HSPs were acquired for primer design and cloning purposes.

The 'HSP seed 1' genes were subjected to a set of exclusion criteria, removing those insufficiently annotated or those that were unlikely to be expressed, leaving only well-annotated sequences for cloning. The exclusion criteria include: (i) any evidence suggesting that they are a pseudogene (i.e. non-coding); (ii) any sequences which are poorly annotated (i.e. no known ORF start/stop site), and (iii) any genes that encode ORFs larger than 3 kb, as large ORFs will be difficult to clone from cDNA and encoded proteins are unlikely to function properly in yeast (Shulga *et al.*, 2000).

Following application of the exclusion criteria, size exclusion was the only relevant criteria and was used to exclude 14 HSPs (Table 3.2) from the 'HSP seed 1' list, leaving a total of 44 HSPs to be followed up.

Table 3.2

SPG	Gene	ORF size	Exclusion criteria
SPG1	L1CAM	3773	ORF size > 3,000 bp
SPG8	WASHC5	3479	
SPG10	KIF5A	3098	
SPG11	SPG11	7331	
SPG15	ZFYVE26	7619	
SPG30	KIF1A	5375	
SPG39	PNPLA6	4127	
SPG49	TECPR2	4235	
SPG51	AP4E1	3413	
SPG58	KIF1C	3311	
SPG59	USP8	3356	

SPG69	RAB3GAP2	4181	
SPG71	ZFR	3224	
-	ALS2	4973	

Table 3.2. Excluded HSPs. HSP genes excluded from further investigation due to large ORF size.

3.3 Cloning protocol

Having acquired all the DNA sequencing information for the 44 'HSP seed 1' ORFs, the Gateway® cloning strategy was used to generate expression constructs for subsequent experimental studies.

3.3.1 Gateway® cloning

An overview of Gateway® cloning can be seen in Figure 3.1. The Gateway® Technology (Invitrogen) is a universal cloning method used to accelerate the cloning of ORFs into a range of different expression vectors. This technology takes advantage of the lambda recombination system which allows the quick and easy shuttling of DNA sequences between vectors, as long as DNA sequences are flanked by specific recombination sequences (Hartley, Temple and Brasch, 2000).

HSP ORFs were amplified from cDNA using 'Gateway' gene-specific primers, these were designed so that the 5' and 3' end of the ORF was followed with *attB*1 and *attB*2 sequence overhangs, respectively. All Gateway primers, contain the ORF native start and stop codons. Once an *attB*-PCR product is generated this can be used in a BP recombination reaction (termed BP reaction), in which the PCR product is recombined, *in vitro,* with the Gateway® donor vector pDONR223. The donor vector has *attP1* and *attP2* sites which flank the *ccdB* gene (expression of which is lethal to *E. coli*). The BP reaction results in the recombination of the *attB*-PCR product with the *attP*-donor vector in which the *ccdB* gene is flipped out and replaced by the HSP ORF to create an *attL*-flanking HSP ORF pDONR223 entry clone.

Figure 3.1

A

Gateway_F:
5'-GAA TTC ACA AGT TTG AAA AAA GCA GGC TGG ATGXXX-3'
Gateway_R:
5'-GTC GAC CAC TTT GTA CAA GAA AGC TGG GTGYYY-3

B

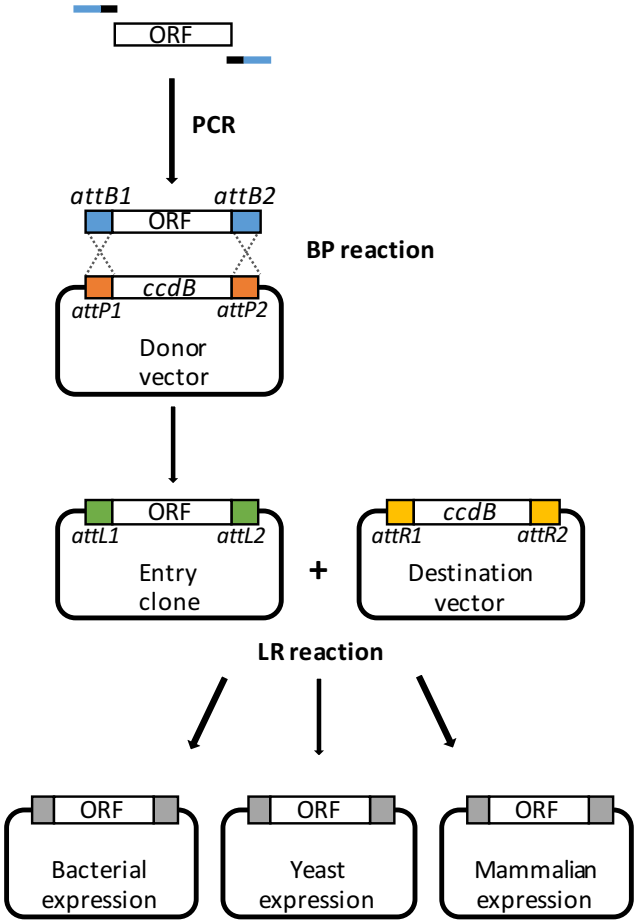

Figure 3.1. The Gateway® system. (A) Primer design includes the Gateway® *attB* recombination site sequences (blue), XXX = first gene-specific codon after ATG and YYY = reverse complement of last gene-specific codon. (B) ORFs are amplified using Gateway primers (as in A), resulting in *attB1* and *attB2* overhangs (blue). The *attB* sites allow the PCR product to be recombined with the *attP1* and *attP2* sites (orange) of a donor vector, producing an *attL*-containing entry clone, in what is called a BP reaction. This entry clone can undergo further recombination with the *attR1* and *attR2* sites (yellow) of various destination vectors, in what is called an LR reaction, generating *attB*-containing bacterial, yeast and mammalian expression clones.

ORF orientation is important, and by using this system this can be maintained as the *attB1* site only recombines with the *attP1* site (likewise for *attB2* and *attP2*). Following *E. coli* transformation, only pDONR223 entry clones can grow as the *ccdB* gene is no longer be expressed in the recombined vector. The Gateway® pDONR223

vector contains a spectinomycin resistance marker (Rual *et al.*, 2004) allowing for the selection of positively transformed colonies on spectinomycin-containing agar plates.

Generated entry clones contain *attL1* and *attL2* sites which allows ORFs to be shuttled into other expression vectors (destination vectors), in a similar recombination reaction as the BP reaction. The destination vector contains *attR1* and *attR2* and with *an attL*-entry clone, can be used to undergo a LR recombination reaction (termed LR reaction). Following *E. coli* transformation, transformants are selected for growth using antibiotic-containing media (elective towards the destination vector.

3.3.2 Yeast two-Hybrid cloning

The primary aim was to investigate the interaction profiles of HSPs, to provide new insight into the molecular mechanisms of the disease and identify new candidate genes for screening. Initially, the *GAL4* yeast two-hybrid (Y2H) system (reviewed in Chapters 1 and 4) was used for this analysis. HSP ORFs were successfully cloned into the Y2H bait vector pGBAE-B and the Y2H prey vector pACTBE-B for use in 'conventional' yeast two-hybrid screens (discussed further in Chapters 4 and 5).

Several HSPs were known to have transmembrane domains (see Figure 3.2), which, due to their hydrophobic nature can be problematic for 'traditional' Y2H and so the split-ubiquitin membrane yeast two-hybrid (MYTH) system was employed (reviewed in Chapters 1 and 6). HSP ORFs were successfully cloned into MYTH bait vectors pAMBV or pBT3N, for use in MYTH library screens (discussed further in Chapter 6).

Figure 3.2

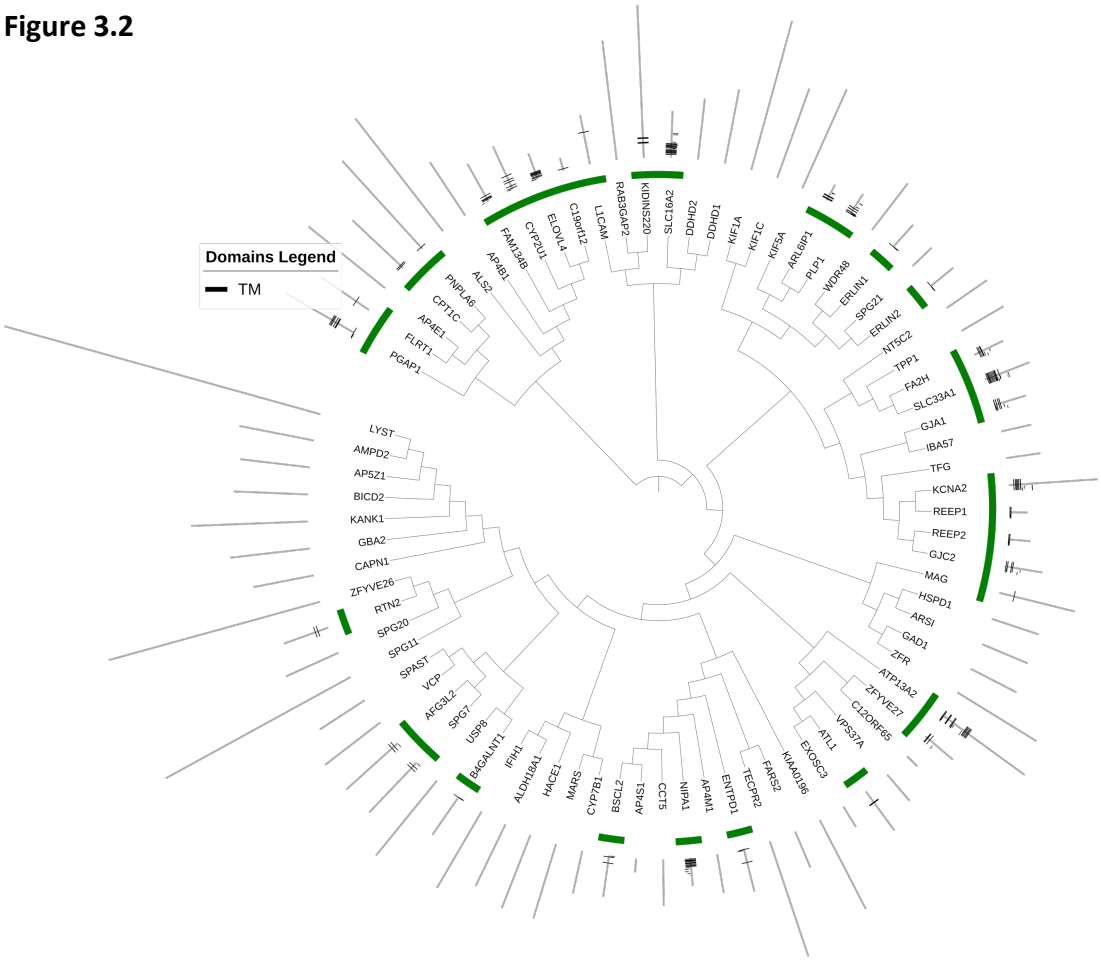

Figure 3.2. Dendrogram of all putative HSP proteins (HSP seed 3) and the representation of transmembrane proteins within the group. Proteins are ordered by their primary sequence using ClustalOmega, a multiple protein sequence alignment tool. Sequence alignment was used to generate a phylogenetic tree using iTOL (Letunic and Bork, 2007). The transmembrane-domain containing proteins are highlighted in green. The position of each transmembrane domain is shown. Abbreviations: TM = transmembrane domain.

3.4 HSP-related proteins interact within a network

For the purpose of network analysis, an annual literature curation was conducted to acquire the most up-to-date list of Entrez Gene IDs for gene entries that encode HSP-related proteins (see Figure 3.3). Ultimately, this resulted in a total of 99 *bona fide* gene entries, corresponding to 83 HSP-related proteins (as shown in Table 1.1), which include 78 spastic gait disease-loci (SPG1-78) and 63 corresponding spastic paraplegia genes, as well as those genes involved in complex forms not referred to as HSP, such as mitochondrial genes MT-ATP6 (Verny *et al.*, 2011) and MT-TI (Corona

et al., 2002), or other causative genes not yet part of the SPG classification system, such as LYST (Shimazaki *et al.*, 2014) and CCT5 (Bouhouche *et al.*, 2005).

3.4.1 HSP protein-protein interaction (PPI) network construction: HSPome

As many cellular processes are mediated by protein-protein interactions, including signal transduction and enzyme activity, large protein-protein interaction networks have often facilitated the identification of common biological pathways and gene function annotation (Vallabhajosyula *et al.*, 2009).

Early in the project, Novarino et al. (2014) generated a predicted HSP interactome network (Novarino *et al.*, 2014). They initially created an expanded global proteome network, combining interaction data from multiple sources which included, iREFINDEX (Razick, Magklaras and Donaldson, 2008), ConsensusPath DB (Kamburov *et al.*, 2009), HumanNet (Lee *et al.*, 2011), literature-curated interactions from STRING (Franceschini *et al.*, 2013) and the Y2H pre-publication dataset (HI-2012) from the Human Interactome Database website (http://interactome.dfci.harvard.edu/H_sapiens/). Following a network propagation-based approach (Vanunu *et al.*, 2010), they were then able to extract already published HSP mutated genes (seeds), candidate HSP genes they identified through whole-exome sequencing of families displaying AR-HSP and their interactors, to derive their HSPome. This 'one-step' subnetwork was composed of 589 proteins. The authors did not make their HSPome freely available and so prior to performing a large-scale targeted Y2H analysis, it was important to generate our own comprehensive predicted HSP interactome network. To achieve this, a global protein network consisting of interaction data from several public databases (BioGRID, HPRD and CCSB), our 'In-house' interactome network (as described in section 2.5.1) and literature-based interaction data was curated. This was used to extract known HSP genes (seeds) and their proximal interactors, creating a 'one-step' HSP subnetwork. Due to the continual discovery of disease-loci and corresponding spastic paraplegia genes, the HSP seed list was updated regularly throughout this project and is shown by the three subnetworks generated (Figure 3.3 A).

Finally, interaction data from several updated public databases, in combination with experimental interaction data from the Human Integrated Protein-Protein Interaction rEference (HIPPIE) and Biophysical Interactions of ORFeome-based complexes (BioPlex) was merged with the global network generated to maximise interaction coverage. This 'expanded' global network, consisted of 22,932 proteins (nodes) and 422,357 interactions(edges), was used to extract the most recent set of known HSP genes (HSP seed 3) and their proximal interactors, creating a 'one-step' HSP subnetwork, termed the 'HSPome' (Figure 3.3 B).

Many of the public interaction databases assign annotations such as a "direct" or "physical" association which can often be confusing. For example, a "physical" association describes molecules in a physical complex, identifying both direct binding partners or indirect protein associations. It was therefore important that in this study all PPIs were annotated according to method of discovery. An interaction was termed "known direct" if discovered via binary methods such as Y2H, whereas a "known indirect" interaction would have been discovered by other techniques such as affinity-capture western or co-immunoprecipitation and finally "predicted direct/indirect" interactions would be assigned to an interolog accordingly.

Figure 3.3

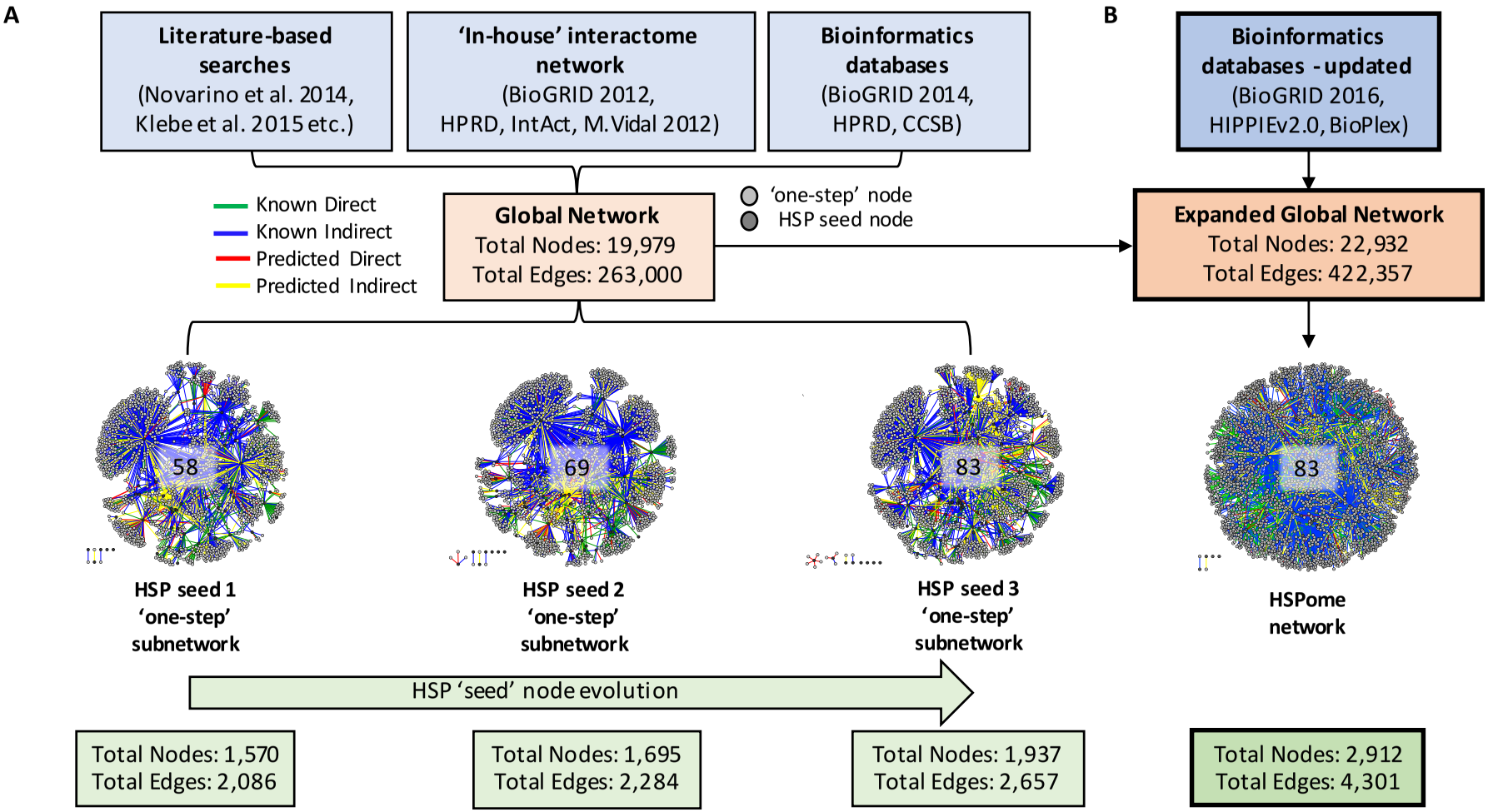
A
Literature-based searches (Novarino et al. 2014, Klebe et al. 2015 etc.)
'In-house' interactome network (BioGRID 2012, HPRD, IntAct, M.Vidal 2012)
Bioinformatics databases (BioGRID 2014, HPRD, CCSB)
Known Direct
Known Indirect
Predicted Direct
Predicted Indirect
Global Network
Total Nodes: 19,979
Total Edges: 263,000
'one-step' node
HSP seed node
B
Bioinformatics databases - updated (BioGRID 2016, HIPPIEv2.0, BioPlex)
Expanded Global Network
Total Nodes: 22,932
Total Edges: 422,357
58
69
83
83
HSP seed 1 'one-step' subnetwork
HSP seed 2 'one-step' subnetwork
HSP seed 3 'one-step' subnetwork
HSPome network
HSP 'seed' node evolution
Total Nodes: 1,570
Total Edges: 2,086
Total Nodes: 1,695
Total Edges: 2,284
Total Nodes: 1,937
Total Edges: 2,657
Total Nodes: 2,912
Total Edges: 4,301

Figure 3.3. Generation of a high-density predicted HSPome network. (A) HSP 'one-step' subnetworks were generated from a combined global human and orthologue network, consisting of interaction data derived from each of the listed databases. Incremental expansion in the number of HSP-associated seed nodes (HSP seed 1 to 3), over the timeline of this project is shown by comparison of the three subnetworks generated, respectively. (B) Final HSP 'one-step' network (HSPome) containing recent data from the HIPPIE, BioPlex and BioGRID databases.

HSP seeds and candidate proteins identified by Novarino et al., (2014) and similarly those identified in the predicted HSPome generated in this study were found to have some degree of overlap (as shown in Figure 3.4). Of the proximal interactors identified by Novarino at al. 6 have since been identified as novel HSP proteins, highlighting the importance and relevance of network analysis.

Figure 3.4

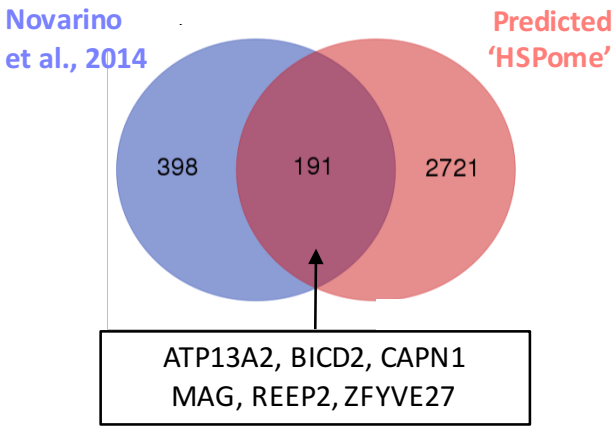

Figure 3.4. Relative expansion of the human 'HSPome'. The degree of overlap between sets of HSP genes previously identified by Novarino et al. (2014) was compared with those in the predicted 'HSPome' generated in this study. Of the 589 genes identified by Novarino et al. (2014), 6 have since been identified as novel HSP proteins and are shown in the box.

3.4.2 Identifying 'hubs' in the HSPome network

Analysis of the topological pattern of interactions observed in large PPI networks often reveals a common feature, the presence of 'hubs' or nodes (proteins) that are highly connected to other nodes within the network. Large networks characterised

by the presence of 'hubs' often possess the 'scale-free' property i.e. the nodal degree distribution of the network is a power-law distribution (Barabasi and Albert, 1999). Even though this property does not identify any degree 'scale', it has become common practice to use an informal threshold or degree scale when analysing protein interaction networks, so that all nodes (proteins) that have a degree higher that the 'threshold' scale are considered special 'hub' nodes (Vallabhajosyula *et al.*, 2009).

Following topological analysis of the HSPome network, 'hub' HSP nodes (proteins) were defined as those most highly connected. The top 10 most highly connected HSP nodes were defined as HSP 'hub' nodes (see Figure 3.5 A). The HSPome network was used to extract these 'hub' HSP nodes and their proximal interactors to create the 'one-step' HSPome degree-based subnetwork as shown in Figure 3.5 B.

Figure 3.5

A

Gene ID	Symbol	No. of interactors	No. of HSP interactors
7415	VCP	698	7
3329	HSPD1	413	5
22948	CCT5	235	2
2697	GJA1	169	0
10342	TFG	165	2
9101	USP8	151	0
823	CAPN1	133	0
57599	WDR48	126	0
4141	MARS	117	0
11160	ERLIN2	110	1

B

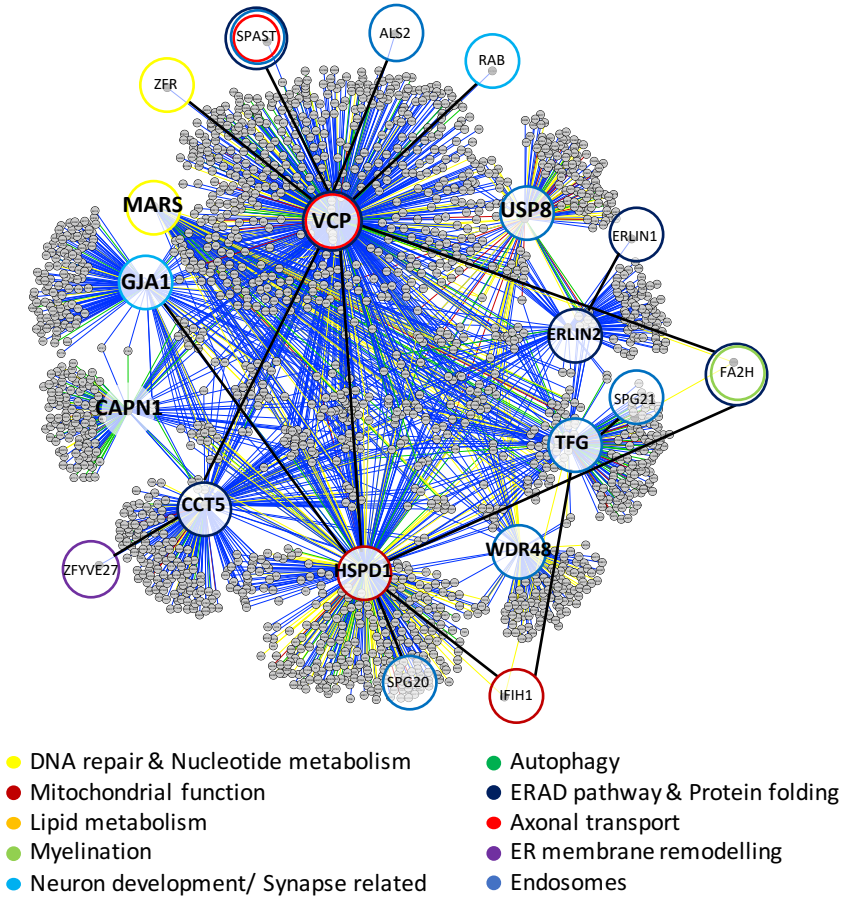

Figure 3.5. Degree-based hubs within the current HSPome. (A) Nodes within the HSPome were ranked to identify the top 10 most highly connected nodes, defined as 'hub' nodes (proteins). The number of total interactors compared to interactions with other HSP proteins is shown. (B) These 'hub' proteins (in bold) were then used to generate the HSPome degree-based subnetwork. Colours represent different functional modules as shown in the key.

3.4.3 Transmembrane HSP subnetwork: construction

Membrane proteins are involved in diverse processes including molecular transport, metabolism and the maintenance of cell structures, with many involved in functions linked to disease (Snider *et al.*, 2010). The identification of membrane protein interactions, and subsequent network generation, would enable a greater understanding of how this class of proteins is able to carry out various cellular roles. However, due to their hydrophobic nature, the use of conventional assays is often difficult or unsuitable (Stagljar and Fields, 2002).

In ‘traditional’ Y2H, the bait and prey are fused to split-transcription factor components and so to activate the reporter genes, the interacting proteins must relocate, with the newly fused transcription factor, to the nucleus (Stagljar and Fields, 2002). This can be considerably difficult for proteins with a high hydrophobic nature such as those with transmembrane domains, and so the split-ubiquitin membrane yeast two-hybrid (MYTH) system was developed for use in such circumstances. Prior to performing a large-scale targeted Y2H analysis, it was therefore important to identify those HSPs with transmembrane domains and use the appropriate technique for further investigation.

Following identification of membrane HSP proteins (Table 3.3), the HSPome network was used to extract HSPs with or without transmembrane domains and their proximal interactors, creating two ‘one-step’ HSPome subnetworks as shown in Figure 3.6.

Figure 3.6

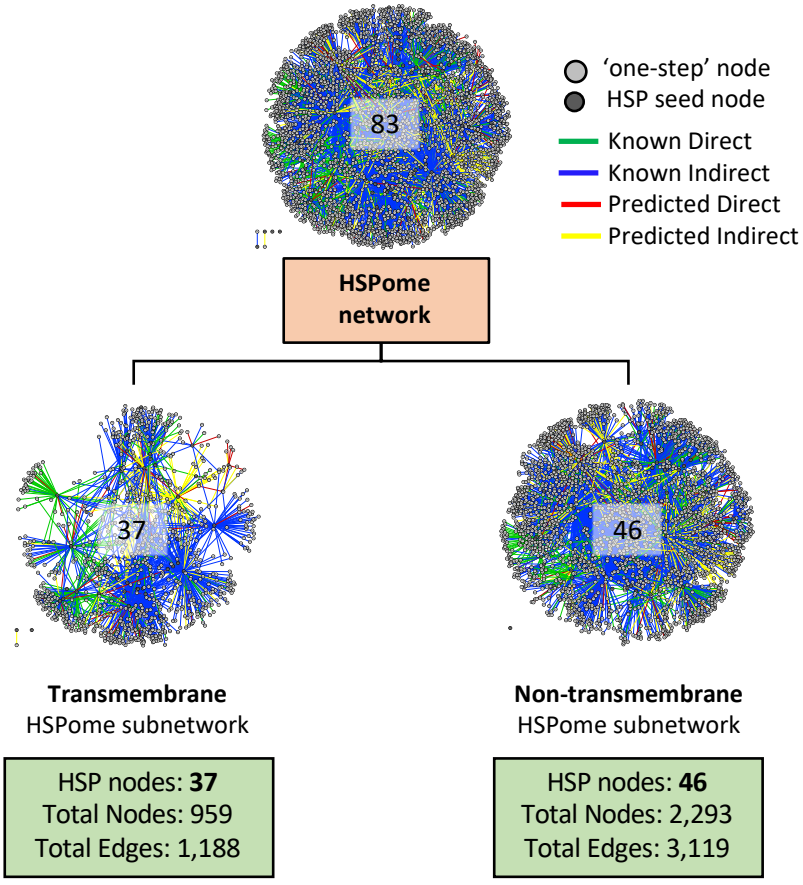

Figure 3.6. Generation of high-density predicted HSPome subnetworks. Lists of HSPs with (37) or without (46) transmembrane domains were used to generate 'one-step' subnetworks from the HSPome network, respectively.

The subnetworks revealed a bias in the number of proteins (nodes) and interactions (edges), more specifically "direct" binary interactions (Table 3.3) identified for non-membrane associated HSP proteins. This in part is reflected in the difficulty membrane proteins pose in the more conventional techniques, and as such the MYTH system was employed for the high-throughput investigation of membrane HSP proteins.

Table 3.3

SPG	Symbol	Gene ID	No. of TM domains	Known Direct Interactions
SPG1	L1CAM	3897	1	14
SPG2	PLP1	5354	4	5
SPG3	ATL1	51062	2	1
SPG4	SPAST	6683	1	3
SPG6	NIPA1	123606	9	0
SPG7	SPG7	6687	2	23
SPG12	RTN2	6253	2	1
SPG17	BSCL2	26580	2	8
SPG18	ERLIN2	11160	1	1
SPG22	SLC16A2	6567	12	0
SPG26	B4GALNT1	2583	1	1
SPG31	REEP1	65055	2	0
SPG33	ZFYVE27	118813	3	2
SPG35	FA2H	79152	4	3
SPG39	PNPLA6	10908	1	1
SPG42	SLC33A1	9197	11	0
SPG43	C19orf12	83636	1	2
SPG44	GJC2	57165	4	0
SPG49	CYP2U1	113612	5	0
SPG61	ARL6IP1	23204	3	41
SPG62	ERLIN1	10613	1	4
SPG64	ENTPD1	953	2	1
SPG67	PGAP1	80055	7	0
SPG68	FLRT1	23769	1	0

SPG72	REEP2	51308	2	1
SPG73	CPT1C	126129	2	0
SPG75	MAG	4099	1	13
SPG78	ATP13A2	23400	12	45
-	AFG3L2	10939	2	5
-	ELOVL4	6785	7	0
-	FAM134B	54463	4	2
-	GJA1	2697	4	7
-	KCNA2	3737	6	6
-	KIDINS220	57498	4	6
-	MT-ATP6	4508	6	1
-	MT-ND4	4538	11	10
-	MT-CO3	4514	7	6

Table 3.3. List of all transmembrane domain-containing HSPs. HSP genes are listed by spastic gait disease-loci (SPG), those not part of the SPG classification system are listed alphabetically. Entrez Gene IDs were obtained from the NCBI database (Maglott *et al.*, 2007). Information regarding transmembrane domains was obtained from UniProt. The number of known direct interactors was identified following analysis of the transmembrane HSPome subnetwork shown in Figure 3.6.

Following identification of membrane HSP proteins, the HSPome network was used to extract HSPs with or without transmembrane domains and their proximal interactors, creating two 'one-step' HSPome subnetworks as shown in Figure 3.6. The subnetworks revealed a bias in the number of proteins (nodes) and interactions (edges), more specifically "direct" binary interactions (Table 3.3) identified for non-membrane associated HSP proteins. This in part is reflected in the difficulty membrane proteins pose in the more conventional techniques, and as such the MYTH system was employed for the high-throughput investigation of membrane HSP proteins.

3.5 Discussion

For the analysis of a given protein family, or in this case a genetically diverse group of disorders, generating a collection of ORFs is a powerful tool to enable a more

systematic, global approach for studying interaction profiles, subcellular localisation or biochemical properties of such proteins.

This chapter describes the process required to generate as complete a set of human HSP ORFs as possible. An initial list of all human putative HSP genes and their corresponding proteins (HSP seed 1) were identified, and all appropriate genetic information extracted following literature-based, and publicly available bioinformatics database searches. The data from several published studies (Fink, 2013; Lo Giudice *et al.*, 2014; Novarino *et al.*, 2014) was extracted so that the initial number of putative HSPs, at the beginning of this study, was set at 58. After removal of 14 HSPs due to their large ORF size, the original 58 was reduced and a new list of 44 human HSPs was compiled and this became the initial ORF acquisition target. DNA sequences representing 41 of the 44 HSPs were acquired, 11 of which were not successfully cloned into the Gateway system, setting the number of genes represented within our collection at 30, and included spastin (SPG4) and its two isoforms (M1 and M87). The majority of HSPs used in this study were full-length and these can be used as a template for the production of truncated ORFs for specific analysis of individual domains separate from the full-length protein. Finally, DNA sequences representing several of the larger ORF-containing HSPs were also used to generate fragments which were successfully cloned into the Gateway® system, for L1CAM and WASHC5, setting the number of genes represented within our collection at 32.

The main aim of this project was to analyse the interaction profiles of human HSPs by Y2H, and so a collection of HSP ORFs in yeast expression vectors had to be successfully constructed. The techniques and reagents for Y2H analysis will be discussed in Chapter 2, and the data generated is compiled in Chapters 4-5. Integral membrane and membrane-associated HSPs were cloned into alternative membrane yeast two-hybrid (MYTH) expression vectors, in the hope to overcome the paucity of data regarding biological function of some of these HSPs, due to the hydrophobic nature of transmembrane domains. The techniques and reagents for membrane Y2H

analysis were discussed in Chapter 2, and data generated will be discussed further in Chapter 6.

Additionally, to further our understanding of HSPs and the biological processes underpinning these disorders, it was essential to generate an initial high coverage protein-protein interaction (PPI) network, which can be continually enriched with experimental data, providing further interaction predictions, as well as annotations with information from literature and other bioinformatics databases, which can serve as a basis for the generation of new hypotheses and prioritization of targets for further investigation.

Chapter 4: Systematic analysis of binary HSP:HSP interactions & the 'edgetic' effect of HSP genetic mutations

4.1 Introduction

Large-scale interactome mapping projects have been successfully used to provide new insight into the composition and organisation of biological processes in several model organisms (Fromont-Racine, Rain and Legrain, 1997; Walhout et al., 2000). Interactome network mapping relies on high-throughput experimental data generated from various methodologies, including yeast two-hybrid (Y2H), which tests direct or 'binary' interactions (Chien et al., 1991; Braun, 2012), or affinity purification and mass spectrometry (AP-MS), which normally involves the isolation of protein complexes, composed of direct and indirect protein interactions (Gingras and Raught, 2012; Walzthoeni *et al.*, 2013). Initially used to investigate the functional relationship of proteins in several model organisms, binary protein-protein interaction mapping can be highly informative (Fromont-Racine, Rain and Legrain, 1997; Walhout *et al.*, 2000), and has since been used to provide insights into a range of human diseases, which result from perturbations in network connectivity (Goh *et al.*, 2007). The approach of systematic protein-protein interaction screening has been successfully used to identify potential interaction partners, as well as to functionally annotate uncharacterised proteins, based on the biological principle known as 'guilt by association'. Interacting proteins usually function within the same molecular machinery or cellular pathway (Schauer and Stingl, 2009).

Yeast two-hybrid is one of the most well-established techniques used to map protein-protein interactions (Walhout and Vidal, 2001), and the use of large-scale high throughput Y2H screens has been the source of most binary protein interaction data currently available (Parrish, Gulyas and Finley, 2006). The Y2H system, as described in Chapter 1, is one of the most standardised *in vivo* techniques used to study protein-protein interactions as it is a relatively simple assay that was originally

developed for high-throughput analyses in the late 1980s (Fields and Song, 1989; Chien *et al.*, 1991).

There are some well-documented examples of HSP:HSP protein interactions reported, which include direct interactions between REEP1, spastin and atlastin-1, all of which are linked to the tubular ER network (Park *et al.*, 2010). However, to date there has not been a systematic investigation of all possible HSP:HSP protein interactions. Therefore, the main aim of the research presented in this chapter was to use the Y2H system to perform an unbiased systematic screen of all possible binary HSP:HSP protein interactions. Data generated from these screens was compared to all available published HSP:HSP protein interaction data, to define novel partner interactions and assess the reproducibility of previously defined interactions. Finally, all reproducible binary HSP:HSP interaction profiles were analysed to assess associated protein functions and/or cellular pathways or processes in which these proteins may act.

Genotype-to-Phenotype:

Genome-wide associated studies and next-generation sequencing has evolved rapidly, generating ever-increasing amounts of genotypic information, which can be used to explore the functional consequences of distinct disease-associated mutations (Karchin and Nussinov, 2016). Genotype-to-phenotype relationships are far more complicated than the original paradigm of 'one-gene/ one-enzyme/ one-function' of the 1940s (Beadle and Tatum, 1941; Sahni *et al.*, 2013), with different mutations affecting the same gene but often leading to clinically diverse phenotypes (Zhong *et al.*, 2009). Additionally, genes and gene products rarely function alone, instead they tend to interact with each other to function as molecular machines, which form part of highly interconnected complex cellular networks, often represented in 'interactome' network models (or graphs) with nodes corresponding to proteins, and edges representing either physical or biochemical interactions (Barabási and Oltvai, 2004; Zhong *et al.*, 2009; Vidal, Cusick and Barabási, 2011).

Missense mutations are some of the most common mutations in Mendelian disorders, accounting for more than half of all reported mutations in the Human Gene Mutation Database (HGMD) (Stenson *et al.*, 2014). Missense mutations may have no functional consequence, however the majority of disease-associated missense mutations cause a complete loss of protein function, through protein misfolding or instability, leading to 'node removal', or alternatively, edge-specific genetic or 'edgetic' perturbations, which can lead to the loss or gain of specific interactions within the network (see Figure 4.1, panel A), giving rise to a host of clinically diverse phenotypes (Zhong *et al.*, 2009; Sahni *et al.*, 2015).

'Edgetic' interaction network studies are emerging as a powerful tool, which can be used to facilitate our understanding of the mechanistic connection between genotype and phenotype (Zhong *et al.*, 2009). Changes in network topology resulting from disease-associated mutations can confer different pathological phenotypes, and a strategy known as 'Edgotyping' can reveal how the loss or gain of specific interactions (edges), can be used to interpret complex genotype-to-phenotype relationships (as shown in Figure 4.1, panel B), allowing improved diagnosis and prognostic prediction (Sahni *et al.*, 2013).

Identification of genetic mutations that contribute to inherited forms of HSP could therefore provide valuable insight into the potential molecular mechanisms involved in the pathogenesis of this group of disorders, which may also improve our understanding of the cellular processes required for axonal maintenance or degeneration. Although there have been many HSP disease-associated mutations identified, to date there has not been any systematic 'edgetic' interaction network studies, investigating the effects of disease-associated mutations on particular interactions as well as on the overall HSP network topology. Therefore, the second aim of the work presented in this chapter was to investigate the 'edgetic' effects of HSP disease-associated mutations on binary wild-type HSP:HSP interactions, in an unbiased systematic method using the Y2H system.

Figure 4.1

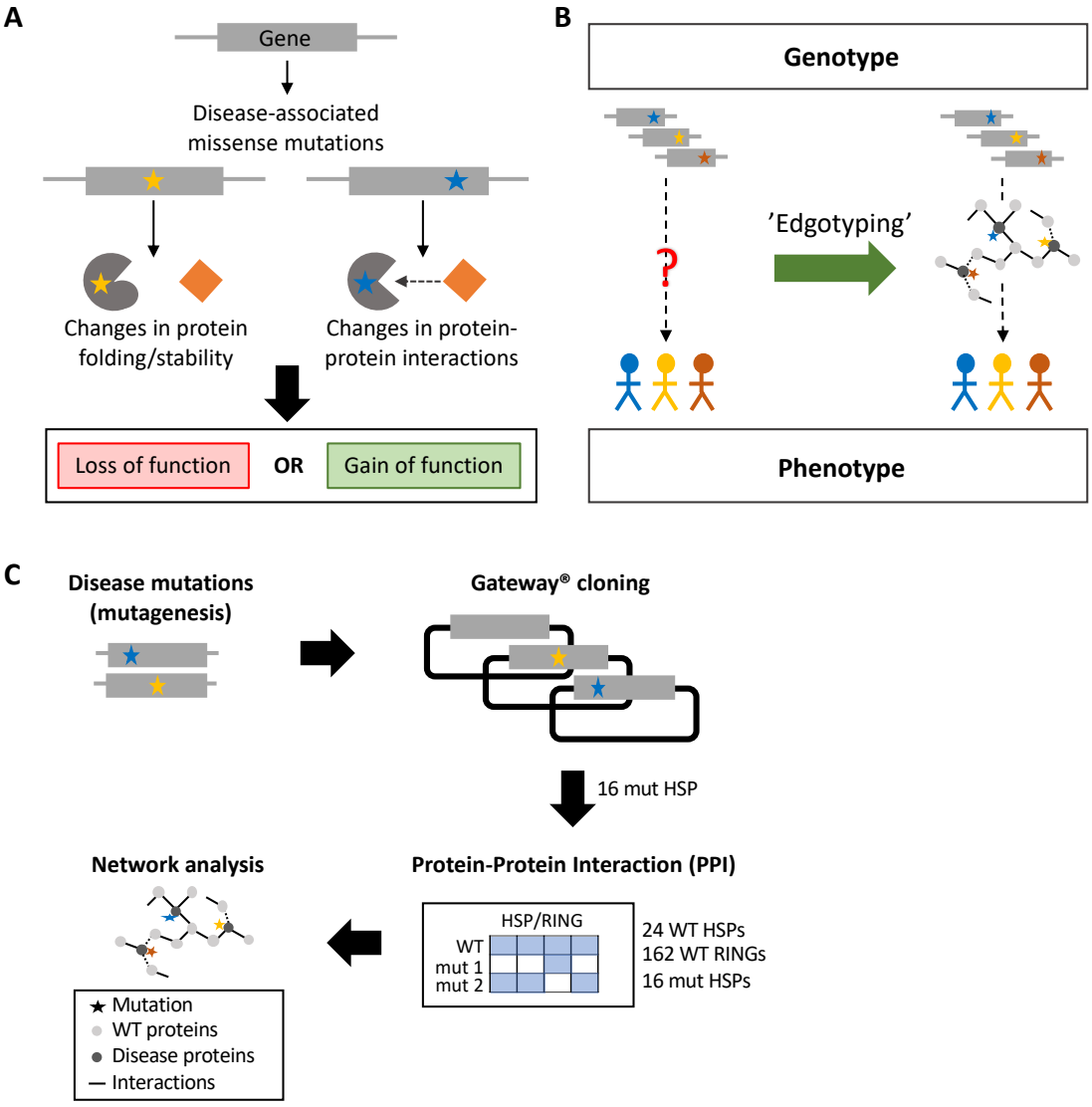

Figure 4.1. Characterisation of disease-associated HSP mutations. (A) Disease-associated missense mutations have the potential to impose changes in protein folding/stability and protein-protein interactions, which in turn may confer a loss or gain of function, leading to phenotypic variation. (B) Changes in network topology resulting from disease-associated mutations can confer different pathological phenotypes. 'Edgotyping' reveals the loss or gain of specific interactions (edges), which can be used to interpret complex genotype-to-phenotype relationships, allowing improved diagnosis and prognostic prediction (Sahni *et al.*, 2013). (C) Experimental workflow for the characterisation of 'edgetic' changes caused by known HSP-associated mutations. Abbreviations: WT (wild-type), mut (mutation). (Adapted from Sahni *et al.*, 2015)

4.2 Targeted Yeast two-Hybrid Screens

4.2.1 Yeast two-Hybrid assay

In this study, the *GAL4* Y2H system was employed. For bait and prey construct transfection the PJ69-4A (MATa) and the switched mating-type PJ69-4α (MATα) host strains were used, respectively (James, Halladay and Craig, 1996; Semple *et al.*, 2005). These host strains carry three independent *GAL4*-responsive reporter genes: *HIS3, ADE2* and *lacZ,* each driven by a different promoter (*GAL1, GAL2* and *GAL7* respectively). The promoter sequences are similar, but not identical, and thus allows for the removal of false positives from promoter-specific reporter activation (Bram, Lue and Kornberg, 1986; Walhout and Vidal, 2001). All three reporter genes can be assayed in parallel, increasing the stringency of Y2H screens (James, Halladay and Craig, 1996; Brückner *et al.*, 2009).

The *HIS3* reporter gene encodes the enzyme, imidazoleglycerol-phosphate dehydratase, which is required for the biosynthesis of histidine (Walhout and Vidal, 2001). Reporter activation allows yeast growth on medium lacking histidine. This reporter gene is very sensitive to low levels of activation, as it has a 'leaky' expression in most yeast strains (Feilotter *et al.*, 1994; James, Halladay and Craig, 1996). Basal levels of expression are conventionally inhibited with the use of 3-aminotriazole (3-AT), a competitive inhibitor of the *HIS3* gene product, increasing stringency and reducing non-specific background growth (James, Halladay and Craig, 1996). The amount of 3-AT used can be titrated depending on the stringency level required, and this is largely dependent on the yeast strain (Van Criekinge and Beyaert, 1999). Previous studies within our laboratory have shown that 2.5 mM 3-AT is the optimal concentration (stringency) required to capture true interactions, whilst preventing false positives. This concentration was used throughout this study, unless stated otherwise.

Activation of the *ADE2* reporter gene allows yeast growth on medium lacking adenine. This reporter gene encodes the enzyme, AIR-carboxylase which is required

for the purine biosynthetic pathway under both specific adenine control and the general amino acid control system (Robert Dorfman, 1969; Gedvilaite and Sasnauskas, 1994).

The *lacZ* gene was first cloned from the lac operon in E. coli (Lederberg, 1948) and encodes the enzyme, beta-galactosidase (β-Gal), which is required for the hydrolysis of β-galactosides (lactose) into monosaccharides (glucose and galactose). The *lacZ* reporter gene is generally more stringent but less sensitive than *HIS3* (Tirode *et al.*, 1997). Yeast colonies can be easily assayed for *lacZ* activity (β-Galactosidase assay) using the colorimetric substrate, X-Gal (5-bromo-4-chloro-3-indolyl-β-D-galactopyranoside) (Brückner *et al.*, 2009). X-Gal is hydrolysed by β-Gal which forms galactose and 5-bromo-4-chloro-3-hydroxyindole, which following spontaneous dimerization, oxidises to form a bright blue insoluble pigment (5,5'-dibromo-4,4'-dichloro-indigo) (Suter *et al.*, 2012).

Upon protein-protein interaction, reporter genes are activated resulting in growth of yeast on selective media and blue colour development in β-Galactosidase assays. Each biosynthetic/enzymatic assay was repeated at least twice and results from each were recorded. Only reproducible interactions were considered to be 'true' interactions.

4.2.2 Generation of HSP Y2H bait and prey constructs

To test binary interactions of HSP proteins, a set of HSP Y2H bait and prey clones were assembled (as described in Chapter 3), resulting in a Gateway® entry clone library consisting of 34 HSP ORFs representing 30 human HSPs. These ORFs were then used to generate corresponding Y2H bait and prey clones for each candidate HSP protein. HSP ORFs were successfully cloned into Y2H expression vectors, pGBAE-B (bait) and pACTBE-B (prey). The pGBAE-B vector contains the *TRP1* gene whilst the pACTBE-B vector contains the *LEU2* gene, both controlled by the ALDH1 promoter, which has been modified to allow moderate expression and stringent selection of N-terminally tagged *GAL4*-fusion proteins (pGBAE-B and pACTBE-B) on synthetic

defined agar plates lacking tryptone (SD-W) or leucine (SD-L), respectively (see Section 2.2). It should be noted that due to problems generating full-length CDS clones for WASHC5 (SPG8) and L1CAM (SPG1) proteins, fragmented domains of each protein was generated in Y2H expression vectors. All Y2H bait and prey clones were tested for auto-activation, resulting in a final collection of 33 HSP Y2H bait clones and 24 HSP Y2H prey clones, representing 29 and 22 human HSPs respectively. This collection of HSP constructs were used to perform systematic Y2H matrix interaction assays.

4.2.3 Generation of HSP disease-associated mutants

To characterise the effect of HSP genetic mutations on the binary HSP network, a set of HSP disease-associated mutants had to be generated. Due to the vast number of known disease-associated HSP proteins, those involved in intracellular trafficking processes were prioritised, resulting in a Gateway® entry clone library of 23 mutant HSP ORFs, representing 10 human HSPs. These mutant HSP ORFs were then transferred into bait and prey Y2H vectors. An outline of the experimental workflow used to investigate HSP 'edgetic' interaction profiles, is shown in Figure 4.1, panel C. Mutant HSP ORFs were successfully cloned into Y2H expression vectors, pGBAE-B (bait) and pACTBE-B (prey). However, many of the pACTBE-B constructs showed signs of auto-activation and were therefore removed from further analysis. For the purposes of this study only pGBAE-B (bait) constructs were used, resulting in 16 mutant HSP Y2H bait clones, representing 9 HSPs as shown in Table 4.1.

Table 4.1

SPG	Gene	Gene ID	Protein	Protein change	Effect on protein
SPG4	SPAST (M87)	6683	Spastin	p.E112K	Missense
				p.R115C	Missense
				p.F124D	Missense
				p.V162I	Missense
				p.N184T	Missense
				p.L195V	Missense
SPG8	WASHC5	9897	WASH complex subunit 5	p.I226T	Missense

				p.N471D	Missense
				p.L619F	Missense
				p.V620A	Missense
				p.V626F	Missense
				p.G696A	Missense
SPG20	SPART	23111	Spartin	p.F24D	Missense
SPG21	SPG21	51324	Maspardin	p.S109A	Missense
SPG50	AP4M1	9179	AP-4 complex subunit mu-1	p.F255A	Missense
				p.R283D	Missense
SPG53	VPS37A	137492	Vacuolar protein sorting-associated protein 37A	p.K382N	Missense
SPG57	TFG	10342	Protein TFG	p.R106C	Missense
SPG61	ARL6IP1	23204	ADP-ribosylation factor-like protein 6-interacting protein 1	p.K193FfsX	Frameshift
SPG62	ERLIN1	10613	Erlin-1	p.R55X	Nonsense
				p.G50V	Missense
				p.del288-289YQ	Frameshift
-	CCT5	22948	T-complex protein 1 subunit epsilon	p.H174R	Missense

Table 4.1. Selection of known HSP disease-associated mutations. List of mutations found in some of the HSP proteins involved in intracellular transport and ER-associated processes. Only successfully cloned, sequence-verified mutants are shown. Red boxes highlight mutant clones that were successfully cloned into pDONR223 but auto-activated when cloned into either bait (pGBAE-B) or prey (pACTBE-B) yeast vectors. The remainder were successfully cloned into Y2H pGBAE-B bait vector.

4.3 Identification of binary HSP:HSP interactions

4.3.1 Targeted Y2H assay reveals 15 binary HSP:HSP interactions

An outline of the targeted Y2H matrix mating methodology used in the HSP:HSP interaction screen is shown in Figure 4.2. As described in Chapter 2, MATα haploid yeast transfected with HSP prey constructs were spotted onto rich medium (YPAD) agar plates, in a 96-well format. MATa haploid yeast cells transfected with HSP bait constructs were spotted on top of prey clones and left for 24 hours to mate. Diploid

yeast were then selected following initial velvet replication onto SD-WL agar plates, followed by a second replication onto SD-WLA and SD-WLH(3-AT) agar plates, to select for positive protein-protein interactions. The *lacZ* reporter activity (β-Gal assays) was also performed on diploid yeast cells, followed by evaluation of blue colouration in a colony filter lift assay as described in Chapter 2. Images were taken every 3-4 days and interactions were annotated as either weak, medium or strong growth. A known positive control was included in every assay to check for efficient mating. All screens were repeated twice, and only interactions observed in both screens were annotated as positive.

Figure 4.2

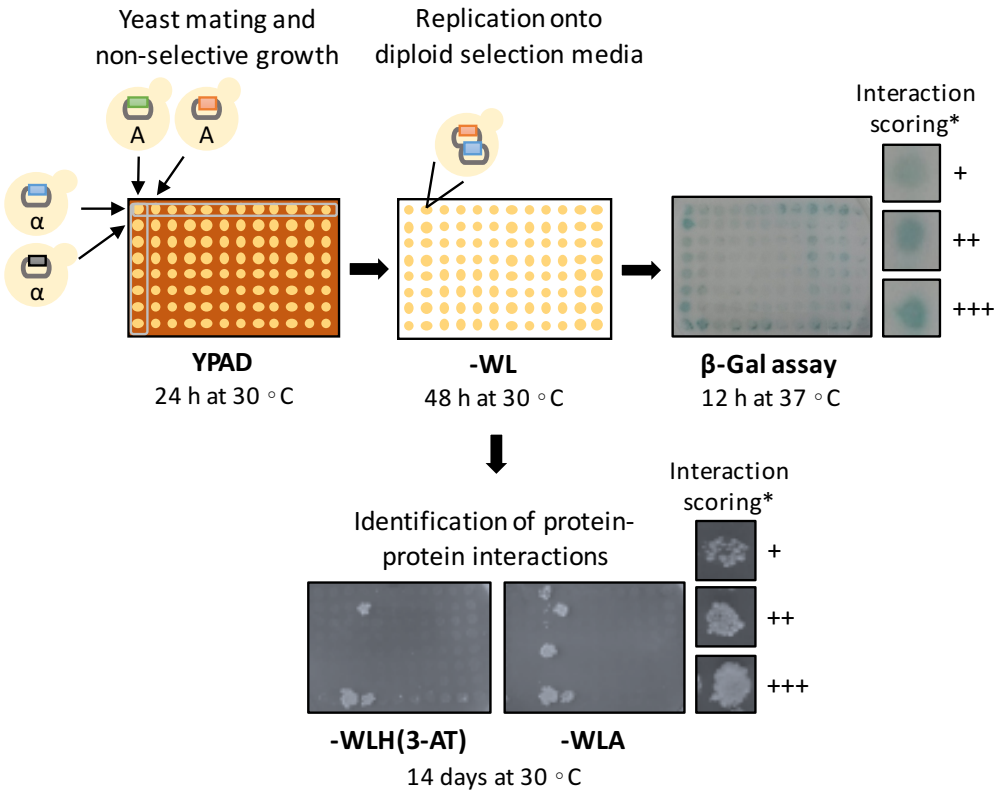

Figure 4.2. Targeted Y2H matrix mating protocol. In the *GAL4* Y2H system, MATa yeast were transfected with pGBAE-B bait constructs while MATα yeast were transfected with pACTBE-B prey constructs and resulting transformants were selected for on –W (pGBAE-B) or –L (pACTBE-B) selective plates respectively. All bait and prey clones were then individually tested for auto-activation (Section 2.2.6) prior to use in subsequent protein-protein interaction assays. Preys were spotted onto non-selective rich media (YPAD), in a 96-well format, and selected baits were spotted on top of each individual prey. Mating on rich medium allowed the growth of diploid yeast, which were selected for on SD-WL medium (-WL). Following diploid selection,

yeast was replicated from SD-WL onto both SD-WLH(3-AT) and SD-WLA triple dropout plates, for the selection of positive protein-protein interactions. The activation of a third reporter, *lacZ* was also analysed using the β-Gal assay on diploid yeast. The level of reporter activation (*) based on yeast colony growth, and growth time (days) for each stage is shown.

In total, a possible 792 binary interactions were tested between 33 HSP bait clones and 24 HSP prey clones (Figure 4.3), and the 15 reproducible positive binary HSP:HSP interactions are presented in Table 4.2. As a general rule, true positive Y2H interactions should be observed on both SD-WLA and SD-WLH(3-AT) selective media, or on the less stringent SD-WLH(3-AT) selection alone. Interactions only detected on SD-WLA, were considered to be false positives and were therefore excluded from the final list of positive interactions in this study. In addition, results from corresponding β-Gal assays (lacZ reporter activity assays) were incorporated with those from the biosynthetic reporter assays and the final list of positive binary interactions includes 7 interactions seen on all three reporters, 5 interactions seen on two reporters and 3 interactions seen on only one reporter. In addition, 3 of the 15 positive HSP:HSP interactions had previously been identified as 'direct' or binary interactions and are highlighted (green) in Table 4.2, leaving 12 novel binary HSP:HSP interactions.

Table 4.2

BAIT Gene ID	BAIT Symbol	PREY Gene ID	PREY Symbol	*HIS3*	*ADE2*	*lacZ*
7415	VCP	7415	VCP	+++	+++	++
10613	ERLIN1	11160	ERLIN2	+++	+++	++
9179	AP4M1	10717	AP4B1	+++	++	+++
51324	SPG21	10342	TFG	+++	++	
137492	VPS37A	137492	VPS37A	+++	+++	+++
51324	SPG21	137492	VPS37A	+++	+++	++
23204	ARL6IP1	11160	ERLIN2	++	+	+
22948	CCT5	137492	VPS37A	++	+	++
51324	SPG21	51324	SPG21	+++	++	
51324	SPG21	23111	SPG20	++	++	
83636	C19orf12	23111	SPG20	++	+	
6683	SPAST (M1)	11160	ERLIN2	+++		++
11160	ERLIN2	11160	ERLIN2	+++		

51324	SPG21	11160	ERLIN2	++		
10717	AP4B1	3897	L1CAM (NT)	+		

Table 4.2. Summary of positive binary HSP:HSP interactions detected in targeted Y2H matrix interaction screens. Entrez Gene IDs and symbols for bait and prey HSPs that showed evidence of positive binary interactions are listed, along with an indication of the relative strength of interaction, as indicated by relative colony growth or intensity of blue signal: strong (+++), medium (++) or weak (+) as defined in Figure 4.2. Previously defined known direct interactions are highlighted in green. Entrez Gene IDs and symbols were obtained from the NCBI database (Maglott *et al.*, 2007).

Figure 4.3

A

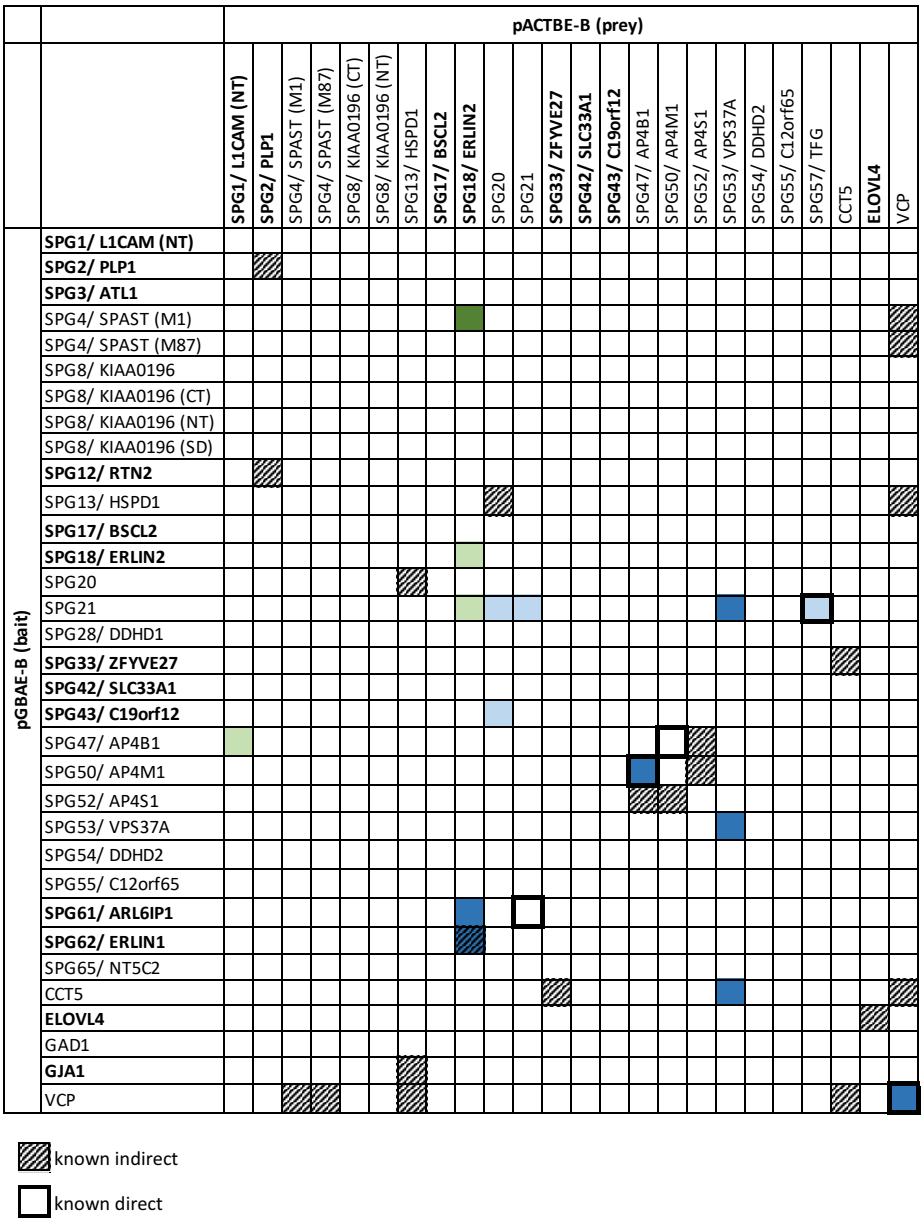

B

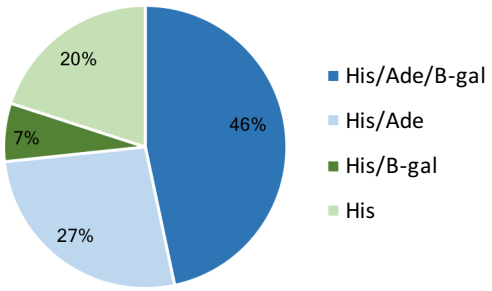

Figure 4.3. Summary of all binary HSP:HSP interactions tested in targeted Y2H matrix interaction assays. A) Matrix showing results of all tested binary HSP:HSP interactions. HSP genes are listed by spastic gait disease-loci (SPG), genes that are not part of the SPG classification system are listed alphabetically. (B) Shows the percentage of positive Y2H interactions observed at each level of reporter stringency. Stringency scoring is ranked as follows: His/Ade/ β-Gal (Dark Blue) > His/Ade (Light Blue) > His/β-Gal (Dark Green) > His (light Green). Corresponding colours are also used to represent relative stringency of individual positive interactions in panel (A). *BOLD = Transmembrane protein.*

4.3.2 Reconfirmation of previously defined interactions

Interaction data from published interaction studies is often manually and/or automatically curated and deposited into publicly available databases such as BioGRID and HPRD. As described in Chapter 3, several of these databases, in combination with our 'in house' interactome data were used to produce the Expanded Global protein interaction network (Figure 3.3). The Expanded Global network (Chapter 3) was used to extract the 58 HSP proteins (using 'seed 1' list), together with their interaction partners, to create the HSP seed 1 'one-step' subnetwork shown in Figure 4.4 A. All previously defined known (direct and indirect) and predicted HSP:HSP interactions were extracted from this global subnetwork, to create the HSP:HSP 'one-step' subnetwork (Figure 4.4 B). A union of HSP:HSP 'one-step' subnetwork and the data generated in this study is presented in Figure 4.4 C. Compared to the initial HSP:HSP 'one-step' subnetwork (Figure 4.4 B), the new 'combined' HSP:HSP subnetwork is composed of 47 interactions between 34 HSP nodes, representing a 10 % increase in the number of HSP nodes and a 31 % increase in the number of interactions (edges) observed.

Figure 4.4

A **Expanded Global seed 1 'one-step' subnetwork**

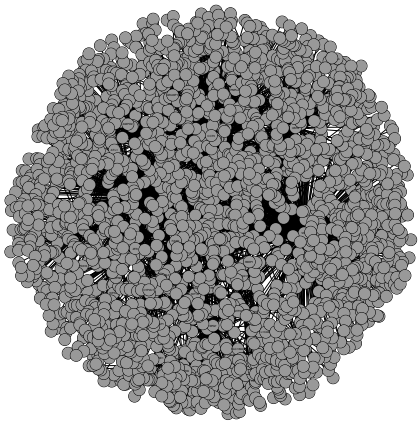

Total nodes: 2,334
Total edges: 3,314

B **HSP:HSP subnetwork**

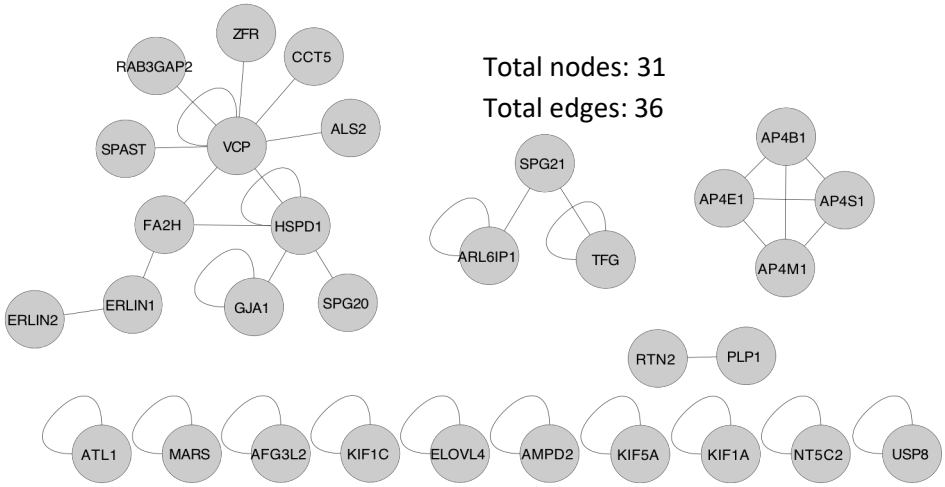

Total nodes: 31
Total edges: 36

C **Combined HSP:HSP subnetwork**

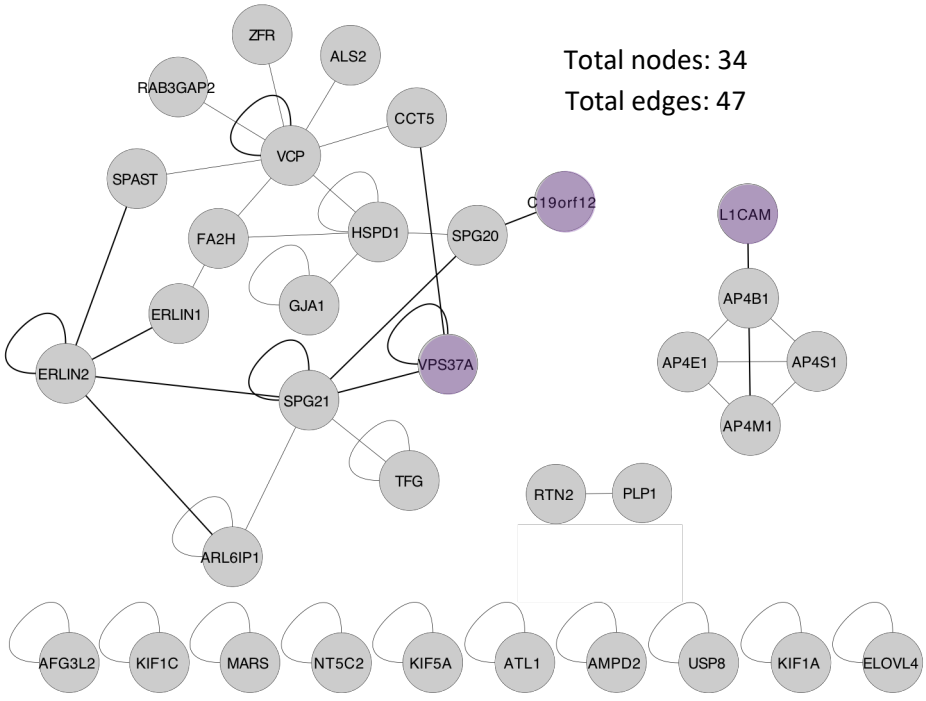

Total nodes: 34
Total edges: 47

Figure 4.4. Generation of an HSP:HSP protein interaction network. (A) HSP seed 1 'one-step' subnetwork was extracted from the expanded global network (shown in Figure 3.3 B), using the HSP seed 1 list (58), as core nodes. All non-HSP nodes and adjacent edges were removed from the network shown in panel A, to generate the HSP:HSP 'one-step' subnetwork (B). (C) The HSP:HSP 'one-step' subnetwork shown in panel (B) with the additional binary interactions identified in this study (represented as bold lines) represented as a network. New HSP partners are shown as purple nodes.

Of the 31 previously known (direct and indirect) HSP:HSP interactions, 16 were re-tested in this study and 4 were reconfirmed. Additionally, 4 of the 16 re-tested known interactions were previously identified as 'direct' or binary interactions, and 75% (3/4) were reconfirmed in this study, compared with 8% (1/12) of the re-tested 'indirect' interactions (from non-Y2H experiments), as presented in Table 4.3. This was the well-defined ERLIN1 (SPFH1) and ERLIN2 (SPFH2) interaction (Pearce *et al.*, 2009; Christianson *et al.*, 2011). The remainder of the re-tested 'indirect' interactions were not found to be positive binary interactions when re-tested in this study.

Table 4.3

Interaction	Direct	Indirect
Known	14	17
Re-tested	4	12
Reconfirmed	3	1
Reconfirmation rate	75%	8%

Table 4.3. Re-tested HSP:HSP protein interactions. Known direct and indirect human HSP:HSP interactions previously defined, were extracted from the expanded global HSP seed 1 'one-step' subnetwork (Figure 4.4 A), and interaction reconfirmation rates were determined.

4.3.3 Common HSP:HSP protein interaction partners

The combined HSP:HSP subnetwork was analysed for common binding partners and cellular pathways in which these proteins might act (Figure 4.5). In the known HSP:HSP 'one-step' subnetwork (Figure 4.4, panel B), SPG20 (spartin) is reported to have one indirect interacting partner, HSPD1 (Milewska, McRedmond and Byrne,

2009). In our study, SPG20 was shown to interact with SPG21 and C19orf12 (Figure 4.4 C). SPG20 (spartin) is a multifunctional protein with roles in endosomal trafficking (Renvoisé *et al.*, 2010), mitochondrial and ER protein folding and degradation of lipid droplet-associated proteins (Milewska, McRedmond and Byrne, 2009). HSPD1 encodes a mitochondrial chaperone protein involved in mitochondrial protein quality control, which also functions as a signalling molecule in the immune system (Landstein, Ulmansky and Naparstek, 2015). C19orf12, encodes a mitochondrial membrane protein (Hartig *et al.*, 2011) which localises to mitochondria and ER (Venco *et al.*, 2015), however not much else is known. Through its interaction with SPG20, and the proteins involved in this subnetwork, C19orf12 could have a role in regulating intracellular trafficking processes or protein quality control.

Figure 4.5

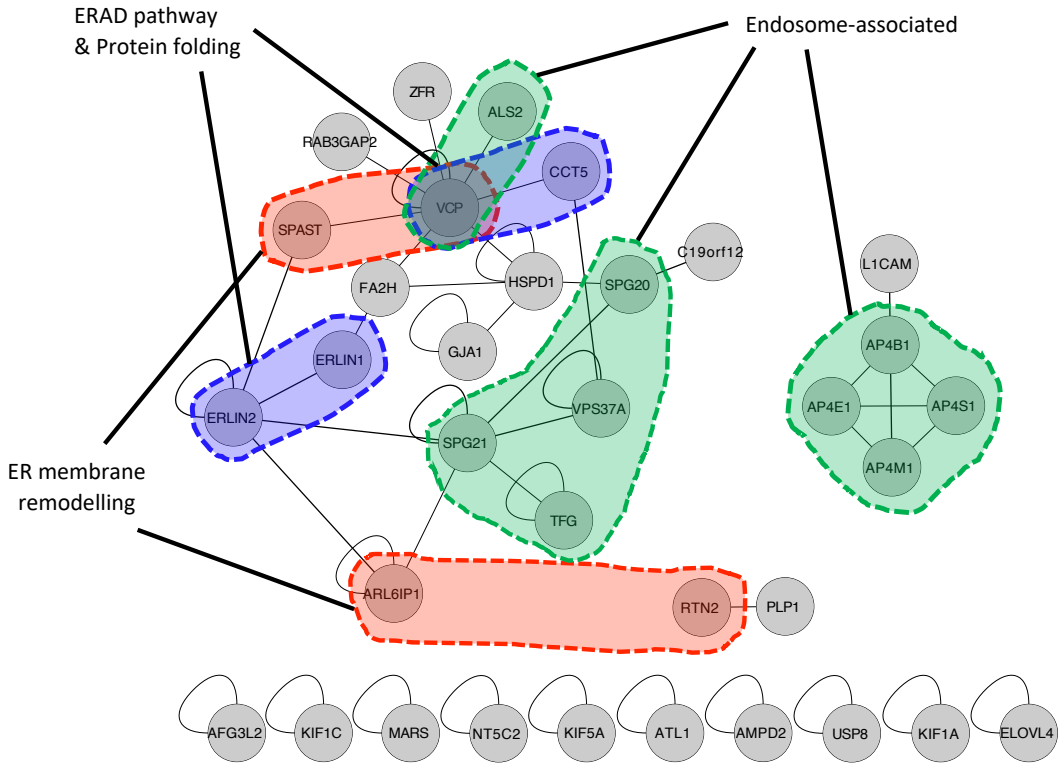

Figure 4.5. Functional annotation of the combined HSP:HSP subnetwork. The nodes (proteins) of the combined HSP:HSP subnetwork (Figure 4.4 C) were functionally annotated based on the previously identified HSP functional modules for which they are predicted to be involved in, as discussed in Chapter 1 (Figure 1.1).

In the HSP:HSP 'one-step' subnetwork as presented in Figure 4.4 B, SPG21 (maspardin) has only two direct interaction partners, TFG and ARL6IP1 (Rolland *et al.*, 2014). SPG21 was initially thought to function as a negative regulatory factor involved in CD4-dependent T-cell activation, due to its interaction with CD4 (Zeitlmann *et al.*, 2001). However, localisation studies showed enrichment at the *trans*-Golgi, late endosomes and lysosomes, suggesting a functional role for SPG21 in the *trans*-Golgi network/endosomal pathway (Hanna and Blackstone, 2009). ARL6IP1 encodes an ER-shaping protein, required for ER and mitochondrial network organisation (Fowler and O'Sullivan, 2016), whilst TFG is a conserved regulator of protein secretion from the ER, where it facilitates the assembly of the COPII coat complex at the interface between ER and ER-Golgi intermediate compartments, to enable the rapid movement of secretory vesicles (Witte *et al.*, 2011; Beetz, Johnson, *et al.*, 2013; Hanna *et al.*, 2017).

Interestingly, in our study ERLIN2, a regulator of the ERAD pathway (Pearce *et al.*, 2007), interacts with both SPG21 and ARL6IP1 as shown in Figure 4.5. ERLIN2 was also shown to interact with SPAST (spastin). Spastin is a microtubule-interacting and trafficking (MIT) domain-containing AAA ATPase (Evans *et al.*, 2005), and the larger isoform, M1 is known to localise and interact with the tubular ER membrane of corticospinal neurons, co-ordinating ER-shaping and microtubule dynamics (Park *et al.*, 2010). Spastin interacts with CHMP1B, a ESCRT-III complex-associated endosomal protein (Reid *et al.*, 2005). Moreover, we identified an interaction between SPG21 and VPS37A. VPS37A encodes a subunit of the endosomal sorting complex required for transport I (ESCRT-I) system (Zivony-Elboum *et al.*, 2012). The ESCRT system is important for intracellular trafficking, maturation of multivesicular bodies (MVB) and regulation of vesicular transport of ubiquitinated cargo proteins for lysosomal degradation (Raiborg and Stenmark, 2009; Lee and Gao, 2012). ESCRT dysfunction has been associated with several human diseases, including neurodegenerative diseases, disrupting neuronal endosomal trafficking and protein degradation (Saksena and Emr, 2009). These findings further demonstrate a potential role for SPG21 in vesicle-mediated trafficking and protein sorting, including ESCRT, providing further evidence to support the idea that defects in intracellular trafficking events

are potentially significant in the pathogenesis of neurodegenerative diseases such as HSP.

4.4 Mutational analysis of HSP 'edgetic' interaction profiles

4.4.1 Y2H analysis of disease-associated mutations on HSP:HSP interaction profiles

An outline of the targeted Y2H matrix mating with improved β-Gal assay methodology, is described in Figure 4.6. As described in Chapter 2, mating arrays were set up on rich medium (YPAD) agar plates, in a 96-well format and left for 24 h at 30 °C, allowing for the mating of MATα and MATa yeast (Chapter 2). Diploid yeast were selected following sequential growth and replication onto SD-WL, followed by SD-WLA and SD-WLH(3-AT) agar plates, to select for positive protein-protein interactions. In this study assessment of *lacZ* reporter activity (β-Gal assay) was changed from the colony lift assay to an agar overlay assay, in which diploid yeast were replicated onto SD-WLH(3-AT) +X-Gal agar plates, as described in Chapter 2. Both methods rely on successful colony transfer and evaluation of blue coloration. We found the agar overlay assay to be more successful in yeast transfer and colour visualisation. Therefore, this approach was adopted for the remainder of the yeast work carried out in this project. As in the conventional Y2H assay, images were taken every 3-4 days and interactions were scored to reflect weak, medium or strong yeast colony growth on selective plates. Again, a known positive control was always included, to check for efficient mating. The interaction screen was repeated twice, and only interactions observed in both screens were annotated as positive.

All 16 mutant HSP Y2H bait clones were screened against 24 HSP Y2H prey clones. 384 possible binary interactions were tested (Figure 4.7), and the 29 reproducible positive binary interactions are presented in Table 4.4. As before, true positive Y2H interactions should be observed on both SD-WLA and SD-WLH(3-AT) or the less stringent SD-WLH(3-AT) selection alone, and interactions detected only on SD-WLA selection media, were considered to be false positives and were removed.

Figure 4.6

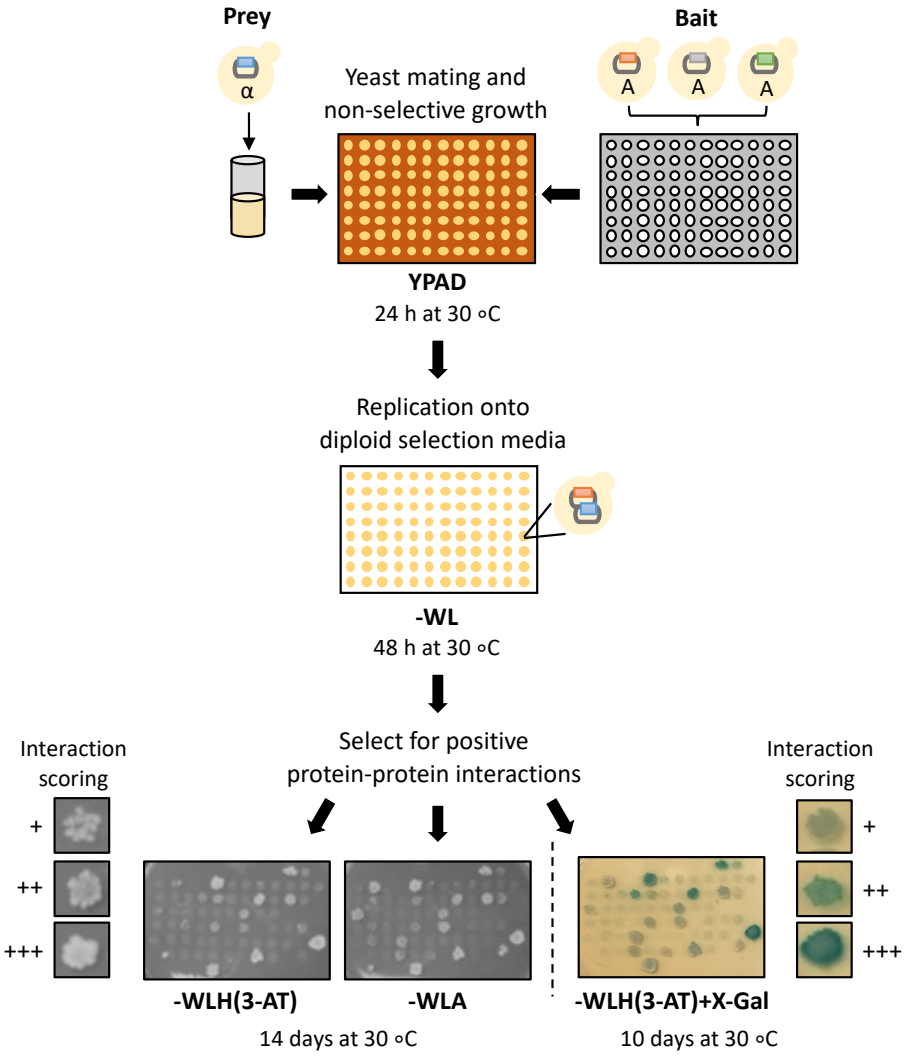

Figure 4.6. Improved targeted Y2H matrix mating procedure. In the *GAL4* Y2H system, MATa yeast were transfected with pGBAE-B bait constructs while MATα yeast were transfected with pACTBE-B prey constructs and resulting transformants were selected for on –W (pGBAE-B) or –L (pACTBE-B) selective plates respectively. All bait and prey clones were then individually tested for auto-activation (Section 2.2.6) prior to use in subsequent protein-protein interaction assays. Preys were spotted onto non-selective rich media (YPAD), in a 96-well format, and the selected bait was spotted on top of each individual prey. Mating on rich medium allowed the growth of diploid yeast, which were selected for on SD-WL medium (-WL). Following the diploid selection, yeast was replicated from SD-WL onto SD-WLA, SD-WLH(3-AT) and SD-WLH(3-AT) +X-Gal triple dropout plates, for the selection of positive protein-protein interactions. The activation of a third reporter, *lacZ* was also analysed using the β-Gal assay on diploid yeast. The level of reporter activation (*) based on yeast colony growth, and growth time (days) for each stage is shown.

The results obtained from the β-Gal assays were incorporated with those from the biosynthetic reporter assays are presented in Table 4.4. The final list of positive binary interactions includes 1 interaction seen on all three reporters, 19 seen on two reporters and 9 seen on one reporter.

Table 4.4

BAIT Gene ID	BAIT Symbol	PREY Gene ID	PREY Symbol	*HIS3*	*ADE2*	*lacZ*
6683	SPAST (M87) N184T	3897	L1CAM (NT)	+	+	
		6683	SPAST (M87)	+	+	
		11160	ERLIN2	+	+	++
23111	SPG20 F24D	3329	HSPD1	+++	+++	
		10342	TFG	+		
51324	SPG21 S109A	6683	SPAST (M1)	+	+	
		3329	HSPD1	++	++	
		137492	VPS37A	+	+	
		10342	TFG	++		
9179	AP4M1 F255D	6683	SPAST (M1)	+	+	
		3329	HSPD1	+++	+++	
		137492	VPS37A	+	+	
	AP4M1 R283D	6683	SPAST (M1)	+	+	
		3329	HSPD1	+++	+++	
137492	VPS37A K382N	3329	HSPD1	+++	+++	
10342	TFG R106C	3329	HSPD1	+++	+++	
		23111	SPG20	++		
23204	ARL6IP1 K193FfsX	3897	L1CAM (NT)	++		
		6683	SPAST (M1)	++	+	
		3329	HSPD1	+++	+++	
		11160	ERLIN2	++		
10613	ERLIN1 G50V	3897	L1CAM (NT)	++		
		3329	HSPD1	+++	+++	
		11160	ERLIN2	++		
	ERLIN1 R55X	3897	L1CAM (NT)	++	+	
		6683	SPAST (M1)	+		
		3329	HSPD1	+++	+++	
		11160	ERLIN2	+++		
22948	CCT5 H147R	3329	HSPD1	+++	+++	

Table 4.4. Summary of disease-associated 'edgetic' changes on the binary HSP:HSP protein interactions detected in targeted Y2H matrix screens. Entrez Gene IDs and symbols for selected mutant HSP bait (pGBAE-B) and wild-type HSP preys (pACTBE-B) that showed evidence of positive binary interactions are listed, along with an indication of the relative strength of interaction: strong (+++), medium (++) or weak (+), as defined previously.

4.4.2 Effect of genetic mutations on HSP:HSP networks

Proteins must be folded correctly to enable correct organelle localisation and protein function, and inherited mutations can affect the folding and subcellular localisation of proteins, resulting in the accumulation of misfolded, non-functional proteins (Valastyan and Lindquist, 2014; Oakes and Papa, 2015). To prevent the toxic build-up of misfolded proteins and protect cells from the damaging effects, cellular responses, including the ER stress response, are activated (Dobson and Ellis, 1998; Kaufman, 1999; Dobson, 2003). However, excessive amounts of misfolded proteins can overwhelm the 'quality control' system and impairs the protective mechanisms of the UPR, leading to ER stress-induced organelle dysfunction and cell death (Rao and Bredesen, 2004). ER stress-mediated cell dysfunction and cell death has been implicated in the pathogenesis of human chronic disorders including neurodegenerative disorders such as Parkinson's disease (PD), Alzheimer's disease (AD) and Amyotrophic Lateral Sclerosis (ALS) (Taylor, Hardy and Fischbeck, 2002; Ross and Poirier, 2005).

Interestingly, Figure 4.7 shows that the edgetic mutation S109A in SPG21 completely abolished interactions with SPG20 and ERLIN2, whilst maintaining interactions with VPS37A and TFG. Both SPG20 and ERLIN2 are involved in protein degradation, so a loss of interaction could result in increased levels of aberrant proteins, leading to ER stress. SPG21 S109A interacts with both SPAST and VPS37A. SPAST is known to interact with two ESCRT-III complex-associated proteins CHMP1B and IST1 (Reid *et al.*, 2005; Allison *et al.*, 2013), whilst VPS37A is also associated with the ESCRT complex, as a component and regulator of ESCRT-I (Zivony-Elboum *et al.*, 2012). More recently, extracellular vesicles formed and released by the ESCRT system have

been identified as important factors for the spread of neurodegenerative disorders (Budnik, Ruiz-Cañada and Wendler, 2016). These findings support the idea that SPG21 could be involved in the ESCRT system, and its involvement in neurodegeneration could provide a link between SPG21 dysfunction and HSP.

Figure 4.7

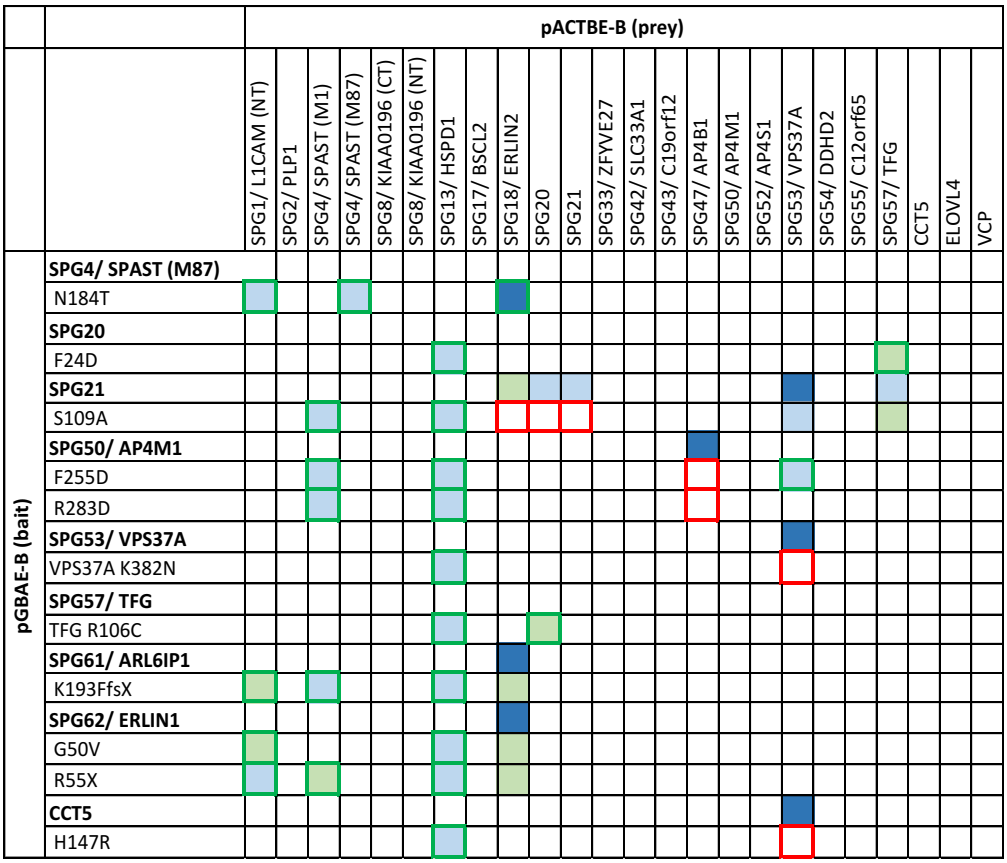

Figure 4.7. Analysis of disease-associated 'edgetic' changes in HSP:HSP interaction profiles. Comparative analysis of wild-type HSP-wild-type HSP or mutant HSP-wild-type HSP partner interaction profiles. Wild-type or mutant HSP bait (pGBAE-B) proteins and wild-type HSP prey (pACTBE-B) Entrez gene ID/symbols are arranged by HSP gene loci. Stringency scoring is ranked as follows: His/Ade/ β-Gal (Dark Blue) > His/Ade (Light Blue) > His/β-Gal (Dark Green) > His (light Green), with corresponding colours used to represent relative stringency of individual positive interactions shown in the table. 'Edgetic' changes are highlighted by green (gain of interaction) or red (loss of interaction) boxes respectively.
BOLD = Wild-type protein.

Additionally, having shown previously that SPG21 is able to form a dimer (Figure 4.3), it is interesting to note that mutant SPG21 S109A loses this interaction, and so this

loss of dimerization could help explain the loss of interactions leading to a loss-of-function phenotype that is observed with mutant SPG21 S109A.

Furthermore, SPG21 S109A was also shown to interact with HSPD1, a highly conserved protein initially identified as a mitochondrial chaperone (Quintana and Cohen, 2011). However, upon exposure to stress stimuli, HSPD1 functions as a signalling molecule in the immune system, activating both adaptive and innate immune responses (Landstein, Ulmansky and Naparstek, 2015).

Interestingly, CCT5 H174R and VPS37A K382N both have abolished interactions with VPS37A, however they both also interact with HSPD1. As the ESCRT system is essential for protein degradation, loss of function could lead to ER stress and so the involvement of HSPD1 may provide a link between ER stress and immune response signalling pathways.

Loss-of-function mutations

One example of loss-of-function observed in our study is provided by mutant SPG50 (AP4M1). AP4M1 is a subunit of the heterotetrameric adaptor protein 4 (AP-4) complex, which is important in vesicular transport. The AP-4 complex is involved in the recognition and sorting of cargo proteins from trans-Golgi network (TGN) to endosomal-lysosomal system, and all AP-4 subunits have been classified as HSP genes (Hirst, Irving and Borner, 2013). The AP-4 phenotype includes early onset, autosomal-recessive complicated form of hereditary spastic paraplegia (HSP), with severe intellectual disability (Hirst, Irving and Borner, 2013). In our study, we observed a loss-of-interaction between both AP4M1 HSP disease-associated mutants F255D and R283D, and SPG47 (AP4B1), which would suggest a loss-of function of the AP-4 complex and this may account for the phenotype observed. Given the importance of the AP-4 complex in vesicular transport and protein sorting, if the AP-4 complex was non-functional there could be a build-up of proteins in the TGN, which could lead to an increase in ER stress, a common feature of neurodegenerative diseases as already mentioned.

Gain-of-function mutations

One example of gain-of-function observed in our study is provided by SPG57 (TFG) R106C mutant. TFG is a regulator of ER protein secretion, regulating ER-derived COPII vesicle secretion, as well as ER morphology (Witte *et al.*, 2011; Beetz, Johnson, *et al.*, 2013). Our study identified a gain-of-interaction with SPG20 (spartin). SPG20 is thought to be involved in regulating endosomal trafficking and mitochondrial function (Renvoisé *et al.*, 2010) and is mutated in Troyer syndrome. Troyer syndrome is an early childhood-onset, autosomal-recessive complicated form of HSP, with additional neurological features including intellectual disability and muscular dystrophy (Proukakis *et al.*, 2004). A gain-of-function mutation could result in an altered protein conformation, which can cause dominant toxic phenotypes (Valastyan and Lindquist, 2014). Previous studies have already identified that the TFG R106C mutant demonstrated a defect in its ability to self-assemble into an oligomeric complex, required for normal TFG function, and inhibition of TFG in cell lines revealed slower ER protein secretion and altered ER morphology, causing a collapse of the ER network (Beetz, Johnson, *et al.*, 2013). During endosomal maturation and trafficking, endosomes are bound to the ER, causing changes to ER morphology (Friedman *et al.*, 2013), therefore the probable altered protein conformation of TFG which interacts with SPG20, likely affecting ER architecture and endosomal trafficking. Given the function of TFG and SPG20, dysfunctional TFG may cause an accumulation of aberrant proteins in the ER, which are unlikely to be degraded, contributing to an increase in ER stress and possible cell death.

4.5 Discussion

Although there are over 75 HSP disease-loci, about 70% of individuals are affected by autosomal dominant mutations (Salinas *et al.*, 2008), most of which affect organelle dynamics, and in particular the endoplasmic reticulum (ER) and ER architecture (Beetz, Johnson, *et al.*, 2013). SPAST, ATL1, and REEP1 (spastin, atlastin-1, and REEP1 proteins, respectively) are some of the most well-characterised HSP genes, which together with reticulons, also implicated in HSP (Saito *et al.*, 2004), regulate ER-shaping and network distribution (Park *et al.*, 2010).

In this study we identified 12 novel binary HSP:HSP interactions, which when integrated with current known HSP interactome data, reveal several functional modules, which are thought to be involved in the pathophysiology of HSPs. These include HSP proteins implicated in endoplasmic reticulum (ER) membrane remodelling (SPAST, ARL6IP1), ER-associated degradation (ERAD) pathway (ERLIN2) and protein folding (CCT5), as well as endosome-associated HSP genes (AP4 complex, VPS37A). ERLIN2 and SPG21, not only interact with each other but they also interact with proteins known to function in each of the functional modules as highlighted in Figure 4.5. Given the recent reports of endosomal involvement in ER dynamics, it is likely that all three functional modules act together as part of the overall dynamics of the ER network.

Interestingly, there are proteins involved in ER network shaping and distribution, which are mutated in HSP and other neurodegenerative disorders, suggesting that correct ER organisation is important for axonal maintenance (Renvoisé and Blackstone, 2010; Beetz, Johnson, *et al.*, 2013), thereby providing a clear link between ER network organisation and neurodegeneration (Beetz, Johnson, *et al.*, 2013).

The ER is a multifunctional organelle involved in a range of processes including protein synthesis, trafficking, and quality control (English, Zurek and Voeltz, 2009). The ER also has an important role in lipid synthesis and distribution, and as a major intracellular calcium store (Matus, Glimcher and Hetz, 2011). Its varied functionality is reflected in its complex architecture (Schwarz and Blower, 2016). The ER is a continuous network of branched tubules and peripheral sheet-like cisternae distributed throughout the cytoplasm, and include the nuclear envelope (Renvoisé and Blackstone, 2010; Beetz, Johnson, *et al.*, 2013). There are a variety of different ER membrane proteins that mediate interactions with other organelles and components of the cytoskeleton, which are thought to be integral to ER shape and distribution (Schwarz and Blower, 2016). These include, (i) ER membrane-bending proteins of the REEP and reticulon families (Voeltz *et al.*, 2006); (ii) the atlastin family of GTPases required for tubular ER network formation (Hu *et al.*, 2009); (iii)

microtubule cytoskeletal regulators required for distribution of ER network (Park and Blackstone, 2010), particularly important for neurons (Renvoisé and Blackstone, 2010) and (iv) components of the early secretory pathway (Renvoisé and Blackstone, 2010; Zanetti *et al.*, 2011). In recent studies, the importance of an endosomal complex regulating nuclear envelope reformation was demonstrated (Olmos *et al.*, 2015; Vietri *et al.*, 2015), suggesting a potential role for ESCRT-III in ER dynamics (Schwarz and Blower, 2016).

The ER is the main site for localised protein synthesis, and even with specific chaperone proteins and enzymes which assist in protein folding, the success rate is low, with less than 20% of proteins translocated into the ER lumen undergo proper folding events, to create a stable and functional protein (Hartl and Hayer-Hartl, 2009; Oakes and Papa, 2015; Schwarz and Blower, 2016). Environmental and genetic factors can disrupt ER function, affecting protein folding processes in the ER lumen. This can cause an imbalance between protein synthesis and the processing of newly synthesised proteins in the ER, leading to an accumulation of misfolded and/or unfolded proteins in the ER lumen, a condition known as ER stress (Oslowski and Urano, 2011). In response to ER stress, cells induce the Unfolded Protein Response (UPR), a highly conserved, adaptive cellular response, which acts to reduce stress and restore protein homeostasis (Malhotra and Kaufman, 2007; Oslowski and Urano, 2011). The UPR is a group of intracellular signal transduction pathways, monitoring conditions in the ER (Walter and Ron, 2011). The UPR is initiated by three major ER transmembrane proteins: inositol requiring kinase 1α (IRE1α), activating transcription factor 6 (ATF6), and protein kinase RNA-like ER kinase (PERK), which function as signal transducers of ER stress (Oslowski and Urano, 2011; Walter and Ron, 2011). Initiation of the UPR is regulated by the ER chaperone, immunoglobulin binding protein (BiP), as it is able to directly interact with each signal transducing sensor (Bertolotti *et al.*, 2000; J. Li *et al.*, 2008). This physical interaction stabilises these ER transmembrane proteins, as they remain in an inactive state. Following increased protein synthesis or abnormal protein folding, there is an increased demand for chaperone-mediated protein stabilisation and so BiP dissociates from the sensors, rendering them active (Bertolotti *et al.*, 2000; Oslowski and Urano,

2011). The activation of each of the ER stress sensors initiates signalling cascades, resulting in transcriptional and translational changes in an attempt to reduce cellular stress, whilst simultaneously inducing protein quality control mechanisms in an attempt to reduce protein misfolding (Sprenkle *et al.*, 2017). In mammalian cells, the UPR adaptive response includes: (i) increased gene transcription of ER-resident chaperones – increase protein folding and handling efficiency, (ii) decreased protein translation - decreasing ER workload and preventing further accumulation of misfolded proteins and (iii) increased ERAD and autophagy components to promote protein clearance and maintain quality control (Anelli and Sitia, 2008; Oslowski and Urano, 2011). Through, ER-associated degradation (ERAD), misfolded proteins are transported back to the cytosol where they undergo ubiquitin-proteasome system (UPS)-dependent degradation (Menendez-Benito *et al.*, 2005; Smith, Ploegh and Weissman, 2011). The UPS is the main pathway responsible for the degradation of cytosolic proteins, however if its function is disrupted this can also lead to ER stress (Ciechanover and Brundin, 2003; Korhonen and Lindholm, 2004). In more severe cases, excessive amounts of misfolded proteins can overwhelm the 'quality control' system leading to ER stress-induced organelle dysfunction and cell death (Rao and Bredesen, 2004; Kim, Xu and Reed, 2008). ER stress-mediated cell dysfunction and cell death has been implicated in the pathogenesis of several human neurodegenerative disorders which include Parkinson's disease (PD), Alzheimer's disease (AD) and Amyotrophic Lateral Sclerosis (ALS) (Taylor, Hardy and Fischbeck, 2002; Ross and Poirier, 2005).

ER stress in neurodegenerative diseases

The accumulation and aggregation of misfolded proteins is a common feature among neurodegenerative diseases such as Alzheimer's disease (AD), Parkinson's disease (PD), Huntington's disease (HD) and amyotrophic lateral sclerosis (ALS) (Kopito and Ron, 2000; Taylor, Hardy and Fischbeck, 2002; Selkoe, 2003; Soto and Estrada, 2008). These can also be referred to as protein conformation disorders or proteinopathies (Soto, 2003). The presence of misfolded proteins triggers cellular stress responses which includes the initiation of the UPR, an adaptive cellular response of the ER, which protects cells against the toxic build-up of misfolded proteins, maintaining

biological processes within the brain during cellular stress (Kopito, 2000; Dobson, 2003; Rao and Bredesen, 2004). Accumulation of misfolded proteins in excessive amounts can overwhelm the 'cellular quality control' system and the prolonged stress observed in neurodegenerative diseases is thought to disrupt the protective mechanisms of the UPR, which ultimately leads to organelle dysfunction and cell death through the activation of inflammation and apoptotic pathways (Rao and Bredesen, 2004; Sprenkle *et al.*, 2017).

Examples in hereditary spastic paraplegia include, the missense mutations in the *BSCL2* gene, which encodes the ER transmembrane protein seipin (BSCL2), causes hereditary spastic paraplegia (HSP) type 17 (SPG17) (Windpassinger *et al.*, 2004). Seipin is involved in lipid droplet morphology and metabolism (Fei *et al.*, 2008). HSP-associated *BSCL2* mutations (N88S and S90L), cause misfolded seipin to accumulate in the ER, leading to ER stress and enhance ubiquitination and degradation (Ito *et al.*, 2008).

More recently, reticulon-like-1 (*Rtnl1*), the Drosophila orthologue of the Hereditary Spastic Paraplegia gene *reticulon 2,* was found to be important in ER organisation and function. Loss of Rtnl1 caused an expansion of the ER sheets which contributed to the overall reorganisation of the ER and significantly increased the ER stress response. Abnormalities within distal motor axons, including disruption of smooth ER (SER), microtubule cytoskeleton and mitochondria, was also observed, linking the pathogenesis of HSP proteins involved in ER morphogenesis and mitochondrial dysfunction (O'Sullivan *et al.*, 2012).

The *tropomyosin-receptor kinase fused gene* (*TFG*) has been implicated in several hereditary neurological disorders which include hereditary spastic paraplegia (Beetz, Johnson, *et al.*, 2013), Charcot-Marie-Tooth (CMT) disease type 2 (CMT2) (Tsai *et al.*, 2014)and the hereditary motor and sensory neuropathy with proximal dominant involvement (HMSN-P) (Ishiura *et al.*, 2012). Each TFG mutation is thought to cause a different disorder, affecting several distinct pathological pathways associated with ER dysfunction (Yagi, Ito and Suzuki, 2016). In cell lines, TFG inhibition slows protein

secretion from the ER and disrupts ER morphology, affecting peripheral ER tubular organisation and the subsequent collapse of the ER network, thereby providing a link between altered ER morphology and neurodegeneration (Beetz, Johnson, *et al.*, 2013). More recently, TFG was shown to function as an inhibitory regulator in the ubiquitin-proteasome system (UPS) and overexpression of wild-type TFG was found to increase ubiquitination of ER-resident protein Seipin, resulting in ER stress (Yagi, Ito and Suzuki, 2014). Furthermore, mutant *TFG* (P285L), causes autosomal-dominant type of HMSN-P, exhibiting an enhanced inhibitory effect on the UPS and the level of ER stress (Yagi, Ito and Suzuki, 2014).

Data from this study show that disease-related mutations of human HSP proteins may re-structure HSP protein interaction networks, which may have the potential to effect ER function and associated cellular processes, this could in turn lead to increased levels of ER stress. ER stress has been suggested to be involved in several human neurodegenerative diseases. Understanding more about the role of ER stress in neurodegenerative diseases, may reveal novel insight into disease mechanisms involved in the progressive axonal degeneration observed in HSPs and other neurodegenerative diseases may be possible, as well as identifying potentially novel therapeutic strategies for these disorders.

Chapter 5: Identification of potential RING E3 ligase and DUB regulators of HSP proteins & the 'edgetic' effect of HSP genetic mutations

5.1. Introduction

The ubiquitin-proteasome system (UPS) is the main pathway for the removal of short-lived, damaged and misfolded proteins in the nucleus and cytoplasm (Dantuma and Bott, 2014). The UPS consists of two distinct and successive steps: ubiquitination and proteasomal degradation (Wilkinson, 1997; Hershko and Ciechanover, 1998).

Ubiquitination is a post-translational modification, whereby ubiquitin, a highly conserved 76-amino acid peptide (Goldknopf and Busch, 1977), is covalently attached to a specific substrate protein via its C-terminal glycine to either the ε-amino group of lysine (Lys) residues or, the less common, amino (N) terminus of the substrate protein itself, forming an isopeptide bond (Pickart, 2001). Ubiquitination is an ATP-dependent process which is catalysed by the sequential action of three enzymes: ubiquitin-activating enzymes (E1), ubiquitin-conjugating enzyme (E2) and ubiquitin ligases (E3) (Ciechanover, 1998; Hershko and Ciechanover, 1998). Initially, the E1 or ubiquitin-activating enzyme, activates ubiquitin using ATP to form a ubiquitin-adenylate intermediate, after which, ubiquitin is transferred to the cysteine residue of the E1 active site, resulting in a thioester linkage between ubiquitin C terminus and the catalytic cysteine on the E1. The activated ubiquitin is then transferred to the cysteine residue of one of the many ubiquitin-conjugating E2 enzymes. Finally, an isopeptide bond is formed between a Lys residue of the target protein and the C-terminal glycine of ubiquitin, with the co-ordination of a ubiquitin ligase E3 which can interact with both E2 and substrate (Ciechanover, 1998; Pickart, 2001). E3s can identify specific protein domains capable of binding the E2-Ub complex, as well as a substrate-specific domain for binding target protein (Bernassola *et al.*, 2008; Deshaies and Joazeiro, 2009). Ubiquitin E3 ligases are a large family which are currently classified into one of three main types based on the presence of specific active and structural domains, and on the mechanism by which ubiquitin is transferred to a substrate protein, and include the Homologous to E6-AP Carboxyl

Terminus (HECT) domain-containing E3s, the Really Interesting New Gene (RING) finger domain-containing E3s, and the RING-between RING-RING (RBR) E3s, analogous to HECT E3s (Morreale and Walden, 2016). The E3 ligases of the HECT domain family, like the RBR E3s, catalyse a two-step ubiquitin transfer reaction where ubiquitin is first transferred to a catalytic cysteine on the E3, and then to the substrate protein, whilst the RING E3s, mediate a direct transfer of ubiquitin, functioning as a scaffold to orient the E2-Ub complex with respect to the substrate protein and stimulating ubiquitin transfer (Metzger, Hristova and Weissman, 2012; Spratt, Walden and Shaw, 2014).

The ubiquitination process can be reversed, by a family of ubiquitin-specific proteases, termed de-ubiquitinating enzymes (DUBs). DUBs can cleave conjugated ubiquitin residues on mono- or poly-ubiquitinated proteins (Wilkinson, 1997; Sun, 2008). DUBs not only reverse ubiquitination to prevent protein degradation, but they can also regulate different cellular pathways. By editing ubiquitin chain linkage and length during ubiquitin chain formation, DUBs can target proteins to specific cellular pathways (Todi and Paulson, 2011).

Ubiquitination is required for many cellular processes, and once ubiquitinated the structural conformation, cellular location and biological function of the target protein will change, and following multiple rounds of ubiquitination, a polyubiquitin chain of four or more ubiquitin moieties at Lys 48 can serve as a signal for degradation, which occurs in the 26S barrel-like complexes known as proteasomes (Ciechanover, 1998; Hershko and Ciechanover, 1998; Cao and Mao, 2011). Most ubiquitinated proteins are in fact destined for degradation by the 26S proteasome, a large, multi-protein complex consisting of one 20S core particle and two 19S regulatory particles (Cao and Mao, 2011). The proteasome unfolds substrates, threading polypeptide chains through the inner channel, where they can be cleaved into short peptides (Bhattacharyya *et al.*, 2014). These short peptides are released from the barrel-like structure of the proteasome, rapidly processed rapidly into amino acids and recycled (Reits *et al.*, 2003).

UPS-dependent protein degradation is initiated when chaperones and ubiquitin ligases recognise abnormalities in protein folding (Ravid and Hochstrasser, 2008). There are several ubiquitin E3 ligases which mediate the ubiquitination of misfolded proteins, and this includes the yeast *S.cerevisiae*, RING finger E3 ligase Ubr1, which, with assistance from chaperones, is responsible for the targeting of misfolded cytosolic proteins to proteasomal degradation (Eisele and Wolf, 2008; Ciechanover and Kwon, 2015b).

Given that the ubiquitin-proteasome system (UPS) is the main pathway for selective protein degradation, it is thought to be a contributing factor in the aetiology of neurodegenerative disorders and in particular those associated with the accumulation or aggregation of misfolded proteins (Dennissen, Kholod and van Leeuwen, 2012). In fact, there are many neurodegenerative diseases, which include AD, PD, HD and ALS, for which the pathogenesis of disease has been associated with the downregulation of the UPS (Hegde and Upadhya, 2011; Dennissen, Kholod and van Leeuwen, 2012). Aging and protein aggregation are two major risk factors associated with reduced UPS activity. Studies have shown that proteasomal activity gradually decreases with age, thereby reducing its ability to degrade misfolded proteins which results in the formation of pathological protein aggregates (Keller, Huang and Markesbery, 2000; Tydlacka *et al.*, 2008). The presence of protein aggregates, on the other hand, can impair proteasome activity, and other UPS components. For example, in Alzheimer's disease, there is an accumulation of hyperphosphorylated and ubiquitinated tau in the brain (Morishima-Kawashima *et al.*, 1993; Cripps *et al.*, 2006), as well as an accumulation of proteasomes and chaperones which suggests that tau aggregation leads to impaired proteolysis, consistent with dysfunction of the UPS (Keck *et al.*, 2003; Tai *et al.*, 2012).

The accumulation and aggregation of misfolded proteins within affected neurons and the surrounding environment, is now a recognised feature among many neurodegenerative diseases, with UPS dysfunction reported in many cases (Ross and Poirier, 2004; Atkin and Paulson, 2014; Ciechanover and Kwon, 2015b). To date, there is very little known about the potential involvement of the UPS in HSP.

Understanding the molecular mechanisms and components responsible for changes in ubiquitination in neurodegenerative diseases, and in particular HSP, may provide valuable insight into the molecular mechanisms involved in the pathogenesis of this group of disorders, as well as potentially identifying novel therapeutic strategies. All of which may improve our understanding of the cellular processes required for axonal maintenance or degeneration.

To do this, we targeted specific components of the ubiquitination process, in particular ubiquitin E3 ligases, which determine the selectivity of the ubiquitination process, and DUBs, direct antagonists of ubiquitin E3 ligases, which together regulate the level and activity of protein substrates and thus cell homeostasis.

The main aim of the research presented in this chapter was to use the Y2H system to perform an unbiased systematic screen of binary HSP:RING E3 ligase or HSP:DUB protein interactions. The second aim was to investigate the 'edgetic' effects of HSP disease-associated mutations on any detected binary wild-type HSP:RING E3 ligase or HSP:DUB interactions, in an unbiased systematic method using the Y2H system.
All data generated was compared to all available published data, to assess the reproducibility of previously defined interactions and identify potentially novel regulators of HSP protein function. Finally, all reproducible data was analysed and used to predict protein function as well as possible cellular pathways/processes in which potential HSP interaction partners may act.

5.2. Use of targeted Y2H assay to investigate binary HSP:RING E3 ligase interactions

5.2.1. The RING E3 ligase prey collection used in this study

The RING E3 ligases constitute the largest type of ubiquitin ligases, with over 600 predicted human E3 ubiquitin ligase genes identified so far, and approximately 300 E3 ligase proteins are currently annotated at RINGs (W. Li *et al.*, 2008). RING E3s can be characterised by the presence of a zinc-binding domain called RING (Really Interesting New Gene) or by a U-box domain, and can function as monomers, homodimers or heterodimers (Morreale and Walden, 2016).

Previous research in our laboratory used a collection of RING E3 ligases, sub-cloned into Y2H prey vectors (pACTBE-B/pACTBD-B), to investigate protein-protein interactions between RING E3 ligases/ RING E3 ligases (Woodsmith, Jenn and Sanderson, 2012) and E2 conjugating enzymes/RING E3 ligases (Markson *et al.*, 2009). The collection consisted of 177 RING E3 ligase genes as presented in Figure 5.1, and a list of all RING E3 ligase genes used was assembled in Appendix 5.1). There were 138 full-length ORF clones and 39 transmembrane (TM) domain-containing RING E3 ligases. As transmembrane domain-containing proteins can be problematic for the 'traditional' Y2H assay, these clones had been previously truncated to generate ORFs encoding the full cytoplasmic RING domain (CRD). These were sub-cloned into the Y2H prey vector (pACTBE-B) generating a collection of TM-RING-E3 proteins (Robert Jenn, University of Liverpool, unpublished data).

5.2.2. The HSP bait collection used in this study

To test binary interactions between human HSP proteins and the set of RING E3 ligase Y2H prey clones, a set of HSP Y2H bait constructs had to be generated. In total, 34 HSP ORFs were sub-cloned into the pGBAE-B (bait) Y2H vector, resulting in 33 HSP Y2H bait clones (Chapter 4, section 4.2.2).

Figure 5.1

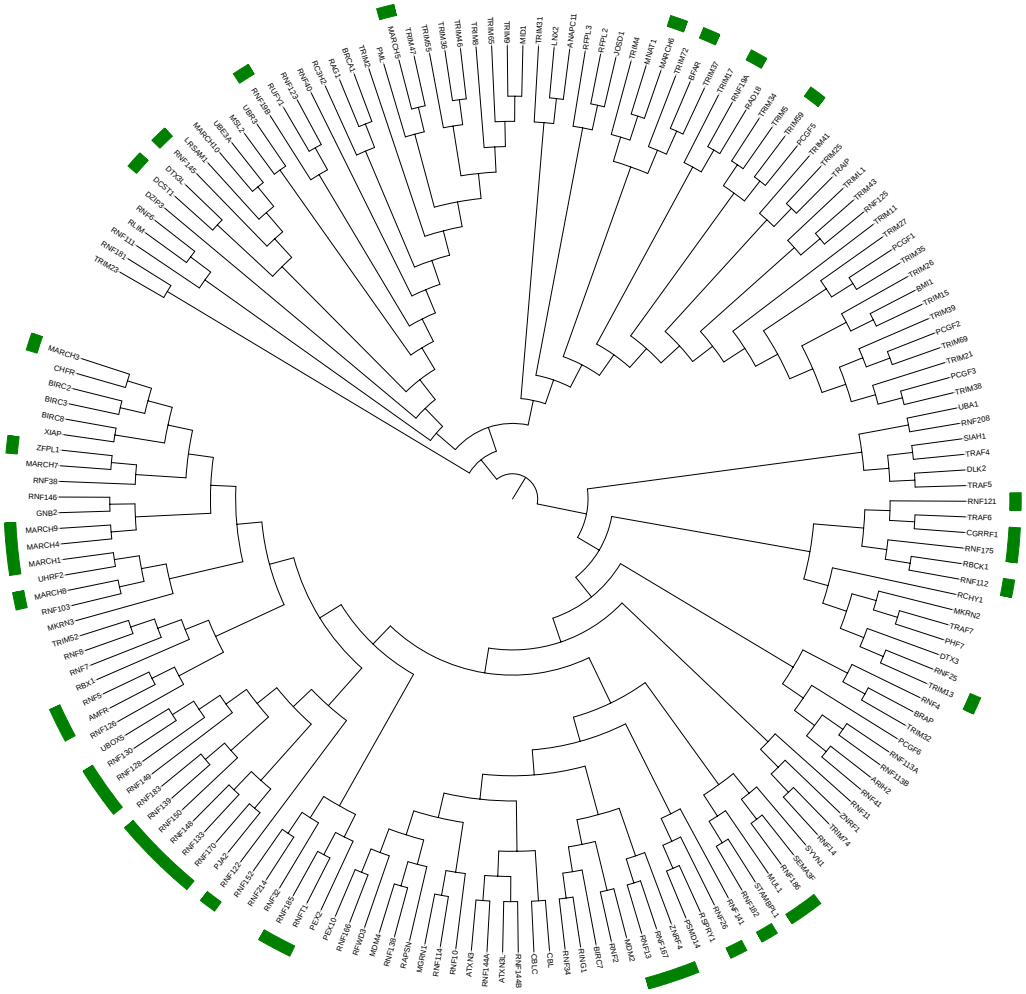

Figure 5.1. RING E3 ligases tested by Y2H. All 177 human RING E3 ligases-domain containing proteins were aligned using ClustalOmega, a multiple protein sequence alignment tool. Sequence alignment was used to generate the phylogenetic tree using iTOL (Letunic and Bork, 2007). TM-RING-E3 ligases are highlighted in green.

5.2.3. The HSP disease-associated mutant bait collection used in this study

To test the 'edgetic' effects on the binary interactions between human HSP proteins and the set of RING E3 ligase Y2H prey clones, a set of mutant HSP Y2H bait constructs had to be generated. In total, 23 mutant HSP ORFs were sub-cloned into the pGBAE-B (bait) Y2H vector, resulting in 16 mutant HSP Y2H bait clones (Chapter 4, section 4.2.3).

5.3. Identification of binary HSP:RING E3 ligase interactions

5.3.1. Y2H screens reveals 88 binary HSP:RING E3 ligase interactions

The improved targeted Y2H matrix mating methodology was used in the HSP:RING E3 ligase interaction screen, as described in Chapter 2. Briefly, MATα haploid yeast cells transfected with RING E3 ligase prey constructs were spotted onto rich medium (YPAD) agar plates, in a 96-well format. MATa haploid yeast cells transfected with the desired HSP bait construct was spotted on top of preys, and they were left for 24 hours to mate. Diploid yeast was selected for following velvet replication onto SD-WL agar plates and left to grow after which yeast cells were replicated onto the SD-WLA and SD-WLH(3-AT) agar plates, to select for positive protein-protein interactions. The *lacZ* reporter activity (β-Gal assay) was altered from the colony lift assay to the agar overlay assay. Diploid yeast was also replicated onto SD-WLH(3-AT) +X-Gal agar plates, as described in Chapter 2, and images taken every 3-4 days. Interactions were annotated as weak, medium or strong according to the relative degree of yeast colony growth on selective plates (see Figure 5.2). A known positive control was always included in each matrix mating assay, to check for efficient detection of interaction. The interaction screen was repeated twice, and only interactions observed in both screens were annotated as positive.

All 33 HSP bait constructs were systematically screened against 177 RING E3 ligase prey constructs, which included 39 TM-RING-E3 proteins. 5,841 possible binary interactions were tested, and the 88 reproducible positive binary HSP:RING E3 ligase interactions are presented in Figure 5.3. Additionally, there were 2 previously defined HSP:RING E3 ligase interactions which were also identified in this study, leaving 86 potentially novel binary HSP:RING E3 ligase interactions. All true positive interactions should be observed on either SD-WLA and SD-WLH(3-AT) or the less stringent SD-WLH(3-AT) alone, interactions detected on SD-WLA alone are considered false positive interactions and were excluded from the final list of positive interactions.

Figure 5.2

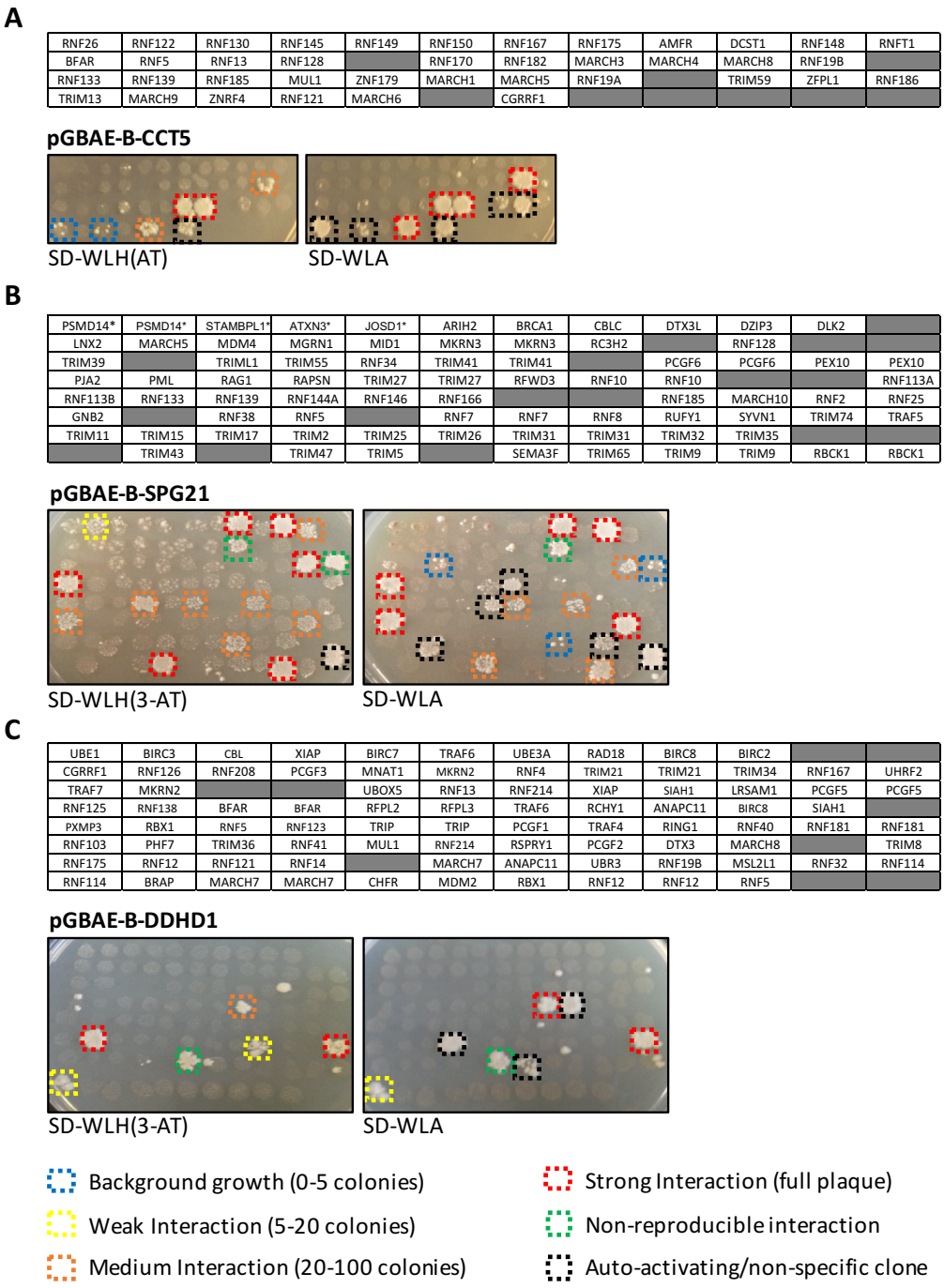

Figure 5.2. HSP:RING E3 ligase interaction data. (A) pGBAE-B-CCT5, (B) pGBAE-B-SPG21 and (C) pGBAE-B-DDHD1 transfected MATa yeast was mated against MATα yeast transfected with either pACTBE-B-TM-RING E3 (panel A) or the full-length pACTBE-B-RING E3 ligase collection (panels B and C), in a matrix array format. Yeast growth was scored on both SD-WLA (most stringent) and SD-WLH(3-AT) (least stringent) agar plates on day 14, shown above. *not E3 RING ligases.

Figure 5.3

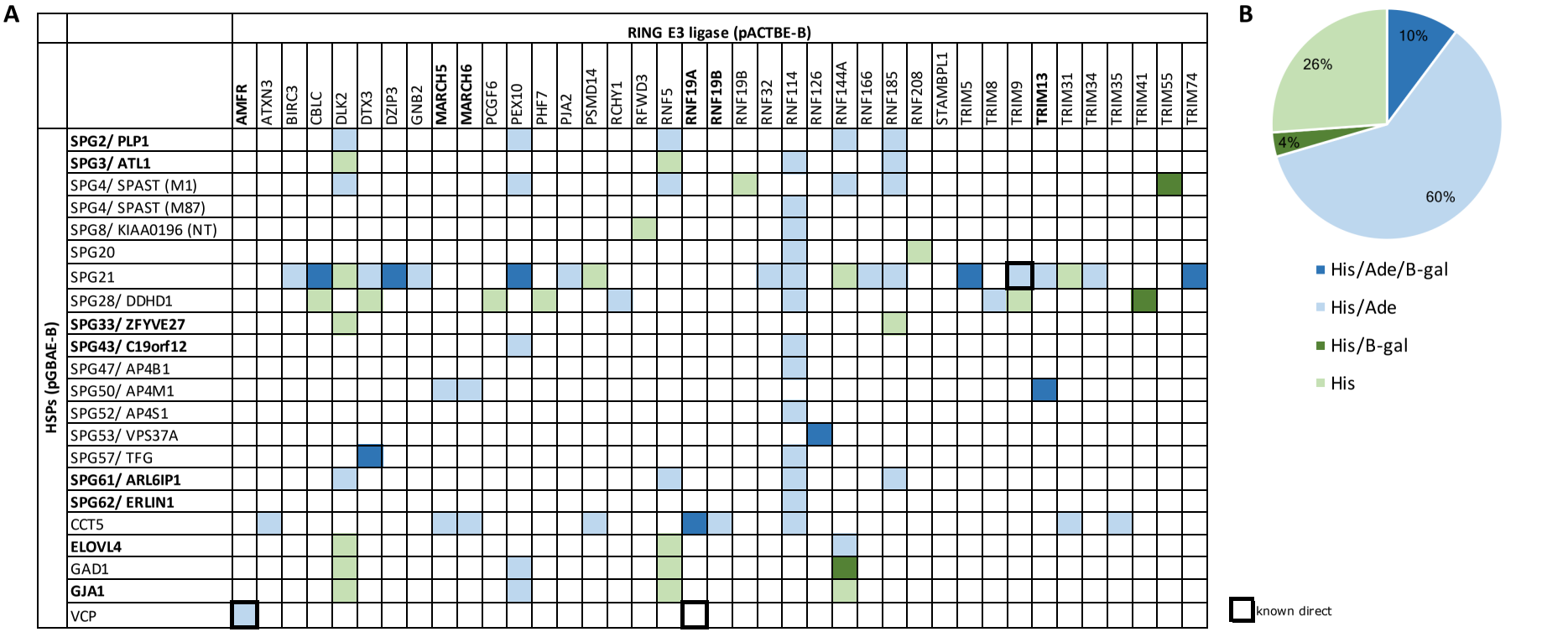

Figure 5.3. All positive binary HSP:RING E3 ligase interactions identified in targeted Y2H matrix interaction screens. (A) Matrix showing all tested Y2H binary interactions involving HSP bait (pGBAE-B) and RING E3 prey (pACTBE-B) clones. HSP bait clones are arranged by spastic gait disease-loci (SPG), those not part of the SPG classification system and are listed alphabetically as are the RING E3 ligase prey clones. (B) Shows the percentage of positive Y2H interactions observed at each level of reporter stringency. Stringency scoring is ranked as follows: His/Ade/ β-Gal (Dark Blue) > His/Ade (Light Blue) > His/β-Gal (Dark Green) > His (light Green). Corresponding colours are also used to represent relative stringency of individual positive interactions in panel (A). *BOLD = Transmembrane HSP/RING protein.*

Results obtained from the β-Gal assays were incorporated with those from the biosynthetic reporter assays and presented in Table 5.1, and the final list of positive binary interactions includes: 9 interactions seen on all three reporters, 56 interactions seen on two reporters and 23 interactions seen on one reporter.

Table 5.1

BAIT Gene ID	BAIT Symbol	PREY Gene ID	PREY Symbol	*HIS3*	*ADE2*	*lacZ*
7415	VCP	267	AMFR	+++	+++	
22948	CCT5	4287	ATXN3	++	+++	
51324	SPG21	330	BIRC3	+++	+++	
51324	SPG21	23624	CBLC	+++	+++	+
80821	DDHD1	23624	CBLC	+		
23204	ARL6IP1	65989	DLK2	+++	+++	
6683	SPAST (M1)	65989	DLK2	+++	+++	
5354	PLP1	65989	DLK2	++	+	
6785	ELOVL4	65989	DLK2	++		
2571	GAD1	65989	DLK2	++		
2697	GJA1	65989	DLK2	++		
51324	SPG21	65989	DLK2	++		
51062	ATL1	65989	DLK2	++		
118813	ZFYVE27	65989	DLK2	++		
10342	TFG	196403	DTX3	+	+	++
51324	SPG21	196403	DTX3	+++	++	
80821	DDHD1	196403	DTX3	++		
51324	SPG21	9666	DZIP3	+++	+++	++
51324	SPG21	2783	GNB2	++	+++	
22948	CCT5	54708	MARCH5	+++	+++	
9179	AP4M1	54708	MARCH5	++	+++	
9179	AP4M1	10299	MARCH6	+++	+++	
22948	CCT5	10299	MARCH6	++	+++	
80821	DDHD1	84108	PCGF6	+		
51324	SPG21	5192	PEX10	+++	++	++
2571	GAD1	5192	PEX10	+++	+++	
2697	GJA1	5192	PEX10	+++	+++	
6683	SPAST (M1)	5192	PEX10	+++	+++	
83636	C19orf12	5192	PEX10	+++	++	
5354	PLP1	5192	PEX10	+	+	

80821	DDHD1	51533	PHF7	+++		
51324	SPG21	9867	PJA2	+++	+++	
22948	CCT5	10213	PSMD14	+	+	
51324	SPG21	10213	PSMD14	+		
80821	DDHD1	25898	RCHY1	++	+++	
9897	KIAA0196 (NT)	55159	RFWD3	+		
137492	VPS37A	55658	RNF126	++	++	++
6683	SPAST (M1)	9781	RNF144A	+++	+++	
6785	ELOVL4	9781	RNF144A	+++	+++	
5354	PLP1	9781	RNF144A	++	+	
2697	GJA1	9781	RNF144A	+++		
2571	GAD1	9781	RNF144A	++		+
51324	SPG21	9781	RNF144A	++		
51324	SPG21	115992	RNF166	+	+	
6683	SPAST (M1)	91445	RNF185	+++	+++	
23204	ARL6IP1	91445	RNF185	+++	+++	
5354	PLP1	91445	RNF185	+	+	
51324	SPG21	91445	RNF185	++	++	
51062	ATL1	91445	RNF185	+	+	
118813	ZFYVE27	91445	RNF185	+		
22948	CCT5	25897	RNF19A	+++	+++	++
22948	CCT5	127544	RNF19B	++	+++	
6683	SPAST (M1)	127544	RNF19B	++		
23111	SPG20	727800	RNF208	++		
51324	SPG21	140545	RNF32	+++	+++	
23204	ARL6IP1	6048	RNF5	+++	+++	
6683	SPAST (M1)	6048	RNF5	+++	+++	
5354	PLP1	6048	RNF5	+	+	
51062	ATL1	6048	RNF5	++		
2697	GJA1	6048	RNF5	++		
6785	ELOVL4	6048	RNF5	+		
2571	GAD1	6048	RNF5	+		
9179	AP4M1	10206	TRIM13	++	+++	+++
51324	SPG21	10206	TRIM13	+++	+++	
22948	CCT5	11074	TRIM31	+	+	
51324	SPG21	11074	TRIM31	++		
51324	SPG21	53840	TRIM34	+++	+++	
22948	CCT5	23087	TRIM35	+++	+++	
80821	DDHD1	90933	TRIM41	+++		+++

51324	SPG21	85363	TRIM5	+++	++	++
6683	SPAST (M1)	84675	TRIM55	++		+
51324	SPG21	378108	TRIM74	++	+++	+++
80821	DDHD1	81603	TRIM8	+++	+++	
51324	SPG21	114088	TRIM9	+++	++	
80821	DDHD1	114088	TRIM9	+		
10342	TFG	55905	RNF114	++	+	
23204	ARL6IP1	55905	RNF114	+	+	
22948	CCT5	55905	RNF114	+	+	
10613	ERLIN1	55905	RNF114	+	+	
23111	SPG20	55905	RNF114	+	+	
80821	DDHD1	55905	RNF114	+	+	
51062	ATL1	55905	RNF114	+	+	
6683	SPAST (M87)	55905	RNF114	+	+	
83636	C19orf12	55905	RNF114	+	+	
10717	AP4B1	55905	RNF114	+	+	
11154	AP4S1	55905	RNF114	+	+	
9897	KIAA0196 (NT)	55905	RNF114	+	+	
51324	SPG21	55905	RNF114	+	+	

Table 5.1. HSP:RING E3 ligase interaction summary. Gene IDs and Gene Symbols are indicated for HSP (pGBAE-B) bait and RING E3 ligase (pACTBE-B) preys that showed reproducible positive interactions in two independent matrix interaction assays. In each case interactions were scored as strong (+++), medium (++) or weak (+), as defined in Chapter 2.

A graphical representation of the data compiled in Table 5.1 is presented in Figure 5.4. HSPs and RING E3 ligases were arranged by degree (number of interactions) using interaction data generated from this screen. This degree sorting results in a cluster of highly-connected HSPs and RING E3 ligases in the top left corner (highlighted by a red box in Figure 5.4). Interestingly, highly connected HSPs do not always interact with highly connected RING E3 ligases, and although there are many interactions formed between HSPs and RING E3 ligases, there still appears to be a high degree of specificity. For example, DDHD1 and CCT5 are highly connected HSPs, yet they do not interact with some of the most highly connected RING E3 ligases.

Figure 5.4

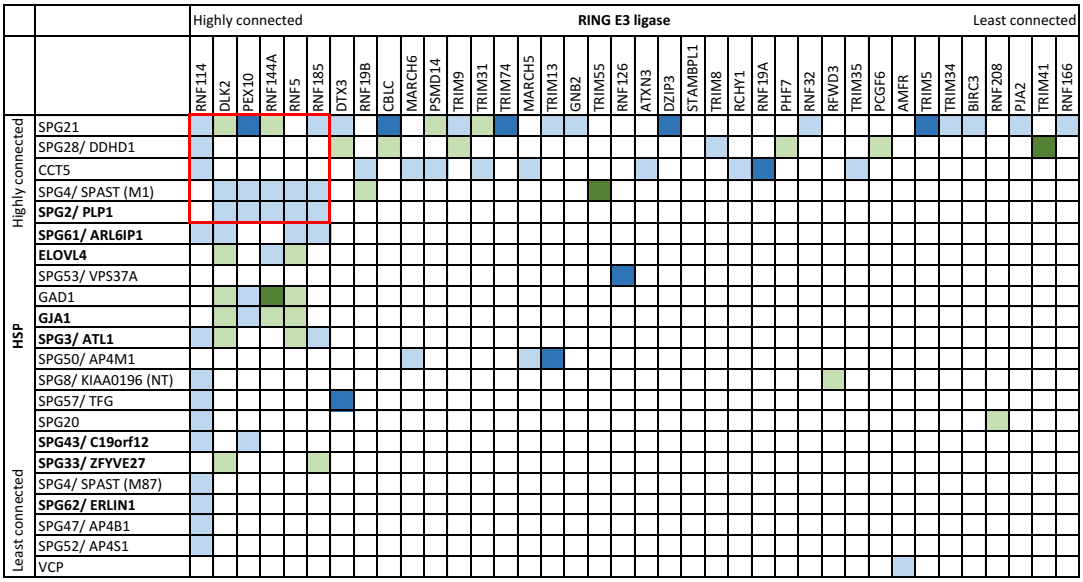

Figure 5.4. Degree clustering of observed HSP:RING E3 ligase protein interaction profiles. Bait HSPs (horizontal) and prey RING E3 ligases (vertical) were sorted by degree, resulting in a highly-connected subset of HSPs and RING E3 ligases highlighted in the top left of the table (red box).

5.3.2. Reconfirmation of previously defined interactions

The Expanded Global network (Figure 3.4 B) was used to extract the 177 RING E3 ligase proteins used in this study, together with their proximal interaction partners, to create an expanded global RING E3 ligase 'one-step' subnetwork shown in Figure 5.5 A. All previously defined known (direct and indirect) and predicted HSP:RING E3 ligase interactions were extracted from this global subnetwork, to create the HSP:RING E3 ligase 'one-step' subnetwork (Figure 5.5 B). A union of the HSP:RING E3 ligase 'one-step' subnetwork and the data obtained from this study is presented in Figure 5.5 C. Compared to the HSP:RING E3 ligase 'one-step' subnetwork (Figure 5.5 B), this new 'combined' HSP:RING E3 ligase interaction network (Figure 5.5 C) contains 156 interactions (edges) between 35 HSPs and 65 RING E3 ligases (nodes), representing a 52 % increase in the number of HSP interactors and a 59 % increase in the number of RING E3 ligase interactors (nodes), which resulted in a 140 % increase in the overall total number of interactions (edges) identified.

Figure 5.5

A **Expanded Global RING E3 ligase subnetwork**

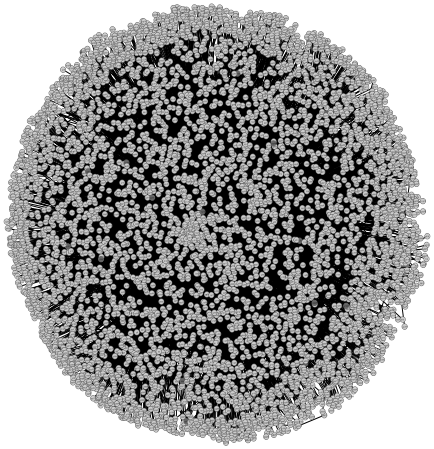

Total nodes: 5,430
Total edges: 11,672

B **HSP:RING E3 ligase subnetwork**

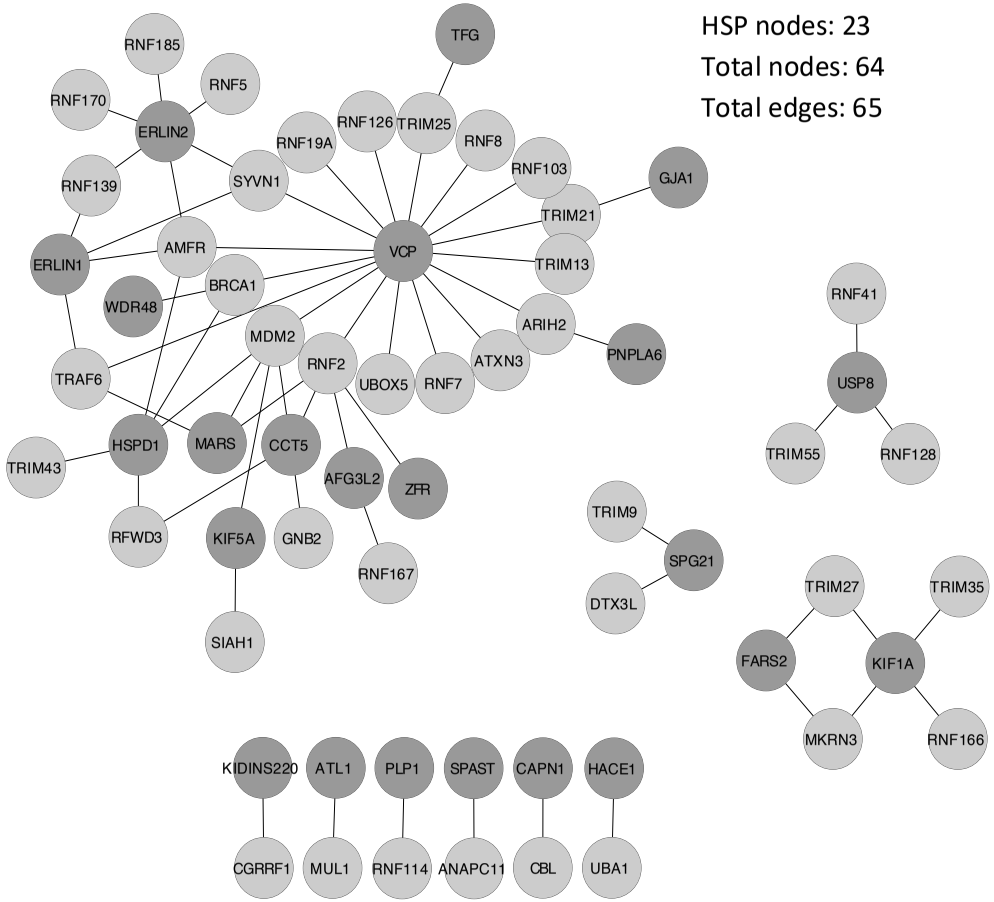

C **Combined HSP:RING E3 ligase subnetwork**

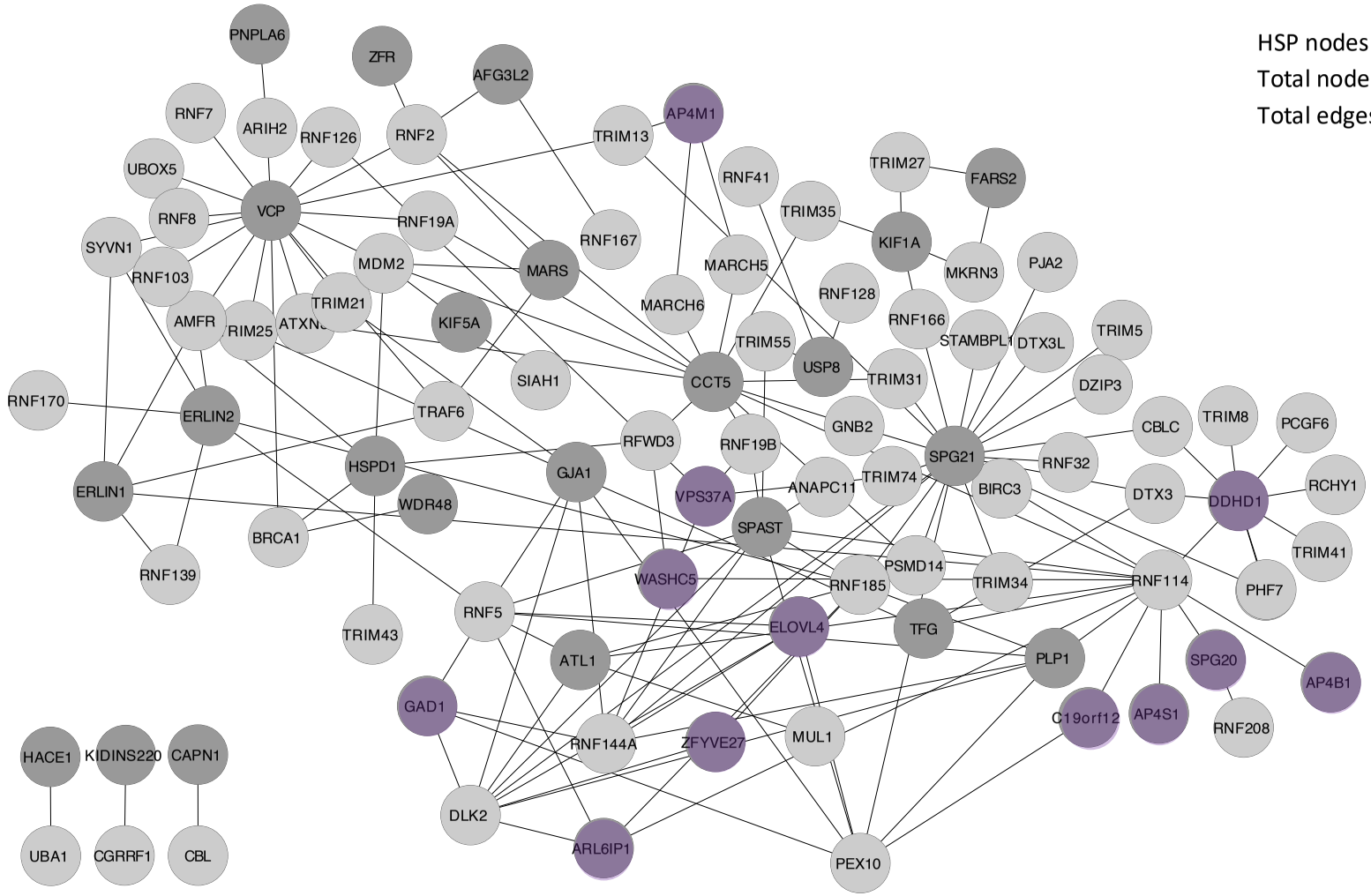

Figure 5.5. Generation of an HSP:RING E3 ligase binary protein interaction subnetwork (A) An initial 'one-step' RING E3 ligase network was extracted from the expanded global network (Figure 3.4 B) using the 177 RINGs used in this study as core nodes. (B) An HSP:RING E3 ligase 'one-step' subnetwork was then derived from the expanded global RING E3 'one-step' network (shown in A) using the 83 'HSP seed 3' genes as core nodes. A union network was then generated from the HSP:RING E3 ligase 'one-step' subnetwork (shown in B) and all interactions observed in this study (bold line) to generate a combined network (C). Newly identified HSPs are highlighted in purple.

Of the 58 previously known (direct and indirect) HSP:RING E3 ligase interactions, 39 were re-tested in this study, and 2 were reconfirmed. Additionally, 6 of the 39 re-tested known interactions were previously identified as 'direct' or binary interactions, and 33% (2/6) were reconfirmed in this study. These include the well-characterised interaction between VCP and AMFR, which was initially discovered via indirect methods (Zhong *et al.*, 2004), but was later confirmed by Y2H to be a direct interaction (Grelle *et al.*, 2006), and the less well-defined SPG21 and TRIM9 interaction (Rolland *et al.*, 2014). None of the retested 'indirect' interactions, were found to be positive binary interactions when tested in this study (Table 5.2).

Table 5.2

Interaction	Direct	Indirect
Known	14	44
Re-tested	6	33
Reconfirmed	2	0
Reconfirmation rate	33 %	-

Table 5.2. Re-tested HSP:RING E3 ligase protein interactions. Previously defined known direct and indirect human HSP:RING E3 ligase interactions, were extracted from the expanded global RING E3 ligase 'one-step' subnetwork (Figure 5.5 A), and interaction reconfirmation rates were determined by comparing them to the results observed in this study.

5.3.3. Common functions of HSP:RING E3 ligase pairs

The Database for Annotation, Visualisation and Integrated Discovery (DAVID, https://david.ncifcrf.gov/home.jsp) is an open-access bioinformatics resource which enables large gene/protein lists to be analysed and the biological/functional information to be extracted, in a high-throughput manner. The DAVID Functional Annotation tool was used to analyse the HSP:RING E3 ligase interaction data generated, in combination with the previously defined HSP:RING E3 ligase interactions as presented in Figure 5.5 C. The RING E3 ligases identified were analysed for gene-GO term enrichment, highlighting the most enriched and statistically significant GO terms associated with the overall list of RING E3 ligase genes.

The Functional Annotation Clustering feature is a novel algorithm, based on the hypothesis that similar gene members have similar annotations thereby clustering similar annotations together. This feature was used to analyse the RING E3 ligase genes, allowing them to be assigned to specific annotation groups/clusters. Following analysis, two clusters which were found to be significantly enriched; Cluster 1: Immune response mechanisms, which included IFN and NF-κB signalling pathways (blue) and, Cluster 2: UPR-associated processes, which included ERAD and protein ubiquitination (green) pathways, as presented in Figure 5.6. This type of analysis allows similar annotations to be grouped together, making the biology clearer and more focused. Following analysis, interacting HSPs were also grouped into functional Clusters 1 and/or 2. All of the functional information gathered was used to annotate the combined HSP:RING E3 ligase network, and is presented in Figure 5.7.

Figure 5.6

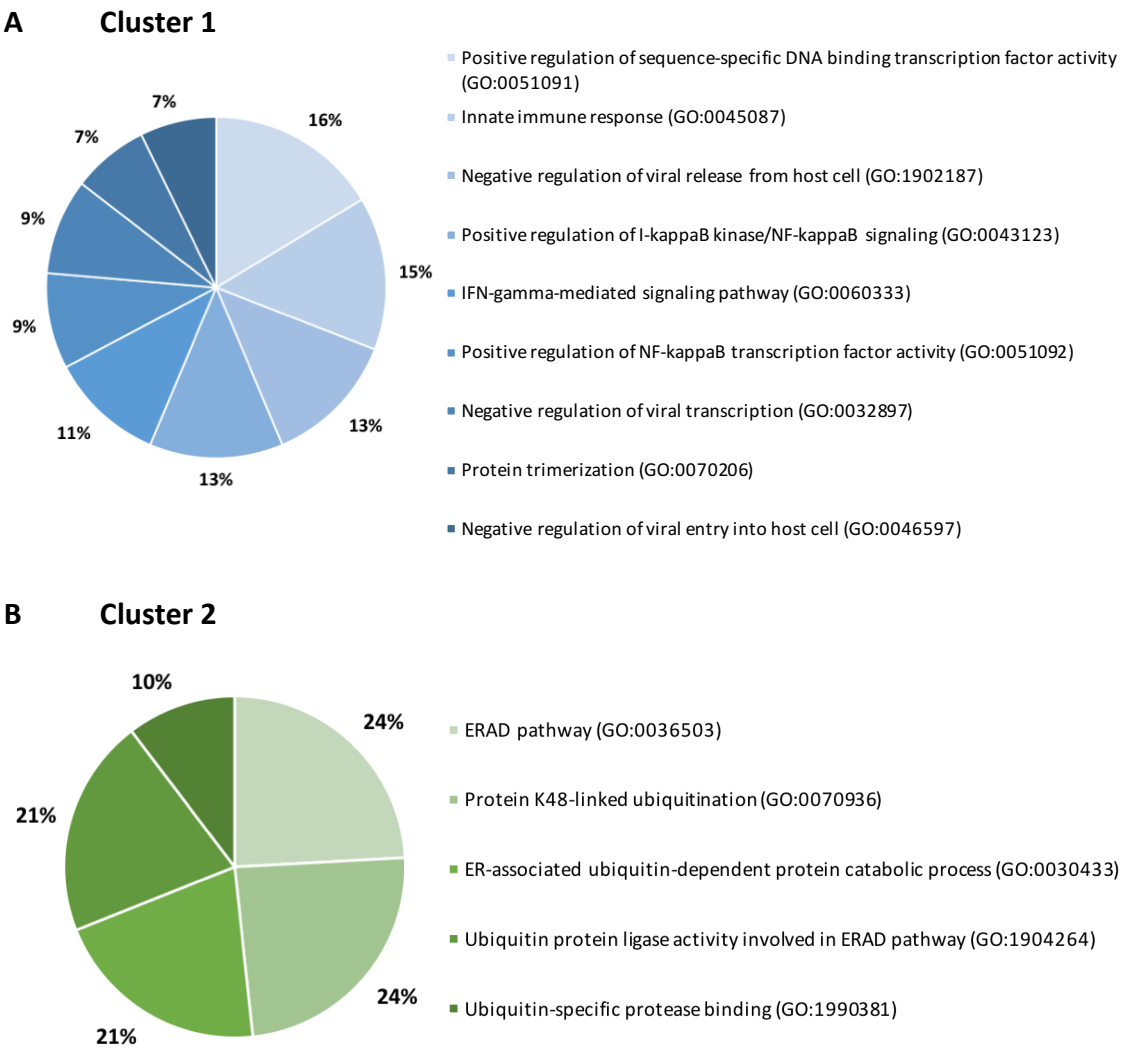

Figure 5.6. Functional annotation of the HSP:RING E3 protein interaction subnetwork. DAVID functional GO term enrichment analysis performed on the HSP interactors (RINGs) identified in the combined HSP:RING E3 ligase subnetwork (Figure 5.5 C). This analysis revealed two significantly enriched (EASE score $p \leq 0.05$) clusters: Cluster 1, highlights partners involved in Immune response mechanisms, such as IFN and NF-κB signalling pathways (A, blue) and Cluster 2, highlights interaction partners involved in unfolded protein response (UPR)-related processes (B, green). The percentage of interactors assigned to each given GO category within each cluster are indicated.

Figure 5.7

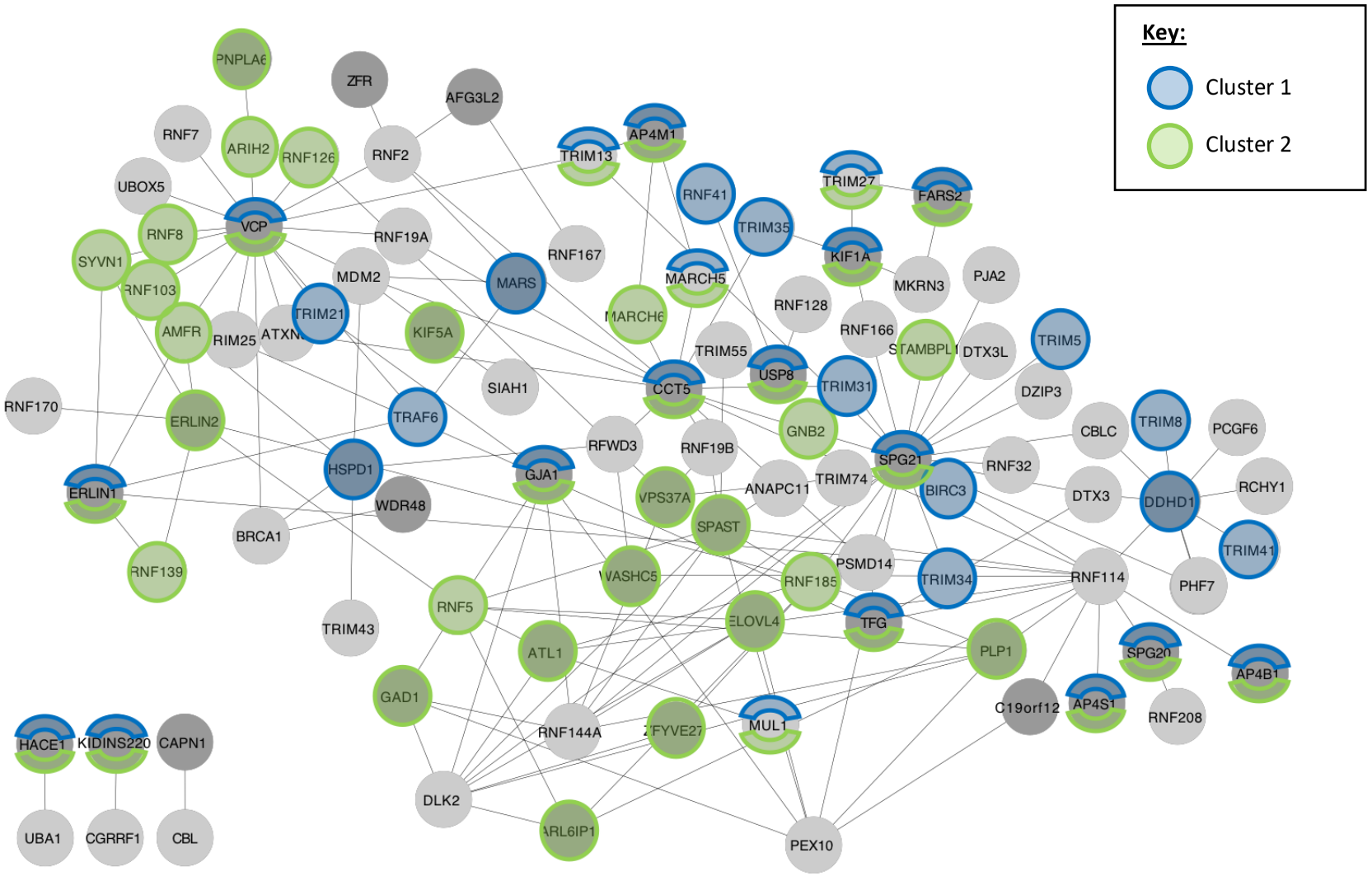
Key:
Cluster 1
Cluster 2
PNPLA6
ZFR
AFG3L2
RNF7
ARIH2
RNF126
RNF2
AP4M1
TRIM13
UBOX5
RNF41
TRIM27
FARS2
VCP
RNF8
RNF19A
TRIM35
SYVN1
RNF167
KIF1A
RNF103
MDM2
MARS
MARCH5
MKRN3
PJA2
AMFR
RIM25
ATXN
TRIM21
KIF5A
MARCH6
RNF128
RNF166
TRIM55
STAMBPL1
DTX3L
TRIM5
USP8
TRIM31
SIAH1
CCT5
DZIP3
RNF170
ERLIN2
TRAF6
GNB2
CBLC
TRIM8
PCGF6
RFWD3
RNF19B
SPG21
RNF32
HSPD1
GJA1
TRIM74
ANAPC11
BIRC3
DTX3
DDHD1
RCHY1
ERLIN1
WDR48
VPS37A
SPAST
BRCA1
TRIM41
RNF139
WASHC5
PSMD14
RNF185
TRIM34
RNF114
PHF7
RNF5
TRIM43
ELOVL4
TFG
ATL1
PLP1
SPG20
AP4B1
GAD1
C19orf12
AP4S1
RNF208
RNF144A
ZFYVE27
MUL1
HACE1
KIDINS220
CAPN1
DLK2
ARL6IP1
PEX10
UBA1
CGRRF1
CBL

Figure 5.7. Functional annotation of the HSP:RING E3 ligase subnetwork. The RING E3 ligases identified in the combined HSP: RING E3 ligase subnetwork (Figure 5.5 C) were functionally annotated according to whether they were involved in either of the assigned GO term enrichment analysis (see Figure 5.6). Cluster 1: Immune response mechanisms, including IFN and NF-κB signalling pathways (blue) and/or Cluster 2: UPR-related processes (green). HSP nodes were also annotated following literature-based curation.

To determine whether there was an inherent bias for RING E3 ligases to naturally cluster within these two functional groups, our collection of 177 human RING E3 ligase-domain containing proteins were analysed using the same DAVID Functional Annotation Clustering feature. The collection of 177 RING E3 ligase that were found to be enriched in several functional clusters (see Figure 5.8), the most significantly enriched being previously identified Cluster 1: Immune response mechanisms, including IFN and NF-κB signalling pathways (blue) and Cluster 2: UPR-associated processes (green). However, comparison with the HSP interactors from the combined HSP:RING E3 ligase subnetwork (Figure 5.5 C) revealed interactor-specific enriched GO terms within these clusters which are specific to the RING E3 ligases identified as potentially novel HSP interactors in this study, suggesting a potential role for those RING E3 ligases which specifically interacted with HSP proteins, in the immune response system and the ubiquitin-proteasome system (UPS).

Figure 5.8

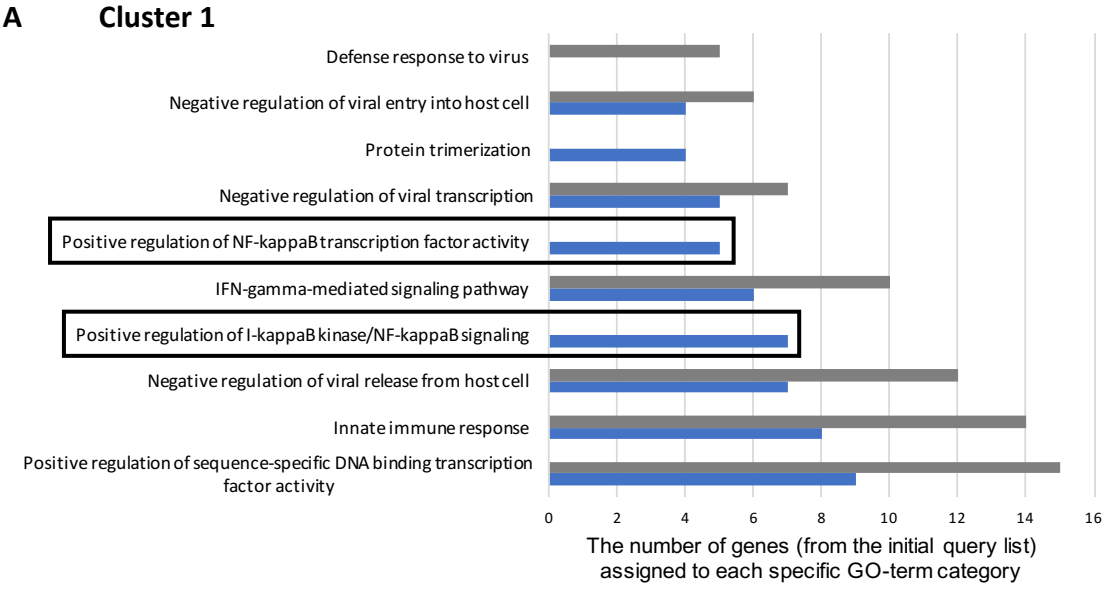

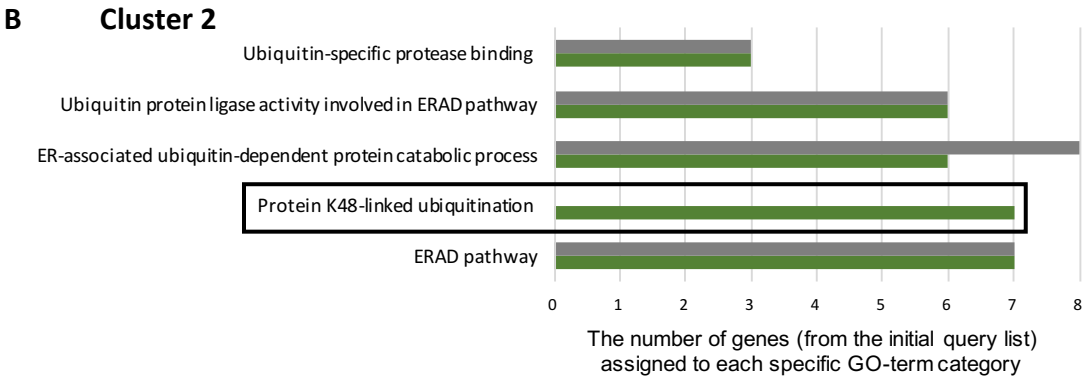

Figure 5.8. RING E3 ligase GO term enrichment analysis. DAVID functional GO term enrichment analysis performed on all 177 RING E3 ligases (grey) used in this study compared with the HSP protein interactors (RINGs) from the combined HSP:RING E3 ligase subnetwork (Figure 5.5 panel C) shown as blue/green bars. This analysis also identified enrichment of previously identified Cluster 1: Immune response mechanisms, including IFN and NF-κB signalling pathways (A, blue) and Cluster 2: UPR-related processes (B, green). The number of interactors assigned to each given GO category within each cluster are indicated, with interactor-specific enrichment highlighted.

5.4. Mutational analysis of HSP 'edgetic' interaction profiles

5.4.1. Y2H analysis of HSP disease-associated mutations on HSP:RING E3 ligase interaction profiles

The improved targeted Y2H matrix mating methodology was used to investigate the 'edgetic' effects of HSP disease-associated mutations on the binary HSP:RING E3 ligase protein interaction summary.

All 16 mutant HSP bait constructs (Table 4.1) were systematically screened against 177 RING E3 ligase prey constructs (including 39 TM-RING-E3 proteins). 2,832 binary interactions were tested, and the 30 reproducible positive binary interactions are presented in Figure 5.9. As before, all true positive interactions should be observed on either SD-WLA and SD-WLH(3-AT) or the less stringent SD-WLH(-AT) alone, interactions detected on SD-WLA alone are considered false positive interactions and were excluded from the final list of positive interactions.

Figure 5.9

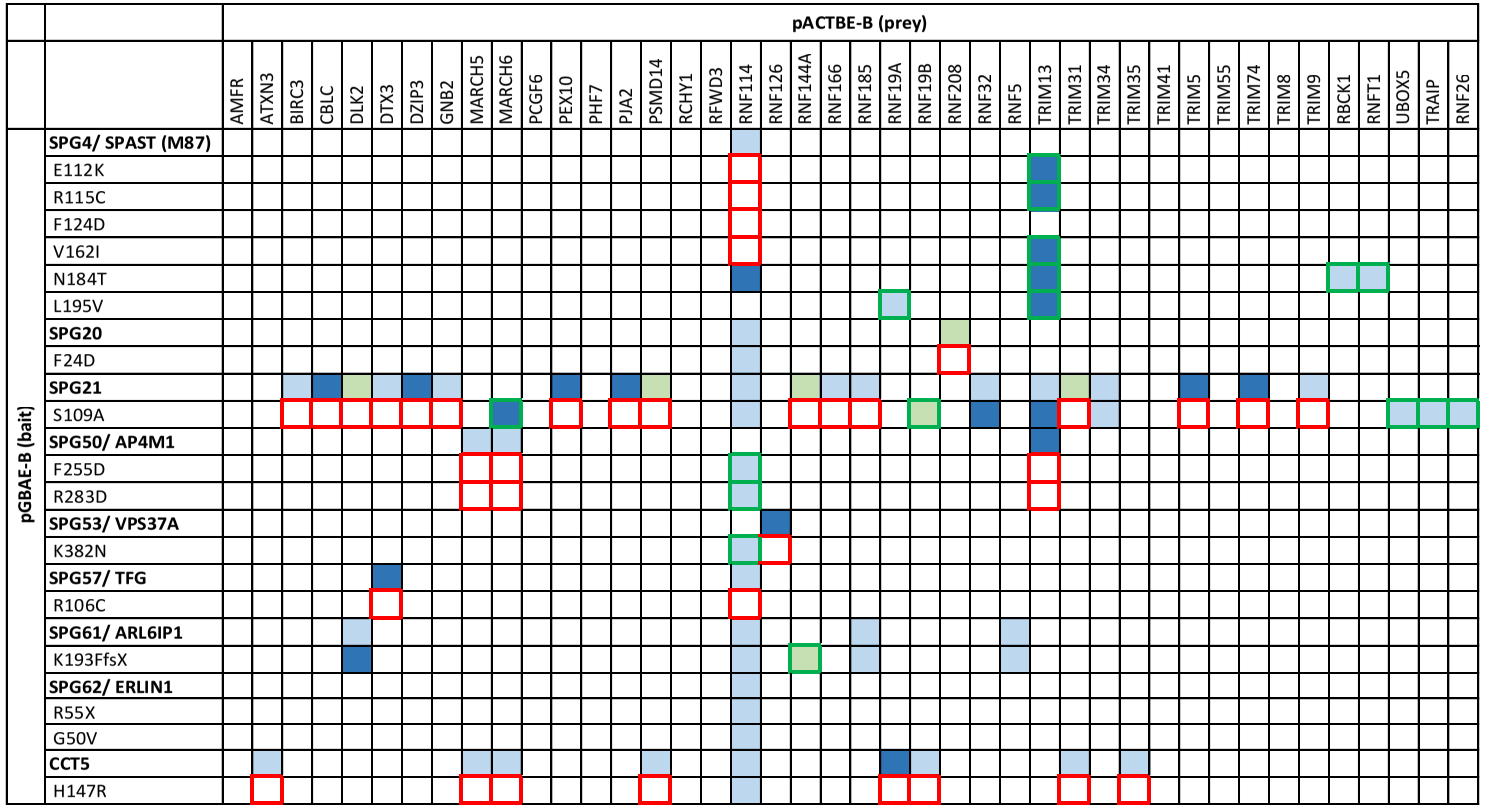

Figure 5.9. Analysis of mutant induced 'edgetic' changes in HSP:RING E3 ligase interaction profiles. Comparative analysis of WT HSP-WT RING E3 ligases or mutant HSP-WT RING E3 ligases partner interaction profiles. WT or mutant HSP bait (pGBAE-B) Entrez gene ID/symbols are ordered according to HSP loci, whilst WT RING E3 ligase prey (pACTBE-B) clones are arranged alphabetically. Stringency scoring is ranked as follows: His/Ade/ β-Gal (Dark Blue) > His/Ade (Light Blue) > His/β-Gal (Dark Green) > His (light Green), with corresponding colours used to represent relative stringency of individual positive interactions shown in the table. 'Edgetic' changes are highlighted by green (gain of interaction)

or red (loss of interaction) boxes respectively. *BOLD = wild-type protein*

Results obtained from the β-Gal assays were incorporated with those from the biosynthetic reporter assays and presented in Table 5.3, and the final list of positive binary interactions includes: 11 interactions seen on all three reporters, 16 interactions seen on two reporters and 3 interactions seen on one reporter.

Table 5.3

BAIT Gene ID	BAIT Symbol	PREY Gene ID	PREY Symbol	*HIS3*	*ADE2*	*lacZ*
6683	SPAST (M87) E112K	10206	TRIM13	+++	+++	++
	SPAST (M87) R115C	10206	TRIM13	+++	+++	+++
	SPAST (M87) V162I	10206	TRIM13	+++	+++	+++
	SPAST (M87) N184T	10206	TRIM13	+++	+++	+++
		51136	RNFT1	+	+	+
		55905	RNF114	+	+	+
		10616	RBCK1	++	++	
	SPAST (M87) L195V	10206	TRIM13	++	++	+++
		25897	RNF19A	+	+	
23111	SPG20 F24D	55905	RNF114	+	+	
51324	SPG21 S109A	10299	MARCH6	++	++	++
		140545	RNF32	++	++	+++
		10206	TRIM13	+	+	+++
		53840	TRIM34	+++	++	
		22888	UBOX5	++	++	
		55905	RNF114	++	++	
		79102	RNF26	+		++
		127544	RNF19B	++		
		10293	TRAIP	+		
9179	AP4M1 F255D	55905	RNF114	+	+	
	AP4M1 R283D	55905	RNF114	+	+	
137492	VPS37A K382N	55905	RNF114	+	+	
23204	ARL6IP1 K193FfsX	65989	DLK2	+++	+++	+
		55905	RNF114	++	++	
		91445	RNF185	++	+	
		6048	RNF5	+	+	

		9781	RNF144A	+		
10613	ERLIN1 G50V	55905	RNF114	+	+	
	ERLIN1 R55X	55905	RNF114	+	+	
22948	CCT5 H147R	55905	RNF114	+	+	

Table 5.3. HSP disease-associated 'edgetic' changes on the binary HSP:RING E3 ligase protein interaction summary. Entrez Gene IDs and symbols for selected mutant HSP bait (pGBAE-B) and RING E3 ligase preys (pACTBE-B) that showed evidence of positive binary interactions are listed, along with an indication of the relative strength of interaction: strong (+++), medium (++) or weak (+), as defined previously.

5.4.2. Effect of genetic mutations on HSP:RING E3 ligase networks

Misfolded proteins trigger cellular stress responses, including the adaptive cellular response of the ER, the UPR, which protects cells against the toxic build-up of misfolded proteins during cellular ER stress (Kopito, 2000; Dobson, 2003; Rao and Bredesen, 2004). Accumulation of misfolded proteins in excessive amounts can overwhelm the 'cellular quality control' system (ERAD and the UPS) and the prolonged stress observed in neurodegenerative diseases is thought to disrupt the protective mechanisms of the UPR, which ultimately leads to organelle dysfunction and cell death through the activation of inflammation and apoptotic pathways (Rao and Bredesen, 2004; Sprenkle *et al.*, 2017).

As a critical regulator of protein homeostasis, the UPS has received particular attention in the study of neurodegenerative disorders (Ciechanover and Brundin, 2003). USP dysfunction has been reported in several neurodegenerative diseases including Alzheimer's disease (AD), Parkinson's disease (PD), Amyotrophic Lateral Sclerosis (ALS), and Huntington's disease (HD) (Keller, Huang and Markesbery, 2000; Bence, Sampat and Kopito, 2001; McNaught *et al.*, 2003; Seo, Sonntag and Isacson, 2004; Lonskaya *et al.*, 2013). We therefore decided to investigate the potential 'edgetic' effects of HSP disease-associated mutations on RING E3 ligase interactions, as key components of ubiquitination and the UPS.

Interestingly, we notice that many HSP disease-associated mutants interact with RNF114, similarly to that observed with the hereditary spastic paraplegia protein, HSPD1 (SPG13). HSPD1 has a dual role as it is involved in the induction and propagation of autoimmune diseases, activating both innate and adaptive immune responses, but it can also activate immunoregulatory pathways which leads to suppression of these diseases (Quintana and Cohen, 2011; Landstein, Ulmansky and Naparstek, 2015). RNF114, also known as zinc-finger protein 313 (ZNF313), binds to K48- and K63-linked polyubiquitin chains both *in vitro* and *in vivo,* and was recently shown to be involved in the regulation of NF-κB activity contributing to the T cell-mediated immune response signalling pathways (Rodriguez *et al.*, 2014).

Additionally, the edgetic mutations E112K, R115C, F124D, V162I and L195V of SPAST (M87) completely abolished interactions with RNF114. Moreover, most SPAST (M87) mutants (E112K, R115C, V162I, N184T and L195V) formed interactions with TRIM13, whereas the remainder of the HSP disease-associated mutants did not interact with TRIM13, and in the case of AP4M1, F255D and R283D both abolished interactions with TRIM13. TRIM13 is an ER-anchored E3 ligase involved in ERAD substrate degradation via proteasome and autophagy degradation pathways (Lerner *et al.*, 2007; Tomar *et al.*, 2012). TRIM13 induced autophagy is crucial in the regulation of ER stress-induced cell death (Tomar *et al.*, 2013). More recently, TRIM13 was shown to be involved in the regulation of NF-κB activity (Tomar and Singh, 2014).

5.5. Use of targeted Y2H assay to investigate HSP:DUB interactions

5.5.1. Analysis of binary HSP:DUB protein interaction profiles

Deubiquitinating enzymes (DUBs) are an essential component of ubiquitin signalling, regulating ubiquitin homeostasis. Almost 100 putative human DUBs have been identified so far, and over 60% remain uncharacterised (Nijman *et al.*, 2005; Hutchins *et al.*, 2013). Previous research in our laboratory resulted in the generation of a library of 63 DUB ORFs representing 59 human DUBs (a list of all DUB genes used is shown in Appendix 5.2). These DUBs were sub-cloned into Y2H bait vector (pGBDU-

GW), and used to investigate the protein-protein interactions between DUBs and RING E3 ligases (Sebastian Hayes, University of Liverpool, unpublished data).

5.5.2. The HSP bait collection used in this study

To test binary interactions with the set of DUB Y2H bait clones, a set of HSP Y2H prey constructs was generated as described in Chapter 4. In total, 34 HSP ORFs were sub-cloned into the pACTBE-B (prey) Y2H vector, resulting in 24 HSP Y2H prey clones. However, due to a lack of pACTBE-B (prey) mutant HSP constructs, a targeted Y2H screen against the pGBDU-GW (bait) DUB collection was not possible.

5.6. Identification of binary HSP:DUB interactions

5.6.1. Targeted Y2H matrix screens reveal 15 binary HSP:DUB interactions

The improved targeted Y2H matrix mating methodology was used in the HSP:RING E3 ligase interaction screen, as described in Chapter 2. Briefly, MATa haploid yeast cells transfected with DUB bait constructs were spotted onto rich medium (YPAD) agar plates, in a 96-well format. MATα haploid yeast cells transfected with the desired HSP prey construct was spotted on top of preys, and they were left for 24 hours to mate. Diploid yeast was then selected following velvet replication onto SD-UL agar plates, and left to grow before colonies were further replicated onto the SD-ULA and SD-ULH(3-AT) agar plates, to select for positive protein-protein interactions. The *lacZ* reporter activity (β-Gal assay) was also assessed using the agar overlay assay. As in the conventional Y2H assay, images were taken every 3-4 days and interactions were annotated as weak, medium or strong activators of reporter expression, based on yeast colony growth (see Figure 5.10). A known positive control was always included, to check for efficient mating and selective growth. The interaction screens were repeated twice, and only interactions observed in both screens were annotated as positive.

Figure 5.10

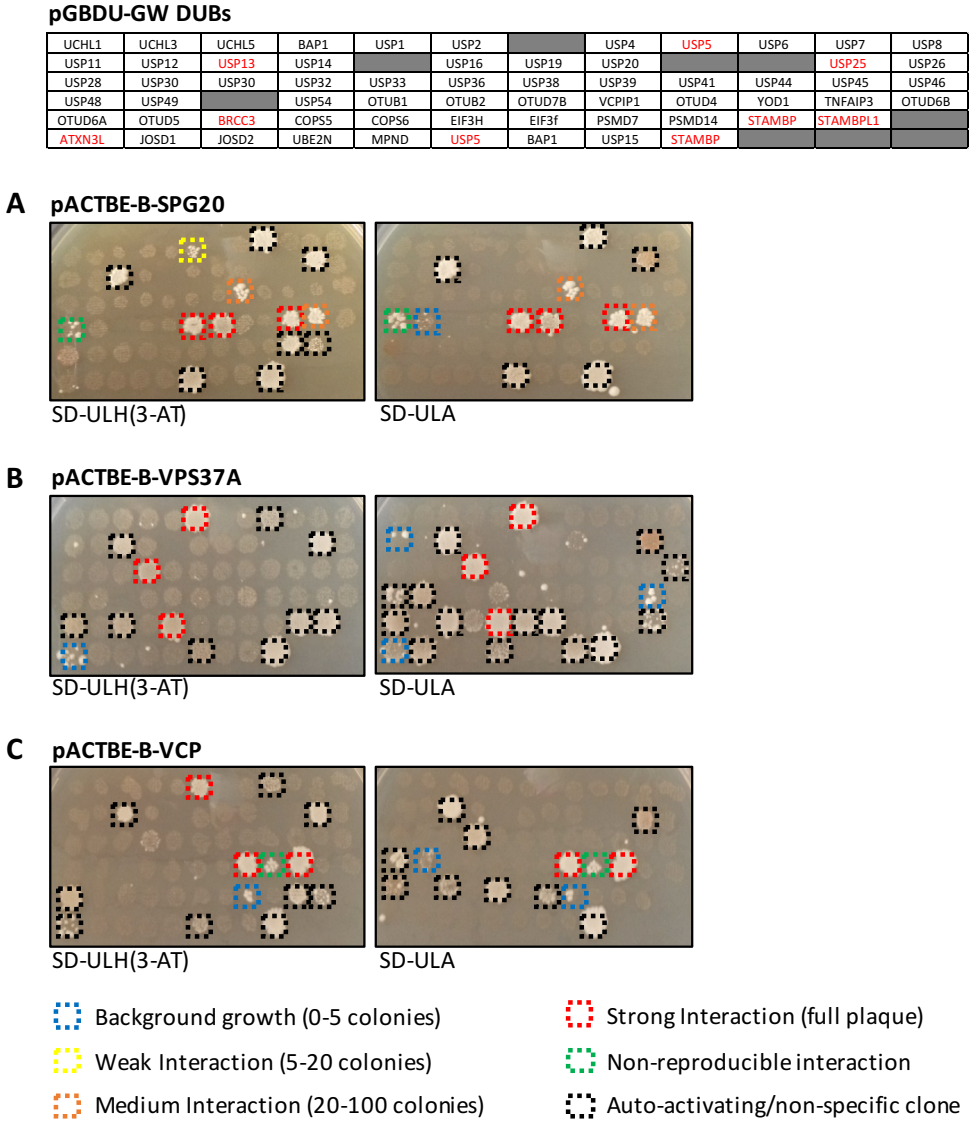

Figure 5.10. HSP:DUB interaction data. (A) pACTBE-B-SPG20, (B) pACTBE-B-VPS37A and (C) pACTBE-B-VCP transfected MATα yeast was mated against Mata yeast transfected with our pGBDU-GW-DUB collection (top panel), in a matrix array format. Yeast growth was scored on both SD-ULA (most stringent) and SD-ULH(3-AT) (least stringent) agar plates on day 14, as shown above.

In total, 24 HSP prey constructs were systematically screened against 59 DUB bait constructs, resulting in the analysis of 1,416 potential binary interactions. Following repeat screening, 15 reproducible positive binary HSP:DUB interactions were detected (Figure 5.11), of which only 2 of the 15 HSP:DUB interactions were previously identified, leaving 13 potentially novel binary HSP:DUB interactions. All

true positive interactions should be observed on either SD-WLA and SD-WLH(3-AT) or the less stringent SD-WLH(3-AT) alone, interactions detected on SD-WLA alone are considered false positive interactions and were excluded from the final list of positive interactions.

Results obtained from the β-Gal assays were incorporated with those from the biosynthetic reporter assays and presented in Table 5.4. The final list of positive binary interactions includes: 3 interactions seen on all three reporters, 7 interactions seen on two and 5 interactions seen on only one reporter.

Table 5.4

BAIT Gene ID	BAIT Symbol	PREY Gene ID	PREY Symbol	*HIS3*	*ADE2*	*lacZ*
55432	YOD1	7415	VCP	+++	+++	+++
55432	YOD1	23111	SPG20	+++	+++	
80124	VCPIP1	7415	VCP	+++	+++	++
80124	VCPIP1	9897	KIAA0196 (NT)	++		
80124	VCPIP1	6683	SPAST (M87)	++		
9099	USP2	137492	VPS37A	+++	+++	
9099	USP2	7415	VCP	+++		
9099	USP2	23111	SPG20	+		
84669	USP32	137492	VPS37A	+++	+++	
10713	USP39	23111	SPG20	++	++	
78990	OTUB2	23111	SPG20	+++	+++	
78990	OTUB2	9897	KIAA0196 (NT)	+		
10980	COPS6	137492	VPS37A	+++	+++	+
56957	OTUD7B	23111	SPG20	+++	+++	
7128	TNFAIP3	23111	SPG20	++	++	

Table 5.4. HSP:DUB interaction summary. Gene IDs and Gene Symbols are indicated for DUB (pGBDU-GW) bait and HSP (pACTBE-B) preys that showed reproducible positive interactions in two independent matrix interaction assays. In each case interactions were scored as strong (+++), medium (++) or weak (+).

Figure 5.11

A

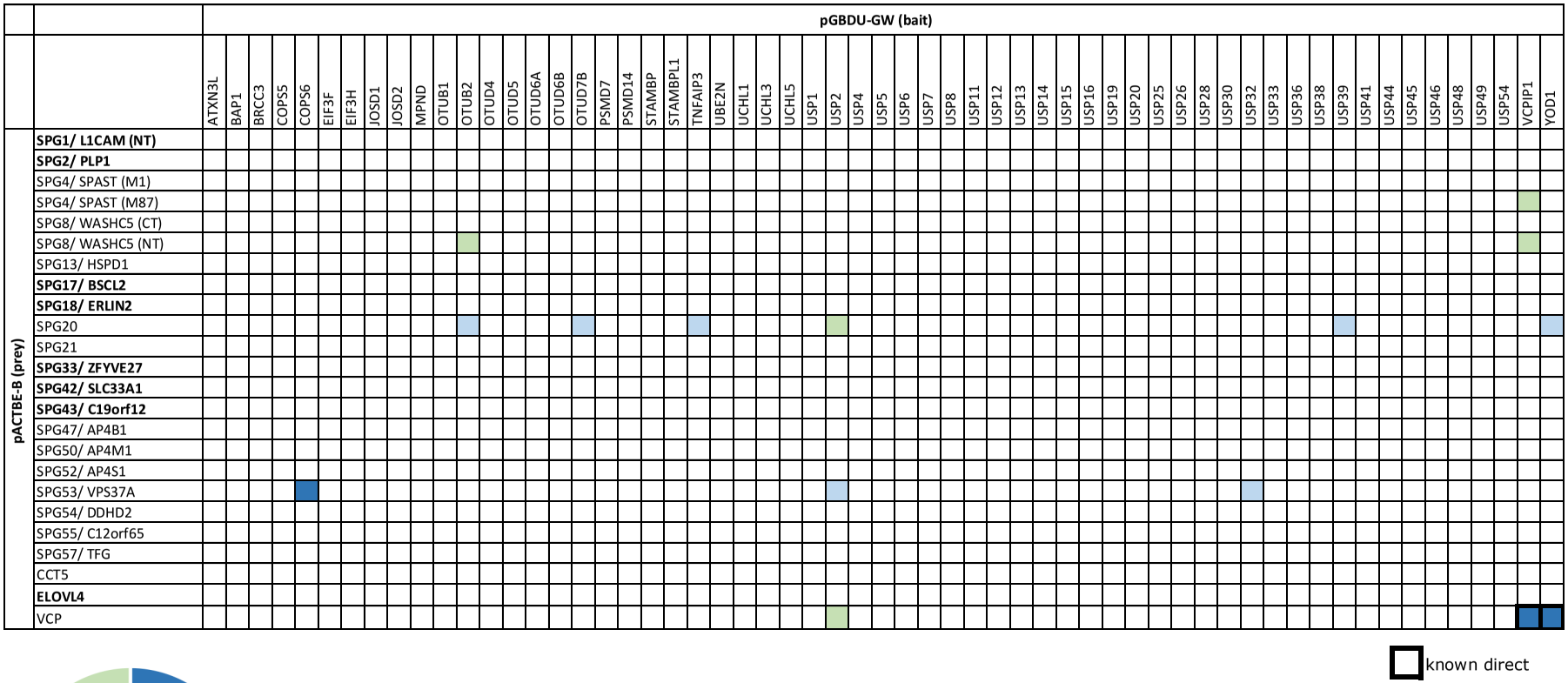

B

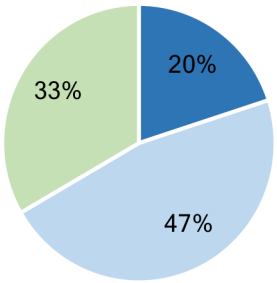

Figure 5.11. Summary of all tested binary HSP:DUB interactions. (A) Matrix showing all tested Y2H binary interaction profiles for DUB bait (pGBDU-GW) and HSP prey (pACTBE-B) clones. HSP prey clones are arranged by spastic gait disease-loci (SPG), those not part of the SPG classification system and are listed alphabetically as are the DUB bait clones. (B) Percentage of positive Y2H interactions observed at each level of reporter stringency. Corresponding colours are also used to represent relative stringency of individual positive interactions in panel (A). *BOLD = Transmembrane protein.*

5.6.2. Reconfirmation of previously defined interactions

The Expanded Global network (Figure 3.4 B) was used to extract the 59 DUB proteins used in this study, together with their proximal (one-step) interaction partners, to create an expanded global DUB 'one-step' subnetwork (Figure 5.12 A). All previously defined known (direct and indirect) and predicted HSP:DUB interactions were then extracted from this global subnetwork, to create the HSP:DUB 'one-step' subnetwork (Figure 5.12 B). A union of the HSP:DUB 'one-step' subnetwork and the data obtained from this study is presented in Figure 5.12 C. Compared to the HSP:DUB 'one-step' subnetwork (Figure 5.12 B), this new 'combined' HSP:DUB interaction network contains 43 interactions (edges) between 17 HSPs and 28 DUBs (nodes), representing a 31 % increase in the number of HSP interactors and a 22 % increase in the number of DUB interactors (nodes), which resulted in a 39 % increase in the overall total number of interactions (edges) identified.

Of the 30 previously known (direct and indirect) HSP:DUB interactions contained in this subnetwork, 8 were re-tested in this study (see Table 5.5). Significantly, 2 of the 8 re-tested known interactions were previously identified as 'direct' or binary interactions, and both were reconfirmed in this study. HSP:DUB interactions reconfirmed in this study include the well-characterised interaction between VCP and VCPIP1 (Sowa *et al.*, 2009; Totsukawa *et al.*, 2011), as well as the VCP and YOD1 interaction (Ernst *et al.*, 2009). None of the retested 'indirect' interactions, were found to be positive binary interactions when tested in this study.

Table 5.5

Interaction	Direct	Indirect
Known	4	26
Re-tested	2	6
Reconfirmed	2	0
Reconfirmation rate	100 %	-

Table 5.5. Re-tested HSP:DUB protein interactions. Previously defined direct and indirect human HSP:DUB interactions were extracted from the global DUB 'one-step' subnetwork (Figure 5.12 A), and interaction reconfirmation rates were determined by comparing them to the results identified in this study.

Figure 5.12

A **Expanded Global DUB subnetwork**

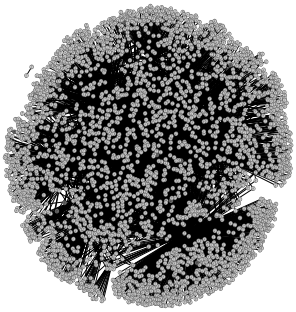

Total nodes: 3,290
Total edges: 5,810

B **HSP:DUB subnetwork**

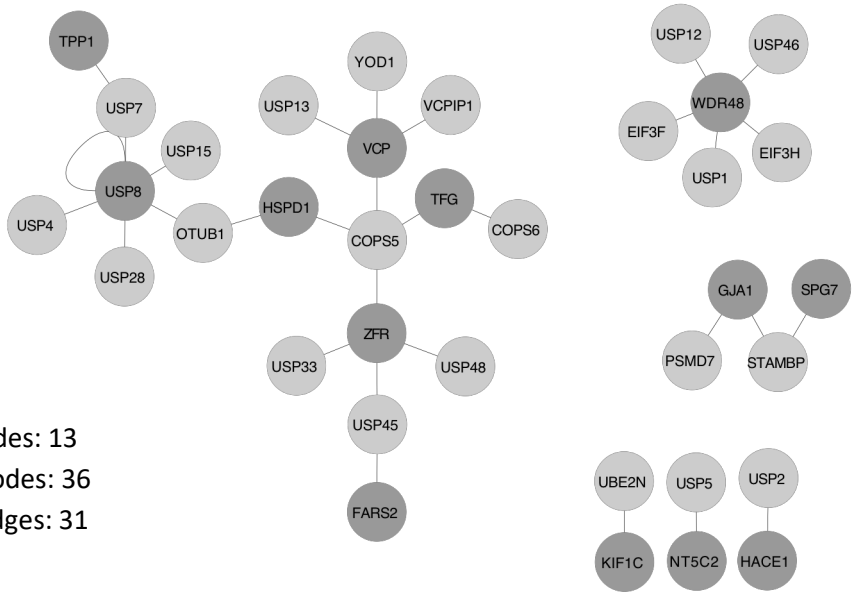

HSP nodes: 13
Total nodes: 36
Total edges: 31

C **Combined HSP:DUB subnetwork**

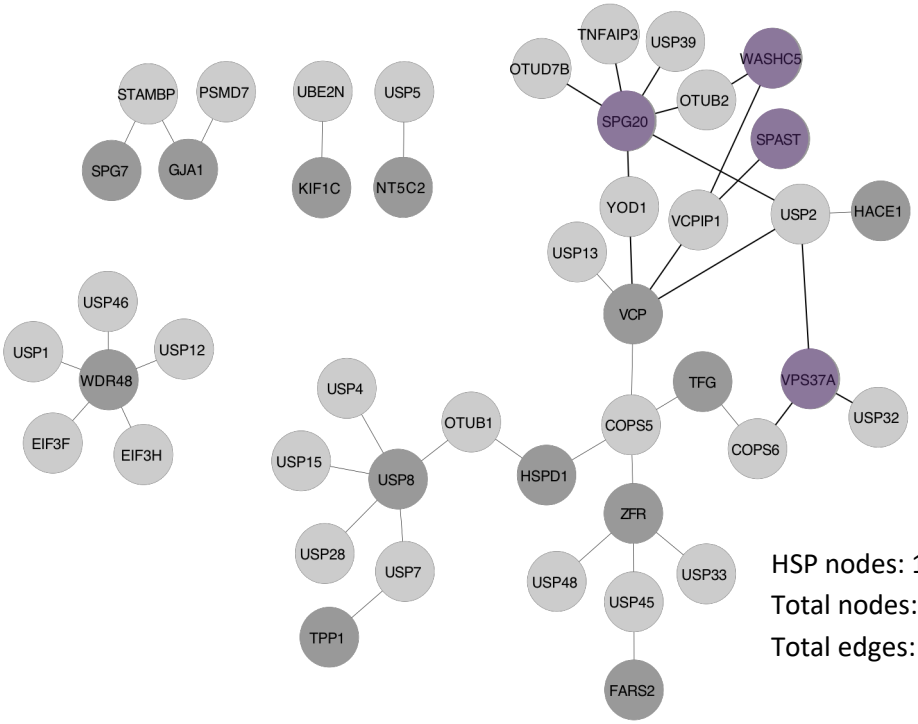

HSP nodes: 17
Total nodes: 45
Total edges: 43

Figure 5.12. Generation of an HSP:DUB binary protein interaction subnetwork. (A) An initial global 'one-step' DUB network was extracted from the expanded global network (shown in Figure 3.4 B) using the 59 DUBs used in our Y2H matrix mating screen, as core nodes. (B) An HSP:DUB 'one-step' subnetwork was then derived from the global DUB 'one-step' network shown in (A) using the 83 'HSP seed 3' genes as core nodes. A union of the HSP:DUB 'one-step' subnetwork shown in (B) and all interactions observed in this study (bold line), was used to generate (C). Newly identified DUB partners, identified in this study are shown as purple nodes.

5.6.3. Common functions of HSP:DUB ligase pairs

The DAVID Functional Annotation tool was used to analyse the newly expanded HSP:DUB interaction network. The DUBs identified were analysed for gene-GO term enrichment, unsurprisingly protein deubiquitination was one of the most relevant GO terms associated with the list of DUBs. However, more interestingly, another enriched GO term associated with these DUBs was the 'negative regulation of IkappaB kinase/NF-kappaB signalling'. As this term was also related to Cluster 1: Immune response mechanisms, which was identified following analysis of binary HSP:RING E3 ligase interactions, we were interested to know whether any of the DUBs listed were known to be involved in either of the processes highlighted previously. As the DAVID functional annotation tool only highlights enriched terms associated with a specific gene list, we manually annotated the known functional associations of each of the DUBs identified. Following literature-based searches, DUBs were annotated according to their involvement in either of the previously identified clusters: Immune response mechanisms, including IFN and NF-κB signalling pathways (blue) and/or UPR-associated processes (green). We identified DUBs that were contained in each of the clusters, as well as three that were identified as having roles in both functional groups/clusters (Figure 5.13).

Figure 5.13

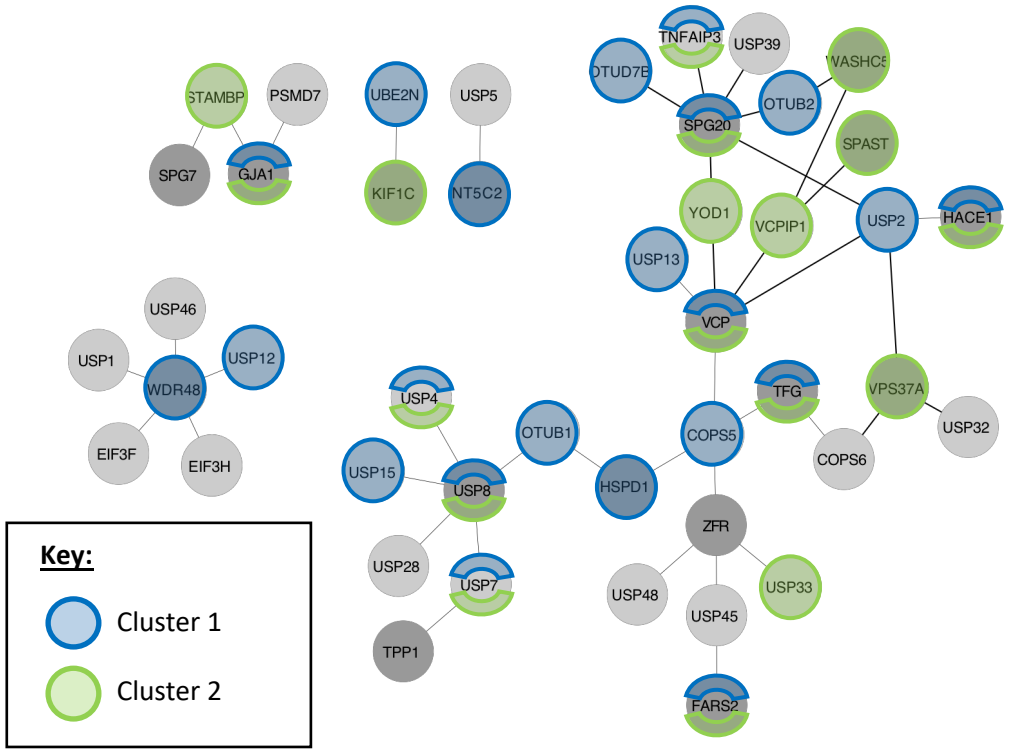

Figure 5.13. Functional annotation of the HSP:DUB protein interaction subnetwork. The DUBs identified in the combined HSP:DUB subnetwork (Figure 5.12, panel C) were functionally annotated according to whether they were involved in either of the assigned GO term enrichment analysis (see Figure 5.6). Cluster 1: Immune response mechanisms, including IFN and NF-κB signalling pathways (blue) and/or Cluster 2: UPR-related processes (green). The HSP nodes were also annotated following literature-based curation.

As both the HSP interacting RING E3 ligases and DUBs seem to fall into these two functional clusters, it is possible that there may be a link between altered patterns of ubiquitination and changes in immune response mechanisms. Therefore, it is possible that over time changes in these processes may contribute to some forms of neurodegeneration.

5.7. Discussion

In this study, we identified a number of novel binary HSP:RING E3 ligase (86) and HSP:DUB (12) interactions, identifying a number of potential HSP regulators. Upon further investigation, two functional clusters appeared to be particularly enriched

within each set of interactions, Cluster 1: Immune response mechanisms, and Cluster 2: unfolded protein response (UPR)-related processes, with a particular emphasis on regulation of NF-κB signalling and protein K48-linked ubiquitination, respectively.

UPR and the immune system

The unfolded protein response (UPR) has traditionally been viewed as an adaptive cellular response to ER stress, activated by an accumulation of unfolded or misfolded proteins, which is aimed at reducing cellular stress and restoring ER homeostasis by co-ordinating the expression of ER stress response signal transducers during ER stress (Oslowski and Urano, 2011; Walter and Ron, 2011). This results with the initiation of several signalling cascades, resulting in transcriptional and translational changes, reducing cellular stress, whilst simultaneously inducing protein quality control mechanisms to reduce protein misfolding (Sprenkle *et al.*, 2017). However, the UPR is also able to mediate inflammatory pathways, essential for an innate immune response.

Inflammation is part of the non-specific immune response of the innate immune system to infection or tissue injury, and this initial response under normal conditions is self-limiting. However, prolonged or chronic inflammation is damaging and can lead to a host of diseases which includes: arthritis, diabetes, cardiovascular disease and even cancer (Shacter and Weitzman, 2002; Hansson and Libby, 2006; Rosenfeld, 2013). The UPR is able to activate several primary inflammatory signalling proteins which include the Mitogen Activated Protein Kinase (MAPK) family proteins: c-Jun N-terminal kinase (JNK) and p38, and the Nuclear Factor-kappa-light-chain-enhancer of activated B cells (NF-κB) (Sprenkle *et al.*, 2017). NF-κB is a transcription factor with a crucial role in the inflammatory response, regulating the expression of many inflammatory cytokine genes, as well as in biological processes including cell survival, innate and adaptive immune responses (Wang *et al.*, 2006; Ghosh and Hayden, 2008; Baltimore, 2009). In the absence of harmful stimuli, NF-κB resides in the cytoplasm where it is bound to a member of the family of inhibitors of NF-κB (IκB), which are

constitutively expressed, and thus NF-κB remains in an inactive state (Zhang and Kaufman, 2008).

NF-κB activation pathways can be subdivided into two kinase-dependent pathways, the canonical/classical pathway and the non-canonical/alternative pathway (Bonizzi and Karin, 2004). Ubiquitin-mediated protein degradation activates both canonical and non-canonical NF-κB pathways. In the canonical pathway, NF-κB activation is initiated by the signal-induced IκB kinase (IKK) complex activation and subsequent IκB phosphorylation (Israel, 2010) by various stimuli. Phosphorylated IκBs undergo proteasome-mediated degradation which frees NF-κB exposing its nuclear-localisation signal, allowing NF-κB dimers to translocate to the nucleus where it binds to κB promoter sites to activate transcription of NF-κB target genes (Ghosh and Hayden, 2008; Baltimore, 2009). The non-canonical NF-κB pathway involves the processing of NF-κB precursors (p100) by the proteasome (Pomerantz and Baltimore, 2002). Ubiquitination has an important role in regulating signal transduction in the NF-κB pathways, it not only controls IκB degradation and the processing of NF-κB precursors (p100) via the proteasome, but it also regulates IκB kinase (IKK) activation, an important regulatory step in NF-κB regulation, via proteasomal-independent mechanisms (Liu and Chen, 2011; Tam *et al.*, 2012).

NF-κB can be activated by a number of different stimuli which include infection, inflammatory signals: tumour necrosis factor alpha (TNFα), interleukin-1 (IL-1) and lipopolysaccharide (LPS), and also various cellular stresses, including DNA damage (Hayden and Ghosh, 2004) and ER stress. ER-associated NF-κB activation can occur as a result of the oxidative stress from excessive protein folding and/or ER-stress-mediated leakage of calcium, increasing levels of cytosolic calcium (Pahl and Baeuerle, 1996; Tabary *et al.*, 2006; Deniaud *et al.*, 2008). Abnormal NF-κB activation occurs in many pathological conditions such as auto-inflammatory diseases (Iwai, 2012). NF-κB provides an important link between the UPR and the immune system, and any changes in the UPR or ubiquitination may well have significant effects on the immune response.

Immune system and neurodegenerative diseases

Inflammation is an initial protective response of the immune system, carried out by different immune and inflammatory cells, which include T-cells, neutrophils, macrophages etc., to repair, regenerate and remove damaged tissues/cells and harmful stimuli from the body (Kulkarni *et al.*, 2016).

Microglia are the main innate immune cells of the brain, that serve to constantly review the microenvironment. Under physiological conditions, they remain in an 'inactive' state, associated with the production of anti-inflammatory and neurotrophic factors (Streit and Kincaid-Colton, 1995). However, in response to pathogens or tissue damage, they become 'active', thereby promoting an inflammatory response, also known as neuroinflammation (Glass *et al.*, 2010). Neuroinflammation is the initial protective response mechanism of the CNS, carried out by microglia and the inflammatory mediators they release, to restore damaged glial cells and neuronal cells (Shabab *et al.*, 2017). However, sustained or chronic inflammation, can be extremely damaging, resulting in the production of neuroinflammatory and neurotoxic factors, which include activation of MAPKs and NF-κB (Prinz and Priller, 2014; Sofroniew, 2015). Interestingly, a direct inflammatory response has been associated with Alzheimer's disease (AD) for over 20 years (Akiyama, 1994), and subsequent neurodegenerative diseases such as Parkinson's disease (PD), Multiple Sclerosis (MS) and amyotrophic lateral sclerosis (ALS) have documented inflammatory components (Glass *et al.*, 2010). Although inflammation is not usually an initiating factor, sustained inflammatory responses are thought to be a crucial factor in the onset and progression of disease, as well as neuronal cell loss in neurodegenerative disease (Glass *et al.*, 2010; Chen, Zhang and Huang, 2016; Kempuraj *et al.*, 2016).

Ubiquitination has an important role in regulating signal transduction in NF-κB pathways, and the RING E3 ligases and DUBs identified in this study may function as regulators of NF-κB signalling. As such abnormalities in UPR-mediated inflammatory pathways may lead to sustained neuroinflammation in hereditary spastic paraplegias (HSPs), contributing to the onset and progression of disease.

Chapter 6: Identification of novel interaction partners of HSP proteins

6.1 Introduction

HSPs are characterised by progressive lower limb spasticity and pyramidal weakness (Harding, 1983), a defining clinical feature which is thought to be caused by length-dependent axonopathy affecting the distal ends of corticospinal tract axons (Harding, 1983; DeLuca, Ebers and Esiri, 2004), for which gene mutation is a major causative factor. Recent advances in molecular genetics has led to the identification of over 75 HSP disease-loci with over 55 corresponding genes (Klebe, Stevanin and Depienne, 2015; de Souza *et al.*, 2016). The identification of disease-loci/genes implicated in HSPs, has been critical to our understanding of the clinical and pathological features of this group of disorders, as well as improving our understanding of the cellular processes required for axonal maintenance or degeneration (Blackstone, O'Kane and Reid, 2011).

We hypothesize that, proteins that interact with known disease-causing HSP proteins, could in some cases also acquire mutations, which may contribute to specific HSP-related phenotypes. It is therefore important to generate high-density protein-protein interaction (PPI) data of human HSP-related proteins, as identification of proteins that interact with known HSP proteins or exist in common molecular complexes may provide detailed insight into the molecular mechanisms that are fundamental to the pathogenesis of this group of disorders.

The main aim of the work presented in this section was to identify novel interaction partners of HSP proteins by performing systematic unbiased cDNA library screens. This chapter describes the various Y2H library screens performed, with a particular focus on the membrane yeast two-hybrid (MYTH) system, which was optimised and used to screen integral membrane HSP proteins. All data generated was compared to all PPI data available in public databases to assess the confidence of each of the Y2H systems employed, as well as the reproducibility of any previously observed interactions. The resulting data was then incorporated, with additional data gathered

throughout this study, to generate an updated HSPome which can be used for bioinformatics analyses to predict areas of interest and functional relevance, as well as for future hypothesis-driven research.

6.2 Matchmaker ® Yeast two-Hybrid library screens

6.2.1 Matchmaker® yeast two-hybrid system

In this study, the *GAL4*-based Y2H system was employed, using the PJ69-4A (MATa) and the switched mating-type PJ69-4α (MATα) host strains (James, Halladay and Craig, 1996; Semple *et al.*, 2005) for pGBAE-B bait and pACT2 prey K562 cDNA library transfection, respectively. The K-562 cDNA library is derived from the human K562 chronic myelogenous leukaemia (CML) cell-line (Lozzio and Lozzio, 1975). As previously described, the host strain carries three independent *GAL4*-responsive reporter genes: *HIS3, ADE2* and *lacZ,* each driven by a different promoter (*GAL1, GAL2* and *GAL7,* respectively), and all three reporter genes can be assayed in parallel, increasing the stringency of Y2H screens (James, Halladay and Craig, 1996; Brückner *et al.*, 2009). To increase confidence of the interactions identified in the Y2H screens performed, all library hits were re-confirmed by performing an *in vivo* recombination (gap repair) of prey library hits into the frame-shift prey vector pACTBE-B, followed by a reconfirmation mating with the original and a negative control bait clone. The reconfirmation 'gap repair' facilitates the removal of false positive, non-specific background colonies, through a red/white selection protocol (Semple *et al.*, 2005). The reconfirmation mating allows the confirmation of genuine positive clones, whilst allowing the removal of any auto-activating or non-specific prey clones.

6.2.2 The HSP bait collection used in this study

To identify novel HSP interaction partners, a set of HSP Y2H bait constructs had to be generated and individually screened against the K-562 cDNA prey library containing a random collection of ORFs and ORF fragments. In total, 34 HSP ORFs were sub-cloned into the pGBAE-B (bait) Y2H vector, resulting in 33 HSP Y2H bait clones (see Chapter 4, section 4.2.2).

6.2.3 Matchmaker® Y2H library screen reveals 51 potentially novel HSP interactors

A schematic depiction of the Matchmaker® Y2H library screening methodology used to identify novel interaction partners of HSP proteins, is shown in Figure 6.1. In Brief, MATa haploid yeast cells transfected with a HSP bait construct were mated against the K-562 cDNA prey library, pre-transformed into MATα haploid yeast cells, on a rich medium (YPAD) agar plate and incubated for 6 hours. The mated yeast suspension was then plated onto SD-WLA agar plates and left to grow for up to 14 days, to select for positive diploid colonies. To increase confidence of the interactions identified from these library screens, all prey library hits identified were re-confirmed. The library prey inserts were amplified from diploid colonies and cloned into the frame-shift pACTBE-B prey vector for reconfirmation mating with the original or negative control (empty vector) bait. Only those that selectively activate all three reporters (*ADE2, HIS3, lacZ*) with the original bait and not the negative control bait, were selected for DNA sequencing to identify the encoded prey proteins.

In total, 9 HSP bait clones were successfully screened against the K-562 cDNA prey library (Clontech), identifying a total of 51 potentially novel HSP interactors. The identification of a previously known interaction provides confidence in the other novel interactors identified. The successfully reconfirmed interaction partners identified in each individual library screen, are presented in Table 6.1. The function and subcellular localisation was manually curated from the literature a well as web sources such as UniProt, which provided functional context to partner interactions.

The interaction between CCT5 and TCP1, was previously identified by affinity capture-MS techniques and as such was annotated as a non-direct interaction (Gingras *et al.*, 2005). However, following identification in the Matchmaker® Y2H library screens, this interaction can now be annotated as a binary or direct interaction.

Figure 6.1

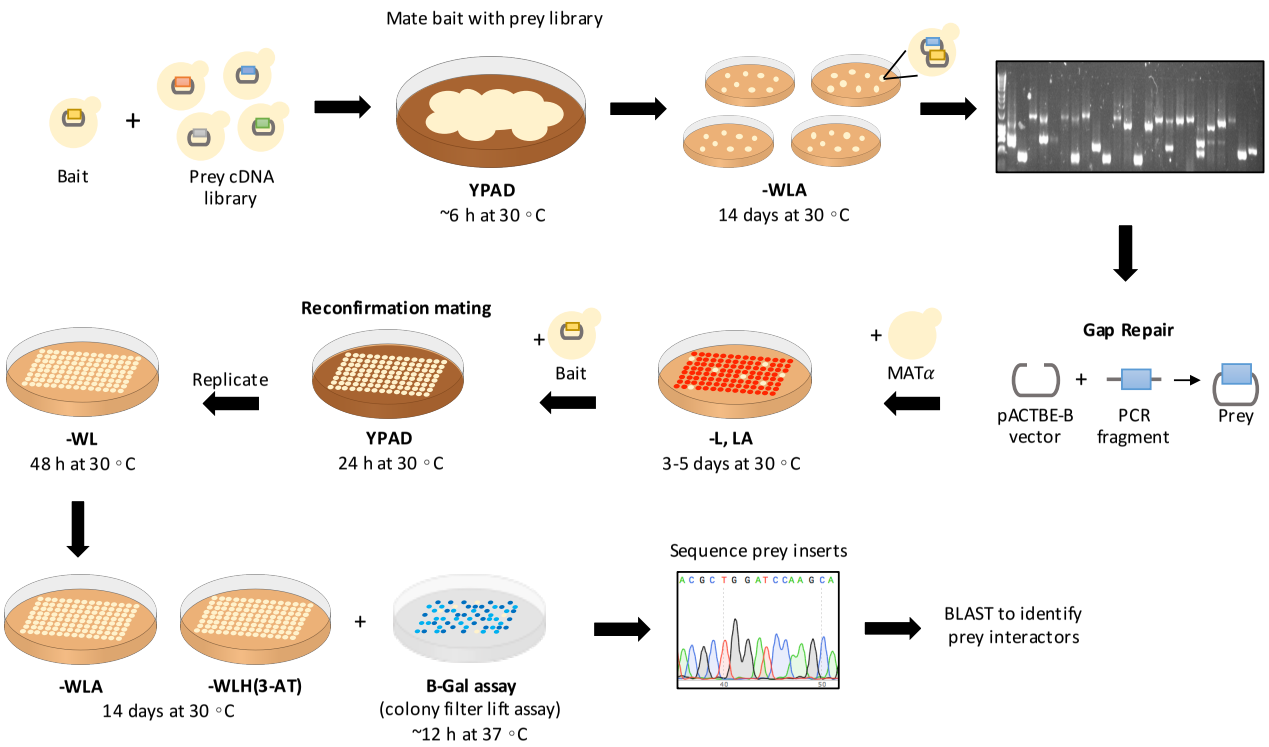

Figure 6.1. Schematic representation of 'traditional' Matchmaker® yeast two-hybrid library screening. pGBAE-B bait construct was mated against the K-562 prey cDNA library on YPAD rich media for 6 h, before plating onto triple selection plates (SD-WLA) for 14 days. Up to 2 x 96 diploid colonies were selected for amplification of prey insert by YC-PCR and subsequent gap repair cloning into linearised pACTBE-B vector. Red colonies (prey clones) were picked and re-mated with the original bait (positive control) or LSM2 bait (negative control), on YPAD media. Diploid yeast were selected on SD-WL medium, before replication onto higher stringency interaction selection plates (SD-WLA/-WLH(3-AT)) or filter paper for β-Galactosidase (β-Gal) assay. Only yeast clones that selectively activate all three reporters (*ADE2, HIS3* and *lacZ*) with the original and not the negative control bait, were selected for DNA sequencing and prey identification via NCBI BLASTN.

Table 6.1

SPG2/ PLP1	This is the major myelin protein from the central nervous system. It plays an important role in myelin formation and maintenance.	Plasma membrane

Gene	Protein Name (UniProt)	Function	Localisation (UniProt)
APLP2	Amyloid-like protein 2	Member of the Amyloid Precursor Protein (APP) family. Works with APP in roles such as neuromuscular transmission, spatial learning and synaptic plasticity	Membrane, Nucleus
CD63	CD63 antigen	Cell surface glycoprotein known to complex with integrins, and is involved in various cellular signalling cascades	-
CD81	CD81 antigen	Cell surface glycoprotein known to complex with integrins, may be involved in signal transduction	Extracellular, Plasma membrane
DCTN2	Dynactin subunit 2	Involved in a number of cellular functions, including axonogenesis, ER-to-Golgi transport and the movement of lysosomes and endosomes	Cytoplasm, Membrane
DDA1	DET1- and DDB1-associated protein 1	May be involved in the ubiquitination and proteasomal degradation of target proteins	
MCM2	DNA replication licensing factor MCM2	Component of the mini-chromosome maintenance (MCM) complex, which is involved in the initiation of eukaryotic genome replication	
RNF5	E3 ubiquitin-protein ligase RNF5	ER membrane-bound ubiquitin ligase. Regulates antiviral response and cell motility.	

SPG12/ RTN2	Required for proper generation of tubular ER. May be involved in intracellular vesicular transport.	ER

Gene	Protein Name (UniProt)	Function	Localisation (UniProt)
DCTN2	Dynactin subunit 2	Involved in a number of cellular functions, including axonogenesis, ER-to-Golgi transport and the movement of lysosomes and endosomes	Cytoplasm, Membrane
ELF1	ETS-related transcription factor Elf-1	Regulates transcription for various genes, acting as enhancer and repressor. Involved in T-cell-receptor-mediated activation of HIV-2 gene expression	Nucleus

SPG21	May act as a negative regulatory factor in CD4-dependent T-cell activation	Cytosol, Golgi app., endosomes

Gene	Protein Name (UniProt)	Function	Localisation (UniProt)
ARIH2	E3 ubiquitin-protein ligase ARIH2	E3 ubiquitin-protein ligase, polyubiquitinating proteins tagging them for degradation	Nucleus, Cytoplasm
C12orf10	UPF0160 protein MYG1, mitochondrial	-	Nucleus, Mitochondrion
C7orf50	Uncharacterized protein C7orf50	-	-
CDV3	Protein CDV3 homolog	-	Cytoplasm
COX6C	Cytochrome c oxidase subunit 6C	Subunit of cytochrome c oxidase, the terminal enzyme of the mitochondrial respiratory chain. May also function in the regulation and assembly of the complex.	Mitochondrion
NOTCH1	Neurogenic locus notch homolog protein 1	Member of the NOTCH family of proteins. Notch signalling is a conserved intracellular signalling pathway regulating interactions between physically adjacent cells.	Cell membrane
LSR	Lipolysis-stimulated lipoprotein receptor	May be involved in the removal of triglyceride-rich lipoprotein from blood	Cell membrane
NLRP2	NACHT, LRR and PYD domains-containing protein 2	Important regulator of immune responses, interacting with components of IKK complex and regulating caspase-1 and NF-kB activity	Cytoplasm
NQO2	Ribosyldihydronicotinamide dehydrogenase [quinone]	Quinone reductase. Mutations have been associated with neurodegenerative diseases	Cytoplasm
PSMD8	26S proteasome non-ATPase regulatory subunit 8	Component of 26S proteasome which participates in numerous cellular processes	Cytosol, Extracellular, Nucleus
RBMX	RNA-binding motif protein, X chromosome	RNA-binding protein involved in the regulation or pre- and post-transcriptional processes	Nucleus
RBMX2	RNA-binding motif protein, X-linked 2	-	-
SDHB	Succinate dehydrogenase [ubiquinone] iron-sulfur subunit, mitochondrial	Subunit of Complex II of the respiratory chain, where it is involved in the oxidation of succinate.	Mitochondrion
SLC26A8	Testis anion transporter 1	DIDS-sensitive anion transporter	Membrane
SPECC1	Cytospin-B	Belongs to cytospin-A family. It's involvement in chromosomal translocation may be a cause of juvenile myelomonocytic leukaemia	Nucleus
SRPX2	Sushi repeat-containing protein SRPX2	May be involved in the development of speech and language centres in the brain. May also be involved in angiogenesis	Cytoplasm
TRIM56	E3 ubiquitin-protein ligase TRIM56	E3 ubiquitin-protein ligase, which plays a key role in innate immunity.	Cytoplasm

Table 6.1. continued

SPG28/ DDHD1	Cytosolic protein, preferentially hydrolyses phosphatidic acid. Some mitochondrial localisation, where it is thought to play a role in the regulation of mitochondrial dynamics.	Cytoplasm, Mitochondrion

Gene	Protein Name (UniProt)	Function	Localisation (UniProt)
C1QBP	Complement component 1 Q subcomponent-binding protein, mitochondrial	Multifunctional and multicompetent protein involved in a number of processes including; apoptosis regulation, ribosome biogenesis and inflammation and infection processes	Mitochondrion, Cell membrane, Nucleus, Cytoplasm
EEF1G	Elongation factor 1-gamma	Subunit of EF-1 complex responsible for enzymatic delivery of aminoacyl tRNAs to the ribosome, may also be involved in anchoring the complex to other cellular components	Cytoplasm, cytosol, Membrane, Nucleus
FLOT2	Flotillin-2	Caveolae-associated membrane protein, which may be involved in neuronal signalling	Cell membrane, Endosome
POLR2G	DNA-directed RNA polymerase II subunit RPB7	Component of RNA polymerase II transcriptional machinery, which synthesises mRNA precursors and non-coding RNAs	Nucleus
PRAME	Melanoma antigen preferentially expressed in tumours	Transcriptional repressor inhibiting retinoic acid signalling	Nucleus, Cell membrane
RPAIN	RPA-interacting protein	Involved in the translocation of RPA, and therefore its function in DNA metabolism	Nucleus, Cytoplasm
RPL7	60S ribosomal protein L7	Component of the 60S ribosomal subunit, has a regulatory role in the translation apparatus	Cytoplasm, Membrane, Nucleus
TAF10	Transcription initiation factor TFIID subunit 10	TFIID is a protein complex involved in the initiation of transcription by RNA polymerase II	Nucleus
TOR3A	Torsin-3A	Novel interferon response gene	Cytoplasm, ER

SPG43/ C19orf12		ER, Mitochondrion

Gene	Protein Name (UniProt)	Function	Localisation (UniProt)
FUS	RNA-binding protein FUS	Component of the hnRNP complex. May be involved in the regulation of gene expression and maintenance of genomic integrity	Nucleus
HNRNPH3	Heterogeneous nuclear ribonucleoprotein H3	Belongs to hnRNP subfamily, and is involved in the splicing process and early heat shock-induced splicing arrest	Nucleus
PLIN3	Perilipin-3	Interacts with mannose 6-phosphate receptors, transporting them from the endosomes to trans-Golgi network (TGN)	Cytoplasm, Endosome, Lipid droplet
RPL7	60S ribosomal protein L7	Component of the 60S ribosomal subunit, has a regulatory role in the translation apparatus	Cytoplasm, Membrane, Nucleus
RUFY2	RUN and FYVE domain-containing protein 2	-	Nucleus

SPG47/ AP4B1	Subunit of adapter-like complex 4, involved in targeting protein from trans-Golgi network (TGN) to endosomal-lysosomal system	Golgi apparatus, Membrane

Gene	Protein Name (UniProt)	Function	Localisation (UniProt)
TK1	Thymidine kinase, cytosolic	Cytosolic enzyme involved in the first step in the biosynthesis of dTTP, component required for DNA replication	Cytoplasm

SPG48/ AP5Z1	Subunit of a adaptor protein complex 5, which may be involved in endosomal transport.	Cytoplasm, Nucleus

Gene	Protein Name (UniProt)	Function	Localisation (UniProt)
COPS5	COP9 signalosome complex subunit 5	Protease subunit of COP9 signalosome complex (CSN) involved in cellular and developmental processes.	Cytoplasm, Cytoplasmic vesicles, Nucleus

SPG55/ C12orf65	Mitochondrial matrix protein, directing the peptide chain termination in the mitochondrial translation machinery.	Mitochondrion

Gene	Protein Name (UniProt)	Function	Localisation (UniProt)
DIAPH1	Protein diaphanous homolog 1	May be involved in regulating actin polymerisation in hair cells of the inner ear	Cytoplasm, Cell membrane
HMGA1	High mobility group protein HMG-I/HMG-Y	Involved in a number of processes including gene transcription regulation	Nucleus
ADGRL1	Adhesion G protein-coupled receptor L1	Member of latrophilin subfamily G-protein coupled receptors (GPCR), involved in cell adhesion and signal transduction	Cell membrane
MRPS18A	39S ribosomal protein S18a, mitochondrial	28S ribosomal subunit protein of the ribosomal protein S18P family	Mitochondrion
NUBP2	Cytosolic Fe-S cluster assembly factor NUBP2	Component of the cytosolic Fe/S protein assembly (CIA) machinery	Nucleus, Cytoplasm
TIMM13	Mitochondrial import inner membrane translocase subunit Tim13	Functions as a chaperone, importing proteins from cytoplasm to the mitochondrial inner membrane	Mitochondrion
TUBA1B	Tubulin alpha-1B chain	Major constituent of microtubules	Cytoplasm

Table 6.1 continued

CCT5	Molecular chaperone involved in the folding of proteins following ATP hydrolysis (including actin and tubulin)	Cytoskeleton, Cytosol, Extracellular, Nucleus

Gene	Protein Name (UniProt)	Function	Localisation (UniProt)
BCCIP	BRCA2 and CDKN1A-interacting protein	May promote cell cycle arrest. May be required for repair following DNA damage.	Nucleus
C12orf10	UPF0160 protein MYG1, mitochondrial	-	Nucleus, Mitochondrion
CCT5	T-complex protein 1 subunit epsilon	Molecular chaperone, involved in the folding of proteins following ATP hydrolysis (Inc. actin and tubulin)	Cytoskeleton, Cytosol, Extracellular, Nucleus
PRPF8	Pre-mRNA-processing-splicing factor 8	Acts as a scaffold in the assembly of spliceosomal proteins and snRNAs	Nucleus
TCP1	T-complex protein 1 subunit alpha	Molecular chaperone, involved in the folding of proteins following ATP hydrolysis (Inc. actin and tubulin)	Cytoplasm

Table 6.1. Matchmaker® K-562 cDNA yeast two-hybrid library screen results. Refined list of potential interaction partners identified from Matchmaker® K-562 Y2H library screens, function and localisation established for each using UniProt and NCBI. Previously identified interactions are highlighted in green (known indirect).

6.2.4 Functional relevance of Matchmaker® Y2H library hits

The interaction data generated from these Matchmaker® K-562 cDNA library screens was analysed to gain a better understanding of the novel interactions identified and their functional relevance.

PLP1(SPG2):

The Y2H library screens identified a total of 7 binary PLP1 (SPG2) interaction partners, all of which were novel. RNF5 was identified as an interactor of PLP1, which interestingly was also identified as a relatively weak PLP1 partner in our targeted RING E3 ligase Y2H matrix screens (Chapter 5).

DCTN2, encodes a subunit of dynactin, a multiprotein complex which works with the cytoplasmic dynein-1 motor (dynein) transporting cargo along the microtubule cytoskeleton (Gill *et al.*, 1991; Urnavicius *et al.*, 2015), and was also identified as an interactor of PLP1. In neurons, dynein is involved in retrograde axonal transport (Hirokawa *et al.*, 1990) and more interestingly, disruption of dynein/dynactin was found to inhibit axonal transport in motor neurons with the onset of progressive motor neuron degeneration (LaMonte *et al.*, 2002). The interaction between PLP1 and RTN2 was also recently identified through affinity capture-MS (Huttlin *et al.*, 2017), and interestingly we identified DCTN2 as a novel binary interactor for both PLP1 (SPG2) and RTN2 (SPG12). Therefore, the identification of a common interactor demonstrates a potential cellular function/pathway in which these proteins might act.

SPG21:

The Y2H library screens identified in total 17 binary SPG21 interaction partners, all of which were novel. ARIH2, an E3 ubiquitin ligase protein, was identified as an interactor of SPG21 and interestingly, it was also previously identified as a weak interactor of SPG21 following the targeted RING E3 ligase Y2H matrix screens but was not annotated as a positive hit at the time, as it was only observed once. Reconfirmation of this interaction would indicate that this is a true positive interaction.

NQO2, also known as quinone reductase 2 (QR2), is another SPG21 interaction partner. It is a cytosolic flavoenzyme which catalyses substrate-specific reduction and enhances the production of damaging activated quinone and reactive oxygen species (ROS) (Benoit *et al.*, 2010). NQO2 expression was observed ubiquitously in brain and is particularly enriched in the neurons of the hippocampus and cortex (Hashimoto and Nakai, 2011). High levels of ROS are associated with age-related learning and memory deficits, as well as in Alzheimer's disease (Serrano and Klann, 2004; Benoit *et al.*, 2010). Moreover, significantly higher levels of NQO2 were identified in the hippocampus of Alzheimer's disease patients compared to control (Hashimoto and Nakai, 2011), whilst NQO2 knock-out mice, demonstrated enhanced cognitive behaviour (Benoit *et al.*, 2010).

NLRP2, is a cytoplasmic protein which inhibits NF-κB activation (Bruey *et al.*, 2004), it was more recently shown to associate with ASC and caspase-1, forming a functional inflammasome, in human astrocytes. Inflammasomes are essential for the activation of caspase-1 and the production of pro-inflammatory cytokines, following CNS injury. The NLRP2 inflammasome is now recognised as an important component of the CNS inflammatory response (Minkiewicz, de Rivero Vaccari and Keane, 2013).

Another SPG21 interaction partner, TRIM56, regulates innate immune responses by associating with and promoting the ubiquitination of STING (stimulator of interferon genes), an ER transmembrane protein that functions as an innate immune signalling adaptor, enhancing cytosolic dsDNA-induced IFN production (Shen *et al.*, 2012).

<u>C19orf12 (SPG43):</u>

Y2H library screens identified 5 binary C19orf12 (SPG43) interaction partners, all of which were novel. Perilipin-3 (PLIN3) was identified as an interactor of C19orf12, following successful library screening. PLIN3 is required for mannose-6-phosphate receptor (MPR) transport from endosomes to the *trans*-Golgi network (TGN) (Díaz and Pfeffer, 1998). We previously identified SPG20, an endosome-associated, multifunctional protein known to be involved in regulating endosomal trafficking (Renvoisé and Blackstone, 2010), as an C19orf12 (SPG43) interaction partner in our

targeted HSP:HSP Y2H matrix screens (Chapter 4). As very little is known about the function of C19orf12, it is interesting that these findings demonstrate a potential role for C19orf12 in endosomal trafficking, providing further evidence to support the idea that defects in intracellular trafficking events are potentially significant in the pathogenesis of neurodegenerative diseases such as HSP.

The RNA-binding protein FUS (FUsed in Sarcoma), was also identified as an interactor of C19orf12. Interestingly, mutations in the FUS protein are known to be either causative or risk factors for several neurodegenerative diseases, including amyotrophic lateral sclerosis (ALS), frontotemporal dementia (FTD) and essential tremor (Vance *et al.*, 2009; Chen *et al.*, 2011; Merner *et al.*, 2012). Abnormal FUS protein aggregates may also suggest a potentially important role for FUS in neurodegenerative diseases (Deng, Gao and Jankovic, 2014).

Unfortunately, many of the 33 Y2H HSP bait constructs used in this study were unsuccessful in the Matchmaker® Y2H library screens and did not yield any true-positive prey interactions when screened against the prey K-562 cDNA library. There are a couple of factors that may contribute to the high failure rate, which need to be considered. First, the yeast cell viability of the prey library aliquots may have decreased over time, affecting library screening quality. Second, there are several HSPs that are known to have transmembrane domains (see Chapter 3) and because of their hydrophobic nature, this can often prove to be problematic for use in 'traditional' Y2H systems.

Given all of the above, a new commercial pre-transformed Matchmaker® Gold Y2H library system was bought and optimised for use with HSP proteins which do not have transmembrane domains. Additionally, the membrane yeast two-hybrid (MYTH) (provided by Dr Igor Stagljar, University of Toronto, Canada) was set-up and optimised for use with HSP proteins that encode one or more transmembrane domain.

6.3 Matchmaker® Gold Yeast two-Hybrid

6.3.1 Matchmaker® Gold yeast two-hybrid system

Again, the *GAL4* Y2H system was employed, such that the bait protein was expressed as a fusion to the *GAL4* DNA-binding domain (BD) using the DNA-BD cloning vector, pGBKT7, whilst the library of prey proteins were expressed as fusions to the *GAL4* activation domain (AD) using the AD cloning vector, pGADT7 (Fields and Song, 1989; Chien *et al.*, 1991). When the bait and library prey proteins interact, the DNA-BD and AD are brought into close proximity to each other, which in the Matchmaker® Gold Y2H system, results in the transcription of four independent reporter genes (*HIS3, ADE2*, *MEL1* and *AUR1-C*).

In this study, the Y2HGold and Y187 host strains, were used for bait and prey library transfection, respectively. The Y187 library host strain carries two reporter genes: *lacZ* and *MEL1*, each driven by a different promoter (*GAL1* and *MEL1*, respectively). Whilst the Y2HGold host strain, a derivative of PJ69-2A (James, Halladay and Craig, 1996), carries four reporter genes: *HIS3, ADE2* and *MEL1/AUR1-C,* under the control of three distinct *GAL4*-responsive promoter elements (*GAL1, GAL2* and *MEL1* respectively).

MEL1 encodes the enzyme, α-galactosidase (α-Gal), which is required for the hydrolysis of the terminal alpha-galactosyl moiety of melibiose into glucose and galactose (Buckholz and Adams, 1981; Liljeström, 1985). Yeast colonies can be assayed for *MEL1* activity (α-Gal assay), without the need to lyse cells, using the chromogenic substrate, X-α-Gal (5-bromo-4-chloro-3-indolyl-α-D-galactopyranoside) (Aho *et al.*, 1997). X-α-Gal can be detected with significantly higher sensitivity than β-Gal (Lazo, Ochoa and Gascón, 1978). Secretion of the α-galactosidase, in response to *GAL4* activation, leads to the hydrolysis of X-α-Gal to yield a blue precipitate, and so interaction detection and strength can be easily assessed. The Y2HGold yeast strain is unable to synthesise histidine or adenine and is therefore unable to grow on media lacking these essential amino acids. Upon

protein-protein interaction, reporter genes are activated resulting in growth of yeast on selective media and blue colour development in the α-Gal assay.

AUR1, on the other hand, encodes the essential yeast enzyme, inositol phosphoryl ceramide synthase, which can be inhibited be Aureobasidin A (AbA), a potent yeast antibiotic known to kill *S. cerevisiae* at low concentrations (Takesako *et al.*, 1993). The dominant mutant *AUR1-C*, encodes a mutant enzyme which confers resistance to AbA (Hashida-Okado *et al.*, 1996), which can be used as an effective selectable yeast marker. Reporter activation allows yeast to grow on media supplemented with AbA, with extremely low background as AbA kills sensitive cells as opposed to slowing growth, and so AbA-based selection favours the growth of genuinely positive interactions.

The protein-binding sites within the three promoters are different, except for the short protein binding sites in the upstream activation sequence (UAS), which are recognised and specifically bound by the *GAL4* BD (Giniger, Varnum and Ptashne, 1985; Giniger and Ptashne, 1988). All four reporter genes, each under the control of different promoters, can be assayed in parallel and the high stringency screening protocols of the Matchmaker® Gold Y2H system is designed to decrease the incidence of false positives. In addition, to increase confidence of the interactions identified in the Matchmaker® Gold Y2H screens, all library hits were also re-confirmed by performing an *in vivo* recombination (gap repair) of prey library hits back into the pGADT7 prey vector, followed by a reconfirmation mating with the original bait clone and a negative control (empty pGBKT7). This reconfirmation 'gap repair' facilitates the removal of non-specific background colonies. In addition, reconfirmation mating allows the confirmation of genuine positive clones, whilst removing auto-activating/ non-specific prey (false positive) clones.

6.3.2 Generation of HSP Matchmaker® Gold Y2H bait constructs

To identify additional novel HSP interaction partners, a set of HSP Matchmaker® Gold Y2H bait constructs had to be generated and individually screened against the

Matchmaker® Gold human brain cDNA prey library. Due to time constraints, we prioritised those HSP proteins known to be involved in intracellular transport and degradation processes.

As described in Chapter 3, the cloning efforts ultimately resulted in the generation of a Gateway® entry clone library representing 30 human HSPs, from which HSPs involved in intracellular trafficking processes were prioritised resulting in the selection of 16 HSP ORFs. The HSP ORFs were cloned in-frame with the *GAL4* DNA-binding domain of the pGBKT7 bait vector, followed by transformation into the Y2H Gold yeast strain (Chapter 2, section 2.3.2). The pGBKT7 vector contains the *TRP1* gene under the control of the modified ALDH1 promoter, which allows moderate expression and stringent selection of the N-terminal tagged *GAL4*-fusion bait proteins on synthetic defined agar plates lacking tryptone (SD-W). It should be noted that fragmented domains of SPG8 (WASHC5) were also cloned into the pGBKT7 Y2H bait expression vector. HSP pGBKT7 bait constructs which showed signs of auto-activation or toxicity in yeast were removed, resulting in 9 HSP pGBKT7 bait clones representing 8 human HSPs: full-length and spectrin domain of SPG8 (WASHC5 and WASHC5-SD), SPG18 (ERLIN2), SPG20, SPG21, SPG52 (AP4S1), SPG57 (TFG), SPG59 (USP8) and CCT5.

6.3.3 Matchmaker® Gold Y2H library screen reveals 34 potentially novel HSP interactors

An outline of the Matchmaker® Gold Y2H library screen methodology used is described in Figure 6.2. In brief, Y2HGold yeast cells transfected with a HSP bait construct was mated against Y187 yeast cells transfected with the Matchmaker® Gold human brain cDNA library, on a rich medium (YPAD) agar plate. Following a 5-hour incubation, mated yeast were plated onto low stringency (SD-WL/AbA) plates and left to grow for 3-5 days to select for positive diploid colonies. These colonies were then transferred onto higher stringency (SD-WLAH/X-α-Gal/AbA) plates and left to grow for up to 14 days. To increase confidence of the interactions identified from these screens, all prey library hits were re-confirmed. The library prey inserts

were amplified from diploid colonies and cloned back into the pGADT7 prey vector for reconfirmation mating with the original or negative control (empty vector) bait. Only those that selectively activate all four reporters (*ADE2, HIS3, MEL1* and *AUR1-C*) with the original and not the negative control bait were selected for DNA sequencing.

Unfortunately, 6 HSP pGBKT7 bait clones were unsuccessful in the Matchmaker® Gold Y2H library screens and did not yield any true-positive prey interactions when screened against the human brain cDNA library. In total, 3 HSP pGBKT7 bait clones were successfully screened against the Matchmaker® Gold human brain cDNA prey library (Clontech), identifying a total of 34 potentially novel HSP interactors. The successfully reconfirmed interaction partners identified in each individual library screen and are presented in Table 6.2. The function and subcellular localisation was manually curated from literature and web sources such as UniProt, again to provide functional context to partner interactions.

AKIRIN2 and TCF4 are both known binary interactors of SPG21 (Rual *et al.*, 2005; Rolland *et al.*, 2014), whilst TFG (SPG57) and CEP126 are both known binary interactors of TFG (Stelzl *et al.*, 2005), and all of these were also identified in the Matchmaker® Gold Y2H library screens. The identification of previously known interactions provides confidence in other novel binary/direct interactors identified in these screens. Moreover, the interactions between SPG21 and PSMD8, as well as CCT5 and CCT5, were both previously identified as novel binary interactions in the Matchmaker® K-562 cDNA library (Figure 6.3). The identification of interactions previously identified in other Y2H screens, provides additional confidence in the overall data generated from the Y2H library screens.

Figure 6.2

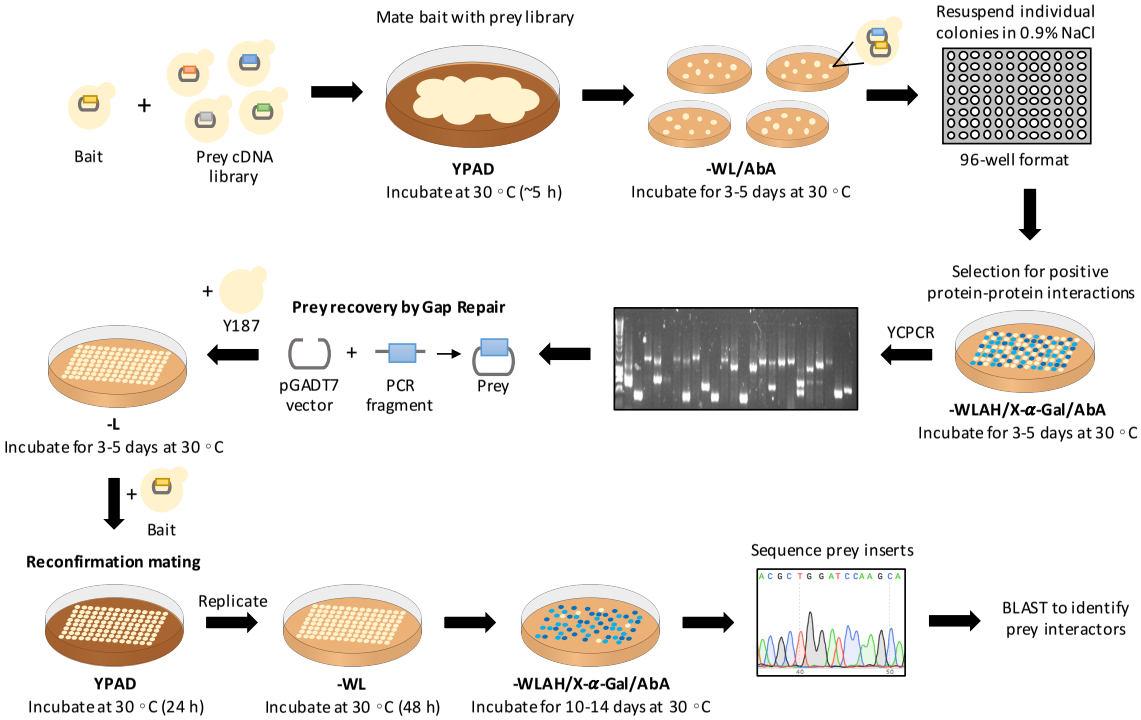

Figure 6.2. Schematic representation of Matchmaker® Gold yeast two-hybrid library screening. Y2HGold yeast transfected with a pGBKT7 bait was mated against the prey cDNA library on YPAD rich media, before being plated onto lower stringency interaction selection media (SD-WL/AbA) for 3-5 days. Positive protein-protein interactions were further analysed by selection on higher stringency (SD-WLAH/X-α-Gal/AbA) plates. Prey inserts were amplified from positive clones by YC-PCR following prey regenerated by gap repair, in Y187 yeast. Successfully regenerated prey clones were re-mated with the original bait (positive control) or empty bait vector (negative control), on YPAD media. Diploid yeast were selected on SD-WL plates, before replication onto higher stringency interaction selection plates (SD-WLAH/X-α-Gal/AbA). Yeast clones that activated all four reporters (*ADE2, HIS3, MEL1* and *AUR1-C*) with the original bait and not negative control, were selected for DNA sequencing and prey identification via NCBI BLASTN.

Table 6.2

SPG21	May act as a negative regulatory factor in CD4-dependent T-cell activation	Cytosol, Golgi app., endosomes

Gene	Protein Name (UniProt)	Function	Localisation (UniProt)
AKIRIN2	Akirin-2	Important for the innate immune response	Nucleus
ATP5O	ATP synthase subunit O, mitochindrial	Mitochondrial F-type ATP synthase, may be involved in transmission of conformational changes or proton conductance	Extracellular, Mitochondrion, Nucleus, Plasma membrane
COG1	Conserved oligomeric Golgi complex subunit 1	Component of the Golgi-localized complex (COG) involved in membrane trafficking. It is also required for normal Golgi morphology and function	Golgi app.
COQ3	Ubiquinone biosynthesis O-methyltransferase, mitochondrial	Catalyzes the 2 O-methylation steps in the ubiquinone (coenzyme Q) biosynthetic pathway	Mitochondrion
ERCC3	TFIIH basal transcription factor complex helicase XPB subunit	ATP-dependent DNA helicase involved in nucleotide excision repair (NER) of DNA	Nucleus
FAM104B	Protein FAM104B	-	Nucleus
GPM6B	Neuronal membrane glycoprotein M6-b	Proteolipid protein thought to be involved in membrane trafficking and cell-to-cell communication	Plasma membrane
LDHB	L-lactate dehydrogenase B chain	Catalyzes the interconversion of pyruvate and lactate whilst simultaneously catalysing the interconversion of NADH and NAD+ in a post-glycolysis process	Cytosol, Extracellular, Mitochondrion
MAGT1	Magnesium transporter protein 1	Associates with N-oligosaccharyl transferase and may therefore be involved in N-glycosylation	Plasma membrane, ER
PSMD8	26S proteasome non-ATPase regulatory subunit 8	Component of 26S proteasome which partcipates in numerous cellular processes	Cytosol, Extracellular, Nucleus
PUM1	Pumilio homolog 1	RNA-binding protein involved in various post-transcriptional processes	Cytosol
TCF4	Transcription factor 4	Involved in the initiation of neuronal differentiation and may play a role in the nervous system development	Nucleus

SPG57/ TFG	Plays a role in the normal function of the endoplasmic reticulum (ER) and its associated microtubules. May play a role in the NF-κB pathway	Cytosol, Golgi apparatus, Extracellular

Gene	Protein Name (UniProt)	Function	Localisation (UniProt)
ABCG2	ATP binding cassette sub-family G member 2	A membrane-associated ATP-binding cassette (ABC) transport protein	Nucleus, Plasma membrane
ANKRD36	Ankyrin repeat domain-containing protein 36A	-	Nucleus
ATL1	Atlastin 1	GTPase and Golgi body transmembrane protein. Functions in ER tubular network biogenesis, may also regulate Golgi biogenesis and axonal development	ER, Golgi apparatus
CEP126	Centrosomal protein of 126kDa	Participates in cytokinesis. Necessary for microtubules and mitotic spindle organization Involved in primary cilium formation	Cytoplasm, Cytoskeleton, Centrosome
FAM13A	Protein FAM13A	May be involved in GPCR and Rho GTPase signalling pathways	Cytosol
FAM13B	Protein FAM13AB	May be involved in GPCR and Rho GTPase signalling pathways	Cytosol
GLMN	Glomulin	Essential for normal development of the vasculature. May function as a membrane anchoring protein	Cytosol
HHLA3	HERV-H LTR-Associating 3	-	Nucleus
HNRNPC	Heterogeneous Nuclear Ribonucleoprotein C1/C2	Binds to pre-mRNAs and is involved in the assembly of 40S hnRNP particles	Cytosol, Extracellular, Nucleus
KIAA1755	uncharacterised protein KIAA1755	-	
NAP1L2	Nucleosome Assembly Protein 1 -Like 2	Nucleosome Assembly Protein (NAP) member which interacts with chomatin to regulate neuronal cell proliferation	Nucleus
PARG	Poly(ADP-Ribose) Glycohydrolase	Major enzyme responsible for the catabolism of poly(ADP-ribose), a reversible covalent-modifier of chromosomal proteins	Mitochondrion, Nucleus
POLR2C	DNA-directed RNA Polymerase II Subunit RPB3	Synthesizes mRNA precursors and many functional non-coding RNAs	Cytoskeleton, Nucelus
RPL27A	60S Ribosomal Protein L27a	A component of the 60S ribosomal subunit	Cytosol
RSL24D1	Probable ribosome biogenesis protein RLP24	Involved in the biogenesis of the 60S ribosomal subunit	Cytosol, Nucleus
SNRPG	Small Nuclear Ribonucleoprotein G.	Component of the spliceosomal U1,2,4 and 5 snRNPs - playing a role in the splicing of cellular pre-mRNAs	Cytosol, Nucleus
TANK	TRAF family member Associated NF-κB activator	Adapter protein involved in I-kappa-B-kinase (IKK) regulation-role in innate immunity. Negatively regulates NF-κB signaling and cell survival after DNA damage	Cytosol
TFG	Protein TFG	Plays a role in the normal function of the ER and its associated microtubules, may be involved in the NF-κB pathway	Cytosol, Golgi apparatus, Extracellular
SNX6	Sorting Nexin 6.	Soritng nexin family member involved in several stages of intracellular trafficking, including endosome-to-trans-Golgi-network retrograde transport	Endosome
USO1	General vesiclar transport factor p115	Peripheral membrane protein required for intercisternal transport in the Golgi, transcytotic fusion and/or binding of vesicle to target membrane	Cytosol, Golgi apparatus, Nucleus
YBX1	Nuclease-sensitive element-binding protein 1	Functions as both a DNA and RNA binding protein and has been implicated in numerous cellular processes including regulation of transcription and translation	Extracellular, Nucleus
ZNF251	Zinc finger protein 251	May be involved in transcriptional regulation	Nucleus

Table 6.2 continued

CCT5	Molecular chaperone involved in the folding of proteins following ATP hydrolysis (including actin and tubulin)		Cytoskeleton, Cytosol, Extracellular, Nucleus

Gene	Protein Name (UniProt)	Function	Localisation (UniProt)
COMMD7	COMM domain-containing 7	May modulate the activity of cullin-RING E3 ubiquitin ligase (CRL) complexes. Associates with NF-κB complex to suppress its transcriptional activity	Extracellular
CDK5RAP2	CDK5 regulatory subunit-associated Protein 2	Localizes to the centrosome and Golgi complex, plays a role in centriole engagement and microtubule nucleation	Cytoskeleton, Cytosol, Extracellular, Golgi app.
RBMX	RNA-binding motif protein, X chromosome	RNA-binding protein that has several roles in the regulation of pre- and post-transcriptional processes	Extracellular
CCT5	T-complex protein 1 subunit epsilon	Molecular chaperone, involved in the folding of proteins following ATP hydrolysis (inc actin and tubulin)	Cytoskeleton, Cytosol, Extracellular, Nucleus
PUM1	Pumilio homolog 1	RNA binding protein involved in various post-transcriptional processes	Cytosol

Table 6.2. Matchmaker® Gold human brain cDNA yeast two-hybrid library screen results. Refined list of potential interaction partners identified from Matchmaker® Gold Y2H library screens. Previously identified binary interactions (known direct), are highlighted in orange.

Figure 6.3

A Matchmaker® K-562

pGBAE-B (bait)	Library hits (prey)
	ADGRL1 APLP2 ARIH2 BCCIP C12orf10 C1QBP C7orf50 CCT5 CD63 CD81 CDV3 COPS5 COX6C DCTN2 DDA1 DIAPH1 EEF1G ELF1 FLOT2 FUS HMGA1 HNRNPH3 LSR MCM2 MRPS18A NLRP2 NOTCH1 NQO2 NUBP2 PLIN3 POLR2G PRAME PRPF8 PSMD8 RBMX RBMX2 RNF5 RPAIN RPL7 RUFY2 SDHB SLC26A8 SPECC1 SRPX2 TAF10 TCP1 TIMM13 TK1 TOR3A TRIM56 TUBA1B
SPG2/ PLP1	APLP2, DCTN2, DDA1, MCM2, RNF5
SPG12/ RTN2	DCTN2, EEF1G
SPG21	ARIH2, C12orf10, C7orf50, COPS5, MRPS18A, NLRP2, NOTCH1, NQO2, PSMD8, RBMX, RBMX2, SDHB, SLC26A8, SPECC1, SRPX2, TRIM56
SPG28/ DDHD1	C1QBP, EEF1G, ELF1, FLOT2, NUBP2, PLIN3, POLR2G, RPL7, RUFY2, TCP1, TOR3A
SPG43/ C19orf12	FUS, HMGA1, PLIN3, RPL7, RUFY2
SPG47/ AP4B1	TIMM13
SPG48/ AP5Z1	COPS5
SPG55/ C12orf65	ADGRL1, FUS, MRPS18A, NUBP2, TIMM13, TRIM56
CCT5	BCCIP, C12orf10, CCT5, PRPF8, TCP1

B Matchmaker® Gold Human brain

pGBKT7 (bait)	Library hits (prey)
	ABCG2 AKIRIN2 ANKRD36 ATL1 ATP5O CCT5 CDK5RAP2 CEP126 COG1 COMMD7 COQ3 ERCC3 FAM104B FAM13A FAM13B GLMN GPM6B HHLA3 HNRNPC KIAA1755 LDHB MAGT1 NAP1L2 PARG POLR2C PSMD8 PUM1 PUM1 RBMX RPL27A RSL24D1 SNRPG SNX6 TANK TCF4 TFG USO1 YBX1 ZNF251
SPG21	AKIRIN2, CEP126, TCF4
SPG57/ TFG	ABCG2, ANKRD36, ATL1, CDK5RAP2, CEP126, GLMN, HHLA3, HNRNPC, KIAA1755, LDHB, MAGT1, NAP1L2, PARG, POLR2C, PSMD8, RBMX, RPL27A, RSL24D1, SNRPG, SNX6, TANK, TFG, USO1, YBX1, ZNF251
CCT5	CCT5, COG1, COMMD7, COQ3, PUM1, PUM1

Known Direct

Known Indirect

C

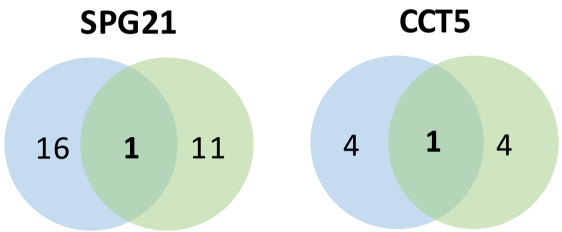

Figure 6.3. Traditional yeast two-hybrid library screen results summary comparison. (A) Table showing refined list of potential interaction partners identified from Matchmaker® Y2H library screens. pGBAE-B bait HSPs (horizontal) and pACTBE-B prey library hits (vertical) are ordered alphabetically. **(**B) Table showing refined list of potential interaction partners identified from Matchmaker® Gold Y2H library screens. pGBKT7 bait HSPs (horizontal) and pGADT7 prey library hits (vertical) are ordered alphabetically. The overlap of the proteins identified as potential interaction partners for SPG21 and CCT5 in each corresponding library screen are shown in (C), colours match accordingly. Previously identified (known) interactions, are annotated as such in the tables above.

6.3.4 Functional relevance of Matchmaker® Gold Y2H library hits

The interaction data generated from these Matchmaker® Gold human brain cDNA library screens was analysed to gain a better understanding of the novel interactions identified and their functional relevance.

SPG21:

The Y2H library screens identified 12 binary SPG21 interaction partners, 10 of which were found to be novel SPG21 interactors. An overview of 6, particularly interesting interactors, are given here.

As already mentioned, AKIRIN2 and TCF4 are both known binary interactors of SPG21 identified in previous screens as well as our own. AKIRIN2 is an evolutionary conserved nuclear protein, which stimulates pro-inflammatory gene transcription during innate immune responses to viral or bacterial infection in mouse macrophages (Tartey *et al.*, 2014). TCF4, often referred to as immunoglobulin transcription factor 2 (ITF2) is known to have an important role in various developmental processes, including regulation of gene expression during neurodevelopment (Forrest *et al.*, 2014). This is particularly interesting given the association of human *TCF4* variants with a range of common diseases including, schizophrenia and intellectual disability (Stefansson *et al.*, 2009; Hamdan *et al.*, 2014).

GPM6B is a transmembrane glycoprotein that belongs to the proteolipid family, described as the structural proteins of the CNS myelin. Other members of this family include GPM6A and PLP1 (SPG2), both also major structural components of the myelin sheath (Mikoshiba *et al.*, 1991). As GPM6B and PLP1 share a high degree of protein sequence similarity (Yan, Lagenaur and Narayanan, 1993), GPM6B may be a potential HSP candidate gene.

COG1, a component of the multi-subunit membrane protein Conserved Oligomeric Golgi (COG) complex, which has an important role in Golgi-associated membrane trafficking and glycol-conjugate synthesis (Oka *et al.*, 2005; Vasile *et al.*, 2006). COG

appears to be involved in retrograde vesicular transport, and it has multiple features associated with maintaining Golgi structure and function (Ungar *et al.*, 2006).

MAGT1 is a magnesium-specific transporter located in the plasma membrane, which is ubiquitously expressed. MAGT1 loss or deficiency leads to the absence of a T cell antigen receptor (TCR)-stimulated Mg^{2+} flux and attenuation of T cell activation which was found to result in a novel primary immunodeficiency, XMEN disease (Li *et al.*, 2014).

TFG (SPG57):

The Y2H library screens identified 22 binary TFG interaction partners, 20 of which were found to be novel TFG interactors. A brief overview of 6, particularly interesting interactors, are given here.

As already mentioned, TFG and CEP126 are both known binary interactors of TFG, which were also identified in this study. TFG is thought to self-associate to form hexamers facilitating its role as a regulator of protein secretion from the ER (Witte *et al.*, 2011), therefore identification of the known TFG-TFG interaction gives added confidence in the novel interactors identified. CEP126 is thought to be involved in regulating pericentriolar-satellite transport to the centrosome, where it appears to indirectly regulate the microtubule anchoring to the centrosome through its interaction with dynactin $p150^{Glued}$, affecting other crucial cellular functions. It is therefore important in regulating centrosome-based functions, and is crucial for correct intracellular organisation (Bonavita *et al.*, 2014).

TANK (TRAF family member-associated NF-κB activator) negatively regulates NF-κB activation by DNA damage by inhibiting TRAF6 ubiquitination (Wang *et al.*, 2015).

SNX6 (sorting nexin 6), a member of the evolutionary conserved family of proteins involved in membrane trafficking and protein sorting. SNX6, now known to be a component of the retromer complex (Wassmer *et al.*, 2006), interacts with dynactin

p150^{Glued} to mediate retrograde transport from endosome-to-trans Golgi network (Hong *et al.*, 2009).

USO1 (vesicle transport factor) is involved in vesicle trafficking and Golgi organisation (Puthenveedu and Linstedt, 2001). Uso1 is an essential ER-to-Golgi tethering factor in yeast vesicular transport (Noda, Yamagishi and Yoda, 2007), as it binds to the ER-derived COPII vesicles budded from the ER (Cao, Ballew and Barlowe, 1998). The packaging of cargo and formation of vesicles at the ER membrane is mediated by the COPII complex (McCaughey *et al.*, 2016), and COPII-dependent export of secretory cargo from the ER is essential for the normal function of all mammalian cells (Zanetti *et al.*, 2011). TFG is also involved as it was previously identified as a Sec16-interacting protein regulating COPII-dependent budding form the ER (Witte *et al.*, 2011), directing the organisation of the very earliest stages of COPII-dependent budding (McCaughey *et al.*, 2016). HSP-associated mutations of TFG, appear to be related to changes in ER architecture (Beetz, Johnson, *et al.*, 2013), which given these results, could arise from defects in vesicular transport and protein secretion (McCaughey *et al.*, 2016).

Interestingly, ATL1 (SPG3) was identified as a novel binary interactor of TFG. ATL1 is one of the most well-characterised HSP genes, regulating ER morphology and network organisation (Park *et al.*, 2010). Interestingly, TFG is also involved in regulating ER morphology (Beetz, Johnson, *et al.*, 2013). TFG may also regulate intracellular protein homeostasis in the ER as it was recently shown to function as an inhibitory regulator of the UPS (Yagi, Ito and Suzuki, 2014). This interaction may therefore provide pathological insight, as we concluded that the pathogenesis of HSP may be associated with the disruption of intracellular protein homeostasis and ER stress.

<u>CCT5:</u>

The Y2H library screens identified in total 5 binary CCT5 interaction partners, all of which were novel. COMMD7, a member of the COpper Metabolism MURR I Domain-Containing (COMMD) family of structurally conserved proteins which appear to have

specific roles in the termination of canonical NF-κB signalling (Bartuzi, Hofker and van de Sluis, 2013). Lacking in catalytic activity, it is suggested that they function as scaffolding proteins, facilitating the assembly of molecular components involved in the control of various biological processes, including NF-κB signalling (Esposito *et al.*, 2016).

6.4 Membrane Yeast two-Hybrid (MYTH) library screens

6.4.1 Membrane yeast two-hybrid (MYTH) system

The traditional yeast two-hybrid system is a powerful tool for *in vivo* analysis of protein-protein interactions (Bartel and Fields, 1995), however this system is more suited to the analysis of soluble proteins or soluble domains of membrane proteins, which means that interactions between integral membrane proteins can be problematic and as such are not well studied (Stagljar *et al.*, 1998). As a result, the split-ubiquitin based membrane yeast two-hybrid (MYTH) system was developed (as described in Chapter 1), which allows the high-throughput identification of interactions between a membrane protein (full-length integral or membrane-associated) and a membrane or soluble protein, in an *in vivo* environment (Stagljar *et al.*, 1998; Fetchko and Stagljar, 2004). Briefly, if there is a direct interaction between a bait and prey proteins, the two fragments of ubiquitin are brought into close proximity, allowing for the spontaneous reconstitution of the 'pseudo-ubiquitin' molecule which can be recognised by the cytosolic proteases, DUBs (Johnsson and Varshavsky, 1994; Stagljar *et al.*, 1998; Snider *et al.*, 2010). As a result, the artificial transcription factor (LexA-VP16) is released from the membrane-bound bait, which allows it to translocate to the nucleus, where it activates reporter gene transcription (e.g. *HIS3, ADE2* and *lacZ*) under the control of promoters containing LexA binding sites (Snider *et al.*, 2010). Reporter genes typically used in the MYTH screen are the same as those used in the 'classical' Y2H system, which include the more commonly used auxotrophic growth markers (e.g. *HIS3,* and *ADE2*) as well as the *lacZ* gene, allowing interactions to be specifically selected for using appropriate selective media (Iyer *et al.*, 2005).

6.4.2 Generation of HSP membrane yeast two-hybrid (MYTH) bait constructs

The MYTH system can be used to identify novel interactions between a membrane protein (full-length integral or membrane-associated) and a cytosolic/ membrane-associated interaction partner. For the MYTH system to function properly, the protein of interest must have either its N and/or C terminus in the cytosol of the cell.

To identify additional novel HSP interaction partners for membrane HSP proteins, a set of HSP membrane yeast two-hybrid (MYTH) bait constructs had to be generated and screened against the MYTH human brain cDNA prey library. Initially, the membrane topology of each HSP was analysed in order to select HSP candidates that would be appropriate for analysis using the MYTH system. Protter, a web-based tool that automatically integrates reference protein annotation sources (e.g. UniProt) for the visual analysis of predicted membrane protein topology (Omasits *et al.*, 2014), was used to analyse the membrane topology for each HSP candidate protein known to contain one or more transmembrane domain and is presented in Table 6.3.

Table 6.3

SPG	Symbol	Gene ID	No. of TM domains	Membrane Topology
SPG1	L1CAM	3897	1	C
SPG2	PLP1	5354	4	N/C
SPG3	ATL1	51062	2	N/C
SPG4	SPAST	6683	1	N
SPG6	NIPA1	123606	9	C
SPG7	SPG7	6687	2	-
SPG12	RTN2	6253	2	-
SPG17	BSCL2	26580	2	N/C
SPG18	ERLIN2	11160	1	N
SPG22	SLC16A2	6567	12	N/C
SPG26	B4GALNT1	2583	1	N
SPG31	REEP1	65055	2	-
SPG33	ZFYVE27	118813	3	N
SPG35	FA2H	79152	4	N/C
SPG39	PNPLA6	10908	1	C
SPG42	SLC33A1	9197	11	N
SPG43	C19orf12	83636	1	N
SPG44	GJC2	57165	4	N/C
SPG49	CYP2U1	113612	5	C

SPG61	ARL6IP1	23204	3	N/C
SPG62	ERLIN1	10613	1	N
SPG64	ENTPD1	953	2	N/C
SPG67	PGAP1	80055	7	N
SPG68	FLRT1	23769	1	C
SPG72	REEP2	51308	2	-
SPG73	CPT1C	126129	2	N/C
SPG75	MAG	4099	1	C
SPG78	ATP13A2	23400	12	N/C
-	AFG3L2	10939	2	N/C
-	ELOVL4	6785	7	C
-	FAM134B	54463	4	N/C
-	GJA1	2697	4	N/C
-	KCNA2	3737	6	N/C
-	KIDINS220	57498	4	N/C
-	MT-ATP6	4508	6	-
-	MT-ND4	4538	11	N
-	MT-CO3	4514	7	N

Table 6.3. List of HSP proteins with one or more transmembrane domain. HSP genes are listed by spastic gait disease-loci (SPG), those not part of the SPG classification system are listed alphabetically. Entrez Gene IDs were obtained from the NCBI database. Information regarding transmembrane domains was obtained from UniProt, whilst membrane topology was analysed using Protter (Omasits *et al.*, 2014). HSPs selected for MYTH analysis are highlighted in green.

The chosen HSP ORFs were cloned in-frame with the C_{ub}-LexA-VP16 tag of an appropriate vector, using either C-terminal vectors (pAMBV4, pCMBV4 or pTMBV4) and/or N-terminal vectors (pBT3N or pTLB1), depending on membrane topology (Chapter 2, section 2.4.3). Bait constructs that showed signs of auto-activation or toxicity in yeast (SPG18 and ELOVL4) were removed, resulting in 10 HSP MYTH bait clones, representing 10 human HSPs.

6.4.3 MYTH library screen reveals 124 potentially novel HSP interactors

An outline of the optimised MYTH library screen used is described in Figure 6.4. In brief, NMY51 yeast cells transfected with a HSP bait construct was transformed with the human embryonic brain cDNA library. The transformation yeast mixture was plated onto SD-WLAH (±3-AT depending on control test) and left to grow for 3-5 days,

to select for positive protein-protein interactions. To increase confidence of the interactions identified from these library screens, all prey library hits identified were re-confirmed. The library prey inserts were amplified from diploid colonies and cloned back into the pPR3N prey vector for reconfirmation mating with the original or negative control (empty vector) bait. Only those that selectively activate all three reporters (*ADE2, HIS3* and *lacZ*) with the original bait and not the negative control (empty) bait, were selected for DNA sequencing to identify the encoded prey proteins.

In total, 10 HSP MYTH bait clones were individually screened against the human embryonic whole brain cDNA prey library, identifying a total of 235 interactions. After removing previously identified false positive interactors (Passantino *et al.*, 2013), a total of 195 potentially novel interactions remained, identifying 124 potentially novel HSP interactors. The identification of previously identified interactions provides additional confidence in the overall MYTH system and the data generated. Successfully reconfirmed interaction partners identified in each individual library screen, including functional annotations, are presented in Table 6.4.

Figure 6.4

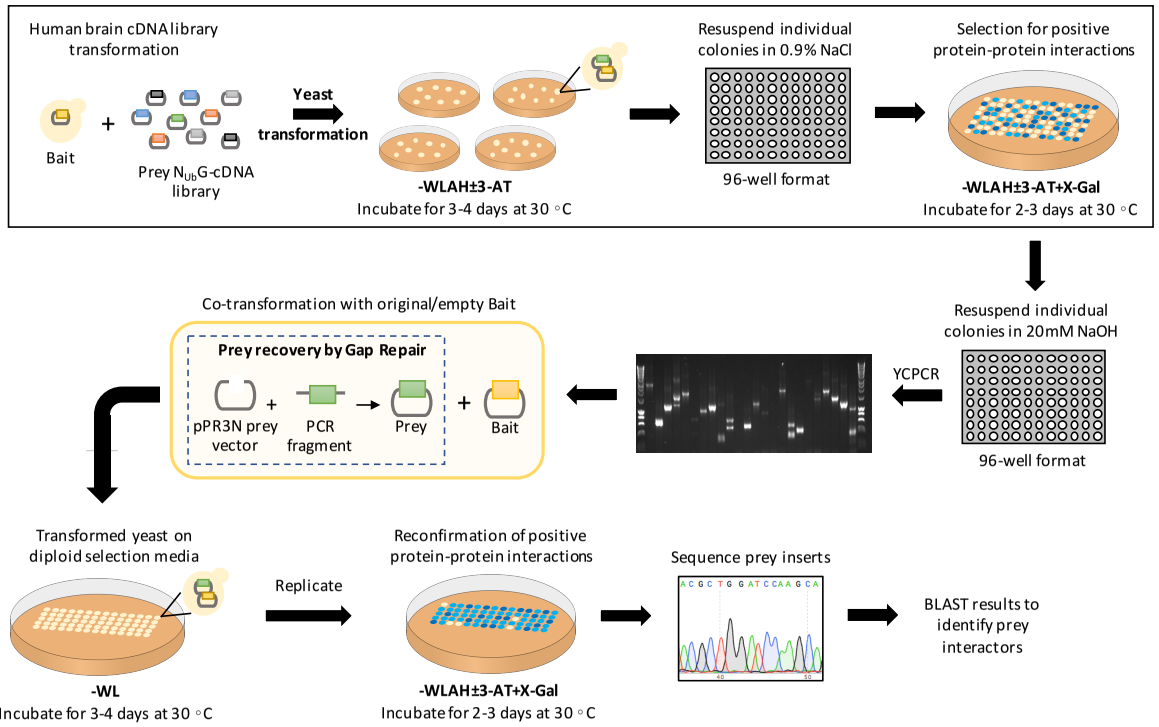

Figure 6.4. Schematic representation of the optimised MYTH library screening procedure used in this study. NMY51 yeast transfected with either pAMBV or pBT3N bait construct was transformed with the human brain N_{ub}G-cDNA prey library before being plated onto SD-WLAH selective plates containing optimal levels of 3-AT, as defined in bait N_{ub}G/N_{ub}I control tests. Positive PPIs were picked and selected for on SD-WLAH±3-AT+X-Gal triple selection plates. To reconfirm potential positive interactions, the NMY51 yeast strain was transformed with a combination of prey PCR product, linearised pPR3N prey vector and either the original bait or an empty bait vector. Diploid yeast (bait and regenerated prey) were selected for on SD-WL medium. Yeast was replicated onto SD-WLAH±3-AT+X-Gal triple selection plates, allowing for the

selection of positive protein-protein interactions. Only those that selectively activate all three reporters (*ADE2, HIS3* and *lacZ*) with the original bait and not the empty bait vector were selected for DNA sequencing and prey identification via NCBI BLASTN.

Table 6.4

A

SPG2/ PLP1	This is the major myelin protein from the central nervous system. It plays an important role in myelin formation and maintenance.	Plasma membrane

Gene	Protein Name (UniProt)	Function	Localisation (UniProt)
ATP13A2	Probable cation-transporting ATPase 13A2	Member of the ATPase P5 subfamily and may have a role in intracellular cation homeostasis and the maintenance of neuronal integrity	Endosome, Lysosome, Plasma membrane, Vacuole
ATP5G2	ATP synthase F(0) complex subunit C2, mitochondrial	Encodes subunit of the proton channel involved in mitochondrial ATP synthase	Mitochondrion
ATP5G3	ATP synthase F(0) complex subunit C3, mitochondrial	Encodes subunit of the proton channel involved in mitochondrial ATP synthase	Mitochondrion
ATP6AP2	Renin receptor	Renin and pro-renin receptor	Extracellular, Plasma membrane
ATP6V0B	V-type proton ATPase 21 kDa proteolipid subunit	Encodes V0 domain of vacuolar ATPase (v-ATPase), important for acidifying various intracellular compartments	Vacuole
CD320	CD320 antigen	Encodes a receptor required for cellular uptake of vitamin B12, B-cell proliferation and immunoglobulin secretion	Extracellular, Plasma membrane, ER, Endosome
CD63	CD63 antigen	Cell surface glycoprotein known to complex with integrins, and is involved in various cellular signaling cascades	Endosome, Lysosome membrane
CD81	CD81 antigen	Cell surface glycoprotein known to complex with integrins, may be involved in signal transduction	Extracellular, Plasma membrane
DPM2	Dolichol phosphate-mannose biosynthesis regulatory protein	Regulates dolichol phosphate-mannose (DPM) biosynthesis	ER
FAM177A1	Protein FAM177A1	-	Nucleus
GLIPR1	Glioma pathogenesis-related protein 1	-	Plasma membrane
PCDHB family	Protocadherin beta family	May be involved in establishing and maintaining specific neuronal connections in the brain	-
RPL17	60S ribosomal protein L17	Component of the 60S ribosomal subunit	-
SHISA4	Protein shisa-4	-	-
SLC25A3	Phosphate carrier protein, mitochondrial	Catalyses the transport of phosphate groups from cytosol into mitochondrial matrix	Extracellular, Plasma membrane, Mitochondrion, Nucleus
SPCS1	Signal peptidase complex subunit 1	Removes signal peptides from nascent proteins translocating into the ER lumen	ER
TMEFF2	Tomoregulin-2	Transmembrane protein which may be a survival factor for hippocampal and mesencephalic neurons	Extracellular
GPM6B	**Neuronal membrane glycoprotein M6-b**	**May be involved in membrane trafficking and cell-cell communication as well as neural development**	**Plasma membrane**
RNF41	**E3 ubiquitin-protein ligase NRDP1**	**Plays a role in type 1 cytokine receptor signaling**	**Cytosol**
TMEM14A	**Transmembrane protein 14A**	-	**Membrane**
YIPF6	**Protein YIPF6**	-	**Membrane**

SPG3/ ATL1	GTPase and Golgi body transmembrane protein. Functions in ER tubular network biogenesis, may also regulate Golgi biogenesis and axonal development.	ER, Golgi app.

Gene	Protein Name (UniProt)	Function	Localisation (UniProt)
ADCY8	Adenylate cyclase type 8	Membrane-bound enzyme that catalyses the formation of cyclic AMP from ATP	Plasma membrane
ARL6IP5	ADP-ribosylation factor-like protein 6-interacting protein 1	Involved in the formation and stabilisation of ER tubules	ER, Plasma membrane
ATP10B	Probable phospholipid-transporting ATPase VB	Catalyses ATP hydrolysis coupled with aminophospholipid translocation through various membranes	ER, Extracellular, Plasma membrane
BCAP31	B-cell receptor-associated protein 31	Chaperone protein - most abundant protein in ER and is involved recognition and targeting or proteins to the ERAD	ER, Plasma membrane, Cytosol
C10orf35	Uncharacterised protein C10orf35	-	-
C18orf32	UPF0729 protein C18orf32	May activate NF-κB signaling pathway	Extracellular
C4orf3	Uncharacterised protein C4orf3	-	Cytosol, Plasma membrane
CCDC167	Coiled-coil domain-containing protein 167	-	Cytosol
COPA	Coatomer subunit alpha	Component of cytosolic protein complex that mediates protein transport between ER and Golgi compartments	Cytosol, Extracellular, Golgi app.
CYB5B	Cytochrome b5 type B	Membrane-bound hemoprotein, may act as an electron carrier for various membrane-bound oxygenases	Mitochondrion
EIF3B	Eukaryotic translation initiation factor 3 subunit B	RNA-binding component of the eIF-3 complex, required for the initiation of protein synthesis	Cytosol, Extracellular, Nucleus
EMC7	ER membrane protein complex subunit 7	-	ER
FAM177A1	Protein FAM177A1	-	Nucleus
FZD1	Frizzled-1	Receptor for Wnt signaling proteins	-
HDDC2	HD domain-containing protein 2	-	Extracellular, mitochondrion
IARS2	Isoleucine-tRNA ligase, mitochondrial	Member of the Class I aminoacyl-tRNA synthetase family	Mitochondrion

Table 6.4 continued

MKRN1	E3 ubiquitin-protein ligase makorin-1	E3 ubiquitin ligase and transcriptional co-regulator thereby controlling cell cycle arrest and apoptosis	Nucleus
NIN	Ninein	Important for centrosomal function - involved in positioning and anchoring microtubule minus-end in epithelial cells	Cytoskeleton, Nucleus
PCDHB10	Protocadherin beta-10	May be involved in establishing and maintaining specific neuronal connections in the brain	-
REEP5	Receptor expression-enhancing protein 5	May promote expression of functional cell surface olfactory receptors	Extracellular
RPS8	40S ribosomal protein S8	Component of the 40S ribosomal subunit	Cytosol, Extracellular, Nucleus
RTN4	Reticulon-4	Developmental neurite outgrowth regulator	ER, Extracellular, Nucleus, Plasma membrane
SLC35B1	Solute carrier family 35 member B1	Nucleotide sugar transporter	ER
TMEM147	Transmembrane protein 147	-	ER
TMEM230	Transmembrane protein 230	Involved in the trafficking and recycling of synaptic vesicles	Plasma membrane
YIF1A	Protein YIF1A	May be involved in transport between ER and Golgi	Cytoskeleton, ER, Golgi app.
C14orf1	**Probable ergosterol biosynthetic protein 28**		**ER**
RNF41	**E3 ubiquitin-protein ligase NRDP1**	**Plays a role in type 1 cytokine receptor signaling**	**Cytosol**
SELENOK	**Selenoprotein K**	**Involved in ERAD and in the protection of cells from ER stress-induced apoptosis**	**ER, Plasma membrane**
TMEM14A	**Transmembrane protein 14A**	-	**Membrane**
YIPF6	**Protein YIPF6**	-	**Membrane**

SPG17/ BSCL2	Necessary for correct lipid storage and lipid droplet maintenance, as well as regulating lipid catabolism.	ER

Gene	**Protein Name (UniProt)**	**Function**	**Localisation (UniProt)**
ANKRD39	Ankyrin repeat domain-containing protein 39	-	Cytosol
ATP10B	Probable phospholipid-transporting ATPase VB	Catalyses ATP hydrolysis coupled with aminophospholipid translocation through various membranes	ER, Plasma membrane
ATP6AP2	Renin receptor	Renin and pro-renin receptor	Extracellular, Plasma membrane
CCDC167	Coiled-coil domain-containing protein 167	-	Cytosol
CD63	CD63 antigen	Cell surface glycoprotein known to complex with integrins, and is involved in various cellular signaling cascades	-
CEND1	Cell cycle exit and neuronal differentiation protein 1	Neuron-specific protein involved in neuronal differentiation	-
CFL1	Cofilin-1	Intracellular actin-modulating protein - various roles including regulation of cell morphology and cytoskeletal organisation	Extracellular, Nucleus
GABBR2	Gamma-aminobutyric acid receptor-associated protein-like 2	Ubiquitin-like modifier involved in intra-Golgi traffic	Cytosol, Vacuole, Golgi app.
MAP1LC3A	Microtubule-associated proteins 1A/1B light chain 3A	Associates with microtubule-associated proteins which mediate interactions between microtubules and cytoskeletal components	Cytosol, Vacuole
MFSD5	Molybdate-anion transporter	Mediates intracellular uptake of molybdenum	Plasma membrane
NDUFB11	NADH dehydrogenase [ubiquinone] 1 beta subcomplex subunit 11, mitochondrial	Subunit of the NADH:ubiquinone oxidoreductase (complex I), where it transfers electrons from NADH to ubiquinone.	Mitochondrion
NFXL1	NF-X1-type zinc finger protein NFXL1	-	Nucleus
NSDHL	Sterol-4-alpha-carboxylate 3-dehydrogenase, decarboxylating	Involved in cholesterol biosynthesis	ER
REEP5	Receptor expression-enhancing protein 5	May promote expression of functional cell surface olfactory receptors	Extracellular
RPL13A	60S ribosomal protein L13a	Component of the 60S ribosomal subunit, but also has a role in the repression of inflammatory genes	Cytosol, Extracellular, Nucleus
RPL34	60S ribosomal protein L34	Component of the 60S ribosomal subunit	Cytosol, Extracellular, Nucleus
RPLP1	60S acidic ribosomal protein P1	Component of the 60S ribosomal subunit and is important in the elongation step of protein synthesis	Cytosol, Extracellular
SLC35B1	Solute carrier family 35 member B1	Nucleotide sugar transporter	ER
SUMO1	Small ubiquitin-related modifier 1	Ubiquitin-like modifier involved in a variety of cellular processes such as nuclear transport and signal transduction	Cytosol, Nucleus, Plasma membrane
TMEM134	Transmembrane protein 134	-	Plasma membrane
TMEM230	Transmembrane protein 230	Involved in the trafficking and recycling of synaptic vesicles	Plasma membrane
TXNDC15	Thioredoxin domain-containing protein 15	-	-
YIF1A	Protein YIF1A	May be involved in transport between ER and Golgi	Cytoskeleton, ER, Golgi app.
C14orf1	**Probable ergosterol biosynthetic protein 28**		**ER**
GPM6B	**Neuronal membrane glycoprotein M6-b**	**May be involved in membrane trafficking and cell-cell communication as well as neural development**	**Plasma membrane**
RNF41	**E3 ubiquitin-protein ligase NRDP1**	**Plays a role in type 1 cytokine receptor signaling**	**Cytosol**
YIPF6	**Protein YIPF6**	-	**Membrane**

Table 6.4 continued

SPG61/ ARL6IP1	Important role in the formation and stabilisation of ER tubules. Also, negatively regulates apoptosis	ER

Gene	Protein Name (UniProt)	Function	Localisation (UniProt)
ACOT7	Cytosolic acyl coenzyme A thioester hydrolase	Hydrolyses the CoA thioester of palmitoyl-CoA and other long-chain fatty acids. May play an important physiological function in the brain	Cytosol, Extracellular, Mitochondrion, Nucleus
ADCY8	Adenylate cyclase type 8	Membrane-bound enzyme that catalyses the formation of cyclic AMP from ATP	Plasma membrane
ARL6IP1	ADP-ribosylation factor-like protein 6-interacting protein 1	Important role in the formation and stabilisation of ER tubules. Also, negatively regulates apoptosis	ER
ARL6IP5	ADP-ribosylation factor-like protein 6-interacting protein 1	Involved in the formation and stabilisation of ER tubules	ER, Plasma membrane
ATP10B	Probable phospholipid-transporting ATPase VB	Catalyses ATP hydrolysis coupled with aminophospholipid translocation through various membranes	ER, Plasma membrane
C10orf35	Uncharacterised protein C10orf35	-	-
C4orf3	Uncharacterised protein C4orf3	-	Cytosol, Plasma membrane
CCDC167	Coiled-coil domain-containing protein 167	-	Cytosol
CYB5B	Cytochrome b5 type B	Membrane-bound hemoprotein, may act as an electron carrier for various membrane-bound oxygenases	Mitochondrion
EEF1A1	Elongation factor 1-alpha 1	Responsible for the GTP-dependent delivery of aminoacyl tRNA to ribosomes during protein biosynthesis	Cytoskeleton, Cytosol, Extracellular, Nucleus, Plasma membrane, Vacuole
EMC7	ER membrane protein complex subunit 7	-	ER
GABABR2	Gamma-aminobutyric acid type B receptor subunit 2	Belongs to GABA-B receptor subfamily, inhibiting neuronal activity through the regulation of neurotransmitter release, ion channels and adenylyl cyclase	Plasma membrane
HERPUD1	Homocysteine-responsive endoplasmic reticulum-resident ubiquitin-like domain member 1 protein	Involved in ER-associated protein degradation (ERAD)	ER, Cytosol
HMOX2	Heme oxygenase 2	Essential enzyme in heme catabolism	ER, Plasma membrane, Cytosol
IARS2	Isoleucine-tRNA ligase, mitochondrial	Member of the Class I aminoacyl-tRNA synthetase family	Mitochondrion
INPP5K	Inositol polyphosphate 5-phosphatase K	5-phosphatase activity towards polyphosphate inositol, may negatively regulate actin cytoskeleton	Cytosol, ER, Golgi app., Nucleus, Plasma membrane
JAGN1	Protein jagunal homolog 1	Involved in vesicle-mediated transport in the early secretory pathway, where it is required for neutrophil differentiation and survival	ER
MGAT4C	Alpha-1,3-mannosyl-glycoprotein 4-beta-N-acetylglucosaminyltransferase C	-	Golgi app.
NFXL1	NF-X1-type zinc finger protein NFXL1	-	Nucleus
NUP107	Nuclear pore complex protein Nup107	Essential component of nuclear pore complex (NPC) required for assembly and maintenance	Cytoskeleton, Cytosol, Nucleus
RABAC1	Prenylated Rab acceptor protein 1	Rab protein regulator required for vesicle formation from Golgi complex	Golgi app., Plasma membrane
REEP5	Receptor expression-enhancing protein 5	May promote expression of functional cell surface olfactory receptors	Extracellular
RPL3	60S ribosomal protein L3	Component of the 60S ribosomal subunit	Cytosol, Extracellular, Nucleus
RTN4	Reticulon-4	Developmental neurite outgrowth regulator	ER, Extracellular, Nucleus, Plasma membrane
SPCS1	Signal peptidase complex subunit 1	Removes signal peptides from nascent proteins translocating into the ER lumen	ER
SSR3	Translocon-associated protein subunit gamma	Glycosylated ER membrane receptor required for the regulation of protein translocation across ER membrane	ER
STMN4	Stathmin-4	Associated with microtubule-destabilizing activity	Golgi app.
YIF1A	Protein YIF1A	May be involved in transport between ER and Golgi	Cytoskeleton, ER, Golgi app.
C14orf1	**Probable ergosterol biosynthetic protein 28**		**ER**
RNF41	**E3 ubiquitin-protein ligase NRDP1**	**Plays a role in type 1 cytokine receptor signaling**	**Cytosol**
TMEM14A	**Transmembrane protein 14A**	**-**	**Membrane**

GJA1	Component of gap junctions, which contain arrays intracellular channels allowing the diffusion of low molecular weight materials from cell to cell	ER, Extracellular, Mitochondrion, Golgi app.

Gene	Protein Name (UniProt)	Function	Localisation (UniProt)
ADGRB3	Adhesion G protein-coupled receptor B3	Brain-specific angiogenesis inhibitor	-
ANKRD46	Ankyrin repeat domain-containing protein 46	-	-
AQP4	Aquaporin-4	Water-selective channels, has a specific role in brain water homeostasis	Plasma membrane
ARV1	Protein ARV1	Acts as a mediator of sterol homeostasis in the ER as well as regulation of bile acid homeostasis	ER

Table 6.4 continued

ATP10B	Probable phospholipid-transporting ATPase VB	Catalyses ATP hydrolysis coupled with aminophospholipid translocation through various membranes	ER, Plasma membrane
ATP5G3	ATP synthase F(0) complex subunit C3, mitochondrial	Encodes subunit of the proton channel involved in mitochondrial ATP synthase	Mitochondrion
ATP6V0B	V-type proton ATPase 21 kDa proteolipid subunit	Encodes V0 domain of vacuolar ATPase (v-ATPase), important for acidifying various intracellular compartments	Vacuole
BCAP31	B-cell receptor-associated protein 31	Chaperone protein - most abundant protein in ER and is involved recognition and targeting or proteins to the ERAD	ER, Plasma membrane, Cytosol
BRICD5	BRICHOS domain-containing protein 5	-	Plasma membrane
C10orf35	Uncharacterised protein C10orf35	-	-
C18orf32	UPF0729 protein C18orf32	May activate NF-κB signaling pathway	Extracellular
C4orf3	Uncharacterised protein C4orf3	-	Cytosol, Plasma membrane
CCDC167	Coiled-coil domain-containing protein 167	-	Cytosol
CDC42BPA	Serine/threonine-protein kinase MRCK alpha	Involved in the regulation of cytoskeleton reorganisation and cell migration.	Cytoskeleton, Extracellular
CDKAL1	Threonylcarbamoyladenosine tRNA methylthiotransferase	-	-
CEND1	Cell cycle exit and neuronal differentiation protein 1	Neuron-specific protein involved in neuronal differentiation	-
CYB5B	Cytochrome b5 type B	Membrane-bound hemoprotein, may act as an electron carrier for various membrane-bound oxygenases	Mitochondrion
EMC7	ER membrane protein complex subunit 7	-	ER
FAM177A1	Protein FAM177A1	-	Nucleus
FZD1	Frizzled-1	Receptor for Wnt signaling proteins	-
GHITM	Growth hormone-inducible transmembrane protein	Important for mitochondrial tubular network organisation.	Extracellular, Mitochondrion
HMOX2	Heme oxygenase 2	Essential enzyme in heme catabolism	ER, Plasma membrane, Cytosol
LMNA	Prelamin-A/C	Important for development of peripheral nervous system as it has roles in nuclear assembly, nuclear membrane and telomere dynamics.	Cytoskeleton, Cytosol, Nucleus
MSMO1	Methylsterol monooxygenase 1	May have a role in cholesterol biosynthesis	ER
NACA	Nascent polypeptide-associated complex subunit alpha	Prevents translocation of non-secretory polypeptides to the ER by forming the nascent polypeptide-associated complex (NAC)	Extracellular, Nucleus
NDUFB11	NADH dehydrogenase [ubiquinone] 1 beta subcomplex subunit 11, mitochondrial	Subunit of the NADH:ubiquinone oxidoreductase (complex I), where it transfers electrons from NADH to ubiquinone.	Mitochondrion
NSDHL	Sterol-4-alpha-carboxylate 3-dehydrogenase, decarboxylating	Involved in cholesterol biosynthesis	ER
OST4	Dolichyl-diphosphooligosaccharide--protein glycosyltransferase subunit 4	May be involved in N-glycosylation	ER
PSMA7	Proteasome subunit alpha type-7	Component of the 20S core proteasome complex	Cytosol, Extracellular, Nucleus
REEP5	Receptor expression-enhancing protein 5	May promote expression of functional cell surface olfactory receptors	Extracellular
SPCS1	Signal peptidase complex subunit 1	Removes signal peptides from nascent proteins translocating into the ER lumen	ER
STX4	Syntaxin-4	Plasma membrane t-SNARE involved in vesicle-mediated transport	Cytosol, Endosome, Extracellular, Plasma membrane, Vacuole
TMCC2	TMCC2 protein	-	Nucleus, Plasma membrane
TMEM101	Transmembrane protein 101	May activate NF-κB signaling pathway	Plasma membrane
TMEM134	Transmembrane protein 134	-	Plasma membrane
TMEM184B	Transmembrane protein 184B	May be involved in the activation of MAP kinase signaling pathway	Plasma membrane
TMEM230	Transmembrane protein 230	Involved in the trafficking and recycling of synaptic vesicles	Plasma membrane
TUBA1A	Tubulin alpha-1A chain	Major constituent of microtubules	Cytosol, Endosome, Extracellular, Cytoskeleton, Nucleus
VTI1B	Vesicle transport through interaction with t-SNAREs homolog 1B	Interacts with t-SNAREs on target membrane to mediate vesicle transport pathways	Endosome, Golgi app., Lysosome, Vacuole
WRB	Tail-anchored protein insertion receptor WRB	Receptor involved in the insertion of tail-anchored proteins into the ER membrane	ER, Nucleus
YIF1A	Protein YIF1A	May be involved in transport between ER and Golgi	Cytoskeleton, ER, Golgi app.
ZMYM2	Zinc finger MYM-type protein 2	May acts as a transcription factor	Cytosol, Nucleus
C14orf1	**Probable ergosterol biosynthetic protein 28**		**ER**
RNF41	**E3 ubiquitin-protein ligase NRDP1**	**Plays a role in type 1 cytokine receptor signaling**	**Cytosol**
TMEM14A	**Transmembrane protein 14A**	-	**Membrane**
TMEM128	**Transmembrane protein 128**	-	**Membrane**
SELENOK	**Selenoprotein K**	**Involved in ERAD and in the protection of cells from ER stress-induced apoptosis**	**ER, Plasma membrane**
YIPF6	**Protein YIPF6**	-	**Membrane**

Table 6.4 continued

B

SPG2/ PLP1	This is the major myelin protein from the central nervous system. It plays an important role in myelin formation and maintenance.	Plasma membrane

Gene	Protein Name (UniProt)	Function	Localisation (UniProt)
ATP10B	Probable phospholipid-transporting ATPase VB	Catalyses ATP hydrolysis coupled with aminophospholipid translocation through various membranes	ER, Plasma membrane
ATP5G3	ATP synthase F(0) complex subunit C3, mitochondrial	Encodes subunit of the proton channel involved in mitochondrial ATP synthase	-
ATP6V0B	V-type proton ATPase 21 kDa proteolipid subunit	Encodes V0 domain of vacuolar ATPase (v-ATPase), important for acidifying various intracellular compartments	Vacuole
CCDC167	Coiled-coil domain-containing protein 167	-	Cytosol
CD63	CD63 antigen	Cell surface glycoprotein known to complex with integrins, and is involved in various cellular signaling cascades	-
CDKAL1	Threonylcarbamoyladenosine tRNA methylthiotransferase	-	-
DPM2	Dolichol phosphate-mannose biosynthesis regulatory protein	Regulates dolichol phosphate-mannose (DPM) biosynthesis	ER
FUNDC2	FUN14 domain-containing protein 2	-	Mitochondrion, Nucleus
NUP107	Nuclear pore complex protein Nup107	Essential component of nuclear pore complex (NPC) required for assembly and maintenance	Cytoskeleton, Cytosol, Nucleus
SPCS1	Signal peptidase complex subunit 1	Removes signal peptides from nascent proteins translocating into the ER lumen	ER
TMEM242	Transmembrane protein 242	-	Nucleus
TRO	Trophinin	Mediates cell adhesion between trophoblastic cells and epithelial cells of the endometrium	Plasma membrane
VKORC1L1	Vitamin K epoxide reductase complex subunit 1-like protein 1	Important role in Vitamin K metabolism	ER
YIF1A	Protein YIF1A	May be involved in transport between ER and Golgi	Cytoskeleton, ER, Golgi
C14orf1	**Probable ergosterol biosynthetic protein 28**	**-**	**ER**
GPM6B	**Neuronal membrane glycoprotein M6-b**	**May be involved in membrane trafficking and cell-cell communication as well as neural development**	**Plasma membrane**
RNF41	**E3 ubiquitin-protein ligase NRDP1**	**Plays a role in type 1 cytokine receptor signaling**	**Cytosol**
TMEM128	**Transmembrane protein 128**	**-**	**Membrane**
TMEM14A	**Transmembrane protein 14A**	**-**	**Membrane**

SPG4/ SPAST	ATP-dependent microtubule severing protein. Required for membrane traffic from the endoplasmic reticulum (ER) to the Golgi and endosome recycling.	Cytoskeleton, ER, endosome, Extracellular

Gene	Protein Name (UniProt)	Function	Localisation (UniProt)
ARL6IP5	ADP-ribosylation factor-like protein 6-interacting protein 1	Involved in the formation and stabilisation of ER tubules	ER, Plasma membrane

SPG33/ ZFYVE27	Involved in vesicular trafficking during neurite extension. Involved in formation and stabilisation of the tubular ER network.	ER, endosome, Plasma membrane

Gene	Protein Name (UniProt)	Function	Localisation (UniProt)
ARL6IP5	ADP-ribosylation factor-like protein 6-interacting protein 1	Involved in the formation and stabilisation of ER tubules	ER, Plasma membrane
ATP6AP2	Renin receptor	Renin and pro-renin receptor	Extracellular, Plasma membrane
C4orf3	Uncharacterised protein C4orf3	-	Cytosol, Plasma membrane
CCDC167	Coiled-coil domain-containing protein 167	-	Cytosol
CDKAL1	Threonylcarbamoyladenosine tRNA methylthiotransferase	-	ER
EMC7	ER membrane protein complex subunit 7	-	ER
FUNDC2	FUN14 domain-containing protein 2	-	Mitochondrion, Nucleus
H3F3B	Histone H3.3	replication-independent histone	Extracellular, Nucleus
LRPAP1	Alpha-2-macroglobulin receptor-associated protein	Molecular chaperone for LDL receptor-related proteins, facilitating proper folding and localisation	ER, Extracellular, Plasma membrane
REEP5	Receptor expression-enhancing protein 5	May promote expression of functional cell surface olfactory receptors	Extracellular
RPL17	60S ribosomal protein L17	Component of the 60S ribosomal subunit	Cytosol, Nucleus
RTN4	Reticulon-4	Developmental neurite outgrowth regulator	ER, Extracellular, Nucleus, Plasma membrane
SEC11C	Signal peptidase complex catalytic subunit SEC11C	Component of microsomal signal peptidase complex, associates with nascent proteins as they translocate into lumen of ER	ER
SSR3	Translocon-associated protein subunit gamma	Glycosylated ER membrane receptor required for the regulation of protein translocation across ER membrane	ER
TMEM134	Transmembrane protein 134	-	Plasma membrane

Table 6.4 continued

TMEM230	Transmembrane protein 230	Involved in the trafficking and recycling of synaptic vesicles	Plasma membrane
RNF41	**E3 ubiquitin-protein ligase NRDP1**	**Plays a role in type 1 cytokine receptor signaling**	**Cytosol**
SELENOK	**Selenoprotein K**	**Involved in ERAD and in the protection of cells from ER stress-induced apoptosis**	**ER, Plasma membrane**
TMEM128	**Transmembrane protein 128**	**-**	**Membrane**
TMEM14A	**Transmembrane protein 14A**	**-**	**Membrane**

SPG43/ C19orf12		ER, Mitochondrion

Gene	**Protein Name (UniProt)**	**Function**	**Localisation (UniProt)**
C18orf32	UPF0729 protein C18orf32	May activate NF-κB signaling pathway	Extracellular
COMT	Catechol O-methyltransferase	Catalyses the O-methylation of catecholamine neurotransmitters and catechol hormones, rendering them inactive	Cytosol, Extracellular, Plasma membrane
DCTPP1	dCTP pyrophosphatase 1	Hydrolyses dCTP to dCMP after DNA synthesis	Cytosol
EDF1	Endothelial differentiation-related factor 1	Regulates endothelial cell differentiation, lipid metabolism and hormone-induced cardiomyocyte hypertrophy	Extracellular, Nucleus
FKBP1A	Peptidyl-prolyl cis-trans isomerase FKBP1A	Important in immunoregulation and various cellular processes involving protein folding and trafficking	Cytosol, Extracellular, ER
HMGN2	Non-histone chromosomal protein HMG-17	Binds nucleosomal DNA and associates with transcriptionally active chromatin	Nucleus
MLLT11	Protein AF1q	-	Nucleus
MRPS34	28S ribosomal protein S34, mitochondrial	Component of 28S mitochondrial ribosomal subunit	Mitochondrion
NFXL1	NF-X1-type zinc finger protein NFXL1	-	Nucleus
PSMA1	Proteasome subunit alpha type-1	Component of the 20S core proteasome complex	Cytoskeleton, Cytosol, Extracellular, Nucleus
SOD1	Superoxide dismutase [Cu-Zn]	Acts as a homodimer to destroy naturally occurring harmful radicals	Cytosol, Extracellular, Mitochondrion, Nucleus, Peroxisome
TIRAP	Toll/interleukin-1 receptor domain-containing adapter protein	Adapter protein involved in signaling pathways of the innate immune response resulting in cytokine secretion and the inflammatory response	Cytosol, Nucleus, Plasma membrane
TMEM106C	Transmembrane protein 106C	-	ER
TUBB2A	Tubulin beta-2A chain	Major constituent of microtubules	Cytoskeleton, Extracellular, Nucleus
UQCRB	Cytochrome b-c1 complex subunit 7	Component of the ubiquinol-cytochrome c reductase complex (complex III) of the mitochondrial respiratory chain, involved in redox-linked proton pumping	Mitochondrion
VPS8	Vacuolar protein sorting-associated protein 8 homolog	Involved in vesicle-mediated protein trafficking of the endocytic membrane transport pathway	endosome
C14orf1	**Probable ergosterol biosynthetic protein 28**	**-**	**ER**
RNF41	**E3 ubiquitin-protein ligase NRDP1**	**Plays a role in type 1 cytokine receptor signaling**	**Cytosol**
YIPF6	**Protein YIPF6**	**-**	**Membrane**

SPG62/ ERLIN1	Component of the ERLIN1/ERLIN2 complex which mediates the endoplasmic reticulum-associated degradation (ERAD) of IP3Rs. Involved in regulation of cellular cholesterol homeostasis	ER

Gene	**Protein Name (UniProt)**	**Function**	**Localisation (UniProt)**
APLP1	Amyloid-like protein 1	Membrane-associated glycoprotein that is cleaved, releasing a cytoplasmic fragment that may act as a transcriptional activator.	Extracellular, Plasma membrane
ATP6V0B	V-type proton ATPase 21 kDa proteolipid subunit	Encodes V0 domain of vacuolar ATPase (v-ATPase), important for acidifying various intracellular compartments	Vacuole
DNAJC30	DnaJ homolog subfamily C member 30	DNAJ molecular chaperone homology domain-containing protein family member	Mitochondrion
ETFB	Electron transfer flavoprotein subunit beta	Transfers electrons to the main mitochondrial respiratory chain	Extracellular, Mitochondrion
FLRT2	Leucine-rich repeat transmembrane protein FLRT2	Cell adhesion molecule which regulates early embryonic vascular and neural development	Extracellular, Plasma membrane
H3F3B	Histone H3.3	replication-independent histone	Extracellular, Nucleus
IDS	Iduronate 2-sulfatase	Required for lysosomal degradation of heparan sulfate and dermatan sulfate	lysosome, Vacuole
MGMT	Methylated-DNA--protein-cysteine methyltransferase	DNA repair protein involved in cellular defense	Nucleus
MRPL50	39S ribosomal protein L50, mitochondrial	Component of 39S mitochondrial ribosomal subunit	Mitochondrion
RPL37A	60S ribosomal protein L37a	Component of the 60S ribosomal subunit	Cytosol, Extracellular, Nucleus
RPL4	60S ribosomal protein L4	Component of the 60S ribosomal subunit	Cytosol, Extracellular, Nucleus
RTN4	Reticulon-4	Developmental neurite outgrowth regulator	ER, Extracellular, Nucleus, Plasma membrane

TMSB10	Thymosin beta-10	Important role in cytoskeleton organisation	Cytoskeleton
TMX2	Thioredoxin-related transmembrane protein 2	Member of the disulphide isomerase (PDI) family. Involved in protein folding and thiol-disulphide interchange reactions	ER
TSPAN7	Tetraspanin-7	Cell surface glycoprotein which may be involved in the regulating neurite outgrowth	Plasma membrane
TUBB2A	Tubulin beta-2A chain	Major constituent of microtubules	Cytosol
BNIP3	**BCL2/adenovirus E1B 19 kDa protein-interacting protein 3**	**Pro-apoptotic factor**	**Mitochondrion**
RNF41	**E3 ubiquitin-protein ligase NRDP1**	**Plays a role in type 1 cytokine receptor signalling**	**Cytosol**

Table 6.4. Membrane Yeast Two-Hybrid (MYTH) library screen results. (A) Refined list of potential interactors identified from C-terminally tagged pAMBV and (B) N-terminally tagged pBT3N bait proteins. Potential false positive interaction partners are shown in bold. False positives correspond to proteins that are repeatedly identified in our MYTH library screens and/or commonly identified false positives in previous MYTH library screens (Passantino *et al.*, 2013). Previously identified interactions are highlighted in orange (known direct) or green (known indirect).

Significantly, the MYTH library screens identified several previously identified interactors, increasing our confidence in the MYTH system and the novel interactions identified. Using C-terminally tagged pAMBV bait constructs, multiple known interaction partners (INPP5K, ARL6IP1 and RTN4) were identified for ARL6IP1 (SPG61) (Rual *et al.*, 2005; Rolland *et al.*, 2014). Whilst the interaction between ATL1 (SPG3) and RTN4, which had previously been identified through mass spectrometry (Hu *et al.*, 2009), was also identified and recorded as a novel binary interaction. Similarly, when screening N-terminally tagged pBT3N bait constructs, we identified the interaction between ZFYVE27 (SPG33) and REEP5, which had previously been reported as an indirect interaction via co-immunoprecipitation and co-expression techniques (Chang, Lee and Blackstone, 2013). Data from this study means that these previously identified indirect interactions, can now be re-annotated as novel binary interactions.

A summary of interaction data generated from all MYTH library screens performed is presented in Figure 6.5. Interaction data for C-terminally tagged HSP baits (Figure 6.5 A) was compared with that of the N-terminally tagged HSP baits (Figure 6.5 B), to reveal an 18 % (22/124) overlap between the two (see Figure 6.5 C). It is expected that different partner profiles may result from different bait clone topologies.

6.4.4 Common HSP interaction partners identified in the MYTH library screens

A graphical representation of the data compiled in Table 6.4 is presented in Figure 6.6. HSP interaction partners were arranged by degree (number of interactions) using interaction data generated from the MYTH library screens (Figure 6.6 A). This data shows that 15 % (19/124) of the HSP interactors identified in these library screens interacted with three or more HSP proteins. These highly connected HSP interactors were used to generate the subnetwork as presented in Figure 6.6 B, which was functionally annotated and analysed for common binding partners.

Figure 6.5

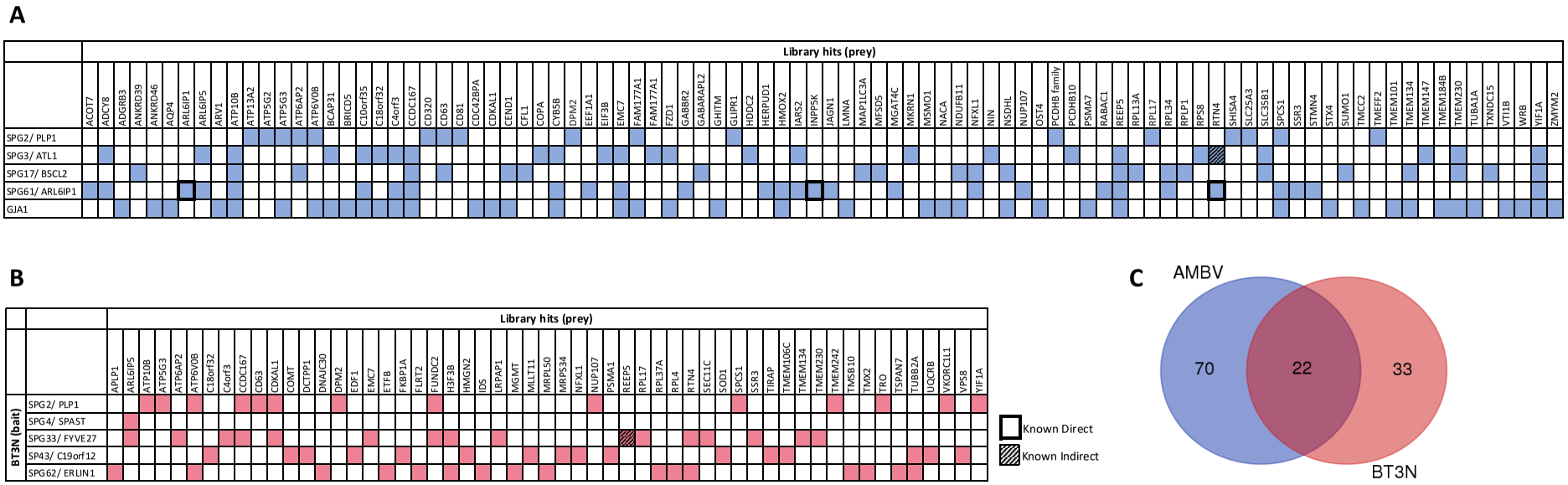

Figure 6.5. Summary of data from all membrane yeast two-hybrid (MYTH) library screens performed in this study. Bait HSPs (horizontal) and prey MYTH library hits (vertical) are ordered alphabetically. C-terminally tagged pAMBV baits are shown in (A) while N-terminally tagged pBT3N baits are shown in (B). The overlap of the proteins identified as potential interaction partners in both A and B MYTH library screens are shown in (C), colours match accordingly. Potential false positives, highlighted in Table 6.4, have been removed. Previously identified (known) interactions, are annotated as such in the tables above.

Figure 6.6

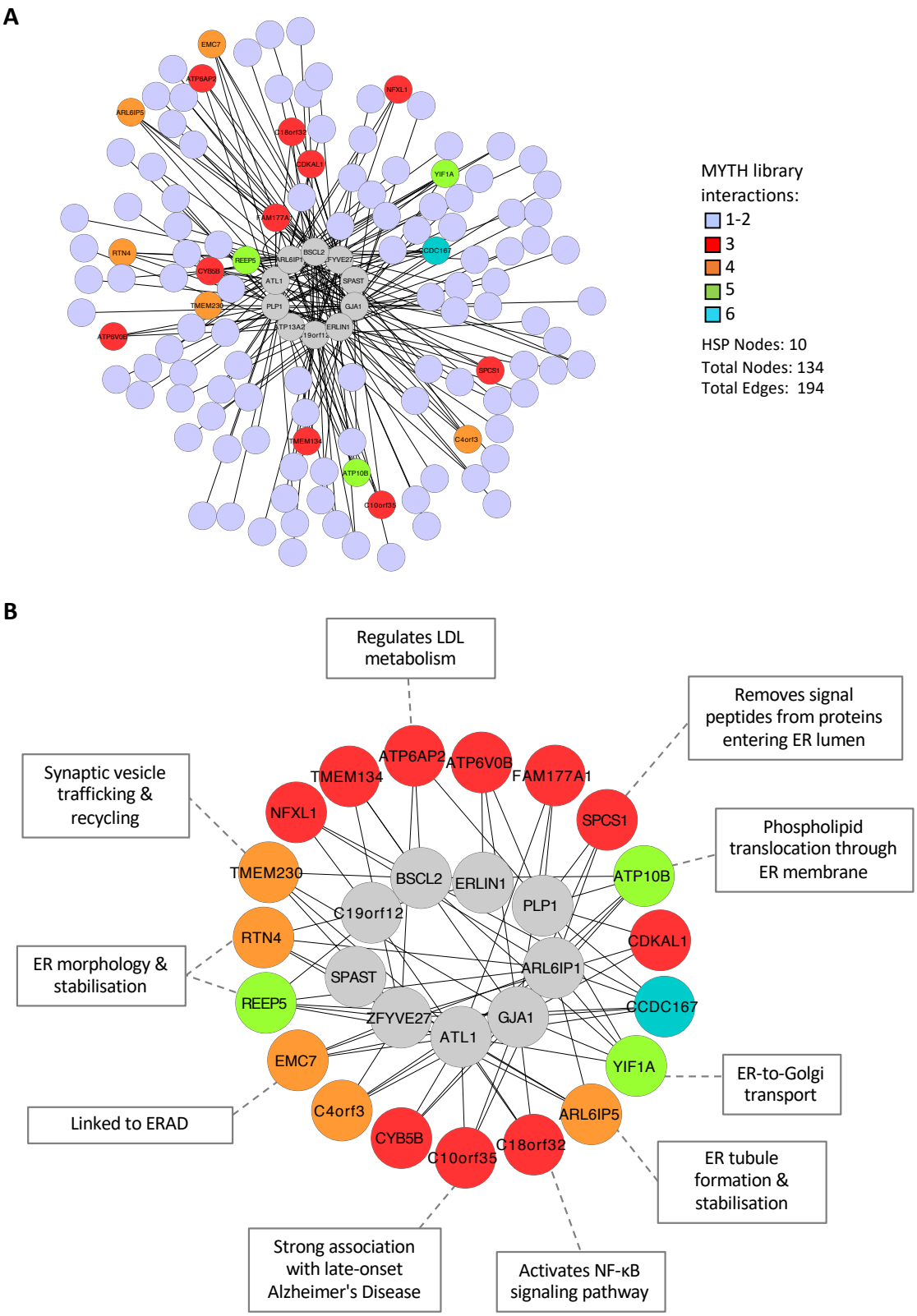

Figure 6.6. Degree clustering of interaction partners identified in MYTH library screens. (A) Interaction partners identified in the MYTH library screens are coloured according to the number of interactions (degree) formed with HSPs screened, as

indicted in the key. HSPs are displayed in grey. Subnetwork (B) was derived from (A), using interactors identified in the MYTH library screens with a degree ≥ 3, and functionally annotated using literature-derived sources.

As already mentioned, ATL1 and ARL6IP1 are previously known RTN4 interaction partners, also identified in our studies, following successful MYTH library screening. RTN4 is a structural ER protein involved in the maintenance of tubular ER structure and function (Voeltz *et al.*, 2006), whilst ARL6IP1 and ATL1 are both ER-shaping proteins required for ER network organisation (Park *et al.*, 2010; Fowler and O'Sullivan, 2016). Interestingly, ZFYVE27, which is known to interact with tubular ER proteins and has a role in ER morphogenesis (Chang, Lee and Blackstone, 2013), and ERLIN1, a component of the ERLIN1/ERLIN2 ER membrane complex which is able to mediate inositol 1,4,5-triphosphate receptors (IP_3Rs) ER-associated degradation (Pearce *et al.*, 2009), were both identified as binary interactors of RTN4 in our study. These RTN4 interactions are of particular interest as another reticulon family member, RTN2 (reticulon 2) is associated with HSP. Mutations in the *RTN2* gene causes the autosomal dominant spastic paraplegia type 12 (SPG12) (Montenegro *et al.*, 2012), therefore RTN4 may be a potential HSP candidate gene.

ARL6IP5 is a microtubule-binding protein which can exert neuroprotective roles against dopaminergic neuron degeneration, through the regulation of intracellular redox status and NF-κB signalling pathway (Miao *et al.*, 2014). ARL6IP5 was shown to interact with ER-shaping proteins ATL1, ARL6IP1 and ZFYVE27, in our studies. Additionally, ARL6IP5 was also identified as a spastin interaction partner. Spastin is an ATP-dependent microtubule-severing protein (Hazan *et al.*, 1999), whose full-length isoform, M1, interacts with tubular ER membrane to co-ordinate ER-shaping (Park *et al.*, 2010).

REEP5, a DP1/REEP/Yop1p family member, is a conserved integral ER membrane protein, involved in shaping the curvature of the tubular ER (Voeltz *et al.*, 2006). We identified binary interactions between REEP5 and the ER-shaping proteins ATL1, ARL6IP1 and ZFYVE27. Interestingly, the 'predicted' indirect interaction between

ATL1 and the REEP5 yeast ortholog, YOP1, was previously inferred by a synthetic rescue study (Anwar *et al.*, 2012). BSCL2 was also identified as a binary interactor of REEP5, in our study. BSCL2 is an ER transmembrane glycoprotein involved in lipid droplet morphology and metabolism (Fei *et al.*, 2008). HSP-associated *BSCL2* mutations (N88S and S90L), cause misfolded seipin to accumulate in the ER, leading to ER stress and enhance ubiquitination and degradation (Ito *et al.*, 2008). These REEP5 interactions are of particular interest as REEP1 is another REEP family member associated with HSP, with mutations in the *REEP1* gene causing the autosomal dominant spastic paraplegia type 31 (SPG31) (Züchner *et al.*, 2006). Like spastin, REEP1 is also able to mediate microtubule interactions with the tubular ER network (Park *et al.*, 2010).

Although these disorders have 75 distinct genetic loci (SPG1-78), more than half of all those affected, harbour autosomal dominant mutations in proteins known to function in ER network formation, most notably spastin (SPG4), atlastin-1 (SPG3A), REEP1 (SPG31) and reticulon-2 (SPG12) (Goyal and Blackstone, 2013). These HSP proteins interact with one another and mediate interactions between the microtubule cytoskeleton and the tubular ER network to co-ordinate tubular ER shaping (Park *et al.*, 2010; Blackstone, 2012).

This study identified common interactors of known HSP proteins, which are involved in various aspects of ER network formation, highlighting the importance for proper ER morphology and distribution in neurons. Given the hydrophobic properties associated with membrane proteins, structural and functional studies remain challenging, and so new methodologies to investigate these candidate proteins are required. It is unlikely that many of the binary interactions identified in the MYTH library screens would have been identified without using this system, or a system like this.

6.5 Network Analysis

6.5.1 Network construction: HSPome+

Each of the positive binary HSP interaction partners identified in this study, through targeted and library yeast two-hybrid screens, were mapped to an Entrez Gene ID. After removing 10 duplicate interactions due to bait/prey configurations, a total of 385 unique interactions were identified (see Appendix 6.1 for all raw interaction data). These were combined with the initial HSPome (Chapter 3) to generate the updated HSPome+ network (Figure 6.7) which contains a total of 4,688 interactions between 3,074 different human proteins.

Figure 6.7

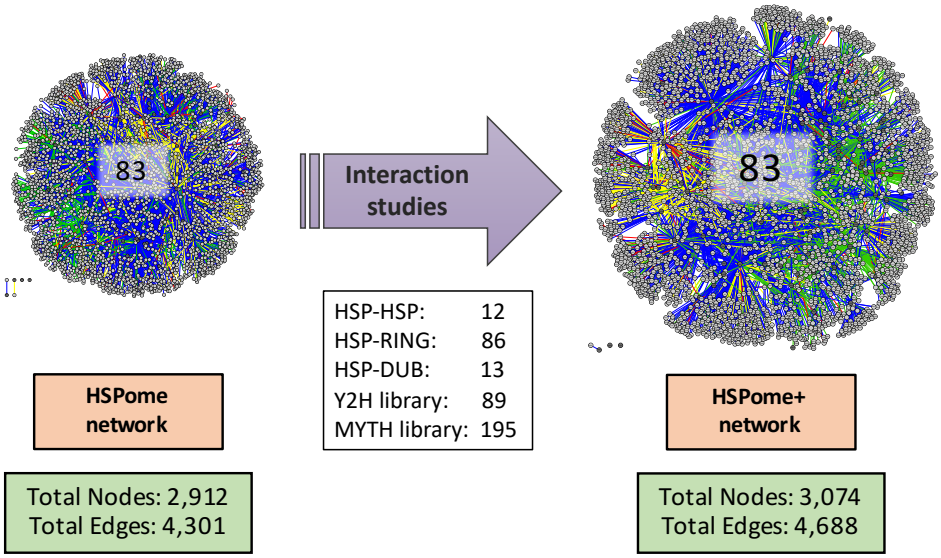

Figure 6.7. Generation of the HSPome+ network. The HSPome was combined with all results from the Y2H targeted matrix matings and Y2H library studies to generate the HSPome+ network.

6.5.2 Network properties

To evaluate the inherent properties of the HSPome+ network, computational analysis of the protein interaction data was performed looking at network structure and function. This type of analysis can be useful as it can be hard to visualise and describe large networks within a functional context.

Figure 6.8

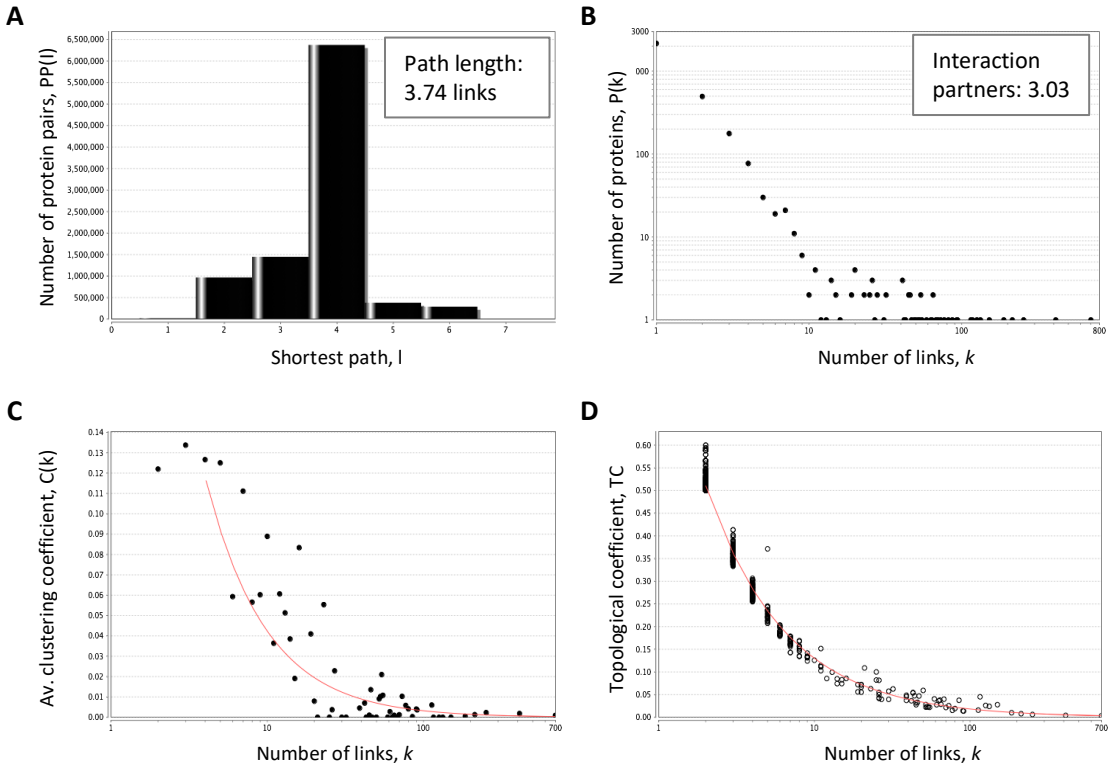

Figure 6.8. Properties of the human predicted HSPome+ Network. (A) Distribution of the shortest path length (l) between pairs of proteins in the predicted HSPome+ network. On average, the path length between any two proteins within the network is 3.74 links. (B) Degree distribution of network proteins. On average, proteins in the network have 3.03 interaction partners. (C) Degree distribution of the clustering coefficients of the network proteins. The average clustering coefficient of all proteins (nodes) with *k* links was plotted against the number of links, *k*. (D) Degree distribution of the topological coefficients of the network proteins. The topological coefficient was calculated for each network protein with >1 interaction partners and plotted against the number of links, *k*.

Path length is a measure of the distance between nodes in the network, calculated as the mean of the shortest distance between all possible node pairs. For the HSPome+ network, a mean shortest path length between any two proteins within the network was calculated as 3.74 links (Figure 6.8 A), which suggests that most proteins are very closely linked ensuring that information spreads easily throughout the network, a property which is often seen in 'small-world' networks. 'Small-world' networks have short path lengths between nodes in the network, as they tend to be more highly clustered than 'random' networks (Watts and Strogatz, 1998). For

example, if node A is linked to node B and node B is linked to node C, then there is an increased probability that A will also be linked to C (Strogatz, 2001).

In the study of networks, the degree of a protein(node) is the number of connections or edges the protein has to other proteins. The degree distribution P(*k*) is the number of proteins in the network with degree, *k*. As shown in Figure 6.8 B, the degree distribution of the HSPome+ network proteins is highly right-skewed, which means that the large majority of proteins have low degree but a small number, known as 'hubs', have a high degree. This observation is common to most networks in the real world and is in agreement with most biological networks (Barabási and Oltvai, 2004). Proteins in the HSPome+ network have on average, 3.03 interaction partners. However, 2,163 proteins have only one partner (which includes 6 HSP protein nodes), whilst there are 42 HSP 'hub' proteins each with more than 30 interaction partners. Studies in yeast have previously demonstrated the importance of protein hubs, as they were shown to be three times more likely to be essential for cells than proteins with fewer interactions (Jeong *et al.*, 2001). It is therefore important for the hubs identified in our HSPome+ network to be analysed further, with regards to cellular function.

Looking at the topological properties of our HSPome+ interaction network, we calculated the average clustering coefficient C(*k*), which is a measure of the tendency of network proteins to form clusters or groups (Barabási and Oltvai, 2004). As shown in Figure 6.8 C, the overall clustering of the HSPome+ network decreased as the number of interactions (links) per protein increased, indicating a potential hierarchical organisation in the HSPome+ network (Ravasz *et al.*, 2002; Ravasz and Barabási, 2003). Interestingly, this hierarchical-type manner of organisation is a key feature in the organisation of complex biological systems, and is particularly associated with the structure and function of neural networks (Kaiser, Hilgetag and Kötter, 2010).

The topological coefficient, was also used to study the topological characteristics of the HSPome+ network. The topological coefficient TC(*k*), is a relative measure for the

tendency of proteins within the network to share common interaction partners (Ravasz *et al.*, 2002; Goldberg and Roth, 2003). Proteins that have no, or one interaction partner are assigned a topological coefficient of 0. As shown in Figure 6.8 D, the topological coefficient also decreased as the number of interactions (links) per protein increased, proving that in the HSPome+ network, 'hub' proteins do not have more common interactors than proteins with fewer links. Therefore, highly-connected proteins do not artificially cluster together. Furthermore, this confirms the modular hierarchical network organisation implicated by the clustering coefficient.

6.5.3 Functional annotation

Some of the known HSP interaction partners, such as RTN4, which interacts with both ATL1 and ARL6IP1, are known to be functionally associated with HSP (Hu *et al.*, 2009). However, the majority of the interactors identified in this study have no prior link with HSP. Therefore, a number of bioinformatics and computational analyses were carried out to investigate functional trends or common themes.

6.5.3.1 Reactome pathway analysis

The Reactome Knowledgebase (www.reactome.org) is a freely available, manually curated and peer-reviewed pathway database, which allows the analysis of complex experimental and computational data. This pathway-based tool identifies human proteins that are enriched in specific cellular pathways linking them to their molecular functions and biological pathways (Croft *et al.*, 2014; Fabregat *et al.*, 2016). Enrichment of a particular pathway or process requires a statistically significant p-value of <0.05.

The HSP seed 3 gene list containing 83 HSP proteins was uploaded onto Reactome and the Pathway Analysis tool was used to analyse the dataset (see Appendix 6.2 for full Reactome dataset). Results from this analysis show an enrichment of proteins involved in vesicle-mediated transport processes, including membrane trafficking, Golgi-to-ER retrograde transport and other transport-related processes (see Figure

6.9 A). The enrichment of proteins in this particular process is important as it is thought to be one of the main functional processes involved in the pathophysiology of HSPs. The pathway analysis tools, were unable to match 22 HSP proteins to any of the pre-defined Reactome pathways.

Figure 6.9

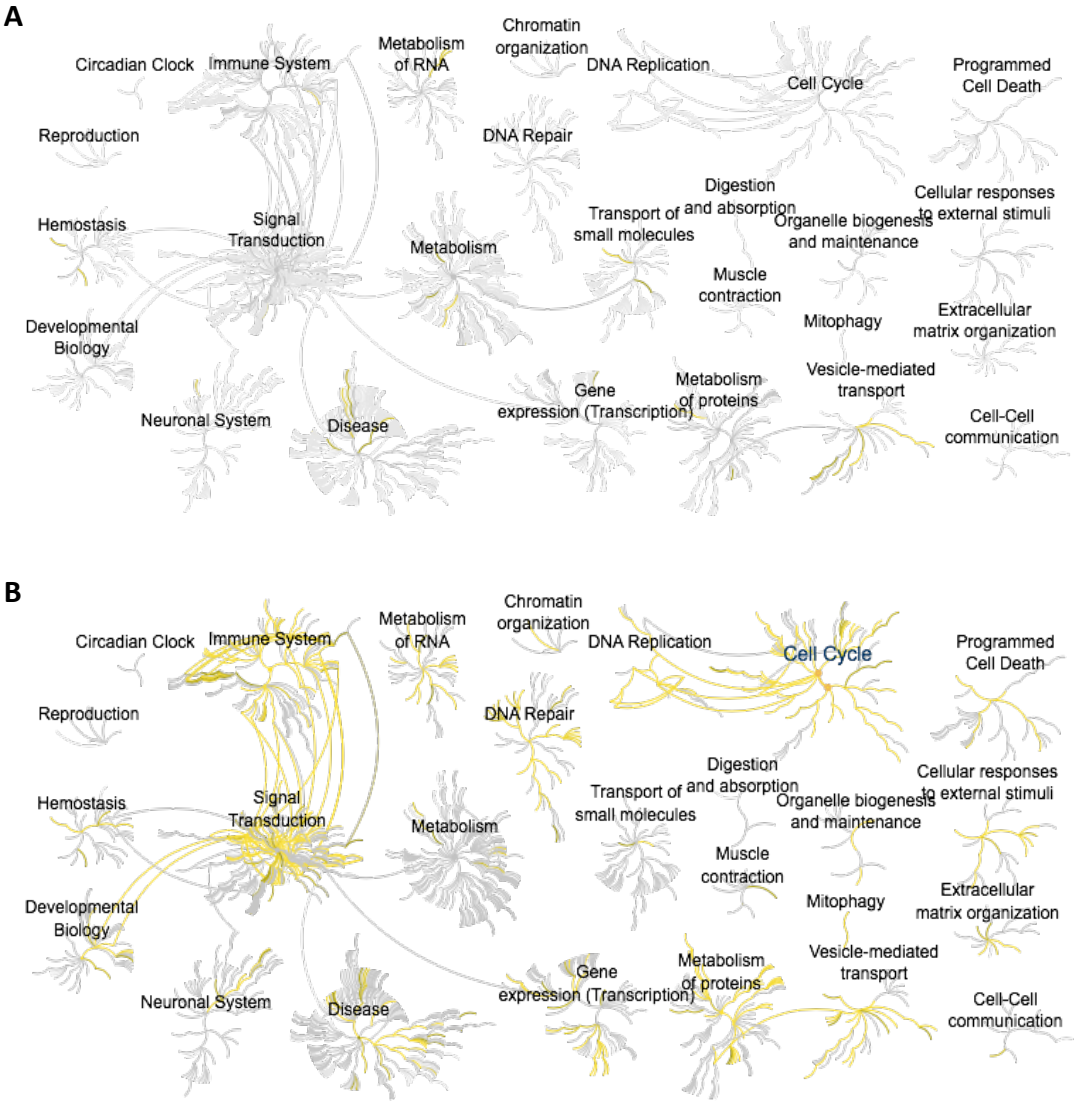

Figure 6.9. Comparative pathway analysis of HSP seed 3 proteins and the predicted HSPome+ network proteins. Reactome pathway enrichment analysis was performed on (A) the HSP seed 3 list (83 proteins), and (B) the HSP interaction partners from the predicted HSPome+ network (3,074 proteins). In each case, enriched pathways are highlighted in yellow.

To understand more about the overall biological processes involved in HSP, the full set of HSP interaction partners identified in the HSPome+ network were subsequently analysed using Reactome and the results were compared with those obtained in the initial analysis (Figure 6.9). As a result, proteins involved in cell cycle, DNA replication, signal transduction and metabolism of proteins were found to be comparatively enriched in the HSPome+ network (Figure 6.9 B). Interestingly, there was also an enrichment of proteins involved in the immune system signalling, focusing on both adaptive and innate immune signalling, involving over 300 proteins, correlating well with results discussed in Chapter 5. Furthermore, upon closer inspection of the proteins implicated in the cell cycle and DNA replication, a number of proteins from each group were found to be involved in the immune system, more specifically NF-κB signalling.

The Reactome pathway analysis tools, were however unable to match 610/ 3,074 HSP interacting proteins to any of the pre-defined Reactome pathways. Moreover, 232/ 610 were HSP interactors identified following the studies described in this thesis. Having identified a considerable number of potentially new HSP-related proteins it is therefore not surprising that a proportion of these are not already pre-defined in Reactome pathways as they are novel and not previously annotated.

6.5.3.2 PANTHER functional analysis

The PANTHER (Protein ANalysis THrough Evolutionary Relationships) Classification System (www.pantherdb.org) is a freely available, manually curated bioinformatics resource, which was designed to classify proteins (and their genes) to facilitate large-scale, high-throughput gene function analysis by combining gene function, ontology and pathway data (Mi *et al.*, 2013). The entire HSPome+ protein interaction data was uploaded into PANTHER and analysed (see Appendix 6.3 for full PANTHER dataset). As shown in Figure 6.10, only gene ontology (GO) categories with a statistically significant p-value of <0.05 are displayed.

Figure 6.10

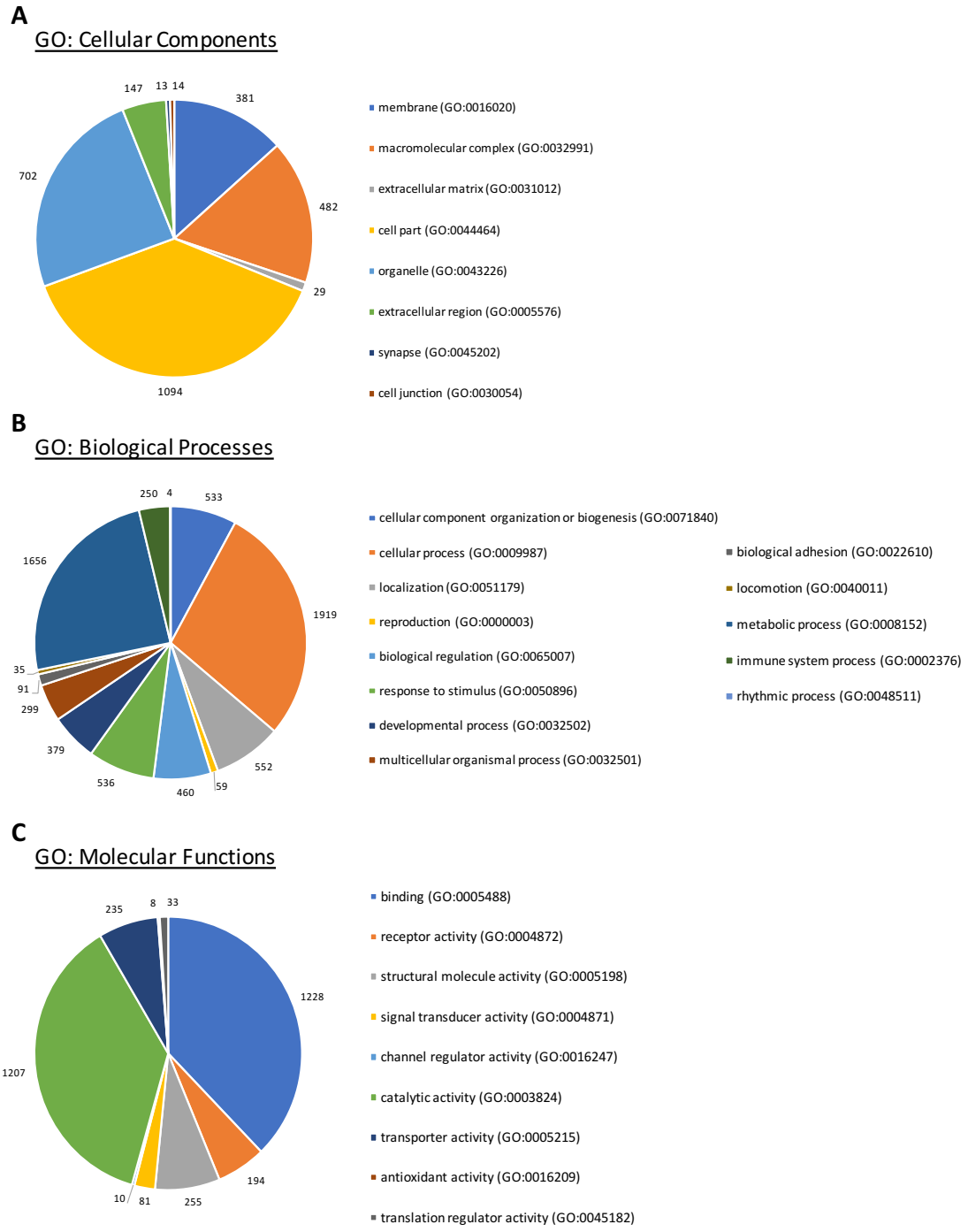

Figure 6.10. PANTHER functional GO term enrichment analysis. PANTHER gene function analysis was performed on HSP interaction partners identified in the HSPome+. The relative representation of cellular components (A), biological processes (B) or molecular functions (C) was compared. In each case, the numbers within each section of the pie chart represent the number of enriched proteins assigned to a given GO category.

The GO Cellular Component analysis (Figure 6.10 A) highlighted a significant proportion of proteins found to be enriched in the Cell Part (GO:0044464), which consisted mainly of cytoplasmic proteins and membrane-bound proteins, including ER-membrane network proteins. Organelle (GO:0043226) was the second largest category identified, and this was found to be predominantly composed of the nucleus and cytoskeleton.

In addition to assessing the enrichment of 'cellular component' identifiers, proteins were also assessed for their involvement in GO Biological Processes (Figure 6.10 B). A large proportion of proteins were found to be associated with Cellular Processes (GO:0009987) such as 'cell communication', 'cell growth' and 'cellular component movement'. A similar number of proteins were also associated with Metabolic Processes (GO:0008152). Interestingly, 250 proteins were enriched in Immune System Processes (GO:0002376), in particular 'immune response'.

Finally, proteins were annotated for GO Molecular Function (Figure 6.10 C). A large proportion of proteins were found to be involved in Binding (GO:0005488), and in particular 'antigen binding' and 'nucleic acid binding'. Another, similarly enriched function was Catalytic Activity (GO:0003824), in particular 'hydrolase activity' and 'transferase activity'. Furthermore, there were over 250 proteins which were found to be enriched for Structural Molecule Activity (GO:0005198), and predominantly involved in the 'structural constituent of the cytoskeleton'.

The re-occurrence of pathways involving cytoskeletal dynamics and immune signalling in the results from different bioinformatics tools and databases provide an increase in confidence in the functional prediction/conclusions gathered following our targeted Y2H studies (as discussed in Chapters 4 and 5).

6.5.4 Disease annotations

Functional annotation using freely available bioinformatics resources, such as Reactome and PANTHER, can provide detailed information regarding the molecular

function of an individual protein and its interactors, as well as its role in an overall biological process. In addition, identification of diseases associated with HSP interaction partners may also provide further insight into the mechanism of development and progression of disease.

6.5.4.1 MGI (Mouse Genome Informatics)

MGI (Mouse Genome Informatics) is online laboratory mouse database which incorporates genomic, genetic and biological data to facilitate the study of human health and disease. MGI has a number of tools, including the Human – Mouse: Disease Connection (HMDC) tool, in which mouse mutation, phenotype and disease model data is integrated with human gene-to-disease relationships from the NCBI, Online Mendelian Inheritance in Man (OMIM), and the Human Phenotype Ontology (HPO), which allows the projection of human gene lists onto mouse phenotype and disease data. This tool generates a list of phenotypes and/or diseases associated with a particular gene, and the potential human relevance where applicable.

The full list of interactors from the HSPome+ network (2,991) was uploaded onto MGI and analysed using the HMDC tool. The HSPome+ human gene IDs were converted into 4,106 mouse genes, of which 2,397 were associated with abnormal mouse phenotypes and more specifically 1,325/2,395 (55.28 %) were associated with defects in 'behaviour/neurological' or 'nervous system' (see Appendix 6.4 for full MGI analysis). There were also 627 human connected proteins associated with human diseases. Interestingly, the mouse-to human connections showed associations with several neurological disorders including, Alzheimer's disease, amyotrophic lateral sclerosis (ALS) and Charcot-Marie-Tooth disease (CMT).

To determine whether there was an inherent bias towards an abnormal neurological phenotype, we performed the same analysis on a 'control' set of 2,991 human gene IDs, which were randomly chosen from the Expanded Global network generated in Chapter 3 using the Excel RAND function. The randomly generated list of human gene IDs were converted into mouse genes and the percentage of the abnormal mouse

phenotypes, more specifically those associated with defects in 'behaviour/neurological' or 'nervous system' was calculated as above (see Appendix 6.4 for full MGI analysis). This was repeated in order for appropriate statistical analysis to be done, see Table 6.5 and 6.6.

Table 6.5

	n	Mean	Std. Deviation	Std. Error Mean
%	20	52.169	0.2675	0.0598

Table 6.5. One-Sample Statistics. Basic statistical information about the selected variable, % of abnormal mouse phenotypes associated with defects in 'behaviour/neurological' or 'nervous system', including sample size (n), mean, standard deviation and standard error.

Table 6.6

	Test Value = 55.28 %			
	t	df	p-value	Mean Difference
%	52.0065	19	5.921E-22	-3.1

Table 6.6. One-Sample Test. Displays the results most relevant to the One-Sample *t* Test, including the test statistic of the one-sample *t* test, denoted *t*, the degrees of freedom for the test (df = *n*-1), the two-tailed p-value corresponding to the test statistic and the mean difference.

These results show that there is a high proportion of proteins associated with abnormal neurological phenotypes, which given the naturally large abundance of proteins expressed in the brain (Uhlen *et al.*, 2015) would seem like a normal background reading. However, these results also show that there is a significant difference in the mean percentage of abnormal mouse phenotypes associated with defects in 'behaviour/neurological' or 'nervous system' between the randomly selected control samples and the HSPome+ ($p < 0.001$), which could suggest a potential role for the HSPome+ proteins in neurological disorders, and this may provide insight into the molecular mechanisms involved in HSP pathology.

The combined functional and disease annotation results provide potential insight into the physiological and pathophysiological processes potentially associated with HSP. Although these analysis tools generate predictions, they may provide new insight into the molecular mechanisms of HSP pathology, which could also be applied to future work and also to other axonopathy-related neurodegenerative diseases.

6.6 Discussion

The interaction partners identified in the various Y2H library screens are involved in a variety of cellular processes, including translational and transcriptional regulation. Some of these proteins are also involved in the pro-inflammatory NF-κB pathway, which could be significant given the strong evidence for functional crosstalk between innate inflammatory responses and neurodegeneration (Glass et al., 2010). In addition, many of the interacting proteins identified are involved in various aspects of ER dynamics, including the mechanisms underlying ER network formation. Several of these proteins were found to be participating in a network of interactions among HSP proteins involved in ER shaping (Figure 6.10 B), which further supports the hypothesis that abnormal ER morphology and distribution is a pathogenic mechanism in HSP and related neurologic disorders, such as amyotrophic lateral sclerosis (ALS) (Goyal and Blackstone, 2013).

Neurodegeneration is a condition in which changes in neuronal structure and function lead to a decrease in neuronal survival and an increase in neuronal death in the CNS (Kempuraj et al., 2016). Despite the extensive heterogeneity associated with hereditary spastic paraplegia (HSP), there is a relatively small number of common pathogenic themes which link sets of HSP proteins to different function modules including endoplasmic reticulum (ER) shaping/distribution, mitochondrial function, myelination, lipid/cholesterol metabolism and endocytic sorting (Blackstone, O'Kane and Reid, 2011; Blackstone, 2012).

The ER is a continuous membranous network comprising the nuclear envelope and a dynamic network of branched, highly curved tubules and peripheral sheet-like

cisternae, often studded with ribosomes, and distributed throughout the cytoplasm (Montenegro et al., 2012). Highly polarised cells such as neurons can be large and complex in nature, which can present issues for shaping and distribution of the ER network (Renvoisé and Blackstone, 2010). Disruption in the tubular ER network in cells has emerged as a key pathogenic theme in HSP (Blackstone, O'Kane and Reid, 2011; Blackstone, 2012), indicating the importance of proper ER morphology and distribution, which likely plays an important role in neuronal maintenance (Renvoisé and Blackstone, 2010; Beetz, Johnson, *et al.*, 2013). Protein synthesis, transport and quality control in the ER are well-studied, however, the mechanisms underlying the distinct ER architecture have only more recently emerged, with the identification of several protein families known to be involved (Park and Blackstone, 2010; Goyal and Blackstone, 2013). Significantly, many of the proteins involved are known to harbour autosomal dominant mutations associated with some of the most common forms of HSP: SPAST, ATL1 and REEP1 (spastin, atlastin-1, and REEP1 proteins, respectively) (Blackstone, O'Kane and Reid, 2011; Blackstone, 2012).

The main ER-shaping protein families include the curvature-stabilizing reticulon and REEP/DP1/Yop1p families (Montenegro *et al.*, 2012). Although these protein families, have little sequence homology, they do share common elongated hydrophobic segments, which are important for targeting to different ER domains and contribute to ER shaping (Voeltz *et al.*, 2006; Ronchi *et al.*, 2008). These segments are predicted to be partially membrane-spanning hairpin (or wedge) domains, which contribute to 'hydrophobic wedging', thus inducing membrane curvature, as the majority of the hydrophobic segment is located in the outer leaflet of the membrane (Collins, 2006; Hu *et al.*, 2008). These ER-shaping proteins are essential for generating and stabilising the high membrane curvature found in both ER tubules and sheets (Montenegro *et al.*, 2012). In addition to producing highly-curved ER tubules, the ER-shaping reticulon and REEP/DP1/Ypo1p families also interact with the atlastin/RHD3/Sey1p family to mediate the formation of three-way junctions in the ER (Rismanchi *et al.*, 2008; Hu *et al.*, 2009), enabling the fusion of tubules required to generate the characteristic tubular ER network. The atlastin family of dynamin-related GTPases are large, multimeric, integral membrane proteins located mainly on highly-curved ER

membranes, which include ER tubules and sheets (Zhu *et al.*, 2003; Rismanchi *et al.*, 2008; Hu *et al.*, 2009).

Furthermore, links between the microtubule cytoskeleton and ER proteins can provide additional information with regards to the overall distribution dynamics of the ER network (Goyal and Blackstone, 2013). Atlastins can also interact with the hydrophobic hairpin domain of the microtubule-severing AAA ATPase protein, spastin, located near the N-terminus of the larger isoform, M1 (Sanderson *et al.*, 2006; Park *et al.*, 2010). Atlastins and M1 spastin, can also interact directly with REEPs/DP1 and reticulons in the tubular ER (Park *et al.*, 2010). The human REEP family is composed of 6 members: REEP1-6, which can be divided into two structurally and phylogenetically distinct groups, comprising REEP1-4 and REEP5-6 (Park *et al.*, 2010). REEP1-4 are directly involved in ER shaping, like REEP5-6, however they are also involved in ER network remodelling as they can interact directly with microtubules through the C-terminal cytoplasmic domain (Park *et al.*, 2010).

Additionally, ZFYVE27 (protrudin), was more recently identified as a protein involved in the formation of the tubular ER, and like the reticulon and REEP/DP1/Yop1p families, it too has hydrophobic hairpins that generate high curvature in ER tubules. ZFYVE27 also interacts with other ER-shaping proteins such as REEP1, ATL1 (Chang et al., 2013) and SPAST (Mannan *et al.*, 2006). In neurons, ER distribution is coupled to cytoskeletal dynamics, involving predominantly microtubules (Blackstone, O'Kane and Reid, 2011) and so it is therefore important that these co-ordinated interactions provide an insight into the potential mechanism for connecting ER membrane remodelling with cytoskeletal dynamics (Park *et al.*, 2010).

Understanding more about ER structural dynamics and its role in neurodegeneration will provide a greater insight into the mechanisms by which loss of ER-shaping proteins may give rise to neurodegeneration in HSPs and other neurodegenerative diseases. The HSPome+ network can be used as a resource to guide future hypothesis-driven research into the physiological mechanisms and functional

relevance of these interactions, providing a greater insight into the potential molecular mechanisms of HSP pathology.

Chapter 7: Discussion

7.1 Introduction

The study of protein-protein interactions is essential in understanding how biological processes work, since most proteins function as part of dynamic multi-protein complexes.

Human disease is usually a result from the imposed perturbation of protein-protein interactions (PPIs), which confer a net functional change of various pathobiological processes within complex global interaction networks. Systematic network-based approaches to human disease, provides an unbiased mechanism to explore the detailed nature of physiological regulation, which may provide new insight into the identification of specific disease modules and pathways, identifying potential novel biomarkers and/or strategies for therapeutic intervention (Barabási, Gulbahce and Loscalzo, 2011). Traditionally, protein interactions were studied individually, through large numbers of relatively small-scale hypothesis-driven approaches (Ng *et al.*, 2003). However, technological advances in proteomics led to the rapid discovery of new proteins, which created a need for high-throughput "binary" and "non-binary" interaction detection methods for the identification of large numbers of protein-protein interactions, such as yeast two-hybrid (Y2H) (Stelzl *et al.*, 2005; Yu *et al.*, 2008) and affinity purification-mass spectrometry (AP/MS) approaches (Guruharsha *et al.*, 2011).

To date, several large-scale high-throughput studies have contributed to the increase in coverage of the human interactome. These include a high-throughput yeast two-hybrid study conducted by Rolland et al. (2014), in which ~14,000 human binary protein-protein interactions were identified. More recently, an affinity purification-mass spectrometry (AP/MS) approach identified interacting partners for 2,594 human proteins, resulting in a network containing 23,744 interactions among 7,668 human proteins, revealing complexes/clusters of functionally-related proteins (Huttlin *et al.*, 2015). The majority of known binary protein-protein interactions are

identified using only a single detection method (Rolland *et al.*, 2014), although using different detection methods generally produces complementary rather than redundant data (Zhao *et al.*, 2005).

Therefore, identifying proteins that either directly or indirectly interact with known HSP proteins, may identify new candidate genes for genetic screening, whilst also providing insights into the molecular mechanisms of HSP pathology. In this context, the main aim of this study was to systematically identify novel HSP interactions, which in conjunction with known interaction profiles could then be used to generate an extended high-confidence map of the human HSP interactome, thereby providing a resource to inform future hypothesis-driven research.

7.2 Increased coverage of the human HSP network

7.2.1 Binary protein-protein interactions (PPIs)

To achieve this aim, a collection of human HSP open reading frames (ORFs) was generated. As described in Chapter 3, an initial search of public databases and literature was undertaken, identifying current HSP-encoding genes, resulting in an initial list of 58 putative HSP-related proteins, with unique gene identifiers, referred to as 'HSP seed 1' in this study. A final panel of 44 unique HSP ORFs were successfully cloned into the Gateway cloning system. These sequence-verified HSP ORFs were used to generate a collection of Y2H HSP bait (33) and HSP prey (24) clones, for use in high-throughput targeted yeast two-hybrid assays to investigate potential binary HSP:HSP protein interactions. Significantly, this targeted Y2H matrix mating approach identified 15 binary HSP:HSP interactions, 12 of which were novel (Chapter 4).

In an attempt to identify new mechanisms of regulating the abundance or function of known HSP proteins, we also investigated the interaction of 33 Y2H HSP bait clones with an existing collection of 177 human RING E3 ligase (including 39 TM-RING-E3) prey clones. Results from targeted Y2H matrix mating assays identified 88 binary HSP:RING E3 ligase interactions, of which 86 were found to be novel. Additionally,

the interaction of 24 Y2H HSP prey clones with an existing collection of 59 deubiquitinating enzymes (DUBs) bait clones, were also investigated. Results from these targeted Y2H matrix mating assays identified 15 binary HSP:DUB interactions, of which 13 of were novel (Chapter 5).

Following targeted Y2H assays, a selection of 10 Y2H HSP bait constructs were successfully generated and individually screened against two, high complexity cDNA prey libraries. The combined results from these screens identified 89 potentially novel binary interactions, and 85 potentially novel HSP interaction partners. As a significant number of HSP proteins contain one or more transmembrane domain. The membrane yeast two-hybrid (MYTH) library system was employed to investigate the interaction profiles for 10 MYTH HSP bait constructs. Each of the MYTH bait constructs were individually screened against a human whole brain cDNA prey library, resulting in the identification of 195 potentially novel interactions and 124 potentially novel HSP interactors (Chapter 6).

7.2.2 Global HSP interactome

In addition to generating a defined high-density binary HSP interaction network, it is also important to know which proteins may associate indirectly with known HSP proteins, as components of large multi-protein complexes. Therefore, all binary HSP interactions identified in this study were combined with the high-density, comprehensive interaction data of the initial HSPome, resulting in an 'updated' HSP network containing 4,688 interactions between 3,074 human proteins. This new high-density network, referred to as the HSPome+ network, represents an increase of >60 % in the number of direct (binary) HSP protein-protein interactions. This high-density, comprehensive HSP interactome can be continually enriched with experimental interactions data and used to inform future hypothesis-driven research, as well as for the development of new strategies for therapeutic intervention.

7.3 Functional significance of novel HSP interactions

As most proteins function as part of dynamic, multiprotein complexes, high-density protein-protein interaction maps can be used to facilitate the identification of common biological pathways, and potential pathophysiological mechanisms of disease (Vallabhajosyula *et al.*, 2009).

ER stress in neurodegenerative diseases

The ongoing identification of HSP-associated loci/genes has been critical to our understanding of the clinical and pathological features of this group of disorders. HSP-related proteins are known to cluster into several functional subgroups or modules, with many HSP proteins functioning in more than one cellular process (as discussed in Chapter 1). Although the number of HSP-related pathogenic themes have evolved over time, it is thought that the largest group of HSP proteins involved in ER membrane trafficking and/or organelle morphogenesis and distribution (Blackstone, O'Kane and Reid, 2011).

Most individuals with HSP are affected by autosomal dominant mutations (Salinas *et al.*, 2008), which predominantly affect organelle dynamics, in particular the ER and ER morphology and distribution (Beetz *et al.*, 2013). Interestingly, we identified links between several functionally-related cellular processes which also have the potential to affect the overall dynamics of the ER network. Therefore, if multiple HSP-related proteins are involved in ER network dynamics, it is pertinent to ask how abnormalities in this process might lead to a neurodegenerative HSP phenotype.

The endoplasmic reticulum (ER) is a multifunctional organelle, which is also essential for the synthesis, modification, quality control and transport of integral membrane and secreted proteins (Oslowski and Urano, 2011). The ER is continuously monitoring protein folding and degradation, in order to avoid the accumulation of misfolded proteins (Vembar and Brodsky, 2008). The accumulation and aggregation of misfolded proteins is a common feature among neurodegenerative diseases such as Alzheimer's disease (AD), Parkinson's disease (PD), Huntington's disease (HD) and

amyotrophic lateral sclerosis (ALS) (Kopito and Ron, 2000; Taylor, Hardy and Fischbeck, 2002; Selkoe, 2003; Soto and Estrada, 2008). The presence of misfolded proteins can trigger cellular stress responses, which activate the UPR, thereby protecting cells against the toxic build-up of misfolded proteins and maintaining normal biological processes within the brain during periods of cellular stress (Kopito, 2000; Dobson, 2003; Rao and Bredesen, 2004). Accumulation of misfolded proteins in excessive amounts can overwhelm the 'cellular quality control' system and the prolonged stress observed in neurodegenerative diseases is thought to disrupt the protective mechanisms of the UPR. Failure of the UPR system to alleviate ER stress can result in chronic ER stress causing cell dysfunction and death through the activation of inflammation and apoptotic pathways, which promote neurotoxicity (Rao and Bredesen, 2004; Kim, Xu and Reed, 2008; Sprenkle *et al.*, 2017). Therefore, understanding more about the role of ER stress in neurodegenerative diseases may provide a novel insight into disease mechanisms involved in the progressive axonal degeneration observed in HSPs and other neurodegenerative diseases, and identifying potentially novel therapeutic strategies for these disorders may be possible.

In addition, it is significant to note that high-throughput interaction profiling performed in this study led to the identification of novel 'edgetic' effects within the HSP interactome. As a consequence, the re-structuring of the HSP protein interaction networks may confer changes in ER structure and/or function as well as associated cellular processes, which in turn may lead to increased levels of ER stress. Furthermore, this study identified interactions between several disease-associated mutant HSP proteins and HSPD1. HSPD1 is a highly conserved protein initially identified as a mitochondrial chaperone (Quintana and Cohen, 2011), which upon exposure to stress stimuli, functions as a signalling molecule in the immune system, activating both adaptive and innate immune responses (Landstein, Ulmansky and Naparstek, 2015), thereby highlighting a potential link between HSP, ER stress and the immune response.

ER stress-linked inflammation in neurodegenerative diseases

Interestingly, we identified 37 RING E3 ligases and 9 DUBs, which interacted with various HSP-related proteins. Interrogation of the publicly available bioinformatics resource DAVID, provided functional data suggesting that immune response mechanisms, more specifically, 'positive regulation of NF-κB signalling', and UPR-related processes, in particular 'protein K48-linked ubiquitination' were two significantly enriched functional clusters. At present, we can only speculate on the functional role that HSPs interacting with RING E3 ligases or DUBs may have. However, if HSP proteins are involved in 'immune response mechanisms' and 'UPR-related processes', then this raises the question of how abnormalities in these processes lead to a neurodegenerative HSP phenotype.

The unfolded protein response (UPR) has traditionally been viewed as a highly conserved, adaptive cellular response to ER stress, which is typically activated by an accumulation of unfolded or misfolded proteins. The UPR aims to reduce cellular stress and restore ER homeostasis by co-ordinating the expression of ER stress response signal transducers during ER stress (Oslowski and Urano, 2011; Walter and Ron, 2011). However, the UPR is also able to mediate inflammatory pathways essential for innate immune response. The UPR is able to activate several primary inflammatory signalling proteins, including the Mitogen Activated Protein Kinase (MAPK) family proteins: c-Jun N-terminal kinase (JNK) and p38, and the Nuclear Factor-kappa-light-chain-enhancer of activated B cells (NF-κB) (Sprenkle *et al.*, 2017). NF-κB is a family of transcription factors which play a crucial role in the inflammatory response, regulating the expression of many inflammatory cytokines (Wang *et al.*, 2006; Ghosh and Hayden, 2008; Baltimore, 2009). Inflammation is an initial protective response of the innate immune system, carried out by different immune and inflammatory cells in order to repair, regenerate and remove damaged tissues/cells and harmful stimuli (Kulkarni *et al.*, 2016). In the brain microglia are the main immune cells which constantly monitor the microenvironment and under physiological conditions, they remain in an 'inactive' state (Streit, 2002). However, in response to pathogens or tissue damage, they become 'active', promoting an inflammatory response (Glass *et al.*, 2010).

In the absence of harmful stimuli, NF-κB resides in the cytoplasm where it is bound to a member of the family of inhibitors of NF-κB (IκB), which are constitutively expressed, thus NF-κB remains in an inactive state (Shih, Wang and Yang, 2015). Ubiquitin-mediated protein degradation has a regulatory role in both canonical and non-canonical NF-κB activation pathways. Abnormal activation occurs in many pathological conditions such as auto-inflammatory diseases (Iwai, 2012).

Innate immune activation appears to be an important factor in the pathology of neurodegenerative diseases. The involvement of immunity was first described over 20 years ago (McGeer *et al.*, 1987; Griffin *et al.*, 1989), however the potential consequences of inflammation in the pathogenesis of neurological disorders is a more recent development (Heneka, Kummer and Latz, 2014). In the CNS, neuroinflammation is the initial protective response mechanism carried out by microglia and astrocytes, to restore damaged glial cells and neuronal cells (Streit and Kincaid-Colton, 1995; Shabab *et al.*, 2017). However, sustained or chronic microglial activation can promote a neurotoxic environment (Prinz and Priller, 2014; Sofroniew, 2015). Abnormalities in UPR-mediated inflammatory pathways may lead to sustained neuroinflammation. Sustained or chronic neuroinflammation is considered to be a potential pathogenic factor contributing to neuronal dysfunction, injury and loss (and hence disease progression) in a number of neurodegenerative diseases, including Alzheimer's disease (AD), Parkinson's disease (PD), Multiple Sclerosis (MS) and amyotrophic lateral sclerosis (ALS) (Glass *et al.*, 2010; Chen, Zhang and Huang, 2016; Kempuraj *et al.*, 2016).

ER stress and neuroinflammation are both pathological features observed in several neurodegenerative diseases, and whilst a connection between the two has been observed in a number of other diseases, including autoimmune disease (Li *et al.*, 2005; Gargalovic *et al.*, 2006) and metabolic disorders (Ozcan *et al.*, 2004, 2006), understanding of the mechanisms by which ER stress mediated neuroinflammation during neurodegeneration remains unclear. However, exploring the cross-talk between ER stress and inflammation may provide us with new insight into whether

targeting cellular stress pathways, such as ER stress in neurodegeneration, may contribute to the control of aberrant neuroinflammation, thereby contributing to neurological disorders (Sprenkle *et al.*, 2017).

7.4 Future directions

The data presented in this study extends our understanding of the potential complexity of the human HSP interactome. However, there are still areas of data paucity. For example, 25 of the 83 known HSP-related proteins have not yet been systematically investigated. As these proteins were only discovered and/or assigned as HSP-related after the start of this study, they were not included in our initial high-throughput Y2H screens, therefore these present as obvious candidates for future investigation. In addition, the 14 HSP proteins from the original 'HSP seed 1' list that were excluded due to size could be truncated and/or fragmented. Truncation and/or fragmentation studies would also be useful for further investigation, identifying specific domains and/or binding sites.

Yeast two-hybrid is a powerful technique to assess binary protein-protein interactions. It is mainly used to obtain qualitative results, which in conjunction with other interaction data can be used to generate protein-protein interaction networks, a useful tool to inform future hypothesis-driven research. However, qualitative genetic and biochemical techniques like yeast two-hybrid or affinity purification-based approaches do not reflect the cellular situation of the dynamic nature of many PPIs. To gain a better understanding of the complex cellular processes, not only do we need to know which proteins interact, but we also need to develop a more comprehensive understanding of the functional characteristics of a particular interaction. This can be done using quantitative PPI detection methods such as, Förster resonance energy transfer (FRET), fluorescence cross-correlation spectroscopy (FCCS) and dual luminescence-based co-immunoprecipitation (DULIP), which can provide quantitative information regarding the interaction strength (Buntru *et al.*, 2016). It would therefore be advisable to expand the current analysis by performing a targeted secondary analysis of these putative interactions, to

confirm the physiological relevance of each interaction in mammalian cells using one of the techniques mentioned.

ER stress and the UPR, are rapidly developing into an important area of research. There is growing evidence for the accumulation of misfolded and unfolded proteins, and the involvement of the UPR in several neurodegenerative diseases. Data presented in this study, also suggest the involvement of these processes in Hereditary Spastic Paraplegia. Although there is strong evidence for the occurrence of ER stress responses in neurodegenerative diseases, the exact role of ER stress and the importance of ER stress and UPR, in terms of the evolution of neurodegeneration, is not clear. To understand more about the role that ER stress may play in neurodegenerative disorders, including HSP, it will be important to target the UPR and the individual UPR master regulators: PERK, IRE1 and ATF6 using both pharmacological and genetic manipulation (Hetz and Mollereau, 2014). A logical initial step would be to characterise how the UPR is affected using an *in vitro* model of a particular HSP, possibly utilising a patient-derived stem cell model as described by Abrahamsen *et al.* (2013), which could be used to assess how the knockdown of each individual UPR master regulator affects cell fate. In addition, there are a number of different animal models available, including a number of mouse models representing different types of HSP (Ferreirinha *et al.*, 2004; Tarrade *et al.*, 2006; Beetz, Johnson, *et al.*, 2013; Khundadze *et al.*, 2013), which would facilitate our understanding of the phenotypic consequence of un-regulated UPR activity. If ER stress is the cause of neurodegeneration in HSP, this raises the possibility of developing new neuroprotective treatment strategies.

Bibliography

Abou Jamra, R. *et al.* (2011) 'Adaptor Protein Complex 4 Deficiency Causes Severe Autosomal-Recessive Intellectual Disability, Progressive Spastic Paraplegia, Shy Character, and Short Stature', *The American Journal of Human Genetics*, 88(6), pp. 788–795. doi: 10.1016/j.ajhg.2011.04.019.

Abrahamsen, G. *et al.* (2013) 'A patient-derived stem cell model of hereditary spastic paraplegia with SPAST mutations.', *Disease models & mechanisms*. The Company of Biologists Ltd, 6(2), pp. 489–502. doi: 10.1242/dmm.010884.

Agbaga, M.-P. *et al.* (2008) 'Role of Stargardt-3 macular dystrophy protein (ELOVL4) in the biosynthesis of very long chain fatty acids.', *Proceedings of the National Academy of Sciences of the United States of America*. National Academy of Sciences, 105(35), pp. 12843–12848. doi:10.1073/pnas.0802607105.

Agromayor, M. *et al.* (2009) 'Essential role of hIST1 in cytokinesis.', *Molecular biology of the cell*. American Society for Cell Biology, 20(5), pp. 1374–87. doi: 10.1091/mbc.E08-05-0474.

Aho, S. *et al.* (1997) 'A Novel Reporter GeneMEL1for the Yeast Two-Hybrid System', *Analytical Biochemistry*, 253(2), pp. 270–272. doi: 10.1006/abio.1997.2394.

Akiyama, H. (1994) 'Inflammatory Response in Alzheimer's Disease.', *The Tohoku Journal of Experimental Medicine*. Tohoku University Medical Press, 174(3), pp. 295–303. doi:10.1620/tjem.174.295.

Akizu, N. *et al.* (2013) 'AMPD2 Regulates GTP Synthesis and Is Mutated in a Potentially Treatable Neurodegenerative Brainstem Disorder', *Cell*, 154(3), pp. 505–517. doi: 10.1016/j.cell.2013.07.005.

Aldahmesh, M. A. *et al.* (2011) 'Recessive Mutations in ELOVL4 Cause Ichthyosis, Intellectual Disability, and Spastic Quadriplegia', *American Journal of Human Genetics*. Elsevier, 89(6), pp. 745–750. doi: 10.1016/j.ajhg.2011.10.011.

Alderson, N. L. *et al.* (2004) 'The Human *FA2H* Gene Encodes a Fatty Acid 2-Hydroxylase', *Journal of Biological Chemistry*, 279(47), pp. 48562–48568. doi: 10.1074/jbc.M406649200.

Aligianis, I. A. *et al.* (2006) 'Mutation in Rab3 GTPase-Activating Protein (RAB3GAP) Noncatalytic Subunit in a Kindred with Martsolf Syndrome', *The American Journal of Human Genetics*, 78(4), pp. 702–707. doi: 10.1086/502681.

Allison, R. *et al.* (2013) 'An ESCRT–spastin interaction promotes fission of recycling tubules from the endosome', *Journal of Cell Biology*. The Rockefeller University Press, 202(3), pp. 527–43. doi: 10.1083/jcb.201211045.

Anelli, T. and Sitia, R. (2008) 'Protein quality control in the early secretory pathway.', *The EMBO journal*. European Molecular Biology Organization, 27(2), pp. 315–27. doi: 10.1038/sj.emboj.7601974.

Antonicka, H. *et al.* (2010) 'Mutations in C12orf65 in patients with encephalomyopathy and a mitochondrial translation defect.', *American journal of human genetics*. Elsevier, 87(1), pp. 115–22. doi: 10.1016/j.ajhg.2010.06.004.

Anwar, K. *et al.* (2012) 'The dynamin-like GTPase Sey1p mediates homotypic ER fusion in *S. cerevisiae*', *The Journal of Cell Biology*, 197(2), pp. 209–217. doi: 10.1083/jcb.201111115.

Atkin, G. and Paulson, H. (2014) 'Ubiquitin pathways in neurodegenerative disease.', *Frontiers in molecular neuroscience*. Frontiers Media SA, 7(63), pp. 1–17. doi: 10.3389/fnmol.2014.00063.

Atorino, L. *et al.* (2003) 'Loss of m-AAA protease in mitochondria causes complex I deficiency and increased sensitivity to oxidative stress in hereditary spastic paraplegia', *The Journal of Cell Biology*, 163(4), pp. 777–787. doi: 10.1083/jcb.200304112.

Attwell, D. and Laughlin, S. B. (2001) 'An Energy Budget for Signaling in the Grey Matter of the Brain', *Journal of Cerebral Blood Flow & Metabolism*, 21(10), pp. 1133–1145. doi:10.1097/00004647-200110000-00001.

Baltimore, D. (2009) 'Discovering NF-kappaB.', *Cold Spring Harbor perspectives in biology*. Cold Spring Harbor Laboratory Press, 1(1), p. a000026. doi: 10.1101/cshperspect.a000026.

Barabasi, A.-L. and Albert, R. (1999) 'Emergence of scaling in random networks', *Science (New York, N.Y.)*. American Association for the Advancement of Science, 286(5439), pp. 509–12. doi: 10.1126/SCIENCE.286.5439.509.

Barabási, A.-L., Gulbahce, N. and Loscalzo, J. (2011) 'Network medicine: a network-based approach to human disease.', *Nature reviews. Genetics*. NIH Public Access, 12(1), pp. 56–68. doi: 10.1038/nrg2918.

Barabási, A.-L. and Oltvai, Z. N. (2004) 'Network biology: understanding the cell's functional organization', *Nature Reviews Genetics*, 5(2), pp. 101–113. doi: 10.1038/nrg1272.

Barbosa, M. D. F. S. *et al.* (1996) 'Identification of the homologous beige and Chediak–Higashi syndrome genes', *Nature*. Nature Publishing Group, 382(6588), pp. 262–265. doi:10.1038/382262a0.

Bartel, P. L. and Fields, S. (1995) 'Analyzing protein-protein interactions using two-hybrid system.', *Methods in enzymology*, 254, pp. 241–63.
Available at:http://www.ncbi.nlm.nih.gov/pubmed/8531690.

Bartuzi, P., Hofker, M. H. and van de Sluis, B. (2013) 'Tuning NF-κB activity: A touch of COMMD proteins', *Biochimica et Biophysica Acta (BBA) - Molecular Basis of Disease*, 1832(12), pp. 2315–2321. doi: 10.1016/j.bbadis.2013.09.014.

Beadle, G. W. and Tatum, E. L. (1941) 'Genetic Control of Biochemical Reactions in Neurospora.', *Proceedings of the National Academy of Sciences of the United States of America*, 27(11), pp. 499–506. Available at: http://www.ncbi.nlm.nih.gov/pubmed/16588492.

Beetz, C., Koch, N., *et al.* (2013) 'A spastic paraplegia mouse model reveals REEP1-dependent ER shaping', *Journal of Clinical Investigation*, 123(10). doi: 10.1172/JCI65665.

Beetz, C., Johnson, A., *et al.* (2013) 'Inhibition of TFG function causes hereditary axon degeneration by impairing endoplasmic reticulum structure.', *Proceedings of the National Academy of Sciences of the United States of America*. National Academy of Sciences, 110(13), pp. 5091–6. doi:

10.1073/pnas.1217197110.

Behrends, C. *et al.* (2010) 'Network organization of the human autophagy system.', *Nature*. NIH Public Access, 466(7302), pp. 68–76. doi: 10.1038/nature09204.

Di Bella, D. *et al.* (2010) 'Mutations in the mitochondrial protease gene AFG3L2 cause dominant hereditary ataxia SCA28', *Nature Genetics*, 42(4), pp. 313–321. doi: 10.1038/ng.544.

Bence, N. F., Sampat, R. M. and Kopito, R. R. (2001) 'Impairment of the Ubiquitin-Proteasome System by Protein Aggregation', *Science*, 292(5521), pp. 1552–1555. doi: 10.1126/science.292.5521.1552.

Benoit, C.-E. *et al.* (2010) 'Behavioral/Systems/Cognitive Loss of Quinone Reductase 2 Function Selectively Facilitates Learning Behaviors', *The Journal of neuroscience : the official journal of the Society for Neuroscience*, 30(38), pp. 12690–12700. doi: 10.1523/JNEUROSCI.2808-10.2010.

Berggård, T., Linse, S. and James, P. (2007) 'Methods for the detection and analysis of protein–protein interactions'. doi: 10.1002/pmic.200700131.

Berlin, I. *et al.* (2010) 'The deubiquitinating enzyme USP8 promotes trafficking and degradation of the chemokine receptor 4 at the sorting endosome.', *The Journal of biological chemistry*. American Society for Biochemistry and Molecular Biology, 285(48), pp. 37895–908. doi:10.1074/jbc.M110.129411.

Bernassola, F. *et al.* (2008) 'The HECT Family of E3 Ubiquitin Ligases: Multiple Players in Cancer Development', *Cancer Cell*, 14(1), pp. 10–21. doi: 10.1016/j.ccr.2008.06.001.

Bertolotti, A. *et al.* (2000) 'Dynamic interaction of BiP and ER stress transducers in the unfolded-protein response.', *Nature Cell Biology*, 2(6), pp. 326–332. doi: 10.1038/35014014.

Bhattacharyya, S. *et al.* (2014) 'Regulated protein turnover: snapshots of the proteasome in action', *Nature Reviews Molecular Cell Biology*, 15(2), pp. 122–133. doi: 10.1038/nrm3741.

Björkhem, I. and Meaney, S. (2004) 'Brain cholesterol: long secret life behind a barrier', *Arteriosclerosis, thrombosis, and vascular*.
Available at: http://atvb.ahajournals.org/content/24/5/806.short.

Blackstone, C. (2012) 'Cellular pathways of hereditary spastic paraplegia.', *Annual review of neuroscience*, 35, pp. 25–47. doi: 10.1146/annurev-neuro-062111-150400.

Blackstone, C., O'Kane, C. J. and Reid, E. (2011) 'Hereditary spastic paraplegias: membrane traffic and the motor pathway.', *Nature reviews. Neuroscience*, 12(1), pp. 31–42. doi: 10.1038/nrn2946.

Block, R. *et al.* (2010) 'Altered cholesterol and fatty acid metabolism in Huntington disease', *Journal of clinical*. Available at: http://www.sciencedirect.com/science/article/pii/S1933287409004371

Blumen, S. C. *et al.* (2003) 'A locus for complicated hereditary spastic paraplegia maps to chromosome 1q24-q32', *Annals of Neurology*, 54(6), pp. 796–803. doi: 10.1002/ana.10768.

Bonavita, R. *et al.* (2014) 'Cep126 is required for pericentriolar satellite localisation to the centrosome

and for primary cilium formation', *Biology of the Cell*, 106(8), pp. 254–267. doi: 10.1111/boc.201300087.

Bonifacino, J. S. and Hurley, J. H. (2008) 'Retromer', *Current Opinion in Cell Biology*, 20(4), pp. 427–436. doi: 10.1016/j.ceb.2008.03.009.

Bonizzi, G. and Karin, M. (2004) 'The two NF-κB activation pathways and their role in innate and adaptive immunity', *Trends in Immunology*, 25(6), pp. 280–288. doi: 10.1016/j.it.2004.03.008.

de Bot, S. T. *et al.* (2012) 'Hereditary spastic paraplegia caused by a mutation in the VCP gene', *Brain*, 135(12), pp. e223–e223. doi: 10.1093/brain/aws201.

Bouhouche, A. *et al.* (2005) 'Mutation in the epsilon subunit of the cytosolic chaperonin-containing t-complex peptide-1 (Cct5) gene causes autosomal recessive mutilating sensory neuropathy with spastic paraplegia', *Journal of Medical Genetics*, 43(5), pp. 441–443. doi: 10.1136/jmg.2005.039230.

Braakman, I. and Hebert, D. N. (2013) 'Protein Folding in the Endoplasmic Reticulum', *Cold Spring Harbor Perspectives in Biology*, 5(5), pp. a013201–a013201. doi: 10.1101/cshperspect.a013201.

Bram, R. J., Lue, N. F. and Kornberg, R. D. (1986) 'A GAL family of upstream activating sequences in yeast: roles in both induction and repression of transcription.', *The EMBO journal*. European Molecular Biology Organization, 5(3), pp. 603–8. Available at: http://www.ncbi.nlm.nih.gov/pubmed/3011415.

Brasaemle, D. L. (2007) '*Thematic review series: Adipocyte Biology* . The perilipin family of structural lipid droplet proteins: stabilization of lipid droplets and control of lipolysis', *Journal of Lipid Research*, 48(12), pp. 2547–2559. doi: 10.1194/jlr.R700014-JLR200.

Braun, P. (2012) 'Interactome mapping for analysis of complex phenotypes: Insights from benchmarking binary interaction assays', *PROTEOMICS*, 12(10), pp. 1499–1518. doi: 10.1002/pmic.201100598.

Bross, P. and Fernandez-Guerra, P. (2016) 'Disease-Associated Mutations in the HSPD1 Gene Encoding the Large Subunit of the Mitochondrial HSP60/HSP10 Chaperonin Complex.', *Frontiers in molecular biosciences*. Frontiers Media SA, 3, p. 49. doi: 10.3389/fmolb.2016.00049.

Browman, D. T. *et al.* (2006) 'Erlin-1 and erlin-2 are novel members of the prohibitin family of proteins that define lipid-raft-like domains of the ER', *Journal of Cell Science*, 119(15), pp. 3149–3160. doi: 10.1242/jcs.03060.

Brückner, A. *et al.* (2009) 'Yeast Two-Hybrid, a Powerful Tool for Systems Biology', *International Journal of Molecular Sciences*, 10(6), pp. 2763–2788. doi: 10.3390/ijms10062763.

Bruey, J. M. *et al.* (2004) 'PAN1/NALP2/PYPAF2, an Inducible Inflammatory Mediator That Regulates NF-κB and Caspase-1 Activation in Macrophages', *Journal of Biological Chemistry*, 279(50), pp. 51897–51907. doi: 10.1074/jbc.M406741200.

Buckholz, R. G. and Adams, B. G. (1981) 'Induction and genetics of two alpha-galactosidase activities in Saccharomyces cerevisiae.', *Molecular & general genetics : MGG*, 182(1), pp. 77–81. Available at: http://www.ncbi.nlm.nih.gov/pubmed/6267434.

Budnik, V., Ruiz-Cañada, C. and Wendler, F. (2016) 'Extracellular vesicles round off communication in the nervous system', *Nature Reviews Neuroscience*, 17(3), pp. 160–172. doi: 10.1038/nrn.2015.29.

Bunge, R. P. (1968) 'Glial cells and the central myelin sheath.', *Physiological reviews*. American Physiological Society, 48(1), pp. 197–251. Available at: http://www.ncbi.nlm.nih.gov/pubmed/4866614.

Buntru, A. *et al.* (2016) 'Current Approaches Toward Quantitative Mapping of the Interactome', *Frontiers in Genetics*. Frontiers, 7, p. 74. doi: 10.3389/fgene.2016.00074.

Burgos, P. V. *et al.* (2010) 'Sorting of the Alzheimer's Disease Amyloid Precursor Protein Mediated by the AP-4 Complex', *Developmental Cell*, 18(3), pp. 425–436. doi: 10.1016/j.devcel.2010.01.015.

Cao, B. and Mao, X. (2011) 'The ubiquitin-proteasomal system is critical for multiple myeloma: implications in drug discovery.', *American journal of blood research*. e-Century Publishing Corporation, 1(1), pp. 46–56. Available at: http://www.ncbi.nlm.nih.gov/pubmed/22432065

Cao, X., Ballew, N. and Barlowe, C. (1998) 'Initial docking of ER-derived vesicles requires Uso1p and Ypt1p but is independent of SNARE proteins', *The EMBO Journal*, 17(8), pp. 2156–2165. doi: 10.1093/emboj/17.8.2156.

Carlton, J. G. and Martin-Serrano, J. (2007) 'Parallels Between Cytokinesis and Retroviral Budding: A Role for the ESCRT Machinery', *Science*, 316(5833), pp. 1908–1912. doi: 10.1126/science.1143422.

Casari, G. *et al.* (1998) 'Spastic paraplegia and OXPHOS impairment caused by mutations in paraplegin, a nuclear-encoded mitochondrial metalloprotease.', *Cell*, 93(6), pp. 973–83. Available at: http://www.ncbi.nlm.nih.gov/pubmed/9635427.

Chang, J., Lee, S. and Blackstone, C. (2013) 'Protrudin binds atlastins and endoplasmic reticulum-shaping proteins and regulates network formation', 110(37), pp. 14954–14959. Available at: http://www.ncbi.nlm.nih.gov/pubmed/23969831.

Chang, J., Lee, S. and Blackstone, C. (2014) 'Spastic paraplegia proteins spastizin and spatacsin mediate autophagic lysosome reformation', *Journal of Clinical Investigation*, 124(12). doi: 10.1172/JCI77598.

de Chaves, E. I. *et al.* (1997) 'Role of lipoproteins in the delivery of lipids to axons during axonal regeneration.', *Journal of Biochemistry*, 272(49), pp. 30766–73. Available at: http://www.jbc.org/content/272/49/30766.short.

Chen, W.-W., Zhang, X. and Huang, W.-J. (2016) 'Role of neuroinflammation in neurodegenerative diseases (Review)', *Molecular Medicine Reports*, 13(4), pp. 3391–3396. doi: 10.3892/mmr.2016.4948.

Chen, Y. *et al.* (2011) 'Expression of human FUS protein in Drosophila leads to progressive neurodegeneration', *Protein & Cell*, 2(6), pp. 477–486. doi: 10.1007/s13238-011-1065-7.

Cheon, J.-E. *et al.* (2002) 'Leukodystrophy in children: a pictorial review of MR imaging features', *Radiographics : a review publication of the Radiological Society of North America, Inc*, 22(3), pp. 461–476. doi: 10.1148/radiographics.22.3.g02ma01461.

Chevalier-Larsen, E. and Holzbaur, E. L. F. (2006) 'Axonal transport and neurodegenerative disease', *Biochimica et Biophysica Acta (BBA) - Molecular Basis of Disease*. Elsevier, 1762(11–12), pp. 1094–1108. Available at: http://www.ncbi.nlm.nih.gov/pubmed/16730956.

Chien, C. T. *et al.* (1991) 'The two-hybrid system: a method to identify and clone genes for proteins that interact with a protein of interest.', *Proceedings of the National Academy of Sciences of the United States of America*, 88(21), pp. 9578–82. Available at: http://www.ncbi.nlm.nih.gov/pubmed/1946372.

Chilton, J. K. (2006) 'Molecular mechanisms of axon guidance', *Developmental Biology*, 292(1), pp. 13–24. doi: 10.1016/j.ydbio.2005.12.048.

Chiurchiù, V., Maccarrone, M. and Orlacchio, A. (2014) 'The Role of Reticulons in Neurodegenerative Diseases', *NeuroMolecular Medicine*. Springer, 16(1), pp. 3–15. doi: 10.1007/s12017-013-8271-9.

Christianson, J. C. *et al.* (2011) 'Defining human ERAD networks through an integrative mapping strategy.', *Nature cell biology*. NIH Public Access, 14(1), pp. 93–105. doi: 10.1038/ncb2383.

Christianson, J. C. and Ye, Y. (2014) 'Cleaning up in the endoplasmic reticulum: ubiquitin in charge', *Nature Structural & Molecular Biology*, 21(4), pp. 325–335. doi: 10.1038/nsmb.2793.

Chua, H. N., Sung, W.-K. and Wong, L. (2006) 'Exploiting indirect neighbours and topological weight to predict protein function from protein-protein interactions', *Bioinformatics*, 22(13), pp. 1623–1630. doi: 10.1093/bioinformatics/btl145.

Chuang, S. S. *et al.* (2004) 'CYP2U1, a Novel Human Thymus- and Brain-specific Cytochrome P450, Catalyzes ω- and (ω-1)-Hydroxylation of Fatty Acids', *Journal of Biological Chemistry*, 279(8), pp. 6305–6314. doi: 10.1074/jbc.M311830200.

Ciccarelli, F. D. *et al.* (2003) 'The identification of a conserved domain in both spartin and spastin, mutated in hereditary spastic paraplegia.', *Genomics*, 81(4), pp. 437–41. Available at: http://www.ncbi.nlm.nih.gov/pubmed/12676568.

Ciechanover, A. (1998) 'The ubiquitin-proteasome pathway: on protein death and cell life.', *The EMBO journal*. European Molecular Biology Organization, 17(24), pp. 7151–60. doi: 10.1093/emboj/17.24.7151.

Ciechanover, A. and Brundin, P. (2003) 'The ubiquitin proteasome system in neurodegenerative diseases: sometimes the chicken, sometimes the egg.', *Neuron*, 40(2), pp. 427–46. Available at: http://www.ncbi.nlm.nih.gov/pubmed/14556719.

Ciechanover, A. and Kwon, Y. T. (2015a) 'Degradation of misfolded proteins in neurodegenerative diseases: therapeutic targets and strategies', *Experimental & Molecular Medicine*. Nature Publishing Group, 47(3), p. e147. doi: 10.1038/emm.2014.117.

Ciechanover, A. and Kwon, Y. T. (2015b) 'Degradation of misfolded proteins in neurodegenerative diseases: therapeutic targets and strategies.', *Experimental & molecular medicine*. Korean Society for Biochemistry and Molecular Biology, 47(3), p. e147. doi: 10.1038/emm.2014.117.

Clapham, D. E. (2007) 'Calcium signaling.', *Cell*. Elsevier, 131(6), pp. 1047–58. doi: 10.1016/j.cell.2007.11.028.

Clarençon, F. *et al.* (2006) 'Spastic paraparesis as a manifestation of Leber's disease.', *Journal of neurology*, 253(4), pp. 525–6. doi: 10.1007/s00415-005-0994-6.

Claudiani, P. *et al.* (2005) 'Spastin subcellular localization is regulated through usage of different translation start sites and active export from the nucleus', *Experimental Cell Research*, 309(2), pp. 358–369. doi: 10.1016/j.yexcr.2005.06.009.

Cohn, M. A. *et al.* (2009) 'UAF1 is a subunit of multiple deubiquitinating enzyme complexes.', *The Journal of biological chemistry*. American Society for Biochemistry and Molecular Biology, 284(8), pp. 5343–51. doi: 10.1074/jbc.M808430200.

Collin, T., Marty, A. and Llano, I. (2005) 'Presynaptic calcium stores and synaptic transmission', *Current Opinion in Neurobiology*, 15(3), pp. 275–281. doi: 10.1016/j.conb.2005.05.003.

Collins, R. N. (2006) 'How the ER Stays in Shape', *Cell*, 124(3), pp. 464–466. doi: 10.1016/j.cell.2006.01.017.

Connell, J. W. *et al.* (2009) 'Spastin couples microtubule severing to membrane traffic in completion of cytokinesis and secretion.', *Traffic*, 10(1), pp. 42–56. doi: 10.1111/j.1600-0854.2008.00847.x.

Cordwell, S. J. and Thingholm, T. E. (2010) 'Technologies for plasma membrane proteomics', *PROTEOMICS*, 10(4), pp. 611–627. doi: 10.1002/pmic.200900521.

Corona, P. *et al.* (2002) 'Novel heteroplasmic mtDNA mutation in a family with heterogeneous clinical presentations', *Annals of Neurology*. John Wiley & Sons, Inc., 51(1), pp. 118–122. doi: 10.1002/ana.10059.

Cosker, K. E. and Segal, R. A. (2014) 'Neuronal signaling through endocytosis.', *Cold Spring Harbor perspectives in biology*. Cold Spring Harbor Laboratory Press, 6(2), pp. 1–15. doi: 10.1101/cshperspect.a020669.

Van Criekinge, W. and Beyaert, R. (1999) 'Yeast Two-Hybrid: State of the Art.', *Biological procedures online*. BioMed Central, 2, pp. 1–38. doi: 10.1251/bpo16.

Cripps, D. *et al.* (2006) 'Alzheimer Disease-specific Conformation of Hyperphosphorylated Paired Helical Filament-Tau Is Polyubiquitinated through Lys-48, Lys-11, and Lys-6 Ubiquitin Conjugation', *Journal of Biological Chemistry*, 281(16), pp. 10825–10838. doi: 10.1074/jbc.M512786200.

Croft, D. *et al.* (2014) 'The Reactome pathway knowledgebase', *Nucleic Acids Research*, 42(D1), pp. D472–D477. doi: 10.1093/nar/gkt1102.

Csermely, P., Agoston, V. and Pongor, S. (2005) 'The efficiency of multi-target drugs: the network approach might help drug design', *Trends in Pharmacological Sciences*, 26(4), pp. 178–182. doi: 10.1016/j.tips.2005.02.007.

Cuervo, A. M. (2004) 'Autophagy: many paths to the same end.', *Molecular and cellular biochemistry*,

263(1–2), pp. 55–72. Available at: http://www.ncbi.nlm.nih.gov/pubmed/15524167.

Dantuma, N. P. and Bott, L. C. (2014) 'The ubiquitin-proteasome system in neurodegenerative diseases: precipitating factor, yet part of the solution', *Frontiers in Molecular Neuroscience*. Frontiers, 7, p. 70. doi: 10.3389/fnmol.2014.00070.

DeLaBarre, B. and Brunger, A. T. (2003) 'Complete structure of p97/valosin-containing protein reveals communication between nucleotide domains', *Nature Structural Biology*, 10(10), pp. 856–863. doi: 10.1038/nsb972.

DeLaBarre, B. and Brunger, A. T. (2005) 'Nucleotide Dependent Motion and Mechanism of Action of p97/VCP', *Journal of Molecular Biology*, 347(2), pp. 437–452. doi: 10.1016/j.jmb.2005.01.060.

DeLuca, G. C., Ebers, G. C. and Esiri, M. M. (2004) 'The extent of axonal loss in the long tracts in hereditary spastic paraplegia', *Neuropathology and Applied Neurobiology*, 30(6), pp. 576–584. doi: 10.1111/j.1365-2990.2004.00587.x.

Deng, H., Gao, K. and Jankovic, J. (2014) 'The role of FUS gene variants in neurodegenerative diseases', *Nature Reviews Neurology*. Nature Research, 10(6), pp. 337–348. doi: 10.1038/nrneurol.2014.78.

Deniaud, A. *et al.* (2008) 'Endoplasmic reticulum stress induces calcium-dependent permeability transition, mitochondrial outer membrane permeabilization and apoptosis', *Oncogene*, 27(3), pp. 285–299. doi: 10.1038/sj.onc.1210638.

Dennissen, F. J. A., Kholod, N. and van Leeuwen, F. W. (2012) 'The ubiquitin proteasome system in neurodegenerative diseases: Culprit, accomplice or victim?', *Progress in Neurobiology*. Pergamon, 96(2), pp. 190–207.
Available at: http://www.sciencedirect.com/science/article/pii/S0301008212000044?via%3Dihub

Derivery, E. *et al.* (2009) 'The Arp2/3 Activator WASH Controls the Fission of Endosomes through a Large Multiprotein Complex', *Developmental Cell*, 17(5), pp. 712–723.
doi: 10.1016/j.devcel.2009.09.010.

Deshaies, R. J. and Joazeiro, C. A. P. (2009) 'RING Domain E3 Ubiquitin Ligases', *Annual Review of Biochemistry*, 78(1), pp. 399–434. doi: 10.1146/annurev.biochem.78.101807.093809.

Díaz, E. and Pfeffer, S. R. (1998) 'TIP47: a cargo selection device for mannose 6-phosphate receptor trafficking.', *Cell*, 93(3), pp. 433–43. Available at: http://www.ncbi.nlm.nih.gov/pubmed/9590177

Dobson, C. M. (2003) 'Protein folding and misfolding', *Nature*, 426(6968), pp. 884–890. doi: 10.1038/nature02261.

Dobson, C. M. and Ellis, R. J. (1998) 'Protein folding and misfolding inside and outside the cell', *The EMBO Journal*, 17(18), pp. 5251–5254. doi: 10.1093/emboj/17.18.5251.

Dor, T. *et al.* (2014) 'KIF1C mutations in two families with hereditary spastic paraparesis and cerebellar dysfunction.', *Journal of medical genetics*, 51(2). doi: 10.1136/jmedgenet-2013-102012.

Dorner, C. *et al.* (1998) 'Characterization of KIF1C, a new kinesin-like protein involved in vesicle

transport from the Golgi apparatus to the endoplasmic reticulum.', *The Journal of biological chemistry*. American Society for Biochemistry and Molecular Biology, 273(32), pp. 20267–75. doi: 10.1074/JBC.273.32.20267.

Dreze, M. *et al.* (2010) 'High-Quality Binary Interactome Mapping', in *Methods in enzymology*, pp. 281–315. doi: 10.1016/S0076-6879(10)70012-4.

Dursun, U. *et al.* (2009) 'Autosomal recessive spastic paraplegia (SPG45) with mental retardation maps to 10q24.3-q25.1.', *Neurogenetics*, 10(4), pp. 325–31. doi: 10.1007/s10048-009-0191-3.

Eastman, S. W., Yassaee, M. and Bieniasz, P. D. (2009) 'A role for ubiquitin ligases and Spartin/SPG20 in lipid droplet turnover.', *The Journal of cell biology*, 184(6), pp. 881–94. doi: 10.1083/jcb.200808041.

Edvardson, S. *et al.* (2008) 'Mutations in the Fatty Acid 2-Hydroxylase Gene Are Associated with Leukodystrophy with Spastic Paraparesis and Dystonia', *The American Journal of Human Genetics*, 83(5), pp. 643–648. doi: 10.1016/j.ajhg.2008.10.010.

Eisele, F. and Wolf, D. H. (2008) 'Degradation of misfolded protein in the cytoplasm is mediated by the ubiquitin ligase Ubr1', *FEBS Letters*, 582(30), pp. 4143–4146. doi: 10.1016/j.febslet.2008.11.015.

Engel, A. and Gaub, H. E. (2008) 'Structure and Mechanics of Membrane Proteins', *Annual Review of Biochemistry*, 77(1), pp. 127–148. doi: 10.1146/annurev.biochem.77.062706.154450.

English, A. R., Zurek, N. and Voeltz, G. K. (2009) 'Peripheral ER structure and function', *Current Opinion in Cell Biology*, 21(4), pp. 596–602. doi: 10.1016/j.ceb.2009.04.004.

Erecinska, M., Cherian, S. and Silver, I. A. (2004) 'Energy metabolism in mammalian brain during development', *Progress in Neurobiology*, 73(6), pp. 397–445. doi: 10.1016/j.pneurobio.2004.06.003.

Erlich, Y. *et al.* (2011) 'Exome sequencing and disease-network analysis of a single family implicate a mutation in KIF1A in hereditary spastic paraparesis.', *Genome research*. Cold Spring Harbor Laboratory Press, 21(5), pp. 658–64. doi: 10.1101/gr.117143.110.

Ernst, R. *et al.* (2009) 'The Otubain YOD1 Is a Deubiquitinating Enzyme that Associates with p97 to Facilitate Protein Dislocation from the ER', *Molecular Cell*, 36(1), pp. 28–38. doi: 10.1016/j.molcel.2009.09.016.

Errico, A., Ballabio, A. and Rugarli, E. I. (2002) 'Spastin, the protein mutated in autosomal dominant hereditary spastic paraplegia, is involved in microtubule dynamics.', *Human molecular genetics*, 11(2), pp. 153–63. Available at: http://www.ncbi.nlm.nih.gov/pubmed/11809724

Esposito, E. *et al.* (2016) 'COMMD7 as a novel NEMO interacting protein involved in the termination of NF-κB signaling', *Journal of Cellular Physiology*, 231(1), pp. 152–161. doi: 10.1002/jcp.25066.

Esteves, T. *et al.* (2014) 'Loss of association of REEP2 with membranes leads to hereditary spastic paraplegia', *American Journal of Human Genetics*, 94(2), pp. 268–277.
doi: 10.1016/j.ajhg.2013.12.005.

Evans, K. *et al.* (2006) 'Interaction of two hereditary spastic paraplegia gene products, spastin and

atlastin, suggests a common pathway for axonal maintenance', *Proc Natl Acad Sci U S A*. National Academy of Sciences, 103(28), pp. 10666–10671. doi: 10.1073/pnas.0510863103.

Evans, K. J. *et al.* (2005) 'Linking axonal degeneration to microtubule remodeling by Spastin-mediated microtubule severing.', *The Journal of cell biology*, 168(4), pp. 599–606. doi: 10.1083/jcb.200409058.

Fabregat, A. *et al.* (2016) 'The Reactome pathway Knowledgebase', *Nucleic Acids Research*, 44(D1), pp. D481–D487. doi: 10.1093/nar/gkv1351.

Fagone, P. and Jackowski, S. (2009) 'Membrane phospholipid synthesis and endoplasmic reticulum function', *Journal of lipid research*. American Society for Biochemistry and Molecular Biology, p. S311-. doi: 10.1194/jlr.R800049-JLR200.

Fei, W. *et al.* (2008) 'Fld1p, a functional homologue of human seipin, regulates the size of lipid droplets in yeast', *The Journal of Cell Biology*, 180(3), pp. 473–482. doi: 10.1083/jcb.200711136.

Fei, W., Du, X. and Yang, H. (2011) 'Seipin, adipogenesis and lipid droplets', *Trends in Endocrinology & Metabolism*, 22(6), pp. 204–210. doi: 10.1016/j.tem.2011.02.004.

Feilotter, H. E. *et al.* (1994) 'Construction of an improved host strain for two hybrid screening.', *Nucleic acids research*. Oxford University Press, 22(8), pp. 1502–1503. Available at: http://www.ncbi.nlm.nih.gov/pubmed/8190644

Ferreirinha, F. *et al.* (2004) 'Axonal degeneration in paraplegin-deficient mice is associated with abnormal mitochondria and impairment of axonal transport', *Journal of Clinical Investigation*, 113(2), pp. 231–242. doi: 10.1172/JCI20138.

Fester, L. *et al.* (2009) 'Cholesterol-promoted synaptogenesis requires the conversion of cholesterol to estradiol in the hippocampus'.
Available at: http://onlinelibrary.wiley.com/doi/10.1002/hipo.20548/full

Fetchko, M. and Stagljar, I. (2004) 'Application of the split-ubiquitin membrane yeast two-hybrid system to investigate membrane protein interactions', *Methods*, 32(4), pp. 349–362. doi: 10.1016/j.ymeth.2003.10.010.

Fields, R. D. (2008) 'White matter in learning, cognition and psychiatric disorders', *Trends in Neurosciences*, 31(7), pp. 361–370. doi: 10.1016/j.tins.2008.04.001.

Fields, S. *et al.* (2000) 'A comprehensive analysis of protein-protein interactions in Saccharomyces cerevisiae.', *Nature*, 403(6770), pp. 623–627. doi: 10.1038/35001009.

Fields, S. and Song, O. (1989) 'A novel genetic system to detect protein–protein interactions', *Nature*, 340(6230), pp. 245–246. doi: 10.1038/340245a0.

Filla, A. *et al.* (1992) 'Prevalence of hereditary ataxias and spastic paraplegias in Molise, a region of Italy.', *Journal of neurology*, 239(6), pp. 351–3.
Available at: http://www.ncbi.nlm.nih.gov/pubmed/1512613

Fink, J. K. (2013) 'Hereditary spastic paraplegia: Clinico-pathologic features and emerging molecular

mechanisms', *Acta Neuropathologica*. doi: 10.1007/s00401-013-1115-8.

Finsterer, J. *et al.* (2012) 'Hereditary spastic paraplegias with autosomal dominant, recessive, X-linked, or maternal trait of inheritance.', *Journal of the neurological sciences*, 318(1–2), pp. 1–18. doi: 10.1016/j.jns.2012.03.025.

Fiskum, G., Murphy, A. N. and Beal, M. F. (1999) 'Mitochondria in Neurodegeneration: Acute Ischemia and Chronic Neurodegenerative Diseases', *Journal of Cerebral Blood Flow & Metabolism*. SAGE PublicationsSage UK: London, England, 19(4), pp. 351–369. doi: 10.1097/00004647-199904000-00001.

Forrest, M. P. *et al.* (2014) 'The emerging roles of TCF4 in disease and development', *Trends in Molecular Medicine*, 20(6), pp. 322–331. doi: 10.1016/j.molmed.2014.01.010.

Fowler, P. C. and O'Sullivan, N. C. (2016) 'ER-shaping proteins are required for ER and mitochondrial network organization in motor neurons', *Human Molecular Genetics*, 25(13), p. ddw139. doi: 10.1093/hmg/ddw139.

Franceschini, A. *et al.* (2013) 'STRING v9.1: protein-protein interaction networks, with increased coverage and integration', *Nucleic Acids Research*, 41(D1), pp. D808–D815. doi: 10.1093/nar/gks1094.

Friedberg, E. C. (2008) 'A brief history of the DNA repair field', *Cell Research*, 18(1), pp. 3–7. doi: 10.1038/cr.2007.113.

Friedman, J. R. *et al.* (2013) 'Endoplasmic reticulum-endosome contact increases as endosomes traffic and mature.', *Molecular biology of the cell*, 24(7). doi: 10.1091/mbc.E12-10-0733.

Fromont-Racine, M., Rain, J.-C. and Legrain, P. (1997) 'Toward a functional analysis of the yeast genome through exhaustive two-hybrid screens', *Nature Genetics*, 16(3), pp. 277–282. doi: 10.1038/ng0797-277.

Gandhi, T. K. B. *et al.* (2006) 'Analysis of the human protein interactome and comparison with yeast, worm and fly interaction datasets.', *Nature genetics*, 38(3), pp. 285–93. doi: 10.1038/ng1747.

Gargalovic, P. S. *et al.* (2006) 'The Unfolded Protein Response Is an Important Regulator of Inflammatory Genes in Endothelial Cells', *Arteriosclerosis, Thrombosis, and Vascular Biology*, 26(11), pp. 2490–2496. doi: 10.1161/01.ATV.0000242903.41158.a1.

Garrus, J. E. *et al.* (2001) 'Tsg101 and the vacuolar protein sorting pathway are essential for HIV-1 budding.', *Cell*, 107(1), pp. 55–65. Available at: http://www.ncbi.nlm.nih.gov/pubmed/11595185

Gedvilaite, A. and Sasnauskas, K. (1994) 'Control of the expression of the ADE2 gene of the yeast Saccharomyces cerevisiae.', *Current genetics*, 25(6), pp. 475–9.
Available at: http://www.ncbi.nlm.nih.gov/pubmed/8082196

Ghosh, S. and Hayden, M. S. (2008) 'New regulators of NF-κB in inflammation', *Nature Reviews Immunology*, 8(11), pp. 837–848. doi: 10.1038/nri2423.

Gill, S. R. *et al.* (1991) 'Dynactin, a conserved, ubiquitously expressed component of an activator of

vesicle motility mediated by cytoplasmic dynein.', *The Journal of cell biology*, 115(6), pp. 1639–50. Available at: http://www.ncbi.nlm.nih.gov/pubmed/1836789

Gingras, A.-C. *et al.* (2005) 'A Novel, Evolutionarily Conserved Protein Phosphatase Complex Involved in Cisplatin Sensitivity', *Molecular & Cellular Proteomics*, 4(11), pp. 1725–1740. doi: 10.1074/mcp.M500231-MCP200.

Gingras, A.-C. and Raught, B. (2012) 'Beyond hairballs: The use of quantitative mass spectrometry data to understand protein-protein interactions.', *FEBS letters*. NIH Public Access, 586(17), pp. 2723–31. doi: 10.1016/j.febslet.2012.03.065.

Giniger, E. and Ptashne, M. (1988) 'Cooperative DNA binding of the yeast transcriptional activator GAL4.', *Proceedings of the National Academy of Sciences of the United States of America*, 85(2), pp. 382–6. Available at: http://www.ncbi.nlm.nih.gov/pubmed/3124106

Giniger, E., Varnum, S. M. and Ptashne, M. (1985) 'Specific DNA binding of GAL4, a positive regulatory protein of yeast.', *Cell*, 40(4), pp. 767–74.
Available at: http://www.ncbi.nlm.nih.gov/pubmed/3886158

Lo Giudice, T. *et al.* (2014) 'Hereditary spastic paraplegia: Clinical-genetic characteristics and evolving molecular mechanisms', *Experimental Neurology*. doi: 10.1016/j.expneurol.2014.06.011.

Glass, C. K. *et al.* (2010) 'Mechanisms underlying inflammation in neurodegeneration.', *Cell*. NIH Public Access, 140(6), pp. 918–34. doi: 10.1016/j.cell.2010.02.016.

Glick, B. S. and Nakano, A. (2009) 'Membrane Traffic Within the Golgi Apparatus', *Annual Review of Cell and Developmental Biology*, 25(1), pp. 113–132. doi: 10.1146/annurev.cellbio.24.110707.175421.

Goh, K.-I. *et al.* (2007) 'The human disease network.', *Proceedings of the National Academy of Sciences of the United States of America*. National Academy of Sciences, 104(21), pp. 8685–90. doi: 10.1073/pnas.0701361104.

Goizet, C. *et al.* (2009) 'CYP7B1 mutations in pure and complex forms of hereditary spastic paraplegia type 5', *Brain*, 132(6). doi: 10.1093/brain/awp073.

Goldberg, D. S. and Roth, F. P. (2003) 'Assessing experimentally derived interactions in a small world.', *Proceedings of the National Academy of Sciences of the United States of America*. National Academy of Sciences, 100(8), pp. 4372–6. doi: 10.1073/pnas.0735871100.

Goldknopf, I. L. and Busch, H. (1977) 'Isopeptide linkage between nonhistone and histone 2A polypeptides of chromosomal conjugate-protein A24.', *Proceedings of the National Academy of Sciences of the United States of America*, 74(3), pp. 864–8. Available at: http://www.ncbi.nlm.nih.gov/pubmed/265581

Goldstein, L. S. B. and Yang, Z. (2000) 'Microtubule-Based Transport Systems in Neurons: The Roles of Kinesins and Dyneins', *Annual Review of Neuroscience*. Annual Reviews 4139 El Camino Way, P.O. Box 10139, Palo Alto, CA 94303-0139, USA , 23(1), pp. 39–71. doi: 10.1146/annurev.neuro.23.1.39.

Gomez, T. S. *et al.* (2012) 'Trafficking defects in WASH-knockout fibroblasts originate from collapsed

endosomal and lysosomal networks', *Molecular Biology of the Cell*, 23(16), pp. 3215–3228. doi: 10.1091/mbc.E12-02-0101.

Gomez, T. S. and Billadeau, D. D. (2009) 'A FAM21-Containing WASH Complex Regulates Retromer-Dependent Sorting.', *Developmental cell*. Elsevier Ltd, 17(5), pp. 699–711. doi: 10.1016/j.devcel.2009.09.009.

Goñi, J. *et al.* (2008) 'A computational analysis of protein-protein interaction networks in neurodegenerative diseases', *BMC Systems Biology*, 2(1), p. 52. doi: 10.1186/1752-0509-2-52.

Goritz, C., Mauch, D. and Pfrieger, F. (2005) 'Multiple mechanisms mediate cholesterol-induced synaptogenesis in a CNS neuron', *Molecular and Cellular Neuroscience*. Available at: http://www.sciencedirect.com/science/article/pii/S104474310500028X

Goyal, U. and Blackstone, C. (2013) 'Untangling the web: Mechanisms underlying ER network formation', *Biochimica et biophysica acta*. NIH Public Access, 1833(11), pp. 2492–2498. doi: 10.1016/j.bbamcr.2013.04.009.

Grelle, G. *et al.* (2006) 'Identification of VCP/p97, Carboxyl Terminus of Hsp70-interacting Protein (CHIP), and Amphiphysin II Interaction Partners Using Membrane-based Human Proteome Arrays', *Molecular & Cellular Proteomics*, 5(2), pp. 234–244. doi: 10.1074/mcp.M500198-MCP200.

Griffin, W. S. *et al.* (1989) 'Brain interleukin 1 and S-100 immunoreactivity are elevated in Down syndrome and Alzheimer disease.', *Proceedings of the National Academy of Sciences of the United States of America*, 86(19), pp. 7611–5. Available at: http://www.ncbi.nlm.nih.gov/pubmed/2529544

Gunawardena, S. *et al.* (2003) 'Disruption of axonal transport by loss of huntingtin or expression of pathogenic polyQ proteins in Drosophila.', *Neuron*, 40(1), pp. 25–40. Available at: http://www.ncbi.nlm.nih.gov/pubmed/14527431

Guo, Y., Sirkis, D. W. and Schekman, R. (2014) 'Protein Sorting at the trans-Golgi Network', *Annu. Rev. Cell Dev. Biol*, 30, pp. 169–206. doi: 10.1146/annurev-cellbio-100913-013012.

Guruharsha, K. G. G. *et al.* (2011) 'A protein complex network of Drosophila melanogaster.', *Cell*, 147(3), pp. 690–703. doi: 10.1016/j.cell.2011.08.047.

Hamdan, F. F. *et al.* (2014) 'De Novo Mutations in Moderate or Severe Intellectual Disability', *PLoS Genetics*. Edited by G. M. Cooper, 10(10), p. e1004772. doi: 10.1371/journal.pgen.1004772.

Hamosh, A. *et al.* (2004) 'Online Mendelian Inheritance in Man (OMIM), a knowledgebase of human genes and genetic disorders', *Nucleic Acids Research*, 33(Database issue), pp. D514–D517. doi: 10.1093/nar/gki033.

Hanein, S. *et al.* (2007) 'A novel locus for autosomal dominant "uncomplicated" hereditary spastic paraplegia maps to chromosome 8p21.1-q13.3.', *Human genetics*, 122(3–4), pp. 261–73. doi: 10.1007/s00439-007-0396-1.

Hanein, S. *et al.* (2008) 'Identification of the SPG15 Gene, Encoding Spastizin, as a Frequent Cause of Complicated Autosomal-Recessive Spastic Paraplegia, Including Kjellin Syndrome', *American Journal*

of Human Genetics, 82(4). doi: 10.1016/j.ajhg.2008.03.004.

Hanna, M. C. and Blackstone, C. (2009) 'Interaction of the SPG21 protein ACP33/maspardin with the aldehyde dehydrogenase ALDH16A1', *neurogenetics*, 10(3), pp. 217–228. doi: 10.1007/s10048-009-0172-6.

Hanna, M. G. *et al.* (2017) 'TFG facilitates outer coat disassembly on COPII transport carriers to promote tethering and fusion with ER–Golgi intermediate compartments', *Proceedings of the National Academy of Sciences*, 114(37), pp. E7707–E7716. doi: 10.1073/pnas.1709120114.

Hansen, J. J. *et al.* (2002) 'Hereditary Spastic Paraplegia SPG13 Is Associated with a Mutation in the Gene Encoding the Mitochondrial Chaperonin Hsp60', *The American Journal of Human Genetics*, 70(5), pp. 1328–1332. doi: 10.1086/339935.

Hansson, G. K. and Libby, P. (2006) 'The immune response in atherosclerosis: a double-edged sword', *Nature Reviews Immunology*, 6(7), pp. 508–519. doi: 10.1038/nri1882.

Harbour, M. E. *et al.* (2010) 'The cargo-selective retromer complex is a recruiting hub for protein complexes that regulate endosomal tubule dynamics', *Journal of Cell Science*, 123(21), pp. 3703–3717. doi: 10.1242/jcs.071472.

Harding, A. E. (1983) 'Classification of the hereditary ataxias and paraplegias.', *Lancet (London, England)*, 1(8334), pp. 1151–5. Available at: http://www.ncbi.nlm.nih.gov/pubmed/6133167

Hartig, M. B. *et al.* (2011) 'Absence of an Orphan Mitochondrial Protein, C19orf12, Causes a Distinct Clinical Subtype of Neurodegeneration with Brain Iron Accumulation', *The American Journal of Human Genetics*, 89(4), pp. 543–550. doi: 10.1016/j.ajhg.2011.09.007.

Hartl, F. U. and Hayer-Hartl, M. (2009) 'Converging concepts of protein folding in vitro and in vivo', *Nature Structural & Molecular Biology*, 16(6), pp. 574–581. doi: 10.1038/nsmb.1591.

Hartley, J. L., Temple, G. F. and Brasch, M. A. (2000) 'DNA cloning using in vitro site-specific recombination.', *Genome research*, 10(11), pp. 1788–95.
Available at: http://www.ncbi.nlm.nih.gov/pubmed/11076863

Hashida-Okado, T. *et al.* (1996) 'AUR1, a novel gene conferring aureobasidin resistance on Saccharomyces cerevisiae: a study of defective morphologies in Aur1p-depleted cells.', *Molecular & general genetics : MGG*, 251(2), pp. 236–44.
Available at: http://www.ncbi.nlm.nih.gov/pubmed/8668135

Hashimoto, T. and Nakai, M. (2011) 'Increased hippocampal quinone reductase 2 in Alzheimer's disease', *Neuroscience Letters*, 502(1), pp. 10–12. doi: 10.1016/j.neulet.2011.07.008.

Hashimoto, Y. *et al.* (2014) 'Protrudin Regulates Endoplasmic Reticulum Morphology and Function Associated with the Pathogenesis of Hereditary Spastic Paraplegia', *Journal of Biological Chemistry*. in Press, 289(19), pp. 12946–12961. doi: 10.1074/jbc.M113.528687.

Hayden, M. S. and Ghosh, S. (2004) 'Signaling to NF- B', *doi.org*. Cold Spring Harbor Laboratory, 18(18), pp. 2195–2224. doi: 10.1101/gad.1228704.

Hazan, J. *et al.* (1999) 'Spastin, a new AAA protein, is altered in the most frequent form of autosomal dominant spastic paraplegia.', *Nature Genetics*, 23(3), pp. 296–303. doi: 10.1038/15472.

Hegde, A. N. and Upadhya, S. C. (2011) 'Role of ubiquitin–proteasome-mediated proteolysis in nervous system disease', *Biochimica et Biophysica Acta (BBA) - Gene Regulatory Mechanisms*, 1809(2), pp. 128–140. doi: 10.1016/j.bbagrm.2010.07.006.

Heneka, M. T., Kummer, M. P. and Latz, E. (2014) 'Innate immune activation in neurodegenerative disease', *Nature Reviews Immunology*, 14(7), pp. 463–477. doi: 10.1038/nri3705.

Henneke, M. *et al.* (2008) 'GJA12 mutations are a rare cause of Pelizaeus-Merzbacher-like disease', *Neurology*, 70(10), pp. 748–754. doi: 10.1212/01.wnl.0000284828.84464.35.

Her, L.-S. and Goldstein, L. S. B. (2008) 'Enhanced Sensitivity of Striatal Neurons to Axonal Transport Defects Induced by Mutant Huntingtin', *Journal of Neuroscience*, 28(50), pp. 13662–13672. doi: 10.1523/JNEUROSCI.4144-08.2008.

Herrmann, J. M. and Spang, A. (2015) 'Intracellular Parcel Service: Current Issues in Intracellular Membrane Trafficking', in *Methods in molecular biology (Clifton, N.J.)*, pp. 1–12. doi: 10.1007/978-1-4939-2309-0_1.

Hershko, A. (2005) 'The ubiquitin system for protein degradation and some of its roles in the control of the cell division cycle*', *Cell Death and Differentiation*, 12(9), pp. 1191–1197. doi: 10.1038/sj.cdd.4401702.

Hershko, A. and Ciechanover, A. (1998) 'The ubiquitin system.', *Annual review of biochemistry*. Annual Reviews 4139 El Camino Way, P.O. Box 10139, Palo Alto, CA 94303-0139, USA, 67, pp. 425–79. doi: 10.1146/annurev.biochem.67.1.425.

Hetz, C. and Mollereau, B. (2014) 'Disturbance of endoplasmic reticulum proteostasis in neurodegenerative diseases', *Nature Reviews Neuroscience*, 15(4), pp. 233–249. doi: 10.1038/nrn3689.

Higgs, H. N. *et al.* (1998) 'Cloning of a phosphatidic acid-preferring phospholipase A1 from bovine testis.', *The Journal of biological chemistry*, 273(10), pp. 5468–77. Available at: http://www.ncbi.nlm.nih.gov/pubmed/9488669

Hiller, M. M. *et al.* (1996) 'ER degradation of a misfolded luminal protein by the cytosolic ubiquitin-proteasome pathway.', *Science (New York, N.Y.)*, 273(5282), pp. 1725–8. Available at: http://www.ncbi.nlm.nih.gov/pubmed/8781238

Hirokawa, N. *et al.* (1990) 'Brain dynein (MAP1C) localizes on both anterogradely and retrogradely transported membranous organelles in vivo.', *The Journal of cell biology*, 111(3), pp. 1027–37. Available at: http://www.ncbi.nlm.nih.gov/pubmed/2143999

Hirokawa, N. *et al.* (1991) 'Kinesin associates with anterogradely transported membranous organelles in vivo.', *The Journal of cell biology*, 114(2), pp. 295–302. Available at: http://www.ncbi.nlm.nih.gov/pubmed/1712789

Hirokawa, N. (1998) 'Kinesin and dynein superfamily proteins and the mechanism of organelle transport.', *Science (New York, N.Y.)*, 279(5350), pp. 519–26. Available at: http://www.ncbi.nlm.nih.gov/pubmed/9438838

Hirst, J. *et al.* (2011) 'The Fifth Adaptor Protein Complex', *PLoS Biology*. Edited by S. L. Schmid. Public Library of Science, 9(10), p. e1001170. doi: 10.1371/journal.pbio.1001170.

Hirst, J., Irving, C. and Borner, G. H. H. (2013) 'Adaptor Protein Complexes AP-4 and AP-5: New Players in Endosomal Trafficking and Progressive Spastic Paraplegia', *Traffic*. John Wiley & Sons A/S, 14(2), pp. 153–164. doi: 10.1111/tra.12028.

Hodgkinson, C. A. *et al.* (2002) 'A novel form of autosomal recessive pure hereditary spastic paraplegia maps to chromosome 13q14.', *Neurology*, 59(12), pp. 1905–9. Available at: http://www.ncbi.nlm.nih.gov/pubmed/12499481

Hoeijmakers, J. H. J. (2001) 'Genome maintenance mechanisms for preventing cancer.', *Nature*, 411(6835), pp. 366–374. doi: 10.1038/35077232.

Hong, Z. *et al.* (2009) 'The retromer component SNX6 interacts with dynactin p150Glued and mediates endosome-to-TGN transport', *Cell Research*, 19(12), pp. 1334–1349. doi: 10.1038/cr.2009.130.

Hooper, C. *et al.* (2010) 'Spartin activates atrophin-1-interacting protein 4 (AIP4) E3 ubiquitin ligase and promotes ubiquitination of adipophilin on lipid droplets.', *BMC biology*, 8(72), pp. 1–11. doi: 10.1186/1741-7007-8-72.

Hu, J. *et al.* (2008) 'Membrane Proteins of the Endoplasmic Reticulum Induce High-Curvature Tubules', *Science*, 319(5867), pp. 1247–1250. doi: 10.1126/science.1153634.

Hu, J. *et al.* (2009) 'A class of dynamin-like GTPases involved in the generation of the tubular ER network.', *Cell*, 138(3), pp. 549–561. doi: 10.1016/j.cell.2009.05.025.

Huber, M. D. *et al.* (2013) 'Erlins restrict SREBP activation in the ER and regulate cellular cholesterol homeostasis', *The Journal of Cell Biology*, 203(3), pp. 427–436. doi: 10.1083/jcb.201305076.

Huotari, J. and Helenius, A. (2011) 'Endosome maturation', *The EMBO Journal*, 30(17), pp. 3481–3500. doi: 10.1038/emboj.2011.286.

Hurley, J. H. (2010) 'The ESCRT complexes.', *Critical reviews in biochemistry and molecular biology*. NIH Public Access, 45(6), pp. 463–87. doi: 10.3109/10409238.2010.502516.

Hurley, J. H. and Yang, D. (2008) 'MIT Domainia', *Developmental Cell*, 14(1), pp. 6–8. doi: 10.1016/j.devcel.2007.12.013.

Hutchins, A. P. *et al.* (2013) 'The repertoires of ubiquitinating and deubiquitinating enzymes in eukaryotic genomes.', *Molecular biology and evolution*. Oxford University Press, 30(5), pp. 1172–87. doi: 10.1093/molbev/mst022.

Huttlin, E. L. *et al.* (2015) 'The BioPlex Network: A Systematic Exploration of the Human Interactome',

Cell. Elsevier, 162(2), pp. 425–440. doi: 10.1016/j.cell.2015.06.043.

Huttlin, E. L. *et al.* (2017) 'Architecture of the human interactome defines protein communities and disease networks', *Nature*. Nature Research, 545(7655), pp. 505–509. doi: 10.1038/nature22366.

Inoue, H. *et al.* (2012) 'Roles of SAM and DDHD domains in mammalian intracellular phospholipase A1 KIAA0725p', *Biochimica et Biophysica Acta (BBA) - Molecular Cell Research*. Elsevier, 1823(4), pp. 930–939. doi: 10.1016/J.BBAMCR.2012.02.002.

Inoue, K. (2005) 'PLP1-related inherited dysmyelinating disorders: Pelizaeus-Merzbacher disease and spastic paraplegia type 2', *Neurogenetics*, 6(1), pp. 1–16. doi: 10.1007/s10048-004-0207-y.

Ishiura, H. *et al.* (2012) 'The TRK-fused gene is mutated in hereditary motor and sensory neuropathy with proximal dominant involvement.', *American journal of human genetics*. Elsevier, 91(2), pp. 320–9. doi: 10.1016/j.ajhg.2012.07.014.

Israel, A. (2010) 'The IKK Complex, a Central Regulator of NF- B Activation', *Cold Spring Harbor Perspectives in Biology*, 2(3), pp. a000158–a000158. doi: 10.1101/cshperspect.a000158.

Ito, D. *et al.* (2008) 'Characterization of seipin/BSCL2, a protein associated with spastic paraplegia 17.', *Neurobiology of disease*, 31(2), pp. 266–77. doi: 10.1016/j.nbd.2008.05.004.

Ito, T. *et al.* (2001) 'A comprehensive two-hybrid analysis to explore the yeast protein interactome', *Proceedings of the National Academy of Sciences*, 98(8), pp. 4569–4574. doi: 10.1073/pnas.061034498.

Iwai, K. (2012) 'Diverse ubiquitin signaling in NF-κB activation', *Trends in Cell Biology*, 22(7), pp. 355–364. doi: 10.1016/j.tcb.2012.04.001.

Iyer, K. *et al.* (2005) 'Utilizing the split-ubiquitin membrane yeast two-hybrid system to identify protein-protein interactions of integral membrane proteins.', *Science's STKE : signal transduction knowledge environment*, 2005(275), p. pl3. doi: 10.1126/stke.2752005pl3.

Jahn, O., Tenzer, S. and Werner, H. B. (2009) 'Myelin proteomics: molecular anatomy of an insulating sheath.', *Molecular neurobiology*. Springer, 40(1), pp. 55–72. doi: 10.1007/s12035-009-8071-2.

James, P., Halladay, J. and Craig, E. A. (1996) 'Genomic libraries and a host strain designed for highly efficient two-hybrid selection in yeast.', *Genetics*, 144(4), pp. 1425–36. Available at: http://www.ncbi.nlm.nih.gov/pubmed/8978031

Jarosch, E. *et al.* (2002) 'Protein Dislocation from the Endoplasmic Reticulum - Pulling Out the Suspect', *Traffic*. Munksgaard International Publishers, 3(8), pp. 530–536. doi: 10.1034/j.1600-0854.2002.30803.x.

Jeong, H. *et al.* (2001) 'Lethality and centrality in protein networks.', *Nature*, 411(6833), pp. 41–2. doi: 10.1038/35075138.

Jinnah, H. A., Sabina, R. L. and Van Den Berghe, G. (2013) 'Metabolic disorders of purine metabolism affecting the nervous system.', *Handbook of clinical neurology*. NIH Public Access, 113, pp. 1827–36.

doi: 10.1016/B978-0-444-59565-2.00052-6.

Johnson, A. *et al.* (2015) 'TFG clusters COPII-coated transport carriers and promotes early secretory pathway organization', *The EMBO Journal*, 34(6), pp. 811–827. doi: 10.15252/embj.201489032.

Johnsson, N. and Varshavsky, A. (1994) 'Split ubiquitin as a sensor of protein interactions in vivo.', *Proceedings of the National Academy of Sciences of the United States of America*. National Academy of Sciences, 91(22), pp. 10340–4. Available at: http://www.ncbi.nlm.nih.gov/pubmed/7937952

Johnston, M. and Dover, J. (1987) 'Mutations that inactivate a yeast transcriptional regulatory protein cluster in an evolutionarily conserved DNA binding domain (GALA/DNA binding protein/Zn2' binding domain/Saccharomyces cerevisiae)', *Genetics*, 84, pp. 2401–2405.
Available at: http://www.pnas.org/content/84/8/2401.full.pdf

Jonsson, P. F. and Bates, P. A. (2006) 'Global topological features of cancer proteins in the human interactome', *Bioinformatics*, 22(18), pp. 2291–2297. doi: 10.1093/bioinformatics/btl390.

Joshi, D. C. and Bakowska, J. C. (2011) 'SPG20 Protein Spartin Associates with Cardiolipin via Its Plant-Related Senescence Domain and Regulates Mitochondrial Ca2+ Homeostasis', *PLoS ONE*. Edited by M. R. Cookson. Public Library of Science, 6(4), p. e19290. doi: 10.1371/journal.pone.0019290.

Jouet, M. *et al.* (1994) 'X–linked spastic paraplegia (SPG1), MASA syndrome and X–linked hydrocephalus result from mutations in the L1 gene', *Nature Genetics*. Nature Publishing Group, 7(3), pp. 402–407. doi: 10.1038/ng0794-402.

Ju, J.-S. and Weihl, C. C. (2010) 'p97/VCP at the intersection of the autophagy and the ubiquitin proteasome system.', *Autophagy*, 6(2), pp. 283–5.
Available at: http://www.ncbi.nlm.nih.gov/pubmed/20083896

Kaiser, M., Hilgetag, C. and Kötter, R. (2010) 'Hierarchy and dynamics of neural networks', *Frontiers in Neuroinformatics*, 4(112), pp. 1–3. doi: 10.3389/fninf.2010.00112.

Kakizuka, A. (2008) 'Roles of VCP in human neurodegenerative disorders', *Biochemical Society Transactions*, 36(1), pp. 105–108. doi: 10.1042/BST0360105.

Kamburov, A. *et al.* (2009) 'ConsensusPathDB—a database for integrating human functional interaction networks', *Nucleic Acids Research*, 37(suppl_1), pp. D623–D628. doi: 10.1093/nar/gkn698.

Kann, O. and Kovács, R. (2007) 'Mitochondria and neuronal activity.', *American journal of physiology. Cell physiology*. American Physiological Society, 292(2), pp. C641-57. doi: 10.1152/ajpcell.00222.2006.

Karchin, R. and Nussinov, R. (2016) 'Genome Landscapes of Disease: Strategies to Predict the Phenotypic Consequences of Human Germline and Somatic Variation.', *PLoS computational biology*, 12(8), p. e1005043. doi: 10.1371/journal.pcbi.1005043.

Karlberg, T. *et al.* (2009) 'Crystal Structure of the ATPase Domain of the Human AAA+ Protein Paraplegin/SPG7', *PLoS ONE*. Edited by N. Gay. Public Library of Science, 4(10), p. e6975. doi: 10.1371/journal.pone.0006975.

Katzmann, D. J., Odorizzi, G. and Emr, S. D. (2002) 'Receptor downregulation and multivesicular-body sorting', *Nature Reviews Molecular Cell Biology*, 3(12), pp. 893–905. doi: 10.1038/nrm973.

Kaufman, R. J. (1999) 'Stress signaling from the lumen of the endoplasmic reticulum: coordination of gene transcriptional and translational controls.', *Genes & development*, 13(10), pp. 1211–33. Available at: http://www.ncbi.nlm.nih.gov/pubmed/10346810

Keck, S. *et al.* (2003) 'Proteasome inhibition by paired helical filament-tau in brains of patients with Alzheimer's disease.', *Journal of Neurochemistry*. Blackwell Science Ltd, 85(1), pp. 115–122. doi: 10.1046/j.1471-4159.2003.01642.x.

Keller, J. N., Huang, F. F. and Markesbery, W. R. (2000) 'Decreased levels of proteasome activity and proteasome expression in aging spinal cord.', *Neuroscience*, 98(1), pp. 149–56. Available at: http://www.ncbi.nlm.nih.gov/pubmed/10858621

Kempuraj, D. *et al.* (2016) 'Neuroinflammation Induces Neurodegeneration.', *Journal of neurology, neurosurgery and spine*. NIH Public Access, 1(1).
Available at: http://www.ncbi.nlm.nih.gov/pubmed/28127589

Kenwrick, S. *et al.* (1986) 'Linkage studies of X-linked recessive spastic paraplegia using DNA probes', *Human Genetics*. Springer-Verlag, 73(3), pp. 264–266. doi: 10.1007/BF00401241.

Kenwrick, S., Watkins, A. and Angelis, E. De (2000) 'Neural cell recognition molecule L1: relating biological complexity to human disease mutations', *Human Molecular Genetics*. Oxford University Press, 9(6), pp. 879–886. doi: 10.1093/hmg/9.6.879.

Khundadze, M. *et al.* (2013) 'A Hereditary Spastic Paraplegia Mouse Model Supports a Role of ZFYVE26/SPASTIZIN for the Endolysosomal System', *PLoS Genetics*. Edited by G. S. Barsh. Public Library of Science, 9(12), pp. 1–16. doi: 10.1371/journal.pgen.1003988.

Kim, I., Xu, W. and Reed, J. C. (2008) 'Cell death and endoplasmic reticulum stress: disease relevance and therapeutic opportunities', *Nature Reviews Drug Discovery*, 7(12), pp. 1013–1030. doi: 10.1038/nrd2755.

Klebe, S., Stevanin, G. and Depienne, C. (2015) 'Clinical and genetic heterogeneity in hereditary spastic paraplegias: From SPG1 to SPG72 and still counting', *Revue Neurologique*. doi: 10.1016/j.neurol.2015.02.017.

Klemm, R. W. *et al.* (2013) 'A Conserved Role for Atlastin GTPases in Regulating Lipid Droplet Size', *Cell Reports*, 3(5), pp. 1465–1475. doi: 10.1016/j.celrep.2013.04.015.

Klionsky, D. J. (2010) 'The Autophagy Connection', *Developmental Cell*, 19(1), pp. 11–12. doi: 10.1016/j.devcel.2010.07.005.

Kopito, R. R. (2000) 'Aggresomes, inclusion bodies and protein aggregation.', *Trends in cell biology*, 10(12), pp. 524–30. Available at: http://www.ncbi.nlm.nih.gov/pubmed/11121744

Kopito, R. R. and Ron, D. (2000) 'Conformational disease.', *Nature Cell Biology*, 2(11), pp. E207–E207. doi: 10.1038/35041139.

Koppen, M. *et al.* (2007) 'Variable and tissue-specific subunit composition of mitochondrial m-AAA protease complexes linked to hereditary spastic paraplegia.', *Molecular and cellular biology*, 27(2), pp. 758–67. doi: 10.1128/MCB.01470-06.

Korade, Z. and Kenworthy, A. (2008) 'Lipid rafts, cholesterol, and the brain', *Neuropharmacology*. Available at: http://www.sciencedirect.com/science/article/pii/S0028390808000646

Korhonen, L. and Lindholm, D. (2004) 'The ubiquitin proteasome system in synaptic and axonal degeneration: a new twist to an ld cycle.', *The Journal of cell biology*. The Rockefeller University Press, 165(1), pp. 27–30. doi: 10.1083/jcb.200311091.

Krämer-Albers, E.-M. *et al.* (2006) 'Perturbed interactions of mutant proteolipid protein/DM20 with cholesterol and lipid rafts in oligodendroglia: implications for dysmyelination in spastic paraplegia.', *The Journal of neuroscience : the official journal of the Society for Neuroscience*, 26(45), pp. 11743–11752. doi: 10.1523/JNEUROSCI.3581-06.2006.

Kulkarni, O. P. *et al.* (2016) 'The Immune System in Tissue Environments Regaining Homeostasis after Injury: Is "Inflammation" Always Inflammation?', *Mediators of Inflammation*. Hindawi, 2016, pp. 1–9. doi: 10.1155/2016/2856213.

Lacy, S. E. *et al.* (1999) 'Identification of FLRT1, FLRT2, and FLRT3: A Novel Family of Transmembrane Leucine-Rich Repeat Proteins', *Genomics*, 62(3), pp. 417–426. doi: 10.1006/geno.1999.6033.

Lamari, F. *et al.* (2013) 'Disorders of phospholipids, sphingolipids and fatty acids biosynthesis: Toward a new category of inherited metabolic diseases', *Journal of Inherited Metabolic Disease*, 36(3), pp. 411–425. doi: 10.1007/s10545-012-9509-7.

LaMonte, B. H. *et al.* (2002) 'Disruption of dynein/dynactin inhibits axonal transport in motor neurons causing late-onset progressive degeneration.', *Neuron*, 34(5), pp. 715–27. Available at: http://www.ncbi.nlm.nih.gov/pubmed/12062019

Landstein, D., Ulmansky, R. and Naparstek, Y. (2015) 'HSP60 - a double edge sword in autoimmunity', *Oncotarget*, 6(32), pp. 32299–32300. doi: 10.18632/oncotarget.5869.

De Las Rivas, J. and Fontanillo, C. (2010) 'Protein-protein interactions essentials: key concepts to building and analyzing interactome networks.', *PLoS computational biology*. Public Library of Science, 6(6), p. e1000807. doi: 10.1371/journal.pcbi.1000807.

Laurenzi, V. De *et al.* (1996) 'Sjögren–Larsson syndrome is caused by mutations in the fatty aldehyde dehydrogenase gene', *Nature Genetics*, 12(1), pp. 52–57. doi: 10.1038/ng0196-52.

Lazo, P. ., Ochoa, A. . and Gascón, S. (1978) 'α-galactosidase (melibiase) from Saccharomyces carlsbergensis: Structural and kinetic properties', *Archives of Biochemistry and Biophysics*. Academic Press, 191(1), pp. 316–324. doi: 10.1016/0003-9861(78)90094-2.

Lederberg, J. (1948) 'Gene control of beta-galactosidase in Escherichia coli.', *Genetics*, 33(6), p. 617. Available at: http://www.ncbi.nlm.nih.gov/pubmed/18100305

Lee, C. W. and Peng, H. B. (2008) 'The function of mitochondria in presynaptic development at the neuromuscular junction.', *Molecular biology of the cell*. American Society for Cell Biology, 19(1), pp. 150–8. doi: 10.1091/mbc.E07-05-0515.

Lee, I. *et al.* (2011) 'Prioritizing candidate disease genes by network-based boosting of genome-wide association data', *Genome Research*, 21(7), pp. 1109–1121. doi: 10.1101/gr.118992.110.

Lee, J.-A. and Gao, F.-B. (2012) 'Neuronal Functions of ESCRTs.', *Experimental neurobiology*. Korean Society for Brain and Neural Science, 21(1), pp. 9–15. doi: 10.5607/en.2012.21.1.9.

Leone, M. *et al.* (1995) 'Hereditary ataxias and paraplegias in Valle d'Aosta, Italy: a study of prevalence and disability.', *Acta neurologica Scandinavica*, 91(3), pp. 183–7. Available at: http://www.ncbi.nlm.nih.gov/pubmed/7793232

Lerner, M. *et al.* (2007) 'The RBCC Gene RFP2 (Leu5) Encodes a Novel Transmembrane E3 Ubiquitin Ligase Involved in ERAD', *Molecular Biology of the Cell*, 18(5), pp. 1670–1682. doi: 10.1091/mbc.E06-03-0248.

Letunic, I. and Bork, P. (2007) 'Interactive Tree Of Life (iTOL): an online tool for phylogenetic tree display and annotation', *Bioinformatics*, 23(1), pp. 127–128. doi: 10.1093/bioinformatics/btl529.

Levine, B. and Kroemer, G. (2008) 'Autophagy in the Pathogenesis of Disease', *Cell*. NIH Public Access, 132(1), pp. 27–42. doi: 10.1016/j.cell.2007.12.018.

Levy-Rimler, G. *et al.* (2001) 'The effect of nucleotides and mitochondrial chaperonin 10 on the structure and chaperone activity of mitochondrial chaperonin 60.', *European journal of biochemistry*, 268(12), pp. 3465–72. Available at: http://www.ncbi.nlm.nih.gov/pubmed/11422376

Lewis, S. A. *et al.* (1996) 'Chaperonin-mediated folding of actin and tubulin.', *The Journal of cell biology*, 132(1–2), pp. 1–4. Available at: http://www.ncbi.nlm.nih.gov/pubmed/8567715

Li, F.-Y. *et al.* (2014) 'XMEN disease: a new primary immunodeficiency affecting Mg2+ regulation of immunity against Epstein-Barr virus.', *Blood*. American Society of Hematology, 123(14), pp. 2148–52. doi: 10.1182/blood-2013-11-538686.

Li, J. *et al.* (2008) 'The unfolded protein response regulator GRP78/BiP is required for endoplasmic reticulum integrity and stress-induced autophagy in mammalian cells', *Cell Death and Differentiation*, 15(9), pp. 1460–1471. doi: 10.1038/cdd.2008.81.

Li, W. *et al.* (2008) 'Genome-Wide and Functional Annotation of Human E3 Ubiquitin Ligases Identifies MULAN, a Mitochondrial E3 that Regulates the Organelle's Dynamics and Signaling', *PLoS ONE*. Edited by H. Ploegh. Public Library of Science, 3(1), p. e1487. doi: 10.1371/journal.pone.0001487.

Li, Y. *et al.* (2005) 'Free Cholesterol-loaded Macrophages Are an Abundant Source of Tumor Necrosis Factor-α and Interleukin-6', *Journal of Biological Chemistry*, 280(23), pp. 21763–21772. doi: 10.1074/jbc.M501759200.

Liang, J.-H. and Jia, J.-P. (2014) 'Dysfunctional autophagy in Alzheimer's disease: pathogenic roles and therapeutic implications', *Neurosci Bull*, 30(2), pp. 308–316. doi: 10.1007/s12264-013-1418-8.

Ligon, L. A. *et al.* (2005) 'Mutant superoxide dismutase disrupts cytoplasmic dynein in motor neurons.', *Neuroreport*, 16(6), pp. 533–6. Available at: http://www.ncbi.nlm.nih.gov/pubmed/15812301

Liljeström, P. L. (1985) 'The nucleotide sequence of the yeast MEL1 gene.', *Nucleic acids research*. Oxford University Press, 13(20), pp. 7257–68.
Available at: http://www.ncbi.nlm.nih.gov/pubmed/2997745

Lind, G. E. *et al.* (2011) 'SPG20, a novel biomarker for early detection of colorectal cancer, encodes a regulator of cytokinesis', *Oncogene*. Nature Publishing Group, 30(37), pp. 3967–3978. doi: 10.1038/onc.2011.109.

Lindahl, T. (1993) 'Instability and decay of the primary structure of DNA', *Nature*, 362(6422), pp. 709–715. doi: 10.1038/362709a0.

Lindahl, T. and Barnes, D. E. (2000) 'Repair of endogenous DNA damage.', *Cold Spring Harbor symposia on quantitative biology*, 65, pp. 127–33. Available at: http://www.ncbi.nlm.nih.gov/pubmed/12760027

Liou, A. K. F., Willison, K. R. and Research, C. (1997) 'Elucidation of the subunit orientation in CCT (chaperonin containing TCP1) from the subunit composition of CCT micro-complexes combinations of possible subunit arrangements within the Immunoprecipitation of intact CCT with a monoclonal', *The EMBO Journal*, 16(14), pp. 4311–4316.
Available at: https://www.ncbi.nlm.nih.gov/pmc/articles/PMC1170057/pdf/004311.pdf

Liu, S. and Chen, Z. J. (2011) 'Expanding role of ubiquitination in NF-κB signaling.', *Cell research*. Nature Publishing Group, 21(1), pp. 6–21. doi: 10.1038/cr.2010.170.

Lombard, D. B. *et al.* (2005) 'DNA Repair, Genome Stability, and Aging', *Cell*, 120(4), pp. 497–512. doi: 10.1016/j.cell.2005.01.028.

Lonskaya, I. *et al.* (2013) 'Tyrosine kinase inhibition increases functional parkin-Beclin-1 interaction and enhances amyloid clearance and cognitive performance.', *EMBO molecular medicine*. Wiley-Blackwell, 5(8), pp. 1247–62. doi: 10.1002/emmm.201302771.

Lopes, C. T. *et al.* (2010) 'Cytoscape Web: an interactive web-based network browser', *Bioinformatics*, 26(18), pp. 2347–2348. doi: 10.1093/bioinformatics/btq430.

Lossos, A. *et al.* (2015) 'Fe/S protein assembly gene IBA57 mutation causes hereditary spastic paraplegia.', *Neurology*, 84(7), pp. 659–67. doi: 10.1212/WNL.0000000000001270.

Love, K. R. *et al.* (2007) 'Mechanisms, biology and inhibitors of deubiquitinating enzymes', *Nature Chemical Biology*, 3(11), pp. 697–705. doi: 10.1038/nchembio.2007.43.

Love, S. (2006) 'Demyelinating diseases.', *Journal of clinical pathology*. BMJ Publishing Group, 59(11), pp. 1151–9. doi: 10.1136/jcp.2005.031195.

Lozzio, C. B. and Lozzio, B. B. (1975) 'Human chronic myelogenous leukemia cell-line with positive Philadelphia chromosome.', *Blood*, 45(3), pp. 321–34. Available at:

http://www.ncbi.nlm.nih.gov/pubmed/163658

Lu, J., Rashid, F. and Byrne, P. C. (2006) 'The hereditary spastic paraplegia protein spartin localises to mitochondria', *Journal of Neurochemistry*, 98(6), pp. 1908–1919. doi: 10.1111/j.1471-4159.2006.04008.x.

Lui, H. M. *et al.* (2003) 'ARMER, apoptotic regulator in the membrane of the endoplasmic reticulum, a novel inhibitor of apoptosis.', *Molecular cancer research : MCR*, 1(7), pp. 508–18. Available at: http://www.ncbi.nlm.nih.gov/pubmed/12754298

Macedo-Souza, L. I. *et al.* (2008) 'Reevaluation of a large family defines a new locus for X-linked recessive pure spastic paraplegia (SPG34) on chromosome Xq25.', *Neurogenetics*, 9(3), pp. 225–6. doi: 10.1007/s10048-008-0130-8.

Maglott, D. *et al.* (2007) 'Entrez Gene: gene-centered information at NCBI.', *Nucleic acids research*. Oxford University Press, 35(Database issue), pp. D26-31. doi: 10.1093/nar/gkl993.

Maglott, D. *et al.* (2011) 'Entrez Gene: gene-centered information at NCBI', *Nucleic Acids Research*, 39(Database), pp. D52–D57. doi: 10.1093/nar/gkq1237.

Malhotra, J. D. and Kaufman, R. J. (2007) 'The endoplasmic reticulum and the unfolded protein response', *Seminars in Cell & Developmental Biology*, 18(6), pp. 716–731. doi: 10.1016/j.semcdb.2007.09.003.

Maness, P. F. and Schachner, M. (2007) 'Neural recognition molecules of the immunoglobulin superfamily: signaling transducers of axon guidance and neuronal migration', *Nature Neuroscience*, 10(1), pp. 19–26. doi: 10.1038/nn1827.

Mannan, A. U. *et al.* (2006) 'ZFYVE27 (SPG33), a novel spastin-binding protein, is mutated in hereditary spastic paraplegia', *American Journal of Human Genetics*, 79(2), pp. 351–357. doi: 10.1086/504927.

Markson, G. *et al.* (2009) 'Analysis of the human E2 ubiquitin conjugating enzyme protein interaction network', *Genome Research*, 19(10), pp. 1905–1911. doi: 10.1101/gr.093963.109.

Martin, L. J. (2008) 'DNA damage and repair: relevance to mechanisms of neurodegeneration.', *Journal of neuropathology and experimental neurology*. NIH Public Access, 67(5), pp. 377–87. doi: 10.1097/NEN.0b013e31816ff780.

Martin, L. J. and Liu, Z. (2002) 'Injury-induced spinal motor neuron apoptosis is preceded by DNA single-strand breaks and is p53- and Bax-dependent', *Journal of Neurobiology*. Wiley Subscription Services, Inc., A Wiley Company, 50(3), pp. 181–197. doi: 10.1002/neu.10026.

Matus, S., Glimcher, L. H. and Hetz, C. (2011) 'Protein folding stress in neurodegenerative diseases: a glimpse into the ER', *Current Opinion in Cell Biology*, 23(2), pp. 239–252. doi: 10.1016/j.ceb.2011.01.003.

Maxfield, F. R. and McGraw, T. E. (2004) 'Endocytic recycling', *Nature Reviews Molecular Cell Biology*, 5(2), pp. 121–132. doi: 10.1038/nrm1315.

McCaughey, J. *et al.* (2016) 'TFG Promotes Organization of Transitional ER and Efficient Collagen Secretion', *Cell Reports*. Elsevier, 15(8), pp. 1648–1659. doi: 10.1016/j.celrep.2016.04.062.

McDermott, C. *et al.* (2000) 'Hereditary spastic paraparesis: a review of new developments.', *Journal of neurology, neurosurgery, and psychiatry*, 69(2), pp. 150–60. Available at: http://www.ncbi.nlm.nih.gov/pubmed/10896685

McDermott, C. J. *et al.* (2003) 'Hereditary Spastic Paraparesis: Disrupted Intracellular Transport Associated with Spastin Mutation', *Ann Neurol*, 54, pp. 748–759. Available at: http://onlinelibrary.wiley.com.liverpool.idm.oclc.org/store/10.1002/ana.10757/asset/10757_ftp.pdf?v=1&t=j6dmfekl&s=200343d1d95c698c6f87b6c678558d7aa547554f.

McGeer, P. L. *et al.* (1987) 'Reactive microglia in patients with senile dementia of the Alzheimer type are positive for the histocompatibility glycoprotein HLA-DR.', *Neuroscience letters*, 79(1–2), pp. 195–200. Available at: http://www.ncbi.nlm.nih.gov/pubmed/3670729

McGinnis, S. and Madden, T. L. (2004) 'BLAST: at the core of a powerful and diverse set of sequence analysis tools', *Nucleic Acids Research*, 32(Web Server), pp. W20–W25. doi: 10.1093/nar/gkh435.

McMonagle, P., Webb, S. and Hutchinson, M. (2002) 'The prevalence of "pure" autosomal dominant hereditary spastic paraparesis in the island of Ireland.', *Journal of neurology, neurosurgery, and psychiatry*, 72(1), pp. 43–6. Available at: http://www.ncbi.nlm.nih.gov/pubmed/11784824

McNaught, K. S. P. *et al.* (2003) 'Altered proteasomal function in sporadic Parkinson's disease.', *Experimental neurology*, 179(1), pp. 38–46. Available at: http://www.ncbi.nlm.nih.gov/pubmed/12504866

Meijer, I. A. *et al.* (2004) 'A novel locus for pure recessive hereditary spastic paraplegia maps to 10q22.1-10q24.1.', *Annals of neurology*, 56(4), pp. 579–82. doi: 10.1002/ana.20239.

Mellman, I. (1996) 'ENDOCYTOSIS AND MOLECULAR SORTING', *Annual Review of Cell and Developmental Biology*, 12(1), pp. 575–625. doi: 10.1146/annurev.cellbio.12.1.575.

Mellman, I. and Warren, G. (2000) 'The road taken: past and future foundations of membrane traffic.', *Cell*, 100(1), pp. 99–112. Available at: http://www.ncbi.nlm.nih.gov/pubmed/10647935

Menendez-Benito, V. *et al.* (2005) 'Endoplasmic reticulum stress compromises the ubiquitin-proteasome system', *Human Molecular Genetics*. Oxford University Press, 14(19), pp. 2787–2799. doi: 10.1093/hmg/ddi312.

Merner, N. D. *et al.* (2012) 'Exome Sequencing Identifies FUS Mutations as a Cause of Essential Tremor', *The American Journal of Human Genetics*, 91(2), pp. 313–319. doi: 10.1016/j.ajhg.2012.07.002.

Metcalf, D. and Isaacs, A. M. (2010) 'The role of ESCRT proteins in fusion events involving lysosomes, endosomes and autophagosomes', *Biochemical Society Transactions*, 38(6). Available at: http://www.biochemsoctrans.org/content/38/6/1469.long#ref-1

Metzger, M. B., Hristova, V. A. and Weissman, A. M. (2012) 'HECT and RING finger families of E3

ubiquitin ligases at a glance', *Journal of Cell Science*, 125(3), pp. 531–537. doi: 10.1242/jcs.091777.

Meyer, H., Bug, M. and Bremer, S. (2012) 'Emerging functions of the VCP/p97 AAA-ATPase in the ubiquitin system', *Nature Cell Biology*, 14(2), pp. 117–123. doi: 10.1038/ncb2407.

Mi, H. *et al.* (2013) 'Large-scale gene function analysis with the PANTHER classification system', *Nature Protocols*. Nature Research, 8(8), pp. 1551–1566. doi: 10.1038/nprot.2013.092.

Miao, S.-H. *et al.* (2014) 'Astrocytic JWA Expression is Essential to Dopaminergic Neuron Survival in the Pathogenesis of Parkinson's Disease', *CNS Neuroscience & Therapeutics*, 20(8), pp. 754–762. doi: 10.1111/cns.12249.

Mikoshiba, K. *et al.* (1991) 'Structure and Function of Myelin Protein Genes', *Annual Review of Neuroscience*. Annual Reviews 4139 El Camino Way, P.O. Box 10139, Palo Alto, CA 94303-0139, USA , 14(1), pp. 201–217. doi: 10.1146/annurev.ne.14.030191.001221.

Milewska, M., McRedmond, J. and Byrne, P. C. (2009) 'Identification of novel spartin-interactors shows spartin is a multifunctional protein', *Journal of Neurochemistry*. Blackwell Publishing Ltd, 111(4), pp. 1022–1030. doi: 10.1111/j.1471-4159.2009.06382.x.

Miller, J. P. *et al.* (2005) 'Large-scale identification of yeast integral membrane protein interactions.', *Proceedings of the National Academy of Sciences of the United States of America*. National Academy of Sciences, 102(34), pp. 12123–8. doi: 10.1073/pnas.0505482102.

Minase, G. *et al.* (2017) 'An atypical case of SPG56/CYP2U1-related spastic paraplegia presenting with delayed myelination', *Journal of Human Genetics*. doi: 10.1038/jhg.2017.77.

Minkiewicz, J., de Rivero Vaccari, J. P. and Keane, R. W. (2013) 'Human astrocytes express a novel NLRP2 inflammasome', *Glia*, 61(7), pp. 1113–1121. doi: 10.1002/glia.22499.

Montenegro, G. *et al.* (2012) 'Mutations in the ER-shaping protein reticulon 2 cause the axon-degenerative disorder hereditary spastic paraplegia type 12', *Journal of Clinical Investigation*, 122(2), pp. 538–544. doi: 10.1172/JCI60560.

Moreno-De-Luca, A. *et al.* (2011) 'Adaptor protein complex-4 (AP-4) deficiency causes a novel autosomal recessive cerebral palsy syndrome with microcephaly and intellectual disability', *Journal of Medical Genetics*, 48(2), pp. 141–144. doi: 10.1136/jmg.2010.082263.

Morikawa, R. K. *et al.* (2009) 'Intracellular Phospholipase A1gamma (iPLA1gamma) Is a Novel Factor Involved in Coat Protein Complex I- and Rab6-independent Retrograde Transport between the Endoplasmic Reticulum and the Golgi Complex', *Journal of Biological Chemistry*, 284(39), pp. 26620–26630. doi: 10.1074/jbc.M109.038869.

Morishima-Kawashima, M. *et al.* (1993) 'Ubiquitin is conjugated with amino-terminally processed tau in paired helical filaments.', *Neuron*, 10(6), pp. 1151–60. Available at: http://www.ncbi.nlm.nih.gov/pubmed/8391280

Morita, E. and Sundquist, W. I. (2004) 'RETROVIRUS BUDDING', *Annual Review of Cell and Developmental Biology*, 20(1), pp. 395–425. doi: 10.1146/annurev.cellbio.20.010403.102350.

Morreale, F. . and Walden, H. (2016) 'Types of Ubiquitin Ligases', *Cell*. Cell Press, 165(1), pp. 248–248. doi: 10.1016/J.CELL.2016.03.003.

Motohashi, K. (2015) 'A simple and efficient seamless DNA cloning method using SLiCE from Escherichia coli laboratory strains and its application to SLiP site-directed mutagenesis', *BMC Biotechnology*. BioMed Central, 15(1), p. 47. doi: 10.1186/s12896-015-0162-8.

Munkonda, M. N. *et al.* (2007) 'Inhibition of human and mouse plasma membrane bound NTPDases by P2 receptor antagonists', *Biochemical Pharmacology*. Elsevier, 74(10), pp. 1524–1534. doi: 10.1016/J.BCP.2007.07.033.

Murmu, R. P. *et al.* (2011) 'Cellular distribution and subcellular localization of spatacsin and spastizin, two proteins involved in hereditary spastic paraplegia', *Molecular and Cellular Neuroscience*, 47(3), pp. 191–202. doi: 10.1016/j.mcn.2011.04.004.

Nagle, D. L. *et al.* (1996) 'Identification and mutation analysis of the complete gene for Chediak–Higashi syndrome', *Nature Genetics*. Nature Publishing Group, 14(3), pp. 307–311. doi: 10.1038/ng1196-307.

Ng, S.-K. *et al.* (2003) 'InterDom: a database of putative interacting protein domains for validating predicted protein interactions and complexes.', *Nucleic acids research*. Oxford University Press, 31(1), pp. 251–4. Available at: http://www.ncbi.nlm.nih.gov/pubmed/12519994

Nicholls, D. G. and Budd, S. L. (2000) 'Mitochondria and neuronal survival.', *Physiological reviews*. American Physiological Society, 80(1), pp. 315–60. Available at: http://www.ncbi.nlm.nih.gov/pubmed/10617771

Nicolson, G. L. (2014) 'Mitochondrial Dysfunction and Chronic Disease: Treatment With Natural Supplements.', *Integrative medicine (Encinitas, Calif.)*. InnoVision Media, 13(4), pp. 35–43. Available at: http://www.ncbi.nlm.nih.gov/pubmed/26770107

Nielsen, K. L. and Cowan, N. J. (1998) 'A single ring is sufficient for productive chaperonin-mediated folding in vivo.', *Molecular cell*, 2(1), pp. 93–9. Available at: http://www.ncbi.nlm.nih.gov/pubmed/9702195

Nijman, S. M. B. *et al.* (2005) 'A Genomic and Functional Inventory of Deubiquitinating Enzymes', *Cell*, 123(5), pp. 773–786. doi: 10.1016/j.cell.2005.11.007.

Nikoletopoulou, V., Papandreou, M.-E. and Tavernarakis, N. (2015) 'Autophagy in the physiology and pathology of the central nervous system', *Cell Death and Differentiation*. Nature Publishing Group, 22(3), pp. 398–407. doi: 10.1038/cdd.2014.204.

Noda, Y., Yamagishi, T. and Yoda, K. (2007) 'Specific membrane recruitment of Uso1 protein, the essential endoplasmic reticulum-to-Golgi tethering factor in yeast vesicular transport', *Journal of Cellular Biochemistry*, 101(3), pp. 686–694. doi: 10.1002/jcb.21225.

Noetzli, L. *et al.* (2014) 'A novel mutation in PLP1 causes severe hereditary spastic paraplegia type 2', *Gene*, 533(1), pp. 447–450. doi: 10.1016/j.gene.2013.09.076.

Nolden, M. *et al.* (2005) 'The m-AAA Protease Defective in Hereditary Spastic Paraplegia Controls Ribosome Assembly in Mitochondria', *Cell*, 123(2), pp. 277–289. doi: 10.1016/j.cell.2005.08.003.

Noreau, A., Dion, P. A. and Rouleau, G. A. (2014) 'Molecular aspects of hereditary spastic paraplegia', *Experimental Cell Research*. doi: 10.1016/j.yexcr.2014.02.021.

Novarino, G. *et al.* (2014) 'Exome sequencing links corticospinal motor neuron disease to common neurodegenerative disorders.', *Science (New York, N.Y.)*. NIH Public Access, 343(6170), pp. 506–511. doi: 10.1126/science.1247363.

O'Sullivan, N. C. *et al.* (2012) 'Reticulon-like-1, the Drosophila orthologue of the Hereditary Spastic Paraplegia gene reticulon 2, is required for organization of endoplasmic reticulum and of distal motor axons', *Human Molecular Genetics*. Oxford University Press, 21(15), pp. 3356–3365. doi: 10.1093/hmg/dds167.

Oakes, S. A. and Papa, F. R. (2015) 'The Role of Endoplasmic Reticulum Stress in Human Pathology', *Annual Review of Pathology: Mechanisms of Disease*, 10(1), pp. 173–194. doi: 10.1146/annurev-pathol-012513-104649.

Oates, E. C. *et al.* (2013) 'Mutations in BICD2 cause dominant congenital spinal muscular atrophy and hereditary spastic paraplegia', *American Journal of Human Genetics*, 92(6). doi: 10.1016/j.ajhg.2013.04.018.

Oertle, T. and Schwab, M. E. (no date) 'Nogo and its paRTNers'. doi: 10.1016/S0962-8924(03)00035-7.

Oka, T. *et al.* (2005) 'Genetic Analysis of the Subunit Organization and Function of the Conserved Oligomeric Golgi (COG) Complex STUDIES OF COG5-AND COG7-DEFICIENT MAMMALIAN CELLS. doi: 10.1074/jbc.M505558200.

Olmos, Y. *et al.* (2015) 'ESCRT-III controls nuclear envelope reformation', *Nature*, 522(7555), pp. 236–239. doi: 10.1038/nature14503.

Omasits, U. *et al.* (2014) 'Protter: interactive protein feature visualization and integration with experimental proteomic data', *Bioinformatics*, 30(6), pp. 884–886.
doi: 10.1093/bioinformatics/btt607.

Orlacchio, A. *et al.* (2005) 'New locus for hereditary spastic paraplegia maps to chromosome 1p31.1-1p21.1', *Annals of Neurology*, 58(3), pp. 423–429. doi: 10.1002/ana.20590.

Orlacchio, A. *et al.* (2008) 'Silver syndrome variant of hereditary spastic paraplegia: A locus to 4p and allelism with SPG4', *Neurology*, 70(21), pp. 1959–1966. doi: 10.1212/01.wnl.0000294330.27058.61.

Orso, G. *et al.* (2009) 'Homotypic fusion of ER membranes requires the dynamin-like GTPase Atlastin', *Nature*, 460(7258), pp. 978–983. doi: 10.1038/nature08280.

Orth, M. and Bellosta, S. (2012) 'Cholesterol: Its Regulation and Role in Central Nervous System Disorders', *Cholesterol*. Hindawi, 2012, pp. 1–19. doi: 10.1155/2012/292598.

Orthmann-Murphy, J. L. *et al.* (2009) 'Hereditary spastic paraplegia is a novel phenotype for GJA12/GJC2 mutations.', *Brain : a journal of neurology*. Oxford University Press, 132(Pt 2), pp. 426–38. doi: 10.1093/brain/awn328.

Oslowski, C. M. and Urano, F. (2011) 'Measuring ER stress and the unfolded protein response using mammalian tissue culture system.', *Methods in enzymology*. NIH Public Access, 490, pp. 71–92. doi: 10.1016/B978-0-12-385114-7.00004-0.

Overington, J. P., Al-Lazikani, B. and Hopkins, A. L. (2006) 'How many drug targets are there?', *Nature Reviews Drug Discovery*, 5(12), pp. 993–996. doi: 10.1038/nrd2199.

Oz-Levi, D. *et al.* (2012) 'Mutation in TECPR2 reveals a role for autophagy in hereditary spastic paraparesis.', *American journal of human genetics*. Elsevier, 91(6), pp. 1065–72. doi: 10.1016/j.ajhg.2012.09.015.

Ozcan, U. *et al.* (2004) 'Endoplasmic reticulum stress links obesity, insulin action, and type 2 diabetes', *Science*, 306(5695), pp. 457–461. doi: 10.1126/science.1103160.

Ozcan, U. *et al.* (2006) 'Chemical chaperones reduce ER stress and restore glucose homeostasis in a mouse model of type 2 diabetes.', *Science*, 313(5790), pp. 1137–1140. doi: 10.1126/science.1128294.

Pahl, H. L. and Baeuerle, P. A. (1996) 'Activation of NF-kappa B by ER stress requires both Ca2+ and reactive oxygen intermediates as messengers.', *FEBS letters*, 392(2), pp. 129–36. Available at: http://www.ncbi.nlm.nih.gov/pubmed/8772190

Pan, T. *et al.* (2008) 'The role of autophagy-lysosome pathway in neurodegeneration associated with Parkinson's disease', *Brain*, 131(8), pp. 1969–1978. doi: 10.1093/brain/awm318.

Pandey, S. and Assmann, S. M. (2004) 'The Arabidopsis putative G protein-coupled receptor GCR1 interacts with the G protein alpha subunit GPA1 and regulates abscisic acid signaling.', *The Plant cell*, 16(6), pp. 1616–32. doi: 10.1105/tpc.020321.

Di Paolo, G. and Kim, T.-W. (2011) 'Linking lipids to Alzheimer's disease: cholesterol and beyond', *Nature Reviews Neuroscience*, 12(5), pp. 284–296. doi: 10.1038/nrn3012.

Papadopoulos, C. *et al.* (2015) 'Spastin Binds to Lipid Droplets and Affects Lipid Metabolism', *PLOS Genetics*. Edited by K. Ashrafi. Public Library of Science, 11(4), p. e1005149. doi: 10.1371/journal.pgen.1005149.

Park, S. H. *et al.* (2010) 'Hereditary spastic paraplegia proteins REEP1, spastin, and atlastin-1 coordinate microtubule interactions with the tubular ER network.', *The Journal of clinical investigation*. American Society for Clinical Investigation, 120(4), pp. 1097–110. doi: 10.1172/JCI40979.

Park, S. H. and Blackstone, C. (2010) 'Further assembly required: construction and dynamics of the endoplasmic reticulum network', *EMBO reports*, 11(7), pp. 515–521. doi: 10.1038/embor.2010.92.

Park, S. Y. and Guo, X. (2014) 'Adaptor protein complexes and intracellular transport.', *Bioscience*

reports. Portland Press Ltd, 34(4). doi: 10.1042/BSR20140069.

Parrish, J. R., Gulyas, K. D. and Finley, R. L. (2006) 'Yeast two-hybrid contributions to interactome mapping', *Current Opinion in Biotechnology*, 17(4), pp. 387–393. doi: 10.1016/j.copbio.2006.06.006.

Passantino, R. *et al.* (2013) 'Identifying protein partners of CLN8, an ER-resident protein involved in neuronal ceroid lipofuscinosis', *Biochimica et Biophysica Acta (BBA) - Molecular Cell Research*, 1833(3), pp. 529–540. doi: 10.1016/j.bbamcr.2012.10.030.

Patel, H. *et al.* (2002) 'SPG20 is mutated in Troyer syndrome, an hereditary spastic paraplegia', *Nature Genetics*, 31(4), pp. 347–8. doi: 10.1038/ng937.

Paumi, C. M. *et al.* (2007) 'Mapping Protein-Protein Interactions for the Yeast ABC Transporter Ycf1p by Integrated Split-Ubiquitin Membrane Yeast Two-Hybrid Analysis', *Molecular Cell*, 26(1), pp. 15–25. doi: 10.1016/j.molcel.2007.03.011.

Pearce, M. M. P. *et al.* (2007) 'SPFH2 Mediates the Endoplasmic Reticulum-associated Degradation of Inositol 1,4,5-Trisphosphate Receptors and Other Substrates in Mammalian Cells', *Journal of Biological Chemistry*, 282(28), pp. 20104–20115. doi: 10.1074/jbc.M701862200.

Pearce, M. M. P. *et al.* (2009) 'An endoplasmic reticulum (ER) membrane complex composed of SPFH1 and SPFH2 mediates the ER-associated degradation of inositol 1,4,5-trisphosphate receptors.', *The Journal of biological chemistry*. American Society for Biochemistry and Molecular Biology, 284(16), pp. 10433–45. doi: 10.1074/jbc.M809801200.

Pensato, V. *et al.* (2014) 'Overlapping phenotypes in complex spastic paraplegias SPG11, SPG15, SPG35 and SPG48', *Brain*, 137(7), pp. 1907–1920. doi: 10.1093/brain/awu121.

Perlson, E. *et al.* (2010) 'Retrograde axonal transport: pathways to cell death?', *Trends in neurosciences*. NIH Public Access, 33(7), pp. 335–44. doi: 10.1016/j.tins.2010.03.006.

Pfenninger, K. H. (2009) 'Plasma membrane expansion: a neuron's Herculean task', *Nature Reviews Neuroscience*. Nature Publishing Group, 10(4), pp. 251–261. doi: 10.1038/nrn2593.

Pickart, C. M. (2001) 'Mechanisms Underlying Ubiquitination', *Annual Review of Biochemistry*, 70(1), pp. 503–533. doi: 10.1146/annurev.biochem.70.1.503.

Pleasure, I. T., Black, M. M. and Keen, J. H. (1993) 'Valosin-containing protein, VCP, is a ubiquitous clathrin-binding protein', *Nature*, 365(6445), pp. 459–462. doi: 10.1038/365459a0.

Polo, J. M. *et al.* (1991) 'Hereditary ataxias and paraplegias in Cantabria, Spain. An epidemiological and clinical study.', *Brain : a journal of neurology*, 114 (Pt 2), pp. 855–66. Available at: http://www.ncbi.nlm.nih.gov/pubmed/2043954

Pomerantz, J. L. and Baltimore, D. (2002) 'Two pathways to NF-kappaB.', *Molecular cell*. Elsevier, 10(4), pp. 693–5. doi: 10.1016/S1097-2765(02)00697-4.

Prinz, M. and Priller, J. (2014) 'Microglia and brain macrophages in the molecular age: from origin to neuropsychiatric disease', *Nature Reviews Neuroscience*, 15(5), pp. 300–312. doi: 10.1038/nrn3722.

Proukakis, C. *et al.* (2004) 'Troyer syndrome revisited', *Journal of Neurology*, 251(9), pp. 1105–10. doi: 10.1007/s00415-004-0491-3.

Pruitt, K. D., Tatusova, T. and Maglott, D. R. (2005) 'NCBI Reference Sequence (RefSeq): a curated non-redundant sequence database of genomes, transcripts and proteins', *Nucleic Acids Research*, 33(Database issue), pp. 501–504. doi: 10.1093/nar/gki025.

Pujana, M. A. *et al.* (2007) 'Network modeling links breast cancer susceptibility and centrosome dysfunction', *Nature Genetics*, 39(11), pp. 1338–1349. doi: 10.1038/ng.2007.2.

Puthenveedu, M. A. and Linstedt, A. D. (2001) 'Evidence that Golgi structure depends on a p115 activity that is independent of the vesicle tether components giantin and GM130.', *The Journal of cell biology*. Rockefeller University Press, 155(2), pp. 227–38. doi: 10.1083/jcb.200105005.

Pye, V. E. *et al.* (2006) 'Going through the motions: The ATPase cycle of p97', *Journal of Structural Biology*, 156(1), pp. 12–28. doi: 10.1016/j.jsb.2006.03.003.

Quintana, F. J. and Cohen, I. R. (2011) 'The HSP60 immune system network.', *Trends in immunology*, 32(2), pp. 89–95. doi: 10.1016/j.it.2010.11.001.

Rabinovich, E. *et al.* (2002) 'AAA-ATPase p97/Cdc48p, a cytosolic chaperone required for endoplasmic reticulum-associated protein degradation.', *Molecular and cellular biology*, 22(2), pp. 626–34. Available at: http://www.ncbi.nlm.nih.gov/pubmed/11756557

Rahman, M. *et al.* (2012) '*Drosophila mauve* Mutants Reveal a Role of LYST Homologs Late in the Maturation of Phagosomes and Autophagosomes', *Traffic*. John Wiley & Sons A/S, 13(12), pp. 1680–1692. doi: 10.1111/tra.12005.

Raiborg, C. and Stenmark, H. (2009) 'The ESCRT machinery in endosomal sorting of ubiquitylated membrane proteins', *Nature*, 458(7237), pp. 445–452. doi: 10.1038/nature07961.

Raine, C. S. (1984) 'Morphology of Myelin and Myelination', in *Myelin*. Boston, MA: Springer US, pp. 1–50. doi: 10.1007/978-1-4757-1830-0_1.

Ramanathan, H. N. and Ye, Y. (2012) 'The p97 ATPase associates with EEA1 to regulate the size of early endosomes', *Cell Research*, 22(2), pp. 346–359. doi: 10.1038/cr.2011.80.

Rao, K. S. (1993) 'Genomic damage and its repair in young and aging brain.', *Molecular neurobiology*, 7(1), pp. 23–48. Available at: http://www.ncbi.nlm.nih.gov/pubmed/8318166

Rao, R. V and Bredesen, D. E. (2004) 'Misfolded proteins, endoplasmic reticulum stress and neurodegeneration', *Curr Opin Cell Biol*, 16(6), pp. 653–662. doi: 10.1016/j.ceb.2004.09.012.

Rapoport, T. A. (2007) 'Protein translocation across the eukaryotic endoplasmic reticulum and bacterial plasma membranes', *Nature*, 450(7170), pp. 663–669. doi: 10.1038/nature06384.

Rass, U., Ahel, I. and West, S. C. (2007) 'Defective DNA Repair and Neurodegenerative Disease', *Cell*, 130(6), pp. 991–1004. doi: 10.1016/j.cell.2007.08.043.

Ravasz, E. *et al.* (2002) 'Hierarchical Organization of Modularity in Metabolic Networks', *Science*, 297(5586), pp. 1551–1555. doi: 10.1126/science.1073374.

Ravasz, E. and Barabási, A.-L. (2003) 'Hierarchical organization in complex networks', *Physical Review*, 67(2), pp. 1–7. doi: 10.1103/PhysRevE.67.026112.

Ravid, T. and Hochstrasser, M. (2008) 'Diversity of degradation signals in the ubiquitin–proteasome system', *Nature Reviews Molecular Cell Biology*, 9(9), pp. 679–689. doi: 10.1038/nrm2468.

Razick, S., Magklaras, G. and Donaldson, I. M. (2008) 'iRefIndex: A consolidated protein interaction database with provenance', *BMC Bioinformatics*, 9(1), p. 405. doi: 10.1186/1471-2105-9-405.
Reddy, P. H. (2008) 'Mitochondrial Medicine for Aging and Neurodegenerative Diseases', *NeuroMolecular Medicine*, 10(4), pp. 291–315. doi: 10.1007/s12017-008-8044-z.

Reid, E. *et al.* (2002) 'A Kinesin Heavy Chain (KIF5A) Mutation in Hereditary Spastic Paraplegia (SPG10)', *The American Journal of Human Genetics*, 71(5), pp. 1189–1194. doi: 10.1086/344210.

Reid, E. *et al.* (2005) 'The hereditary spastic paraplegia protein spastin interacts with the ESCRT-III complex-associated endosomal protein CHMP1B.', *Human molecular genetics*, 14(1), pp. 19–38. doi: 10.1093/hmg/ddi003.

Reits, E. *et al.* (2003) 'Peptide diffusion, protection, and degradation in nuclear and cytoplasmic compartments before antigen presentation by MHC class I.', *Immunity*, 18(1), pp. 97–108. Available at: http://www.ncbi.nlm.nih.gov/pubmed/12530979

Renvoisé, B. *et al.* (2010) 'SPG20 protein spartin is recruited to midbodies by ESCRT-III protein Ist1 and participates in cytokinesis.', *Molecular biology of the cell*, 21(19), pp. 3293–303. doi: 10.1091/mbc.E09-10-0879.

Renvoisé, B. and Blackstone, C. (2010) 'Emerging themes of ER organization in the development and maintenance of axons.', *Current opinion in neurobiology*. NIH Public Access, 20(5), pp. 531–7. doi: 10.1016/j.conb.2010.07.001.

Ribai, P. *et al.* (2006) 'A new phenotype linked to SPG27 and refinement of the critical region on chromosome', *Journal of Neurology*, 253(6), pp. 714–719. doi: 10.1007/s00415-006-0094-2.

Richter, R. *et al.* (2010) 'A functional peptidyl-tRNA hydrolase, ICT1, has been recruited into the human mitochondrial ribosome.', *The EMBO journal*, 29(6), pp. 1116–25. doi: 10.1038/emboj.2010.14.

Rismanchi, N. *et al.* (2008) 'Atlastin GTPases are required for Golgi apparatus and ER morphogenesis', *Human Molecular Genetics*, 17(11), pp. 1591–1604. doi: 10.1093/hmg/ddn046.

Ritz, D. *et al.* (2011) 'Endolysosomal sorting of ubiquitylated caveolin-1 is regulated by VCP and UBXD1 and impaired by VCP disease mutations', *Nature Cell Biology*, 13(9), pp. 1116–1123. doi: 10.1038/ncb2301.

Robay, D. *et al.* (2006) 'Endogenous spartin, mutated in hereditary spastic paraplegia, has a complex subcellular localization suggesting diverse roles in neurons', *Experimental Cell Research*, 312(15), pp.

2764–2777. doi: 10.1016/j.yexcr.2006.05.003.

Robert Dorfman (1969) 'An Economic Interpretation of Optimal Control Theory', *The American Economic Review*, 59(5), pp. 817–831. Available at: https://www.andrew.cmu.edu/course/88-737/optimal_control/papers/dorfman.pdf

Rodríguez-Negrete, E., Bejarano, E. R. and Castillo, A. G. (2014) 'Using the Yeast Two-Hybrid System to Identify Protein–Protein Interactions', in *Methods in molecular biology (Clifton, N.J.)*, pp. 241–258. doi: 10.1007/978-1-62703-631-3_18.

Rodriguez, M. S. *et al.* (2014) 'The RING ubiquitin E3 RNF114 interacts with A20 and modulates NF-κB activity and T-cell activation.', *Cell death & disease*. Nature Publishing Group, 5(8), p. e1399. doi: 10.1038/cddis.2014.366.

Rolland, T. *et al.* (2014) 'A Proteome-Scale Map of the Human Interactome Network', *Cell*, 159(5), pp. 1212–1226. doi: 10.1016/j.cell.2014.10.050.

Ronchi, P. *et al.* (2008) 'Transmembrane domain–dependent partitioning of membrane proteins within the endoplasmic reticulum', *The Journal of Cell Biology*, 181(1), pp. 105–118. doi: 10.1083/jcb.200710093.

Rosenfeld, M. E. (2013) 'Inflammation and Atherosclerosis: Direct Versus Indirect Mechanisms', *Current opinion in pharmacology*. NIH Public Access, 13(2), pp. 154–160. doi: 10.1016/j.coph.2013.01.003.

Ross, C. A. and Poirier, M. A. (2004) 'Protein aggregation and neurodegenerative disease', *Nature Medicine*, 10(7), pp. S10–S17. doi: 10.1038/nm1066.

Ross, C. A. and Poirier, M. A. (2005) 'Opinion: What is the role of protein aggregation in neurodegeneration?', *Nature Reviews Molecular Cell Biology*, 6(11), pp. 891–898. doi: 10.1038/nrm1742.

Row, P. E. *et al.* (2007) 'The MIT Domain of UBPY Constitutes a CHMP Binding and Endosomal Localization Signal Required for Efficient Epidermal Growth Factor Receptor Degradation', *Journal of Biological Chemistry*, 282(42), pp. 30929–30937. doi: 10.1074/jbc.M704009200.

Rual, J.-F. *et al.* (2004) 'Human ORFeome version 1.1: a platform for reverse proteomics.', *Genome research*. Cold Spring Harbor Laboratory Press, 14(10B), pp. 2128–35. doi: 10.1101/gr.2973604.

Rual, J.-F. *et al.* (2005) 'Towards a proteome-scale map of the human protein-protein interaction network.', *Nature*, 437(7062), pp. 1173–8. doi: 10.1038/nature04209.

Ruano, L. *et al.* (2014) 'The global epidemiology of hereditary ataxia and spastic paraplegia: A systematic review of prevalence studies', *Neuroepidemiology*. doi: 10.1159/000358801.

Ruggiano, A., Foresti, O. and Carvalho, P. (2014) 'ER-associated degradation: Protein quality control and beyond', *The Journal of Cell Biology*, 204(6).
Available at: http://jcb.rupress.org/content/204/6/869

Sagona, A. P. *et al.* (2010) 'PtdIns(3)P controls cytokinesis through KIF13A-mediated recruitment of FYVE-CENT to the midbody', *Nature Cell Biology*, 12(4), pp. 362–371. doi: 10.1038/ncb2036.

Saha, A. R. *et al.* (2004) 'Parkinson's disease -synuclein mutations exhibit defective axonal transport in cultured neurons', *Journal of Cell Science*, 117(7), pp. 1017–1024. doi: 10.1242/jcs.00967.

Sahni, N. *et al.* (2013) 'Edgotype: a fundamental link between genotype and phenotype', *Current Opinion in Genetics & Development*, 23(6), pp. 649–657. doi: 10.1016/j.gde.2013.11.002.

Sahni, N. *et al.* (2015) 'Widespread Macromolecular Interaction Perturbations in Human Genetic Disorders', *Cell*, 161(3), pp. 647–660. doi: 10.1016/j.cell.2015.04.013.

Saito, H. *et al.* (2004) 'RTP Family Members Induce Functional Expression of Mammalian Odorant Receptors', *Cell*, 119(5), pp. 679–691. doi: 10.1016/j.cell.2004.11.021.

Saksena, S. and Emr, S. D. (2009) 'ESCRTs and human disease', *Biochemical Society Transactions*, 37(1), pp. 167–172. doi: 10.1042/BST0370167.

Salinas, S. *et al.* (2008) 'Hereditary spastic paraplegia: clinical features and pathogenetic mechanisms.', *Lancet neurology*, 7(12), pp. 1127–38. doi: 10.1016/S1474-4422(08)70258-8.

Salviati, L. *et al.* (2007) 'A novel deletion in the GJA12 gene causes Pelizaeus–Merzbacher-like disease', *Neurogenetics*, 8(1), pp. 57–60. doi: 10.1007/s10048-006-0065-x.

Sanderson, C. M. *et al.* (2005) 'Spastin and atlastin, two proteins mutated in autosomal-dominant hereditary spastic paraplegia, are binding partners', *Human Molecular Genetics*. Oxford University Press, 15(2), pp. 307–318. doi: 10.1093/hmg/ddi447.

Sanderson, C. M. *et al.* (2006) 'Spastin and atlastin, two proteins mutated in autosomal-dominant hereditary spastic paraplegia, are binding partners.', *Human molecular genetics*. Oxford University Press, 15(2), pp. 307–18. doi: 10.1093/hmg/ddi447.

Sato, S. *et al.* (2010) 'Golgi-localized KIAA0725p regulates membrane trafficking from the Golgi apparatus to the plasma membrane in mammalian cells', *FEBS Letters*, 584(21), pp. 4389–4395. doi: 10.1016/j.febslet.2010.09.047.

Satoh, J., Tabunoki, H. and Yamamura, T. (2009) 'Molecular network of the comprehensive multiple sclerosis brain-lesion proteome', *Multiple Sclerosis Journal*, 15(5), pp. 531–541. doi: 10.1177/1352458508101943.

Schauer, K. and Stingl, K. (2009) '‘Guilty by Association’ – Protein-Protein Interactions (PPIs) in Bacterial Pathogens', in *Microbial Pathogenomics*. Basel: KARGER, pp. 48–61. doi: 10.1159/000235762.

Schrattenholz, A., Groebe, K. and Soskic, V. (2010) 'Systems Biology Approaches and Tools for Analysis of Interactomes and Multi-target Drugs', in *Methods in molecular biology (Clifton, N.J.)*, pp. 29–58. doi: 10.1007/978-1-60761-800-3_2.

Schule, R. *et al.* (2009) 'Autosomal dominant spastic paraplegia with peripheral neuropathy maps to

chr12q23-24', *Neurology*, 72(22), pp. 1893–1898. doi: 10.1212/WNL.0b013e3181a6086c.

Schüle, R. *et al.* (2016) 'Hereditary spastic paraplegia: Clinicogenetic lessons from 608 patients', *Annals of Neurology*, 79(4). doi: 10.1002/ana.24611.

Schwartz, C. E. *et al.* (2005) 'Allan-Herndon-Dudley Syndrome and the Monocarboxylate Transporter 8 (MCT8) Gene', *The American Journal of Human Genetics*, 77(1), pp. 41–53. doi: 10.1086/431313.

Schwarz, D. S. and Blower, M. D. (2016) 'The endoplasmic reticulum: structure, function and response to cellular signaling.', *Cellular and molecular life sciences : CMLS*. Springer, 73(1), pp. 79–94. doi: 10.1007/s00018-015-2052-6.

Seaman, M. N. J. (2004) 'Cargo-selective endosomal sorting for retrieval to the Golgi requires retromer', *The Journal of Cell Biology*, 165(1), pp. 111–122. doi: 10.1083/jcb.200312034.

Seaman, M. N. J. (2012) 'The retromer complex - endosomal protein recycling and beyond.', *Journal of cell science*. Company of Biologists, 125(Pt 20), pp. 4693–702. doi: 10.1242/jcs.103440.

Seeligmüller, A. (1876) 'Einige seltenere Formen von Affectionen des Rückenmarks', *DMW - Deutsche Medizinische Wochenschrift*. © Georg Thieme Verlag, Stuttgart, 2(16), pp. 185–186. doi: 10.1055/s-0029-1193358.

Selkoe, D. J. (2003) 'Folding proteins in fatal ways', *Nature*, 426(6968), pp. 900–904. doi: 10.1038/nature02264.

Semple, J. I. *et al.* (2005) 'Two-hybrid reporter vectors for gap repair cloning.', *BioTechniques*, 38(6), pp. 927–34. Available at: http://www.ncbi.nlm.nih.gov/pubmed/16018554

Seo, H., Sonntag, K.-C. and Isacson, O. (2004) 'Generalized brain and skin proteasome inhibition in Huntington's disease', *Annals of Neurology*, 56(3), pp. 319–328. doi: 10.1002/ana.20207.

Sergeeva, O. A. *et al.* (2013) 'Human CCT4 and CCT5 Chaperonin Subunits Expressed in Escherichia coli Form Biologically Active Homo-oligomers.', *The Journal of biological chemistry*. American Society for Biochemistry and Molecular Biology, 288(24), pp. 17734–44. doi: 10.1074/jbc.M112.443929.

Serrano, F. and Klann, E. (2004) 'Reactive oxygen species and synaptic plasticity in the aging hippocampus', *Ageing Research Reviews*, 3(4), pp. 431–443. doi: 10.1016/j.arr.2004.05.002.

Shabab, T. *et al.* (2017) 'Neuroinflammation pathways: a general review', *International Journal of Neuroscience*. Taylor & FrancisNew York, 127(7), pp. 624–633. doi: 10.1080/00207454.2016.1212854.

Shacter, E. and Weitzman, S. A. (2002) 'Chronic inflammation and cancer.', *Oncology (Williston Park, N.Y.)*, 16(2), pp. 217–26, 229–2. Available at: http://www.ncbi.nlm.nih.gov/pubmed/11866137

Sheftel, A. D. *et al.* (2012) 'The human mitochondrial ISCA1, ISCA2, and IBA57 proteins are required for [4Fe-4S] protein maturation.', *Molecular biology of the cell*. American Society for Cell Biology, 23(7), pp. 1157–66. doi: 10.1091/mbc.E11-09-0772.

Shen, Y. *et al.* (2012) 'TRIM56 is an essential component of the TLR3 antiviral signaling pathway.', *The*

Journal of biological chemistry. American Society for Biochemistry and Molecular Biology, 287(43), pp. 36404–13. doi: 10.1074/jbc.M112.397075.

Shih, R.-H., Wang, C.-Y. and Yang, C.-M. (2015) 'NF-kappaB Signaling Pathways in Neurological Inflammation: A Mini Review.', *Frontiers in molecular neuroscience*. Frontiers Media SA, 8(77), pp. 1–8. doi: 10.3389/fnmol.2015.00077.

Shilo, B.-Z. and Schejter, E. D. (2011) 'Regulation of developmental intercellular signalling by intracellular trafficking', *The EMBO Journal*, 30(17), pp. 3516–3526. doi: 10.1038/emboj.2011.269.

Shimazaki, H. *et al.* (2012) 'A homozygous mutation of C12orf65 causes spastic paraplegia with optic atrophy and neuropathy (SPG55).', *Journal of medical genetics*, 49(12), pp. 777–84. doi: 10.1136/jmedgenet-2012-101212.

Shimazaki, H. *et al.* (2014) 'Autosomal-recessive complicated spastic paraplegia with a novel lysosomal trafficking regulator gene mutation', *Journal of Neurology, Neurosurgery & Psychiatry*, 85(9), pp. 1024–1028. doi: 10.1136/jnnp-2013-306981.

Shulga, N. *et al.* (2000) 'Yeast nucleoporins involved in passive nuclear envelope permeability.', *The Journal of cell biology*. The Rockefeller University Press, 149(5), pp. 1027–38. Available at: http://www.ncbi.nlm.nih.gov/pubmed/10831607

Silve, S. *et al.* (1991) 'Membrane insertion of uracil permease, a polytopic yeast plasma membrane protein.', *Molecular and cellular biology*, 11(2), pp. 1114–24. Available at: http://www.ncbi.nlm.nih.gov/pubmed/1846664

Simpson, M. A. *et al.* (2003) 'Maspardin is mutated in mast syndrome, a complicated form of hereditary spastic paraplegia associated with dementia.', *American journal of human genetics*. Elsevier, 73(5), pp. 1147–56. doi: 10.1086/379522.

Siri, L. *et al.* (2010) 'Cognitive Profile in Spastic Paraplegia with Thin Corpus Callosum and Mutations in SPG11', *Neuropediatrics*, 41(1), pp. 35–38. doi: 10.1055/s-0030-1253352.

Słabicki, M. *et al.* (2010) 'A genome-scale DNA repair RNAi screen identifies SPG48 as a novel gene associated with hereditary spastic paraplegia.', *PLoS Biology*. Edited by N. Hastie. Public Library of Science, 8(6), pp. 1–16. doi: 10.1371/journal.pbio.1000408.

Smith, M. H., Ploegh, H. L. and Weissman, J. S. (2011) 'Road to Ruin: Targeting Proteins for Degradation in the Endoplasmic Reticulum', *Science*, 334(6059), pp. 1086–1090. doi: 10.1126/science.1209235.

Snider, J. *et al.* (2010) 'Split-ubiquitin based membrane yeast two-hybrid (MYTH) system: a powerful tool for identifying protein-protein interactions.', *Journal of visualized experiments : JoVE*. MyJoVE Corporation, (36). doi: 10.3791/1698.

Soderblom, C. and Blackstone, C. (2006) 'Traffic accidents: Molecular genetic insights into the pathogenesis of the hereditary spastic paraplegias', *Pharmacology & therapeutics*, 109(1–2), pp. 42–56. doi: 10.1016/j.pharmthera.2005.06.001.

Sofroniew, M. V. (2015) 'Astrocyte barriers to neurotoxic inflammation', *Nature Reviews*

Neuroscience, 16(5), pp. 249–263. doi: 10.1038/nrn3898.

Soler-Lopez, M. *et al.* (2011) 'Interactome mapping suggests new mechanistic details underlying Alzheimer's disease', *Genome Research*, 21(3), pp. 364–376. doi: 10.1101/gr.114280.110.

Solowska, J. M. *et al.* (2008) 'Quantitative and Functional Analyses of Spastin in the Nervous System: Implications for Hereditary Spastic Paraplegia', *Journal of Neuroscience*, 28(9), pp. 2147–2157. doi: 10.1523/JNEUROSCI.3159-07.2008.

Soto, C. (2003) 'Unfolding the role of protein misfolding in neurodegenerative diseases', *Nature Reviews Neuroscience*, 4(1), pp. 49–60. doi: 10.1038/nrn1007.

Soto, C. and Estrada, L. D. (2008) 'Protein Misfolding and Neurodegeneration', *Archives of Neurology*, 65(2), pp. 184–9. doi: 10.1001/archneurol.2007.56.

de Souza, P. V *et al.* (2016) 'Hereditary Spastic Paraplegia: Clinical and Genetic Hallmarks.', *Cerebellum*. doi: 10.1007/s12311-016-0803-z.

Sowa, M. E. *et al.* (2009) 'Defining the Human Deubiquitinating Enzyme Interaction Landscape', *Cell*, 138(2), pp. 389–403. doi: 10.1016/j.cell.2009.04.042.

Spacek, J. and Harris, K. M. (1997) 'Three-dimensional organization of smooth endoplasmic reticulum in hippocampal CA1 dendrites and dendritic spines of the immature and mature rat.', *The Journal of neuroscience : the official journal of the Society for Neuroscience*, 17(1), pp. 190–203. Available at: http://www.ncbi.nlm.nih.gov/pubmed/8987748

Splinter, D. *et al.* (2010) 'Bicaudal D2, Dynein, and Kinesin-1 Associate with Nuclear Pore Complexes and Regulate Centrosome and Nuclear Positioning during Mitotic Entry', *PLoS Biology*. Edited by D. Pellman. Public Library of Science, 8(4), p. e1000350. doi: 10.1371/journal.pbio.1000350.

Spratt, D. E., Walden, H. and Shaw, G. S. (2014) 'RBR E3 ubiquitin ligases: new structures, new insights, new questions', *Biochemical Journal*, 458(3), pp. 421–437. doi: 10.1042/BJ20140006.

Sprenkle, N. T. *et al.* (2017) 'Endoplasmic reticulum stress and inflammation in the central nervous system', *Molecular Neurodegeneration*. BioMed Central, 12(1), p. 42. doi: 10.1186/s13024-017-0183-y.

Stagljar, I. *et al.* (1998) 'A genetic system based on split-ubiquitin for the analysis of interactions between membrane proteins in vivo.', *Proceedings of the National Academy of Sciences of the United States of America*, 95(9), pp. 5187–92. Available at: http://www.ncbi.nlm.nih.gov/pubmed/9560251

Stagljar, I. and Fields, S. (2002) 'Analysis of membrane protein interactions using yeast-based technologies.', *Trends in biochemical sciences*, 27(11), pp. 559–63. Available at: http://www.ncbi.nlm.nih.gov/pubmed/12417131

Stefansson, H. *et al.* (2009) 'Common variants conferring risk of schizophrenia', *Nature*, 460(7256), pp. 744–7. doi: 10.1038/nature08186.

Steinmüller, R. *et al.* (1997) 'Evidence of a third locus in X-linked recessive spastic paraplegia.', *Human*

genetics, 100(2), pp. 287–9. Available at: http://www.ncbi.nlm.nih.gov/pubmed/9254866

Stelzl, U. *et al.* (2005) 'A Human Protein-Protein Interaction Network: A Resource for Annotating the Proteome', *Cell*, 122(6), pp. 957–968. doi: 10.1016/j.cell.2005.08.029.

Stenson, P. D. *et al.* (2014) 'The Human Gene Mutation Database: building a comprehensive mutation repository for clinical and molecular genetics, diagnostic testing and personalized genomic medicine', *Human Genetics*, 133(1), pp. 1–9. doi: 10.1007/s00439-013-1358-4.

Stevanin, G. *et al.* (2007) 'A new locus for autosomal recessive spastic paraplegia (SPG32) on chromosome 14q12-q21.', *Neurology*, 68(21), pp. 1837–40. doi: 10.1212/01.wnl.0000262043.53386.22.

Stokin, G. B. *et al.* (2005) 'Axonopathy and Transport Deficits Early in the Pathogenesis of Alzheimer's Disease', *Science*, 307(5713), pp. 1282–1288. doi: 10.1126/science.1105681.

Streit, W. J. (2002) 'Microglia as neuroprotective, immunocompetent cells of the CNS.', *Glia*, 40(2), pp. 133–9. doi: 10.1002/glia.10154.

Streit, W. J. and Kincaid-Colton, C. A. (1995) 'The brain's immune system.', *Scientific American*, 273(5), pp. 54–5, 58–61. Available at: http://www.ncbi.nlm.nih.gov/pubmed/8966536

Streitberger, K.-J. *et al.* (2012) 'Brain Viscoelasticity Alteration in Chronic-Progressive Multiple Sclerosis', *PLoS ONE*. Edied by W. Zhan. Public Library of Science, 7(1), p. e29888. doi: 10.1371/journal.pone.0029888.

Strogatz, S. H. (2001) 'Exploring complex networks', *Nature*. Nature Publishing Group, 410(6825), pp. 268–276. doi: 10.1038/35065725.

Strümpell, A. (1880) 'Beiträge zur Pathologie des Rückenmarks', *Archiv für Psychiatrie und Nervenkrankheiten*. Springer-Verlag, 10(3), pp. 676–717. doi: 10.1007/BF02224539.

Su, J., Yoon, B.-J. and Dougherty, E. R. (2010) 'Identification of diagnostic subnetwork markers for cancer in human protein-protein interaction network', *BMC Bioinformatics*. BioMed Central, 11(Suppl 6), p. S8. doi: 10.1186/1471-2105-11-S6-S8.

Subramony, S. *et al.* (2009) 'Identification of a new form of autosomal dominant spastic paraplegia', *Clinical Genetics*. Blackwell Publishing Ltd, 76(1), pp. 113–116. doi: 10.1111/j.1399-0004.2008.01122.x.

Sun, S.-C. (2008) 'Deubiquitylation and regulation of the immune response', *Nature Reviews Immunology*, 8(7), pp. 501–511. doi: 10.1038/nri2337.

Suter, B. *et al.* (2012) 'Chapter 4 A Stringent Yeast Two-Hybrid Matrix Screening Approach for Protein–Protein Interaction Discovery', *Methods in Molecular Biology*. Springer Science+Business Media, 812(10). doi: 10.1007/978-1-61779-455-1_4.

Suter, B., Auerbach, D. and Stagljar, I. (2006) 'Yeast-based functional genomics and proteomics technologies: the first 15 years and beyond.', *BioTechniques*, 40(5), pp. 625–44. Available at:

http://www.ncbi.nlm.nih.gov/pubmed/16708762

Suter, B., Kittanakom, S. and Stagljar, I. (2008) 'Two-hybrid technologies in proteomics research', *Current Opinion in Biotechnology*, 19(4), pp. 316–323. doi: 10.1016/j.copbio.2008.06.005.

Swerdlow, R. H. (2011) 'Role and treatment of mitochondrial DNA-related mitochondrial dysfunction in sporadic neurodegenerative diseases.', *Current pharmaceutical design*, 17(31), pp. 3356–73. Available at: http://www.ncbi.nlm.nih.gov/pubmed/21902672

Synofzik, M. *et al.* (2014) 'PNPLA6 mutations cause Boucher-Neuha¨user and Gordon Holmes syndromes as part of a broad neurodegenerative spectrum', *Brain*. Oxford University Press, 137, pp. 69–77. doi: 10.1093/brain/awt326.

Tabary, O. *et al.* (2006) 'Calcium-dependent regulation of NF-κB activation in cystic fibrosis airway epithelial cells', *Cellular Signalling*, 18(5), pp. 652–660. doi: 10.1016/j.cellsig.2005.06.004.

Tai, H.-C. *et al.* (2012) 'The Synaptic Accumulation of Hyperphosphorylated Tau Oligomers in Alzheimer Disease Is Associated With Dysfunction of the Ubiquitin-Proteasome System Hwan-Ching', *The American Journal of Pathology*. American Society for Investigative Pathology, 181(4), pp. 1426–1435. doi: 10.1016/j.ajpath.2012.06.033.

Takesako, K. *et al.* (1993) 'Biological properties of aureobasidin A, a cyclic depsipeptide antifungal antibiotic.', *The Journal of antibiotics*, 46(9), pp. 1414–20. Available at: http://www.ncbi.nlm.nih.gov/pubmed/8226319

Tam, A. B. *et al.* (2012) 'ER Stress Activates NF-κB by Integrating Functions of Basal IKK Activity, IRE1 and PERK', *PLoS ONE*. Edited by M. Koritzinsky. Public Library of Science, 7(10), p. e45078. doi: 10.1371/journal.pone.0045078.

Tarrade, A. *et al.* (2006) 'A mutation of spastin is responsible for swellings and impairment of transport in a region of axon characterized by changes in microtubule composition', *Hum Mol Genet*, 15.

Tartey, S. *et al.* (2014) 'Akirin2 is critical for inducing inflammatory genes by bridging I B- and the SWI/SNF complex', *The EMBO Journal*, 33(20), pp. 2332–2348. doi: 10.15252/embj.201488447.

Taylor, J. P., Hardy, J. and Fischbeck, K. H. (2002) 'Toxic Proteins in Neurodegenerative Disease', *Science*, 296(5575), pp. 1991–1995. doi: 10.1126/science.1067122.

Tesson, C. *et al.* (2012) 'Alteration of Fatty-Acid-Metabolizing Enzymes Affects Mitochondrial Form and Function in Hereditary Spastic Paraplegia', *The American Journal of Human Genetics*, 91(6), pp. 1051–1064. doi: 10.1016/j.ajhg.2012.11.001.

Thaminy, S. *et al.* (2003) 'Identification of novel ErbB3-interacting factors using the split-ubiquitin membrane yeast two-hybrid system.', *Genome research*. Cold Spring Harbor Laboratory Press, 13(7), pp. 1744–53. doi: 10.1101/gr.1276503.

Thiele, C. and Spandl, J. (2008) 'Cell biology of lipid droplets', *Current Opinion in Cell Biology*, 20(4), pp. 378–385. doi: 10.1016/j.ceb.2008.05.009.

Tian, W.-T. *et al.* (2016) 'Novel Mutations in Endoplasmic Reticulum Lipid Raft-associated Protein 2 Gene Cause Pure Hereditary Spastic Paraplegia Type 18.', *Chinese medical journal*. Wolters Kluwer -- Medknow Publications, 129(22), pp. 2759–2761. doi: 10.4103/0366-6999.193444.

Tiranti, V. *et al.* (2000) 'A novel frameshift mutation of the mtDNA COIII gene leads to impaired assembly of cytochrome c oxidase in a patient affected by Leigh-like syndrome.', *Human molecular genetics*, 9(18), pp. 2733–42. Available at: http://www.ncbi.nlm.nih.gov/pubmed/11063732

Tirode, F. *et al.* (1997) 'A conditionally expressed third partner stabilizes or prevents the formation of a transcriptional activator in a three-hybrid system.', *The Journal of biological chemistry*, 272(37), pp. 22995–9. Available at: http://www.ncbi.nlm.nih.gov/pubmed/9287295

Todi, S. V. and Paulson, H. L. (2011) 'Balancing act: deubiquitinating enzymes in the nervous system', *Trends in Neurosciences*, 34(7), pp. 370–382. doi: 10.1016/j.tins.2011.05.004.

Tomar, D. *et al.* (2012) 'TRIM13 regulates ER stress induced autophagy and clonogenic ability of the cells', *Biochimica et Biophysica Acta (BBA) - Molecular Cell Research*. Elsevier, 1823(2), pp. 316–326. doi: 10.1016/J.BBAMCR.2011.11.015.

Tomar, D. *et al.* (2013) 'TRIM13 regulates caspase-8 ubiquitination, translocation to autophagosomes and activation during ER stress induced cell death', *Biochimica et Biophysica Acta (BBA) - Molecular Cell Research*. Elsevier, 1833(12), pp. 3134–3144. doi: 10.1016/J.BBAMCR.2013.08.021.

Tomar, D. and Singh, R. (2014) 'TRIM13 regulates ubiquitination and turnover of NEMO to suppress TNF induced NF-κB activation', *Cellular Signalling*, 26(12), pp. 2606–2613. doi: 10.1016/j.cellsig.2014.08.008.

Topaloglu, A. K. *et al.* (2014) 'Loss-of-Function Mutations in *PNPLA6* Encoding Neuropathy Target Esterase Underlie Pubertal Failure and Neurological Deficits in Gordon Holmes Syndrome', *The Journal of Clinical Endocrinology & Metabolism*, 99(10), pp. E2067–E2075. doi: 10.1210/jc.2014-1836.

Totsukawa, G. *et al.* (2011) 'VCIP135 deubiquitinase and its binding protein, WAC, in p97ATPase-mediated membrane fusion', *The EMBO Journal*, 30(17), pp. 3581–3593. doi: 10.1038/emboj.2011.260.

Tresse, E. *et al.* (2010) 'VCP/p97 is essential for maturation of ubiquitin-containing autophagosomes and this function is impaired by mutations that cause IBMPFD.', *Autophagy*. NIH Public Access, 6(2), pp. 217–27. Available at: http://www.ncbi.nlm.nih.gov/pubmed/20104022

Trushina, E. and McMurray, C. T. (2007) 'Oxidative stress and mitochondrial dysfunction in neurodegenerative diseases.', *Neurscience*. Elsevier Limited, 145(4), pp. 1233–48. doi: 10.1016/j.neuroscience.2006.10.056.

Tsai, P.-C. *et al.* (2014) 'A novel TFG mutation causes Charcot-Marie-Tooth disease type 2 and impairs TFG function', *Neurology*, 83(10), pp. 903–912. doi: 10.1212/WNL.0000000000000758.

Tsang, H. T. H. *et al.* (2006) 'A systematic analysis of human CHMP protein interactions: additional MIT domain-containing proteins bind to multiple components of the human ESCRT III complex.', *Genomics*, 88(3), pp. 333–46. doi: 10.1016/j.ygeno.2006.04.003.

Tsang, H. T. H. H. *et al.* (2009) 'The hereditary spastic paraplegia proteins NIPA1, spastin and spartin are inhibitors of mammalian BMP signalling.', *Human molecular genetics*, 18(20), pp. 3805–21. doi: 10.1093/hmg/ddp324.

Tubbs, A. and Nussenzweig, A. (2017) 'Endogenous DNA Damage as a Source of Genomic Instability in Cancer'. doi: 10.1016/j.cell.2017.01.002.

Tydlacka, S. *et al.* (2008) 'Differential Activities of the Ubiquitin-Proteasome System in Neurons versus Glia May Account for the Preferential Accumulation of Misfolded Proteins in Neurons', *Journal of Neuroscience*, 28(49), pp. 13285–13295. doi: 10.1523/JNEUROSCI.4393-08.2008.

Uchida, Y. *et al.* (2007) 'Fatty Acid 2-Hydroxylase, Encoded by *FA2H* , Accounts for Differentiation-associated Increase in 2-OH Ceramides during Keratinocyte Differentiation', *Journal of Biological Chemistry*, 282(18), pp. 13211–13219. doi: 10.1074/jbc.M611562200.

Uhlen, M. *et al.* (2015) 'Tissue-based map of the human proteome', *Science*, 347(6220), pp. 1260419–1260419. doi: 10.1126/science.1260419.

Uhlenberg, B. *et al.* (2004) 'Mutations in the Gene Encoding Gap Junction Protein α12 (Connexin 46.6) Cause Pelizaeus-Merzbacher–Like Disease', *The American Journal of Human Genetics*, 75(2), pp. 251–260. doi: 10.1086/422763.

Ungar, D. *et al.* (2006) 'Retrograde transport on the COG railway', *Trends in Cell Biology*, 16(2), pp. 113–120. doi: 10.1016/j.tcb.2005.12.004.

Urnavicius, L. *et al.* (2015) 'The structure of the dynactin complex and its interaction with dynein', *Science*, 347(6229), pp. 1441–1446. doi: 10.1126/science.aaa4080.

Valastyan, J. S. and Lindquist, S. (2014) 'Mechanisms of protein-folding diseases at a glance.', *Disease models & mechanisms*. Company of Biologists, 7(1), pp. 9–14. doi: 10.1242/dmm.013474.

Valente, E. M. *et al.* (2002) 'Novel locus for autosomal dominant pure hereditary spastic paraplegia (SPG19) maps to chromosome 9q33-q34.', *Annals of neurology*, 51(6), pp. 681–5. doi: 10.1002/ana.10204.

Vallabhajosyula, R. R. *et al.* (2009) 'Identifying Hubs in Protein Interaction Networks Ravishankar', *PloS one*. Edited by D. Di Bernardo. Public Library of Science, 4(4), pp. 1–10. doi: 10.1371/journal.pone.0005344.

Vance, C. *et al.* (2009) 'Mutations in FUS, an RNA Processing Protein, Cause Familial Amyotrophic Lateral Sclerosis Type 6', *Science*, 323(5918), pp. 1208–1211. doi: 10.1126/science.1165942.

Vanunu, O. *et al.* (2010) 'Associating Genes and Protein Complexes with Disease via Network Propagation', *PLoS Computational Biology*. Edited by W. W. Wasserman. Public Library of Science, 6(1), p. e1000641. doi: 10.1371/journal.pcbi.1000641.

Varga, R. E. *et al.* (2015) 'In Vivo Evidence for Lysosome Depletion and Impaired Autophagic Clearance in Hereditary Spastic Paraplegia Type SPG11', *PLoS Genetics*, 11(8). doi:

10.1371/journal.pgen.1005454.

Vasile, E. *et al.* (2006) 'IntraGolgi distribution of the Conserved Oligomeric Golgi (COG) complex', *Experimental Cell Research*, 312(16), pp. 3132–3141. doi: 10.1016/j.yexcr.2006.06.005.

Vaurs-Barrière, C. *et al.* (2009) 'Pelizaeus-Merzbacher-Like disease presentation of MCT8 mutated male subjects', *Annals of Neurology*. Wiley Subscription Services, Inc., A Wiley Company, 65(1), pp. 114–118. doi: 10.1002/ana.21579.

Vazquez, A. *et al.* (2003) 'Global protein function prediction from protein-protein interaction networks', *Nature Biotechnology*, 21(6), pp. 697–700. doi: 10.1038/nbt825.

Vazza, G. *et al.* (2000) 'A new locus for autosomal recessive spastic paraplegia associated with mental retardation and distal motor neuropathy, SPG14, maps to chromosome 3q27-q28.', *American journal of human genetics*. Elsevier, 67(2), pp. 504–9. doi: 10.1086/303017.

Vembar, S. S. and Brodsky, J. L. (2008) 'One step at a time: endoplasmic reticulum-associated degradation', *Nature Reviews Molecular Cell Biology*, 9(12), pp. 944–957. doi: 10.1038/nrm2546.

Venco, P. *et al.* (2015) 'Mutations of C19orf12, coding for a transmembrane glycine zipper containing mitochondrial protein, cause mis-localization of the protein, inability to respond to oxidative stress and increased mitochondrial Ca^{2+}.', *Frontiers in genetics*. Frontiers Media SA, 6, p. 185. doi: 10.3389/fgene.2015.00185.

Verkhratsky, A. (2005) 'Physiology and Pathophysiology of the Calcium Store in the Endoplasmic Reticulum of Neurons', *Physiological Reviews*, 85(1), pp. 201–279. doi: 10.1152/physrev.00004.2004.

Verny, C. *et al.* (2011) 'Hereditary spastic paraplegia-like disorder due to a mitochondrial ATP6 gene point mutation', *Mitochondrion*, 11(1), pp. 70–75. doi: 10.1016/j.mito.2010.07.006.

Verstreken, P. *et al.* (2005) 'Synaptic Mitochondria Are Critical for Mobilization of Reserve Pool Vesicles at Drosophila Neuromuscular Junctions', *Neuron*, 47(3), pp. 365–378. doi: 10.1016/j.neuron.2005.06.018.

Vidal, M., Cusick, M. E. and Barabási, A.-L. (2011) 'Interactome networks and human disease.', *Cell*. Elsevier, 144(6), pp. 986–98. doi: 10.1016/j.cell.2011.02.016.

Vietri, M. *et al.* (2015) 'Spastin and ESCRT-III coordinate mitotic spindle disassembly and nuclear envelope sealing', *Nature*, 522(7555), pp. 231–235. doi: 10.1038/nature14408.

Voeltz, G. K. *et al.* (2006) 'A Class of Membrane Proteins Shaping the Tubular Endoplasmic Reticulum', *Cell*, 124(3), pp. 573–586. doi: 10.1016/j.cell.2005.11.047.

Walhout, A. J. *et al.* (2000) 'Protein interaction mapping in C. elegans using proteins involved in vulval development.', *Science (New York, N.Y.)*, 287(5450), pp. 116–22. Available at: http://www.ncbi.nlm.nih.gov/pubmed/10615043

Walhout, A. J. M. and Vidal, M. (2001) 'High-Throughput Yeast Two-Hybrid Assays for Large-Scale Protein Interaction Mapping', *Methods*, 24(3), pp. 297–306. doi: 10.1006/meth.2001.1190.

Wallace, D. C. (2005) 'A Mitochondrial Paradigm of Metabolic and Degenerative Diseases, Aging, and Cancer: A Dawn for Evolutionary Medicine', *Annual Review of Genetics*, 39(1), pp. 359–407. doi: 10.1146/annurev.genet.39.110304.095751.

Wallace, D. C. (2012) 'Mitochondria and cancer', *Nature Reviews Cancer*, 12(10), pp. 685–698. doi: 10.1038/nrc3365.

Walter, P. and Ron, D. (2011) 'The Unfolded Protein Response: From Stress Pathway to Homeostatic Regulation', *Science*, 334(6059), pp. 1081–1086. doi: 10.1126/science.1209038.

Walzthoeni, T. *et al.* (2013) 'Mass spectrometry supported determination of protein complex structure', *Current Opinion in Structural Biology*, 23(2), pp. 252–260. doi: 10.1016/j.sbi.2013.02.008.

Wang, B. *et al.* (2004) 'The yeast split-ubiquitin membrane protein two-hybrid screen identifies BAP31 as a regulator of the turnover of endoplasmic reticulum-associated protein tyrosine phosphatase-like B.', *Molecular and cellular biology*. American Society for Microbiology (ASM), 24(7), pp. 2767–78. doi: 10.1128/MCB.24.7.2767-2778.2004.

Wang, W. *et al.* (2015) 'TRAF Family Member-associated NF-κB Activator (TANK) Inhibits Genotoxic Nuclear Factor κB Activation by Facilitating Deubiquitinase USP10-dependent Deubiquitination of TRAF6 Ligase', *Journal of Biological Chemistry*, 290(21), pp. 13372–13385. doi: 10.1074/jbc.M115.643767.

Wang, X. W. *et al.* (2006) 'Evidence for the ancient origin of the NF- B/I B cascade: Its archaic role in pathogen infection and immunity', *Proceedings of the National Academy of Sciences*, 103(11), pp. 4204–4209. doi: 10.1073/pnas.0507044103.

Wassmer, T. *et al.* (2006) 'A loss-of-function screen reveals SNX5 and SNX6 as potential components of the mammalian retromer', *Journal of Cell Science*, 120(1), pp. 45–54. doi: 10.1242/jcs.03302.

Watts, D. J. and Strogatz, S. H. (1998) 'Collective dynamics of "small-world" networks', *Nature*, 393(29), pp. 440–442. doi: 10.1038/30918.

Weimbs, T. and Stoffel, W. (1992) 'Proteolipid protein (PLP) of CNS myelin: positions of free, disulfide-bonded, and fatty acid thioester-linked cysteine residues and implications for the membrane topology of PLP.', *Biochemistry*, 31(49), pp. 12289–96.
Available at: http://www.ncbi.nlm.nih.gov/pubmed/1281423

Welte, M. A. (2007) 'Proteins under new management: lipid droplets deliver', *Trends in Cell Biology*, 17(8), pp. 363–369. doi: 10.1016/j.tcb.2007.06.004.

Werner, E. D., Brodsky, J. L. and McCracken, A. A. (1996) 'Proteasome-dependent endoplasmic reticulum-associated protein degradation: an unconventional route to a familiar fate.', *Proceedings of the National Academy of Sciences of the United States of America*. National Academy of Sciences, 93(24), pp. 13797–801. Available at: http://www.ncbi.nlm.nih.gov/pubmed/8943015

Wheldon, L. M. *et al.* (2010) 'Critical Role of FLRT1 Phosphorylation in the Interdependent Regulation of FLRT1 Function and FGF Receptor Signalling Lee', *PloS one*. Edited by C. Neylon. Public Library of

Science, 5(4), pp. 1–12. doi: 10.1371/journal.pone.0010264.

White, S. R. *et al.* (2007) 'Recognition of C-terminal amino acids in tubulin by pore loops in Spastin is important for microtubule severing', *The Journal of Cell Biology*, 176(7), pp. 995–1005. doi: 10.1083/jcb.200610072.

Wilkinson, K. D. (1997) 'Regulation of ubiquitin-dependent processes by deubiquitinating enzymes.', *FASEB journal : official publication of the Federation of American Societies for Experimental Biology*, 11(14), pp. 1245–56. Available at: http://www.ncbi.nlm.nih.gov/pubmed/9409543

Wilson, C. M. and High, S. (2007) 'Ribophorin I acts as a substrate-specific facilitator of N-glycosylation', *Journal of Cell Science*, 120(4), pp. 648–657. doi: 10.1242/jcs.000729.

Windpassinger, C. *et al.* (2004) 'Heterozygous missense mutations in BSCL2 are associated with distal hereditary motor neuropathy and Silver syndrome', *Nature Genetics*, 36(3), pp. 271–276. doi: 10.1038/ng1313.

Witte, K. *et al.* (2011) 'TFG-1 function in protein secretion and oncogenesis.', *Nature cell biology*. NIH Public Access, 13(5), pp. 550–8. doi: 10.1038/ncb2225.

Woodsmith, J., Jenn, R. C. and Sanderson, C. M. (2012) 'Systematic analysis of dimeric E3-RING interactions reveals increased combinatorial complexity in human ubiquitination networks.', *Molecular & cellular proteomics : MCP*. American Society for Biochemistry and Molecular Biology, 11(7). doi: 10.1074/mcp.M111.016162.

Xu, J. and Li, Y. (2006) 'Discovering disease-genes by topological features in human protein–protein interaction network', *Bioinformatics*, 22(22), pp. 2800–2805. doi: 10.1093/bioinformatics/btl467.

Yagi, T., Ito, D. and Suzuki, N. (2014) 'Evidence of TRK-Fused Gene (TFG1) function in the ubiquitin–proteasome system', *Neurobiology of Disease*, 66, pp. 83–91. doi: 10.1016/j.nbd.2014.02.011.

Yagi, T., Ito, D. and Suzuki, N. (2016) '*TFG* -Related Neurologic Disorders: New Insights Into Relationships Between Endoplasmic Reticulum and Neurodegeneration', *Journal of Neuropathology & Experimental Neurology*, 75(4), pp. 299–305. doi: 10.1093/jnen/nlw009.

Yamamoto, Y. *et al.* (2014) 'Arl6IP1 has the ability to shape the mammalian ER membrane in a reticulon-like fashion', *Biochemical Journal*, 458(1), pp. 69–79. doi: 10.1042/BJ20131186.

Yamashita, A. *et al.* (2010) 'Generation of lysophosphatidylinositol by DDHD domain containing 1 (DDHD1): Possible involvement of phospholipase D/phosphatidic acid in the activation of DDHD1', *Biochimica et Biophysica Acta (BBA) - Molecular and Cell Biology of Lipids*, 1801(7), pp. 711–720. doi: 10.1016/j.bbalip.2010.03.012.

Yan, Y., Lagenaur, C. and Narayanan, V. (1993) 'Molecular cloning of M6: identification of a PLP/DM20 gene family.', *Neuron*. Elsevier, 11(3), pp. 423–31. doi: 10.1016/0896-6273(93)90147-J.

Yang, Y. S. and Strittmatter, S. M. (2007) 'The reticulons: a family of proteins with diverse functions', *Genome Biology*. BioMed Central, 8(12), p. 234. doi: 10.1186/gb-2007-8-12-234.

Yap, C. C. and Winckler, B. (2012) 'Harnessing the power of the endosome to regulate neural development.', *Neuron*. NIH Public Access, 74(3), pp. 440–51. doi: 10.1016/j.neuron.2012.04.015.

Yu, H. *et al.* (2004) 'Annotation transfer between genomes: protein-protein interologs and protein-DNA regulogs.', *Genome research*. Cold Spring Harbor Laboratory Press, 14(6), pp. 1107–18. doi: 10.1101/gr.1774904.

Yu, H. *et al.* (2008) 'High-quality binary protein interaction map of the yeast interactome network.', *Science (New York, N.Y.)*. NIH Public Access, 322(5898), pp. 104–10. doi: 10.1126/science.1158684.

Zaccheo, O. *et al.* (2004) 'Neuropathy Target Esterase and Its Yeast Homologue Degrade Phosphatidylcholine to Glycerophosphocholine in Living Cells', *Journal of Biological Chemistry*, 279(23), pp. 24024–24033. doi: 10.1074/jbc.M400830200.

Zanetti, G. *et al.* (2011) 'COPII and the regulation of protein sorting in mammals', *Nature Cell Biology*. Nature Research, 14(1), pp. 20–28. doi: 10.1038/ncb2390.

Zeitlmann, L. *et al.* (2001) 'Cloning of ACP33 as a novel intracellular ligand of CD4.', *The Journal of biological chemistry*. American Society for Biochemistry and Molecular Biology, 276(12), pp. 9123–32. doi: 10.1074/jbc.M009270200.

Zhang, K. and Kaufman, R. J. (2008) 'From endoplasmic-reticulum stress to the inflammatory response', *Nature*, 454(7203), pp. 455–462. doi: 10.1038/nature07203.

Zhang, X. *et al.* (2000) 'Structure of the AAA ATPase p97', *Molecular Cell*, 6(6), pp. 1473–1484. doi: 10.1016/S1097-2765(00)00143-X.

Zhao, G. *et al.* (2008) 'A novel candidate locus on chromosome 11p14.1-p11.2 for autosomal dominant hereditary spastic paraplegia.', *Chinese medical journal*, 121(5), pp. 430–4. Available at: http://www.ncbi.nlm.nih.gov/pubmed/18364116

Zhao, J. and Hedera, P. (2013) 'Hereditary spastic paraplegia-causing mutations in atlastin-1 interfere with BMPRII trafficking.', *Molecular and cellular neurosciences*. NIH Public Access, 52, pp. 87–96. doi: 10.1016/j.mcn.2012.10.005.

Zhao, R. *et al.* (2005) 'Navigating the Chaperone Network: An Integrative Map of Physical and Genetic Interactions Mediated by the Hsp90 Chaperone', *Cell*, 120(5), pp. 715–727. doi: 10.1016/j.cell.2004.12.024.

Zhao, X. *et al.* (2001) 'Mutations in a newly identified GTPase gene cause autosomal dominant hereditary spastic paraplegia.', *Nature Genetics*, 29(3), pp. 326–331. doi: 10.1038/ng758.

Zhong, Q. *et al.* (2009) 'Edgetic perturbation models of human inherited disorders.', *Molecular systems biology*, 5, p. 321. doi: 10.1038/msb.2009.80.

Zhong, X. *et al.* (2004) 'AAA ATPase p97/Valosin-containing Protein Interacts with gp78, a Ubiquitin Ligase for Endoplasmic Reticulum-associated Degradation', *Journal of Biological Chemistry*, 279(44), pp. 45676–45684. doi: 10.1074/jbc.M409034200.

Zhu, P.-P. *et al.* (2003) 'Cellular Localization, Oligomerization, and Membrane Association of the Hereditary Spastic Paraplegia 3A (SPG3A) Protein Atlastin', *Journal of Biological Chemistry*, 278(49), pp. 49063–49071. doi: 10.1074/jbc.M306702200.

Zhu, X.-H. *et al.* (2012) 'Quantitative imaging of energy expenditure in human brain', *NeuroImage*, 60(4), pp. 2107–2117. doi: 10.1016/j.neuroimage.2012.02.013.

Zivony-Elboum, Y. *et al.* (2012) 'A founder mutation in Vps37A causes autosomal recessive complex hereditary spastic paraparesis', *Journal of Medical Genetics*, 49(7), pp. 462–472. doi: 10.1136/jmedgenet-2012-100742.

Zoller, I. *et al.* (2008) 'Absence of 2-Hydroxylated Sphingolipids Is Compatible with Normal Neural Development But Causes Late-Onset Axon and Myelin Sheath Degeneration', *Journal of Neuroscience*, 28(39), pp. 9741–9754. doi: 10.1523/JNEUROSCI.0458-08.2008.

Zortea, M. *et al.* (2002) 'Genetic mapping of a susceptibility locus for disc herniation and spastic paraplegia on 6q23.3-q24.1.', *Journal of medical genetics*, 39(6), pp. 387–90. Available at: http://www.ncbi.nlm.nih.gov/pubmed/12070243

Züchner, S. *et al.* (2006) 'Mutations in the novel mitochondrial protein REEP1 cause hereditary spastic paraplegia type 31.', *American journal of human genetics*. Elsevier, 79(2), pp. 365–9. doi: 10.1086/505361.

Zurek, N., Sparks, L. and Voeltz, G. (2011) 'Reticulon short hairpin transmembrane domains are used to shape ER tubules.', *Traffic (Copenhagen, Denmark)*. NIH Public Access, 12(1), pp. 28–41. doi: 10.1111/j.1600-0854.2010.01134.x.